**Dr. Balaji Ramakrishnan**
Associate Professor, Department of Civil Engineering
Indian Institute of Technology Bombay
Powai, Mumbai-400 076, India.

27 Nov 2019

**To**
Shri Anil Pruthi
Deputy Director (Engg)
Room no.: 541, Ministry of Shipping, Transport Bhawan, Parliament Street,
New Delhi – 110 001. Email: anil.pruthi@nic.in

Dear Sir,

**Sub.:** Submission of Consolidated Final report -reg.
**Ref.:** Sanctioned R&D scheme, ref. DW/DTO-7/2015 dated 13 Apr 2017

With reference to the above R&D scheme titled "Comprehensive Analysis of Siltation Behavior of Indian Ports and Navigational Channels", please see enclosed the Consolidated Final Report of the project outcome, for your kind reference.

I'm happy to inform you that the siltation behaviour of Deendayal (erstwhile Kandla) Port's (DPT) navigational approach channel is systematically understood through a comprehensive study and suggested for set of silt-curtains as the best option. The suggested silt-curtains, as detailed in the enclosed Executive Summary, *would minimise the silt deposition along the navigational approach channel, from 46% to 56%,* which is expected to reduce the maintenance dredging cost of Deendayal port (*erstwhile Kandla*).

*IIT Bombay would be happy to assist in the process of implementing this solution, if deemed necessary, in association with Ministry of Shipping and or DPT.*

Thank you.

Sincerely,

**[R. BALAJI]**

IIT BOMBAY
Prof. R BALAJI
Department of Civil Engineering

***Encl:*** (i) One original Consolidated Final Report (190 pages)
(ii) Executive Summary of the outcome of the project (5 pages)
(iii) Original UC and SoE.(6 pages)

***Copy to:*** The Chairman, DPT, with kind attention to Shri. V.Raveendra Reddy, Superintending Engineer (Harbour), Deen Dayal Port Trust, Administration office, Gandhidham-Kutch, Pin:320201.

Tel.: (+91) 22 2576 7321 (off), (+91) 98198 57321 (mob), Fax.: (+91) 22 2576 7302
Email: rbalaji@civil.iitb.ac.in, rbalaji@iitb.ac.in
URL: http://www.civil.iitb.ac.in/~rbalaji/

## EXECUTIVE SUMMARY

Ministry of Shipping sanctioned (*vide letter ref.: DW/DTO-7/2015 dated 13 Apr 2017*) a research project titled "*Comprehensive analysis of siltation behavior of Navigation channels and basins of Indian major ports*" to analyze the siltation behavior of Kandla port (*now renamed as Deendayal port-DPT*), to start with, and to suggest suitable strategies to minimize the maintenance dredging quantities and thereby the cost.

The comprehensive study, schematically shown in Fig. 1, taken up by IIT Bombay, includes field measurements (pre- and post-monsoon seasons) of tides & currents (spatial and temporal) and suspended sediment concentration (SSC). An exclusive numerical model is also developed that cover the entire Kandla region to estimate the hydrodynamic conditions, using an open-source software called Delft3D. The spatial variations of SSC are also mapped using satellite imageries based analysis. The results of the numerical model are appropriately calibrated and validated with the help of in-situ measurements. Bathymetry and dredging details, supplied by DPT, are also used for analysis the siltation behavior. The estimates of siltation from the developed numerical simulations of morphodynamics is in agreement with that of siltation quantities estimated by DPT. Glimpses of all the aforementioned activities are given in Fig. 2, in nut-shell.

After gaining confidence on the developed numerical model, options to reduce the siltation are attempted, that include (i) changing alignment of the existing channel and (ii) introducing porous barriers along the sides of the channel. ***However, attempt to change the alignment of approach channel did not give any encouraging solution for the siltation issue, as estimated by the developed numerical model.***

Placing porous barriers of different alignment, length and orientation, along the approach channel, are analysed. In practice, these porous barriers are equivalent to a silt curtain type structure, that have successfully been adopted in several ports across the globe as an effective siltation stopper. ***After extensive modelling for numerous alignments and different positions of silt-curtains on the adjacent sides of the approach channel, one particular alignment, as shown in Fig. 3, is found to reduce siltation by 46% - 54%.***

Typical schematic of such silt-curtain and the anchoring arrangement is shown in Fig. 4. Silt curtains could be made of permeable screen that allow water movement and current circulation with minimal sediment passage. The suggested option shall further be explored from the techno-commercial aspect, for possible implementation in Kandla and to reduce the expenditure towards maintenance dredging.



*Dr. Balaji Ramakrishnan, Dept. of Civil Engg., IIT Bombay, Mumbai-76.*
*Ph.: +91 22 2576 7321 (Off), +91 9819857321(mob), email: rbalaji@iitb.ac.in, rbalaji@civil.iitb.ac.in*

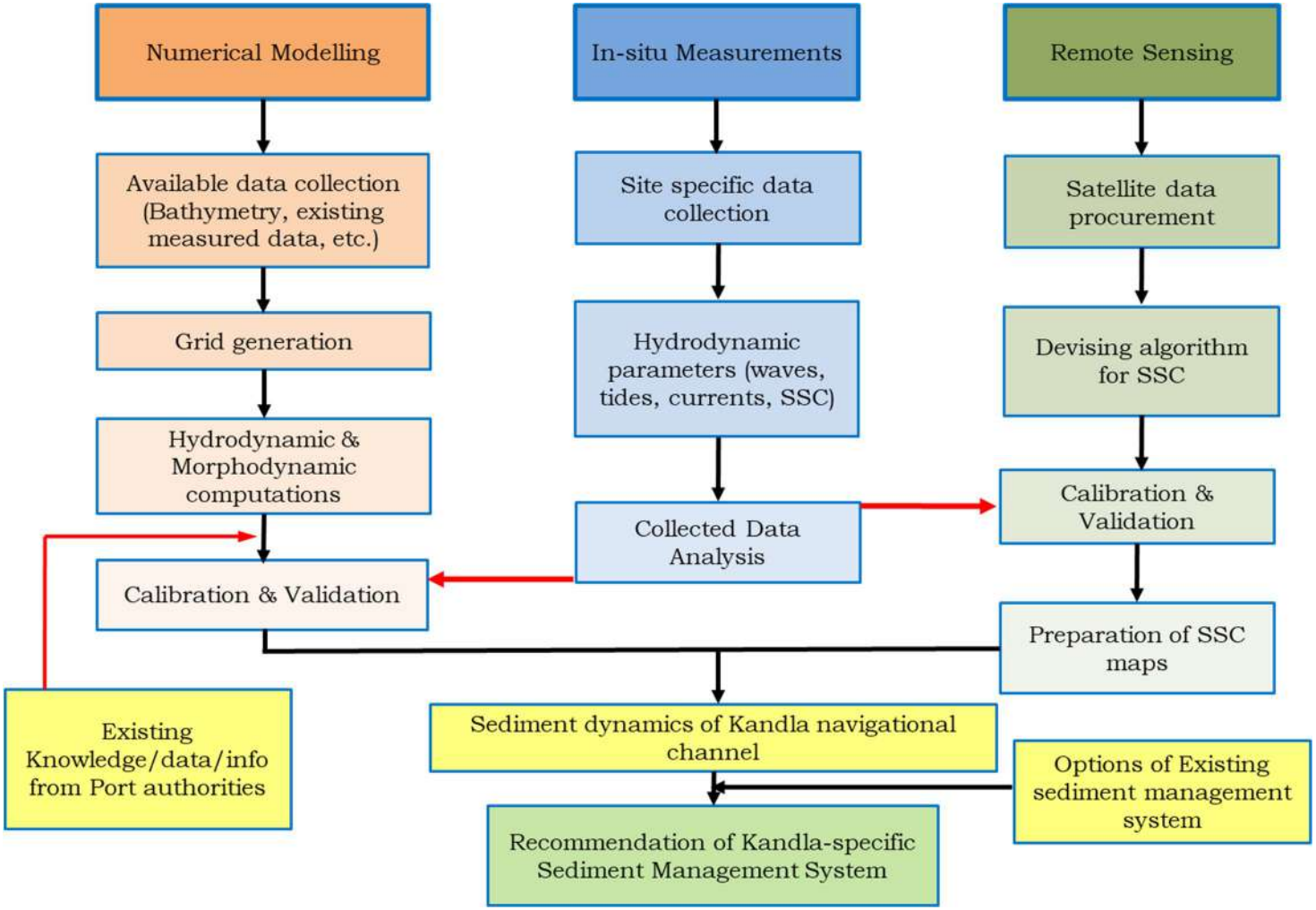


**Fig. 1 Flow-chart of methodology adopted in this study**



*Dr. Balaji Ramakrishnan, Dept. of Civil Engg., IIT Bombay, Mumbai-76.*
*Ph.: +91 22 2576 7321 (Off), +91 9819857321(mob), email: rbalaji@iitb.ac.in, rbalaji@civil.iitb.ac.in*

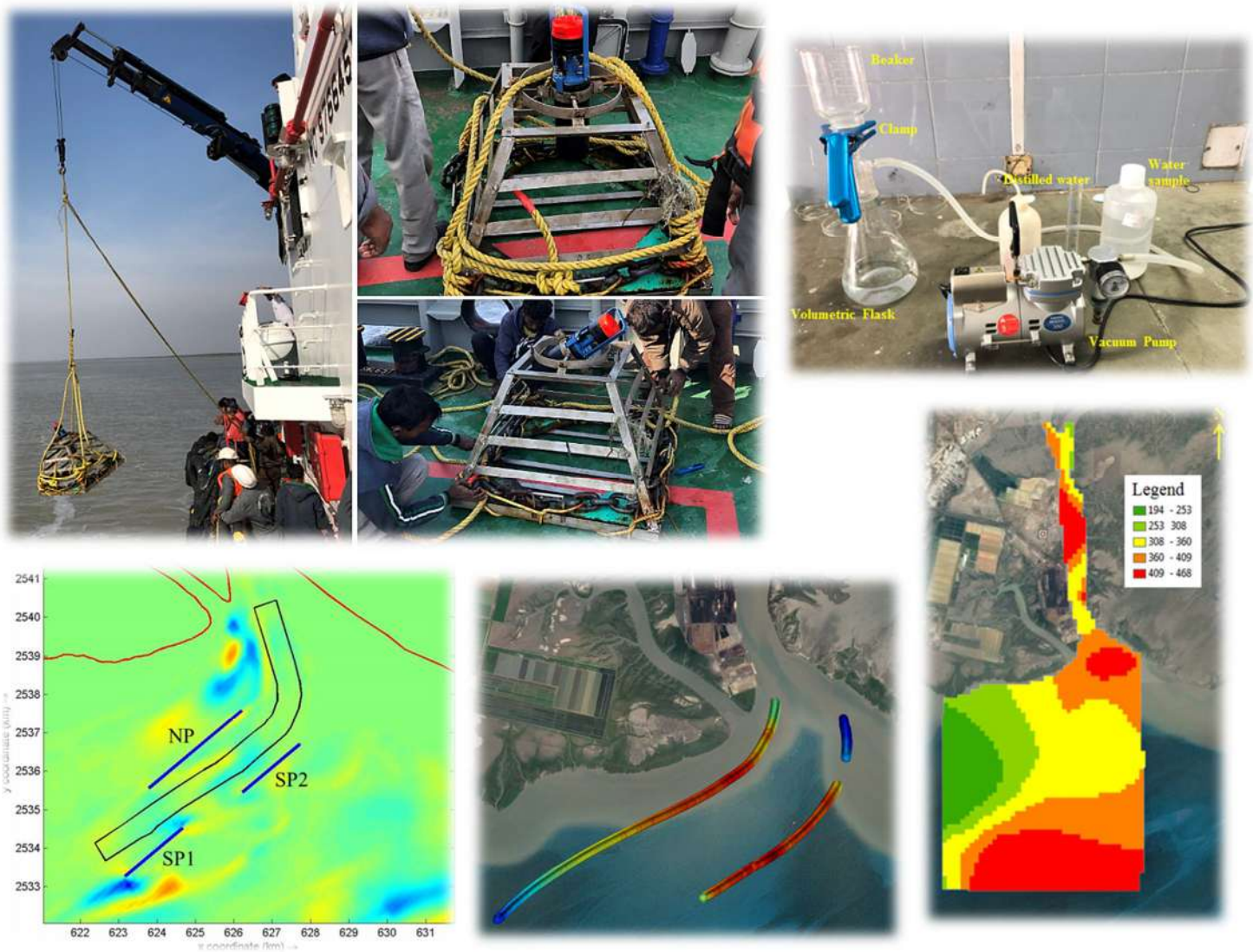


**Fig. 2 Glimpses of various activities of the project, in nut-shell**



*Dr. Balaji Ramakrishnan, Dept. of Civil Engg., IIT Bombay, Mumbai-76.*
*Ph.: +91 22 2576 7321 (Off), +91 9819857321(mob), email: rbalaji@iitb.ac.in, rbalaji@civil.iitb.ac.in*


**Fig. 3 Suggested silt-curtain option for reducing siltation in navigational channel**



*Dr. Balaji Ramakrishnan, Dept. of Civil Engg., IIT Bombay, Mumbai-76.*
*Ph.: +91 22 2576 7321 (Off), +91 9819857321(mob), email: rbalaji@iitb.ac.in, rbalaji@civil.iitb.ac.in*

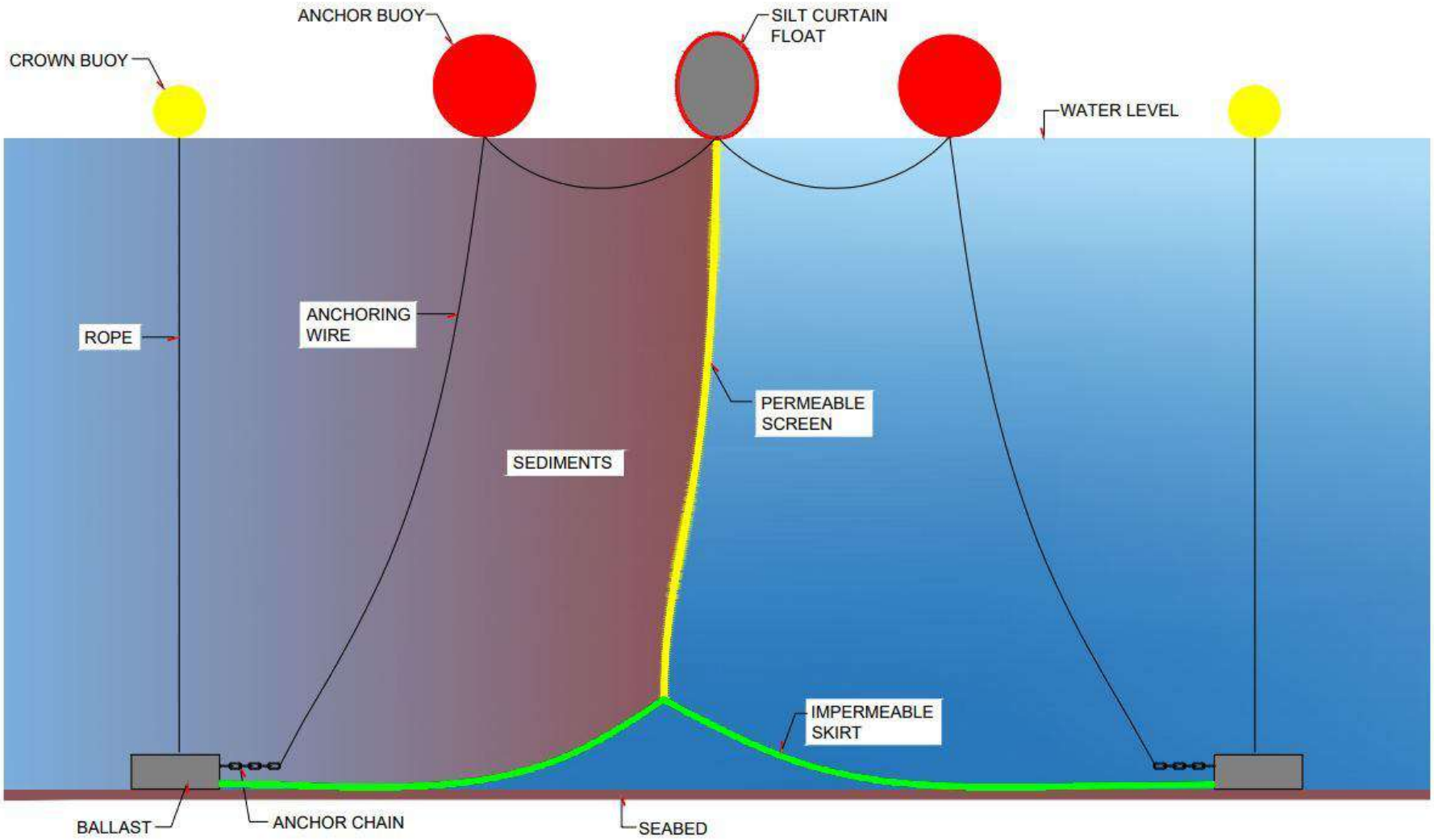


**Fig. 4 Schematic of typical silt curtain arrangement**



*Dr. Balaji Ramakrishnan, Dept. of Civil Engg., IIT Bombay, Mumbai-76.*
*Ph.: +91 22 2576 7321 (Off), +91 9819857321(mob), email: rbalaji@iitb.ac.in, rbalaji@civil.iitb.ac.in*

# Comprehensive analysis of siltation behaviour of Navigation channels and basins of Indian major ports

*Consolidated Final Report for the Siltation of Kandla Port Navigational Channel*

*Submitted to Ministry of shipping, Govt. of India.*

*(Sanction order ref. DW/DTO-7/2015 dated 13 Apr 2017)*

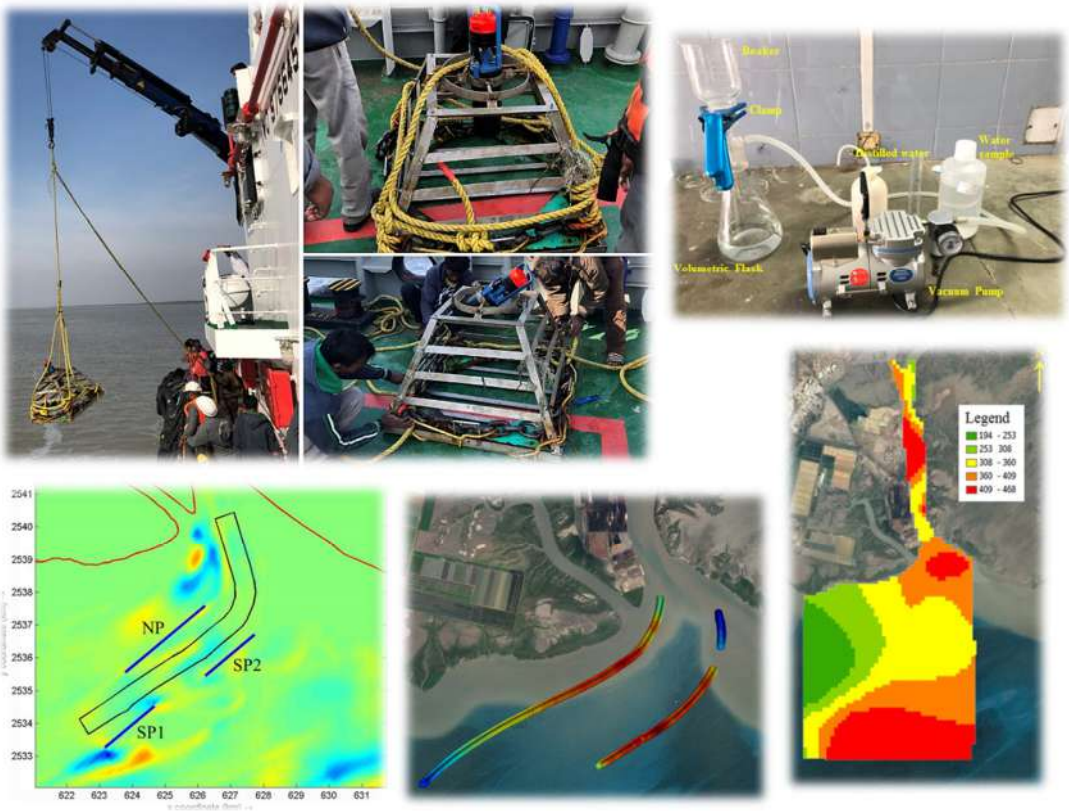


Dr. BALAJI Ramakrishnan
Associate Professor
Department of Civil Engineering
IIT Bombay, Mumbai-400 076.

November 2019

# CONTENTS

# LIST OF FIGURES

# LIST OF TABLES

# EXECUTIVE SUMMARY

Siltation is the physical process of accumulation of sediments, due to natural environmental forcing, in navigational channel intended for vessel movements. Dredging is an inevitable process, in order to keep the channels navigable, that cost significant expenditures to ports, apart from environmental concerns related to fine-sediment-plume spill from dredging process, the transportation and deposition of dredged material. Undoubtedly, it has become a great concern for every port and harbour authorities that necessitates to find some solutions to reduce the siltation and thereby the expenditure.

The project titled "Comprehensive analysis of siltation behaviour of navigational channels and basins of Indian major ports" was proposed by IIT Bombay to the Ministry of Shipping to analyze the siltation behaviour of Deendayal Port (Kandla Port) and thus suggest strategies to minimize the quantity of maintenance dredging of the channel. The primary objective of the project was to analyze about the siltation behaviour of the approach channel and to suggest suitable engineering solutions to reduce siltation, which may help in reducing the expenditure towards dredging.

The comprehensive study, schematically shown in Fig. ES1, taken up by IIT Bombay, started with an initial site visits and followed by detailed field measurements to understand the hydro-morpho-dynamics of the region. The field measurements, carried out during pre- and post-monsoon seasons, include observations of tidal levels, currents (spatial and temporal) and suspended sediment concentration (SSC). A dedicated and exclusive numerical model is also developed, as part of this study, that cover the entire Kandla region to estimate the hydrodynamic conditions. An open-source, freely-available yet reliable software tool called Delft3D is employed for setting up the numerical model. The spatial variations of SSC are also mapped using satellite imageries based analysis. The results of the numerical model are appropriately calibrated and validated with the help of in-situ measurements. Relevant data collected by DPT, such as bathymetry and dredging details along the channel are also used for analysis the siltation behavior.

The estimates of siltation from the developed numerical simulations of morphodynamics is in agreement with that of siltation quantities estimated by DPT. After gaining confidence on the developed numerical model, options to reduce the siltation are attempted through the model studies that included (i) change in the alignment of the existing channel as well as by (ii)

introducing porous barrier structures along the side of the channel to minimize siltation. Porous barriers of different alignment, length and orientation are analysed and a particular option observed to give maximum reduction in the siltation of navigational channel. **Placing these three porous barriers, as shown in Fig. ES2, has resulted in reduction of the siltation by 46-56%, in the main navigation channel of Kandla port.** In practice, these porous barriers are equivalent to a silt curtain type structure, that have successfully been adopted in several ports across the globe as an effective siltation stopper. The suggested option shall further be explored from the techno-commercial aspect, for possible implementation in Kandla and to reduce the expenditure towards maintenance dredging.

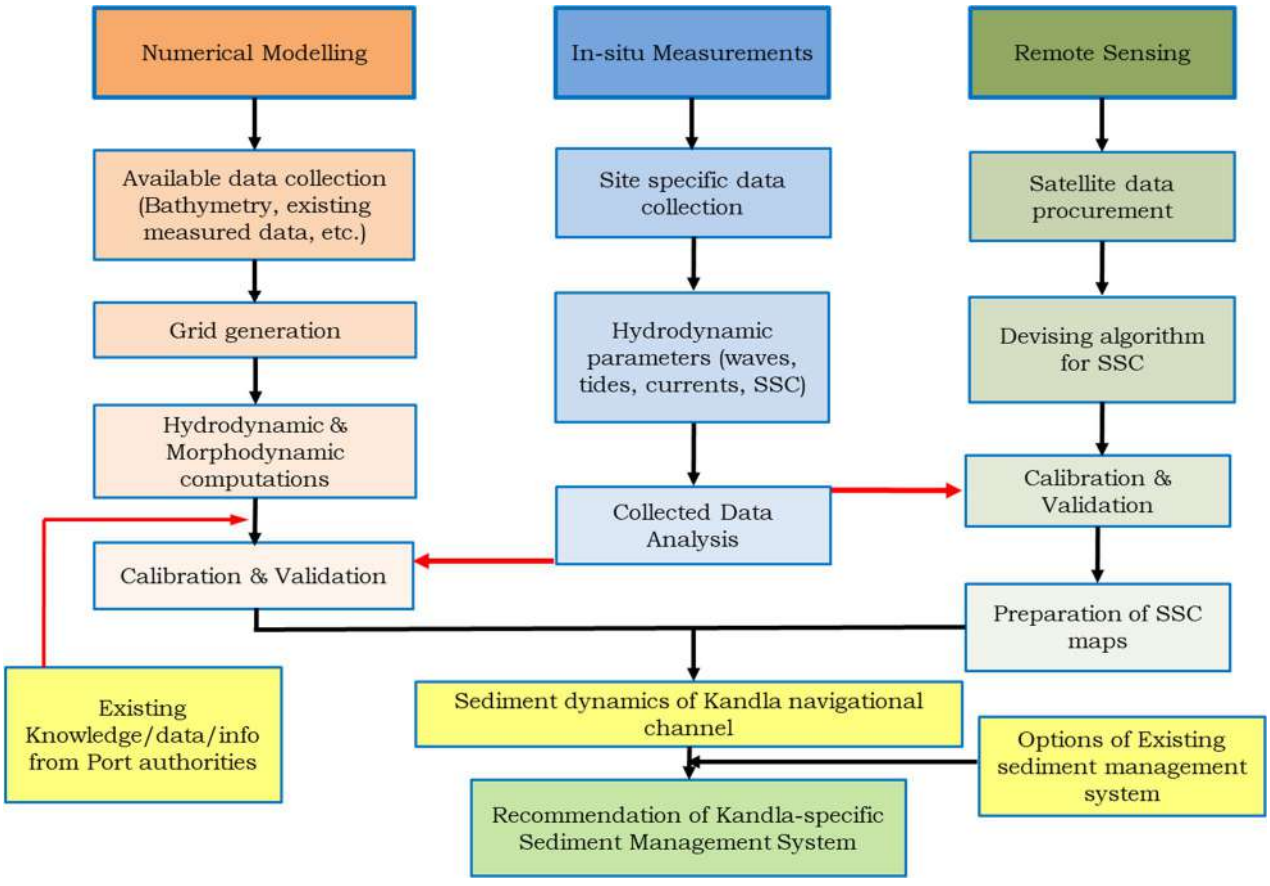


**Fig. ES1 Flow-chart of methodology adopted in this study**


**Fig. ES2 Suggested silt-curtain option for reducing siltation in navigational channel**

# 1. INTRODUCTION

## 1.1 Overview

Ministry of Shipping sanctioned (*vide letter ref.: DW/DTO-7/2015 dated 13 Apr 2017*) a research project titled "*Comprehensive analysis of siltation behaviour of Navigation channels and basins of Indian major ports*" to analyze the siltation behaviour of Kandla port (*now renamed as Deendayal port*), to start with, and to suggest suitable strategies to minimize the maintenance dredging quantities and thereby the cost.

Kandla Port Trust, recently renamed as Deendayal Port Trust, is a seaport in Kutch District of Gujarat state in Western India, near the city of Gandhidham. The Port of Kandla is located, as shown in Fig. 1.1 on the Gulf of Kutch on the northwestern coast of India over 430 nautical miles north-northwest of the Port of Mumbai. The Kandla port-the northwest gateway of India is an example of natural harbor with deep inland water channel to facilitate easy trade. Compared to other coastal ports Kandla has advantage of having dry weather and short spell and scanty monsoon season hence there is hardly any loss of working days in a year.

Out of the 12 major ports in India, Kolkata, Cochin and Kandla ports spend huge costs towards maintenance dredging every year to keep the channel navigable. The met-ocean parameters such as waves, tides, currents and sediment dynamics play a crucial role in the siltation behaviour of Deendayal Port. During the $11^{th}$ five-year plan (2007-2012), an amount of 41.6 million cubic-meter (MCM) of maintenance dredging quantity was targeted for Deendayal port, however only 78% of it could be achieved. The projected quantity of maintenance dredging for the $12^{th}$ five-year plan was increased to 45.5MCM.

In the present study, using the information from the past events and available data from Kandla Port, the problem of siltation is addressed using a combination of numerical modeling, satellite imagery based remote sensing analysis supported by limited field measurements. The three-way approach as expected yielded in a thorough understanding of the hydro and sediment dynamics of the Deendayal Port region. The end result of the study includes a comprehensive sediment management system that would enable the port authorities to effectively manage the problem of siltation. It shall be noted that the Ocean Engineering Division, Department of Civil Engineering, IIT Bombay (IITB) is well equipped with numerical modeling and remote sensing expertise.

A detailed ocean data collection enhanced the understanding of the environmental conditions, further enabled the IITB to utilize it to develop numerical model tools for analyzing siltation behaviour. The currents and tides are found to be the important factors that need to be considered for analysis of siltation behaviour in the creek area. Seasonal collection of samples, laboratory analyses and satellite imageries as well as the numerical model based estimations were done for sediment transport and siltation studies. All the data's collected are used for proper calibration or validation of the numerical model and to train the algorithms for satellite imageries.

Project staff with appropriate educational qualification were exclusively recruited to carryout for the project. A well flourished computational infrastructure facility was also implemented in the institution specifically for carrying out the project progress in full stretch. The existing computational infrastructures with PI were upgraded accordingly to develop a much efficient numerical model.

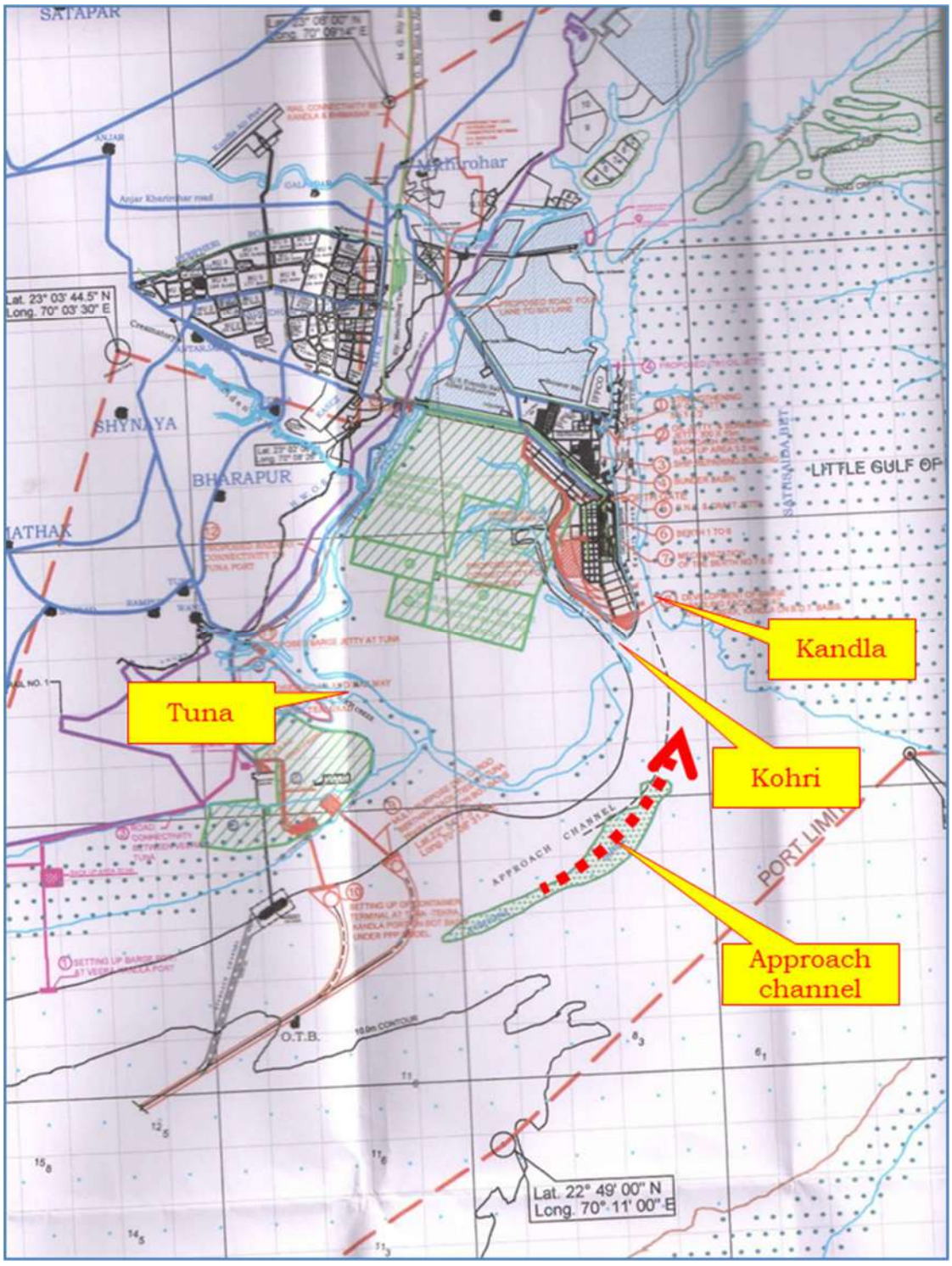


**Fig. 1.1 Location of the project**

## 1.2 Objectives and Scope of the Project

With the advancement of numerical modeling, causative mechanisms for siltation can be identified for Kandla port and based on which a more systematic approach for handling the issues of siltation can be suggested, which would help reduce the cost of maintenance to some extent. The study aims to investigate the behavior of siltation and causative mechanisms along the navigational channel of Kandla port. The hydrodynamic and morphological information obtained from the field data are used in the numerical model. Intensity of sedimentation is there by estimated and a suitable management system is proposed which are studied via the developed numerical model and through remote sensing techniques. On the basis of this scientific rationale, it is anticipated that huge investments involved in maintenance dredging of the Kandla port can be minimized.

The primary objective of the project is to carry out a Comprehensive analysis of the environmental factors that influence the siltation of approach channel of the Kandla Port and to suggest a suitable sedimentation management system to minimize the maintenance dredging.

To fulfill the objectives, following are the proposed scope of works;

- In-situ field measurements of tides, currents and waves near approach channel and Suspended Sediment Concentrations (SSC) at various locations.
- Development of port specific numerical model for the estimation of hydrodynamics & siltation dynamics.
- Finding the characteristics of suspended sediment concentration and bed load sediment.
- Calibration and validation of numerical model results of tidal hydrodynamics using the field measured data.
- Calibration and validation of numerical model results of siltation behaviour, using Deendayal port supplied bathymetry data.
- Develop an algorithm for Remote Sensing to estimate SSC, validate the same using in-situ measurements and prepare maps for temporal and spatial distribution of SSC.
- Based on above analyses, recommend suitable sediment management systems for Deendayal port.

## 1.3 Study Area

The study area lies in the West coast of Indian state of Gujarat, in the north eastern stretch of Arabian Sea, between 68°20’ - 70°40’E and 22°15’ - 23°40’ N covering an area of 7300 Km. It sprawls 180 Km in length in east-west direction, and 70 Km at the mouth to 1 -2 Km at the creeks in the East (Ramaswamy et al., 2007). The depth varies from 60 m near the mouth to 20 m at the eastern end of the Gulf. The Gulf has major ports of Kandla, Mandvi, Mundra, Navlakhi and Okha. There are fresh water sources to the Gulf from Indus River, which lies 100 Km northwest from the mouth of the Gulf. The Gulf of Kutch is shown in Fig. 1.2 and closer view of Kandla port in Fig. 1.3.


**Fig. 1.2 View of study domain in Gulf of Kutch**

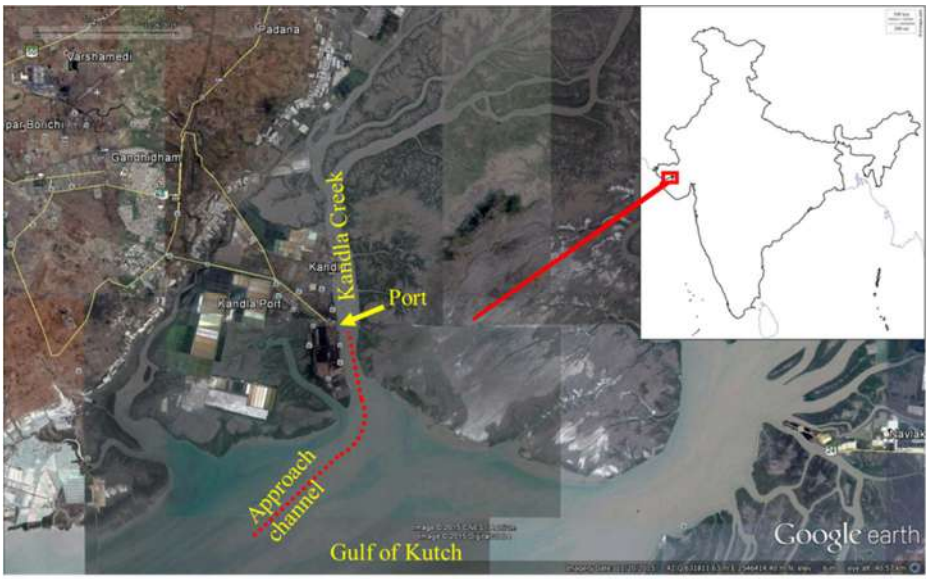


**Fig. 1.3 Detailed view of study domain**

# 2. EQUIPMENT AND COMPUTATIONAL INFRASTRUCTURE

The computational time for a numerical model is primarily dependent on size of the model domain, grid size, resolution of bathymetry and time step in which the model output is expected. In accordance with these factors a proper computational facility should be available so as to simulate and store the results in an efficient way. So the existing facilities available with the PI was upgraded accordingly to complete the task in a much better manner. Apart from the computational facility, it requires proper instruments to be used for procuring the in-situ measurements regarding the study area. For this purpose, various instruments like ADCP, drifters, current meters and other sophisticated instruments were also used for completing this task. A brief description about which will be given in the next sections.

## 2.1 Software Used

Development of model required a number of software in order to creating land boundary, to convert charts into digital form, meshing, editing, simulating hydrodynamic model and post processing the results. A brief description of the software's installed are listed below:

***ArcGIS 10.2***

The current version of ArcGIS is V10.2. It is widely used, Geographic Information System (GIS) software. The applications ranges from creating simple map to shoreline analysis, image analysis, earth quake damage analysis, converting and storing charts, trip planning and routing analysis, extraction of bathymetry etc.

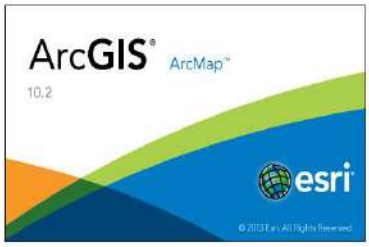


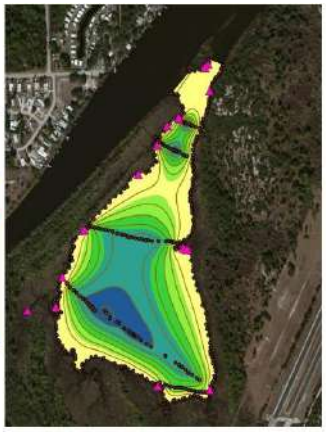

***Admiralty Total Tide (ATT)***

Admiralty total tide is a comprehensive tidal prediction program providing tidal height and tidal stream predictions. The software automates the prediction process, reduces the possibility of user error and

provides an easy means of viewing both under clear and safe overhead clearances. It contains tidal information for over7000 ports and more than 3,000 tidal stream stations worldwide.

***BlueKenue***

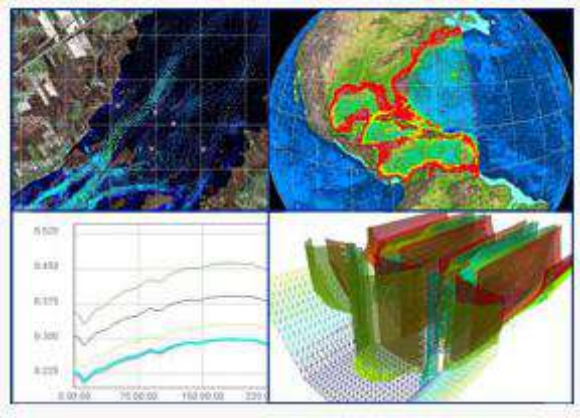

Blue Kenue is an advanced data preparation, analysis, and visualization tool for hydrodynamic modeling. It provides with all the interface, integrating geospatial data with model input and results data. Blue Kenue provides direct import of model results from TELEMAC, ADCIRC and HydroSim. It is used for pre-processing and post-processing of finite-element model for hydrodynamics.

***Autodesk AutoCAD 2016***


Computer – aided design and drafting (CADD) is the process of using a computer with CADD software to design and produce drawings and models according to specific industry and company standards. The terms computer – aided design (CAD)and computer – aided drafting (CAD) refer to specific aspects of CADD process. AutoCAD is used to prepare two-dimensional (2D) drawings, three-dimensional (3D) models, and animations. AutoCAD is a universal CADD software program that applies to any drafting, design or engineering discipline. For this project, AutoCAD is used for processing the bathymetry.

***Delft3D***

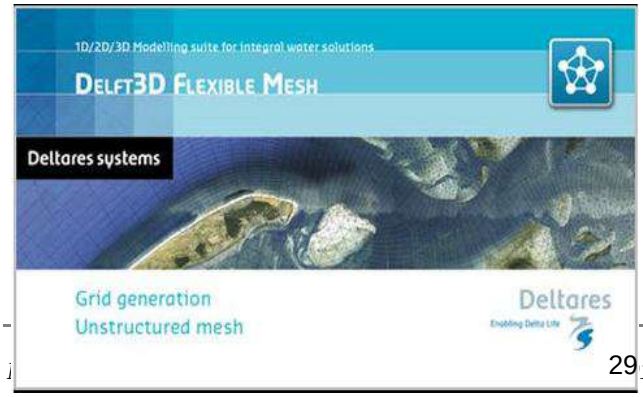


Delft3D is a flexible integrated modeling framework, which simulates two-dimensional (in either the horizontal or a vertical plane) and three-dimensional flow, sediments transport and morphology,

waves, water quality and ecology and is capable of handling the interactions between these processes. Delft3D is composed of a number of modules, each addressing a specific domain of interest, such as grid, flow, water quality, wave generation and propagation, together with pre-processing and post- processing modules. All modules are dynamically interfaced to exchange data and results.

***Matlab***

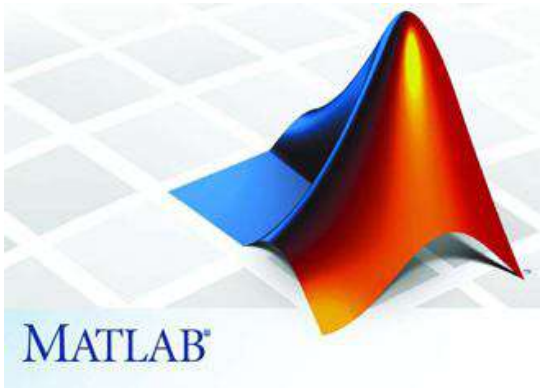


MATLAB is a platform for programming, designing and developing the GUI. It is flexible and has ability to handle many desired input and output formats. MATLAB GUI runs with the help of MATLAB environment which makes it easy for processing huge amount of data like bathymetry data and post processing like displaying texture or contour of the processed data. MATLAB also allows export of the GUI into an executable package which helps us to install this software in other computer which does not run MATLAB.

***Ubuntu***


Ubuntu is an open source Debian-based Linux distribution sponsored by Canonical Ltd. Ubuntu is the most popular operating system running in hosted environments, so–called "clouds". The operating system was intended primarily for personal computers (PCs) but it can also be used on servers. SeaWiFS Data Analysis System (SeaDAS) is installed in Ubuntu for processing, display, analysis, and quality control of ocean color data.

***SeaWiFS Data Analysis System (SeaDAS)***

SeaDAS is a comprehensive software package for the processing, display, analysis, and quality control of ocean color data. While the primary focus of SeaDAS is ocean color data, it is applicable to many satellite-based earth science data analyses. The latest version SeaDAS 7.4 is installed to process MODIS image to assess sediment character.

## 2.2 Instruments Procured

A brief description of the instruments purchased for the project along with its specifications are given below:

### 2.2.1 Wave buoy

The wave buoy is an instrument incorporating advanced technologies that make it an easy to use, reliable for accurate measurement of directional waves. The wave buoy uses GPS to determine its position, store the raw data in its in-built memory card or communicate through RF, in near real time. The wave buoy procured in this project, CX-26D, is shown in Fig 2.1. The following are the technical specifications of the wave buoy;

GPS/GLONASS positioning system:

- Position accuracy 2.5m CEP, velocity with an accuracy 0.1m/s.

Data logger: Micro SD slot: default storage 8Gb.

Data collection:

- Position, current speed, current direction. (validated only for drifting status)
- 3-axis acceleration, pitch, roll, yaw in 4Hz for 10min.
- Significant Wave height, mean wave period, primary wave direction.

Data sampling/transmit interval: 1-Sample/20min. (fastest frequency)

Dimension: Sphere with 26-cm diameter.

**Fig. 2.1 Typical view of Wave buoy CX-26D**

### 2.2.2 Drifters

The drifter is designed to record instantaneous velocity components along the surface of the water with its trajectory. It is easy to use and reliable for accurate measurement. The wave drifter uses GPS to determine its position, stores the data in in-built memory card or through RF system to control station, in near real time. Two different types of drifters are used in this project. Typical view of the RF drifter that is procured through this project, DS-12T, is shown in Fig. 2.2. The technical specifications of the drifters are given below;

***Drifter DS-12T***

GPS/GLONASS positioning system:

- Position accuracy 2.5m CEP, velocity with an Accuracy 0.1m/s.

Data logger: Micro SD slot: default storage 8Gb.

Water temperature measurement: Accuracy 0.03°˚C at 0°˚C, 0.06°˚C at 40°˚C.

Communication range: 1km~15km with data rate varies from 200 Kbps to 10 Kbps.

Data collection: Position, current speed, current direction, water temperature.

Data sampling/transmit interval: 1-Sample/10sec. (fastest frequency)

Dimension: Sphere with 12-cm diameter.

***Drifter CX-12T***

Typical view of these drifters is shown in Fig. 2.3.

GPS/GLONASS positioning system:

- Position accuracy 2.5m CEP, velocity with an accuracy 0.1m/s.

Data logger: Micro SD slot: default storage 8Gb.

Water temperature measurement: Accuracy 0.03°˚C at 0°˚C, 0.06°˚C at 40°˚C.

Data collection: Position, current speed, current direction, water temperature.

Data sampling/transmit interval: 1-Sample/10min. (fastest frequency)

Dimension: Sphere with 26-cm diameter.

**Fig. 2.2 Typical view of RF Drifter DS-12T**

**Fig. 2.3 Typical view of Drifter CX-12T**

### 2.2.3 ADCP (Acoustic Doppler Current Profiler)

An acoustic Doppler current profiler (ADCP) is a hydro acoustic current meter similar to a sonar, used to measure water current velocities over a depth range using the Doppler effect of sound waves scattered back from particles within the water column. The Flow Quest current profiler, procured through this project, is ideal for measuring currents and flow in oceans, harbors, lakes and rivers, and for measuring waves in ocean and coastal areas. Flow Quest

also serves as a focal point for your underwater deployments. A typical Acoustic Current Profiler is shown in Fig. 2.4 with its specification in the below Table.

### 2.2.4 Niskin Sampler

A Niskin sampler (below figure) is an improved version of the Nansen bottle. Instead of the usual metal bottle, the 'bottle' here is a tube made of plastic which is open to the water at both ends. Each end of the tube is equipped with a cap which is either spring-loaded or tensioned by an elastic rope.

**Table 2.1 Acoustic Current Profiler specifications**

| **Water Profiling Range and Depth** | | | |
|---|---|---|---|
| **Model** | FlowQuest 300 | FlowQuest 600 | FlowQuest 1000 |
| **Frequency** | 300 kHz | 600 kHz | 1000 kHz |
| **Maximum Range** | 230 m | 100 m | 40 m |
| **Maximum Cell size** | 8 m | 4 m | 2 m |
| **Standard Depth** | 800 m | 800 m | 800 m |
| **Optional Depth** | | 1500, 3000 or 6000 m | |
| **Blank Distance** | 1.4 m | 0.7 m | 0.4 m |
| **Velocity Specifications** | | | |
| **Model** | FlowQuest 300 | FlowQuest 600 | FlowQuest 1000 |
| **Frequency** | 300 kHz | 600 kHz | 1000 kHz |
| **Accuracy** | 0.5% ± 5 mm/s | 0.25% ± 2.0 mm/s | 0.25% ± 2.0 mm/s |
| **Cell size** | 1 – 8 m | 0.5 – 4 m | 0.25 – 2 m |
| **Maximum Water Velocity** | 20 knots | 20 knots | 20 knots |
| **Number of Cells** | 170 | 170 | 170 |
| **Maximum Ping Rate** | 2/second | 2/second | 5/second |

**Fig. 2.4 Typical view of Acoustic Current Profiler procured**

**Fig. 2.5 Niskin water sampler**

# 3. DEKSTOP DATA COLLECTION

The PI, Dr. Balaji, visited Kandla port on 07 Dec 2015, as per the suggestions of the Ministry of Shipping. During that meeting, the port officials shared the information regarding the measured field data and past reports, as listed below. In this proposed study, the major parameters that have a direct impact on the siltation process are found to be tides, waves, oceans currents, and suspended sediment concentration (turbidity). The details of various stages of data collection as part of the desktop study carried out by IIT Bombay are given in the following sections.

## 3.1 Offshore Bathymetry

The Deendayal port officials had supplied with the required bathymetry data for the project site as shown in the previous section. Fig. 3.1 represents the depth contours of the Gulf of Kutch with the stippled areas representing the marshes (Satish., 1999).

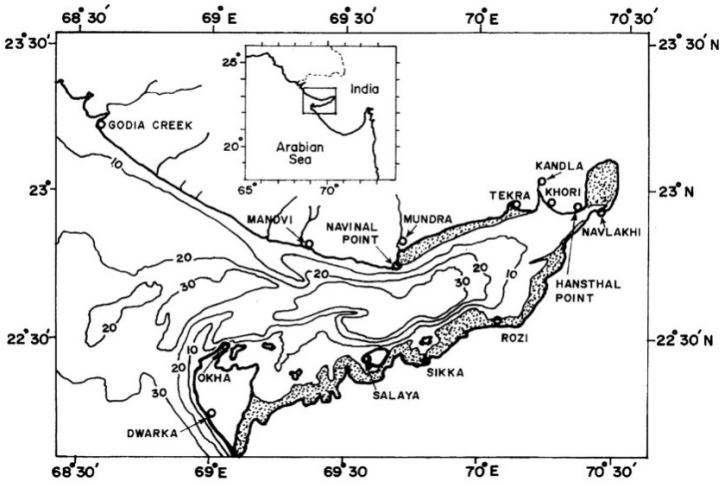


**Fig. 3.1 The Gulf of Kutch, Depth in meters (Satish., 1999)**

## 3.2 Tide & Currents

Tides, rise and fall of water levels on the open ocean due to the gravitational pull of sun and moon on the global ocean water mass, plays a major role in the design of maritime infrastructures, in terms of hydrodynamic. The variations in the tidal water levels dictate the top levels of creek. The various levels associated with tides; Mean, High and Low High Water Levels are also considered for numerical modeling of tidal hydrodynamics.

The currents, induced by the tidal elevations, are also important parameter in the coastal regions. To understand the siltation behavior and to reduce the maintenance dredging need to

be investigated in details to understand the impacts on climate of coastal regions. There was a possibility that the suggestions given to reduce the siltation behavior may deteriorate the natural flushing processes of the Kandla creek, which was also assessed from environmental perspective.

The water level data was obtained from DPT for the locations shown in Fig. 3.7 during the site visit in the proposed site. The maximum water level reaches up to 0.4 – 6.9 m for a period of one-month in Jan 2017 as shown in Fig. 3.2.The widths (in km) along the 10 sections in the Fig. 3.3 shows the distance measured from the mouth (the line joining Godia Creek to Dwarka) along a curve (the broken line in the inset) passing through the mid-points of each section. The continuous line joining the circles shows the linearly interpolated depth that were used in the numerical model. Then mean depth (in m) across the cross-sections; the horizontal line at 16.8 m shows the average of the mean depth of all the cross-sections (Satish., 1999).

The comparison between the observed and the predicted values for the four most significant constituents in the gulf are given in Fig. 3.4. The favorable comparisons from the figure suggests that the model described above, though simple, does capture the most important elements of the dynamics of the tides in the Gulf (Satish., 1999).The solid lines in Fig. 3.5 shows the variation of sea surface elevation at the interior stations as simulated with the barrage while the dashed lines represent the one without the barrage. At Mundra and Rozi, the water levels are slightly higher compared to the no-barrage condition. At Kandla, with the barrage, the level at low tide is found to be less than that without the barrage case (Sinha et al., 2000).

The depth-averaged hydrodynamic model of the Gulf of Kutch was able to simulate the tidal wave propagation realistically. The introduction of realistic bathymetry of the Gulf was very important to simulate the flow correctly. A typical diagram showing the variation of tidal currents approaching Kandla creek after the introduction of barrage is shown in Fig. 3.6. It also shows the tidal stream currents 1.5 hours before and 1.5 hours after the high water, respectively, at Okha location with the barrage (Sinha et al., 2000).

As per the current data obtained from the DPT for the proposed project locations, the maximum current speed during the average tide for 6$^{th}$ of Feb 2016 reaches about 0.8m/s and the direction varies from 50 deg - 180 deg (Buoy no. 10) as shown in Fig. 3.8.The maximum

current speed during the neap tide for 1st of Mar 2016 reaches about 1.2m/s with the direction varying from 20 deg - 220 deg (Buoy no. 4) as shown in Fig. 3.9.

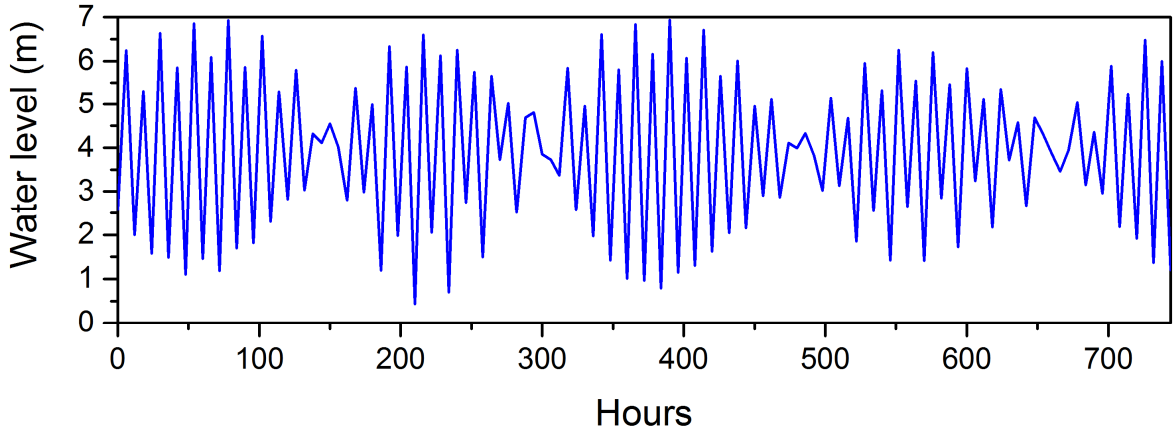


**Fig. 3.2 Typical one lunar tidal cycle in Kandla creek**

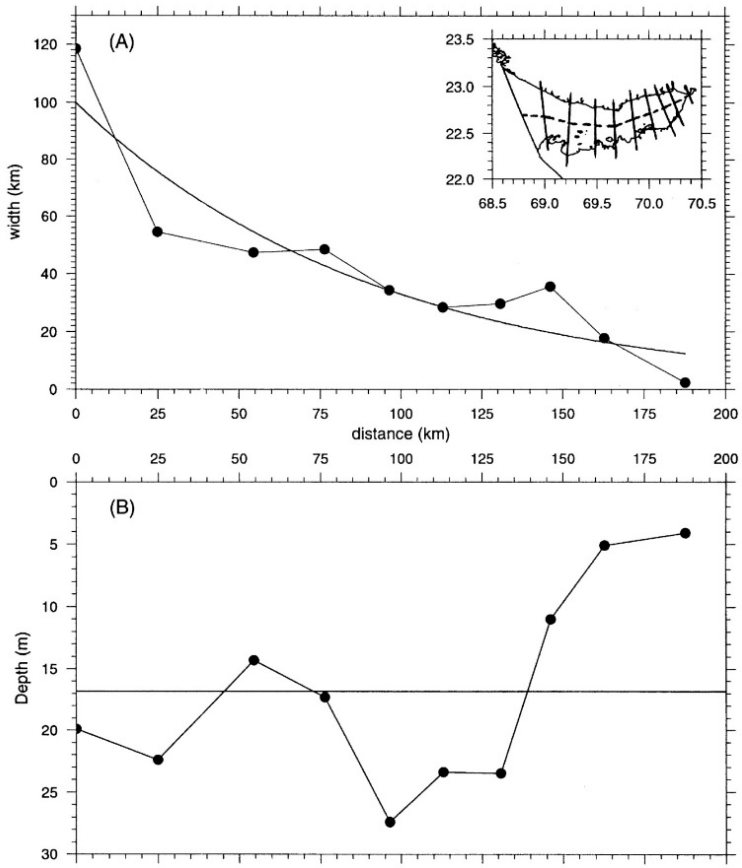


**Fig. 3.3 Gulf of Kutch as function of distance (km) (Satish., 1999)**

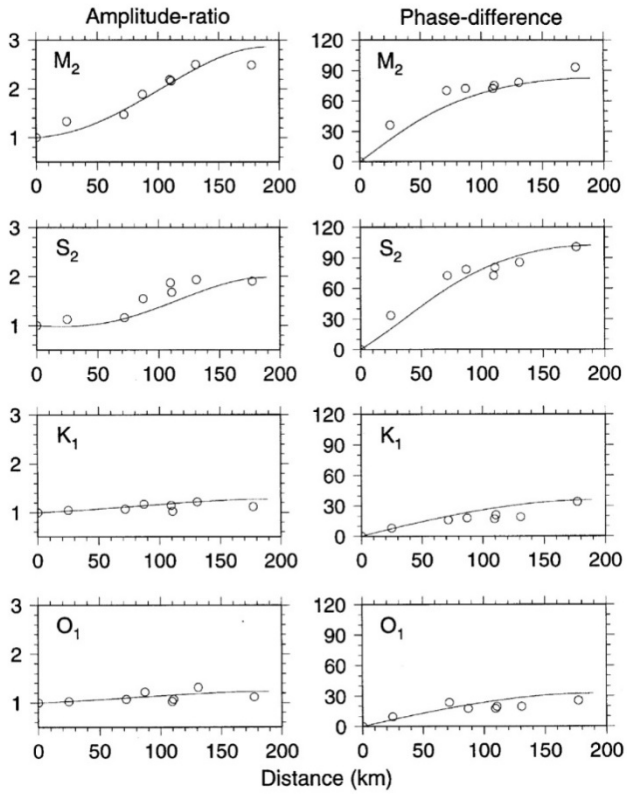


**Fig. 3.4 Comparison between observed and predictions (Satish., 1999)**

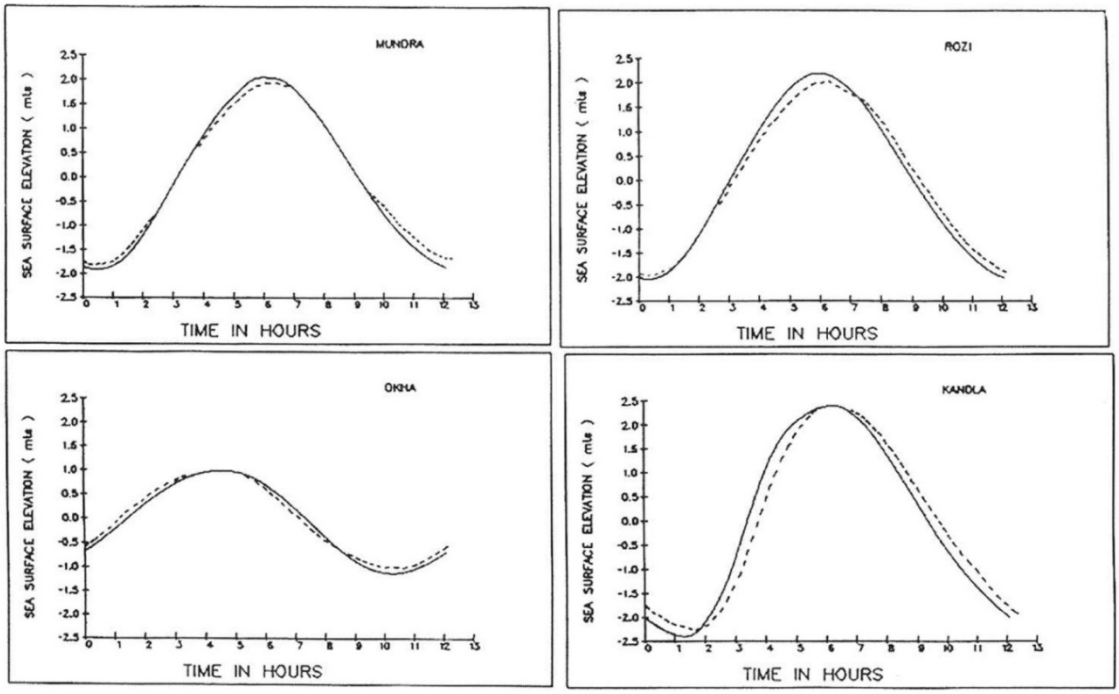


**Fig. 3.5 Variation of sea surface elevations (Sinha et al., 2000)**

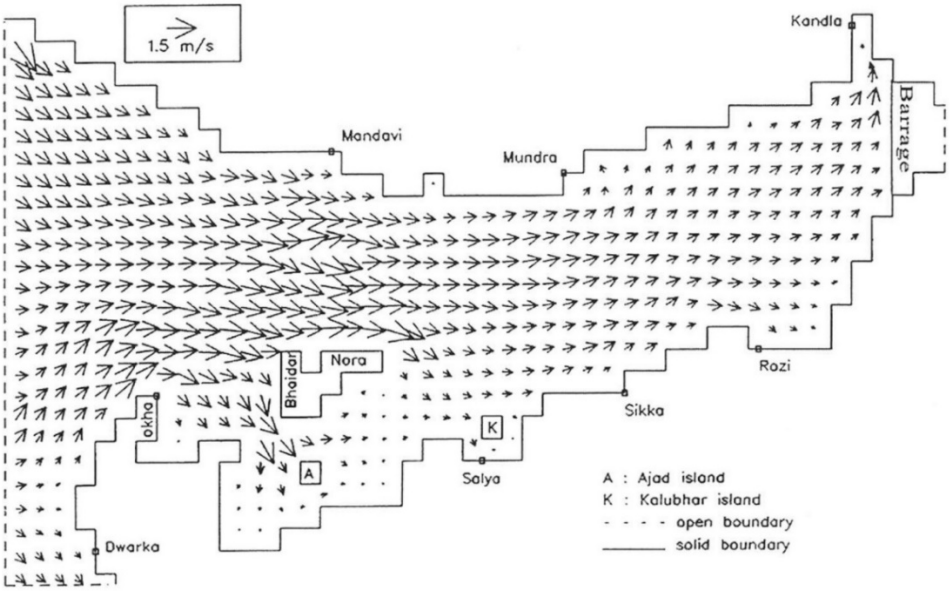


**Fig. 3.6 Tidal stream current (with barrage) (Sinha et al., 2000)**


**Fig. 3.7 Geographical view of absorbed data location**

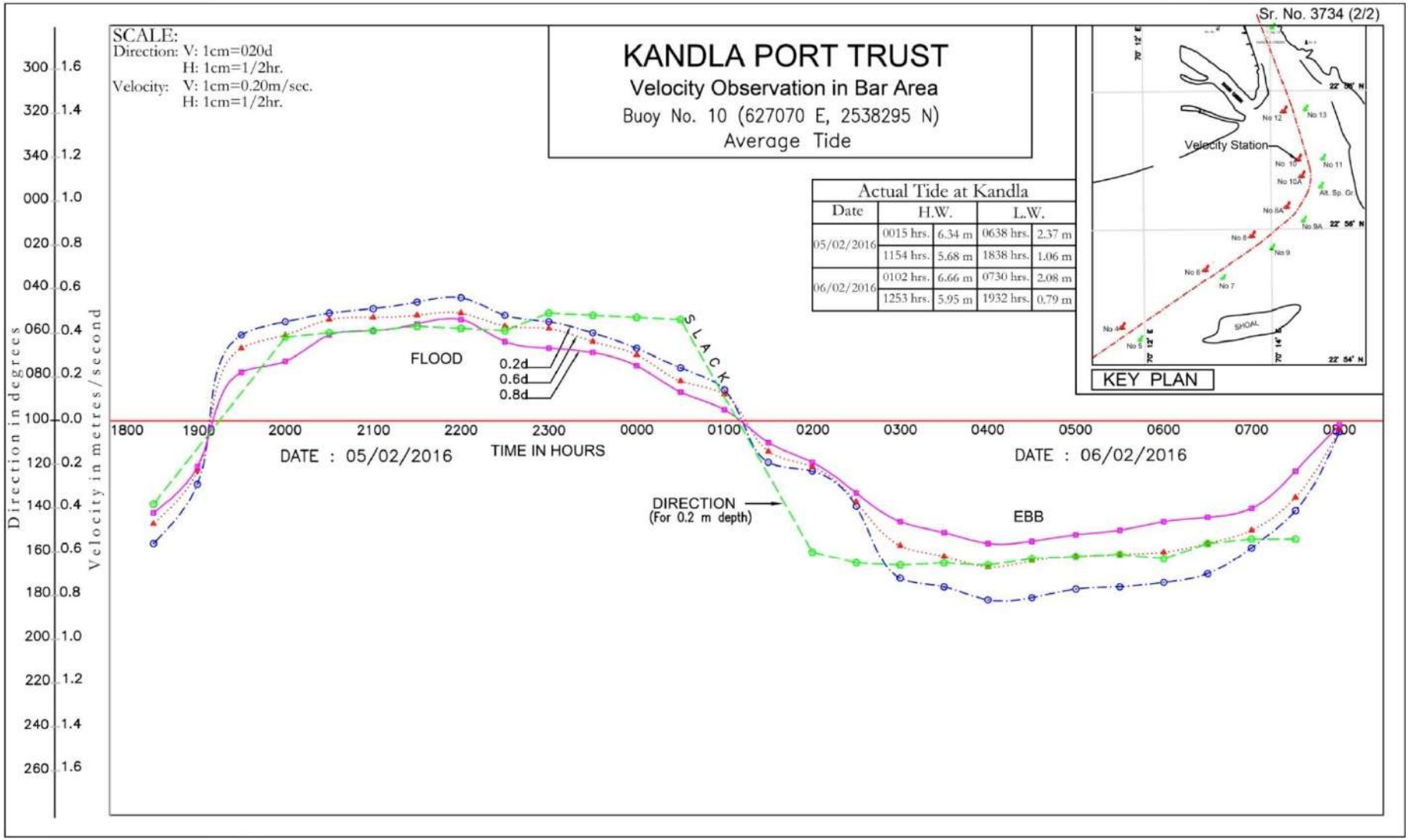


**Fig. 3.8 Typical variation of current speed and directions**

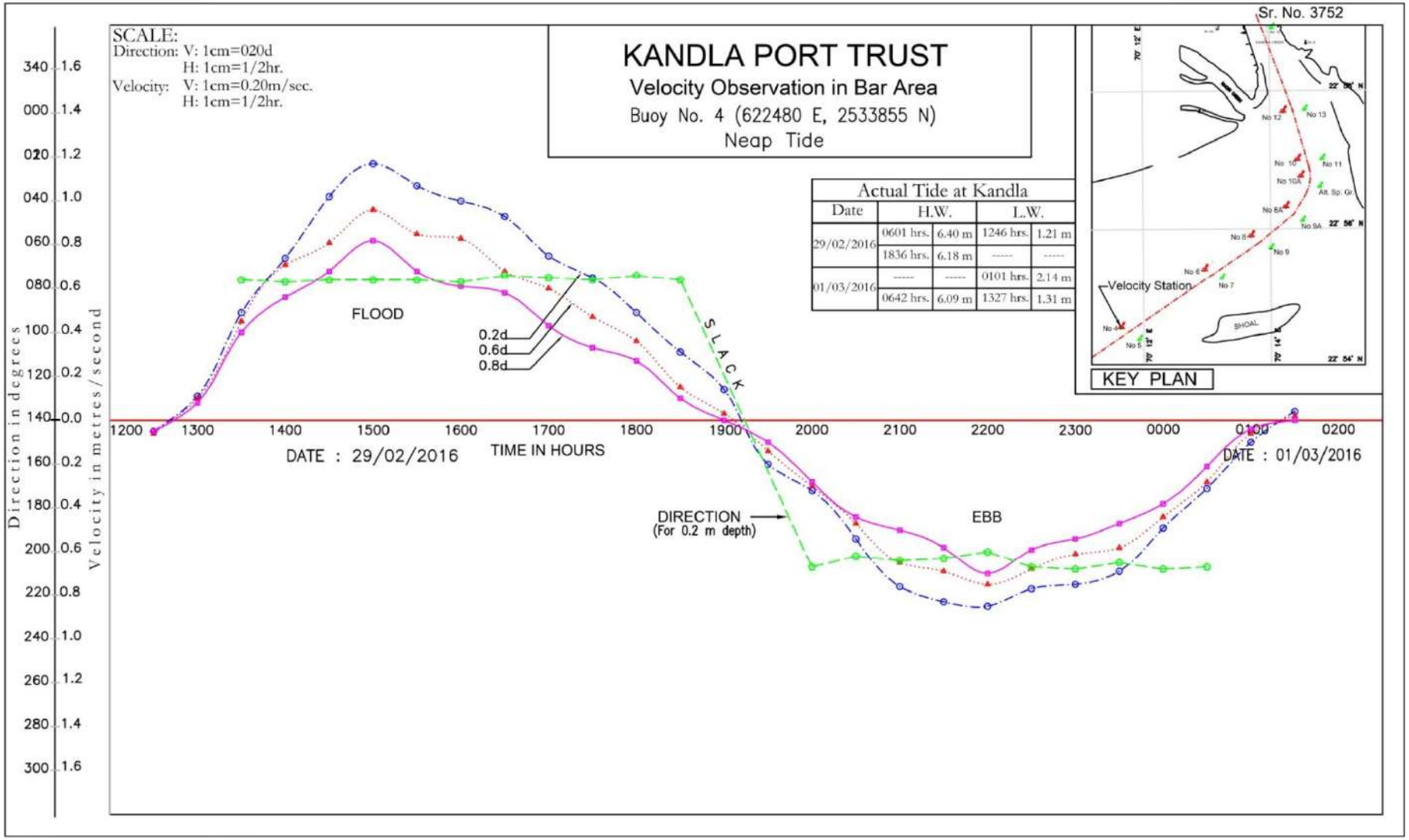


**Fig. 3.9 Typical variation of current speed and direction during neap tide**

## 3.3 Sediment Transport

Sediment transport is one of the most dynamic and complex hydrodynamic processes occurring in coastal regions such as bays, estuaries, and tidal inlets. It pertains to the movement of cohesive or non-cohesive material due to the combination of gravity acting on the particle and the movement of the fluid in which the particle is entrained. Sediments are generally brought in suspension by wave action, and are further transported by coastal currents. Sediment particles varies according to their grain size, shape, density, settling velocity, angle of repose, and volume concentration. Grain size is the most important factor that affects the mobility of the particle in a fluid. Sediments are usually transported along the bottom by the process of rolling, sliding, and saltation. According to Wentworth (1922), particles having grain diameter less than ±60 μm are classified as mud (Table 3.1).

The topography is very irregular at the mouth and the central part of the Gulf and consists of pinnacles and a scarp ranging in height from 6 to 32m is shown in Fig. 3.10Fig. 3.10 Inferred sediment transport direction (Nair et al. 1982) (Nair et al., 1982). A large area of the floor at the mouth of the Gulf, at depths greater than 20 m, is covered with algal limestone, aragonite cemented sandstones and dead corals (Fig. 3.11). On the low-energy margin of the Gulf, especially on the southern side, wide tidal flats with patches of coral in the intertidal zone are present. The remainder of the Gulf is floored by silt and clay with patches of fine sand (Hashimi et al. 1978).

Two FCCs were generated from principal components (PCs) 2, 3 and 4 (RGB) and 1, 2 and 3 (RGB) (Fig. 3.12). These enhanced images were enlarged to locate and decipher various coastal geomorphic units and underwater bed flow structures. Particular attention was paid towards mapping of sediment plumes to understand the distribution and dispersion of suspended and settled sediments. Geomorphic units, distribution and directions of suspended sediments, and current directions are marked on the OCM PC image (Fig. 3.12). Dark blue colors indicate water at offshore, the mouth of the Gulf and the central portion that might be probably the deepest region (depth >20 to <60 m) (Fig. 3.13). Deep submerged shoals ‘Sb’ (light pink color) are the deeper portion (depth between 5 and 20 m), whereas, shallow submerged shoals ‘Ss’ in pink color represents parts (between 0 and 5m) of the Gulf. Suspended sediments in buff color represents variable depths. The Gulf entrance channel with a depth of water varying between 30 and 50m was also visible on the image. The northern and south-western coasts are bordered by sands (blue colour) along coast, mud

(reddish) in intertidal zones and shoals (pink colour) in the deeper part of the Gulf. The depth variation represented by different colours matches fairly with bathymetric contours of the Gulf (Pravin et al., 2003).

**Table 3.1 Grain size classification according to Wentworth (1922)**

| Millimeters | µm | Phi (ϕ) | Wentworth size class | |
|---|---|---|---|---|
| | | -20 | | |
| 4096 | | -12 | Boulder (-8 to -12ϕ) | |
| 1024 | | -10 | | |
| 256 | | -8 | Pebble (-6 to -8ϕ) | |
| 64 | | -6 | | |
| 16 | | -4 | Pebble (-2 to -6ϕ) | Gravel |
| 4 | | -2 | | |
| 3.36 | | -1.75 | | |
| 2.83 | | -1.50 | Gravel | |
| 2.38 | | -1.25 | | |
| 2.00 | | -1.00 | | |
| 1.68 | | -0.75 | | |
| 1.41 | | -0.50 | Very coarse sand | |
| 1.19 | | -0.25 | | |
| 1.00 | | -0.00 | | |
| 0.84 | | 0.25 | | |
| 0.71 | | 0.50 | Coarse sand | |
| 0.59 | | 0.75 | | |
| 1/2 – 0.50 | 500 | 1.00 | | |
| 0.42 | 420 | 1.25 | | |
| 0.35 | 350 | 1.50 | Medium sand | Sand |
| 0.30 | 300 | 1.75 | | |
| 1/4 – 0.25 | 250 | 2.00 | | |
| 0.210 | 210 | 2.25 | | |
| 0.177 | 177 | 2.50 | Fine sand | |
| 0.149 | 149 | 2.75 | | |
| 1/8 – 0.125 | 125 | 3.00 | | |
| 0.105 | 105 | 3.25 | | |
| 0.088 | 88 | 3.50 | Very fine sand | |
| 0.074 | 74 | 3.75 | | |
| 1/16 – 0.0625 | 63 | 4.00 | | |
| 0.0530 | 53 | 4.25 | | |
| 0.0440 | 44 | 4.50 | Coarse silt | |
| 0.0370 | 37 | 4.75 | | |
| 1/32 – 0.0310 | 31 | 5 | | |
| 1/64 0.0156 | 15.6 | 6 | Medium silt | |
| 1/128 0.0078 | 7.8 | 7 | Fine silt | |
| 1/256 – 0.0039 | 3.9 | 8 | Very fine silt | Mud |
| 0.0020 | 2.0 | 9 | | |
| 0.00098 | 0.98 | 10 | | |
| 0.00049 | 0.49 | 11 | Clay | |
| 0.00024 | 0.24 | 12 | | |
| 0.00012 | 0.12 | 13 | | |
| 0.00006 | 0.06 | 14 | | |

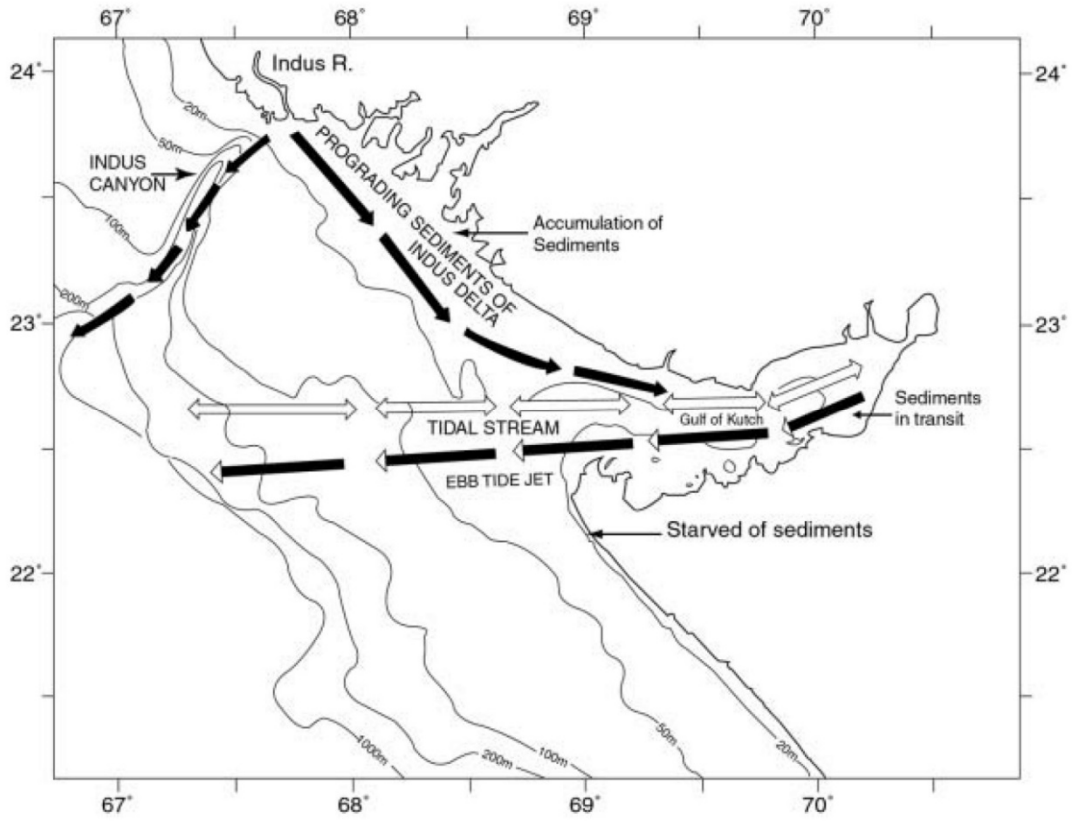


**Fig. 3.10 Inferred sediment transport direction (Nair et al. 1982)**

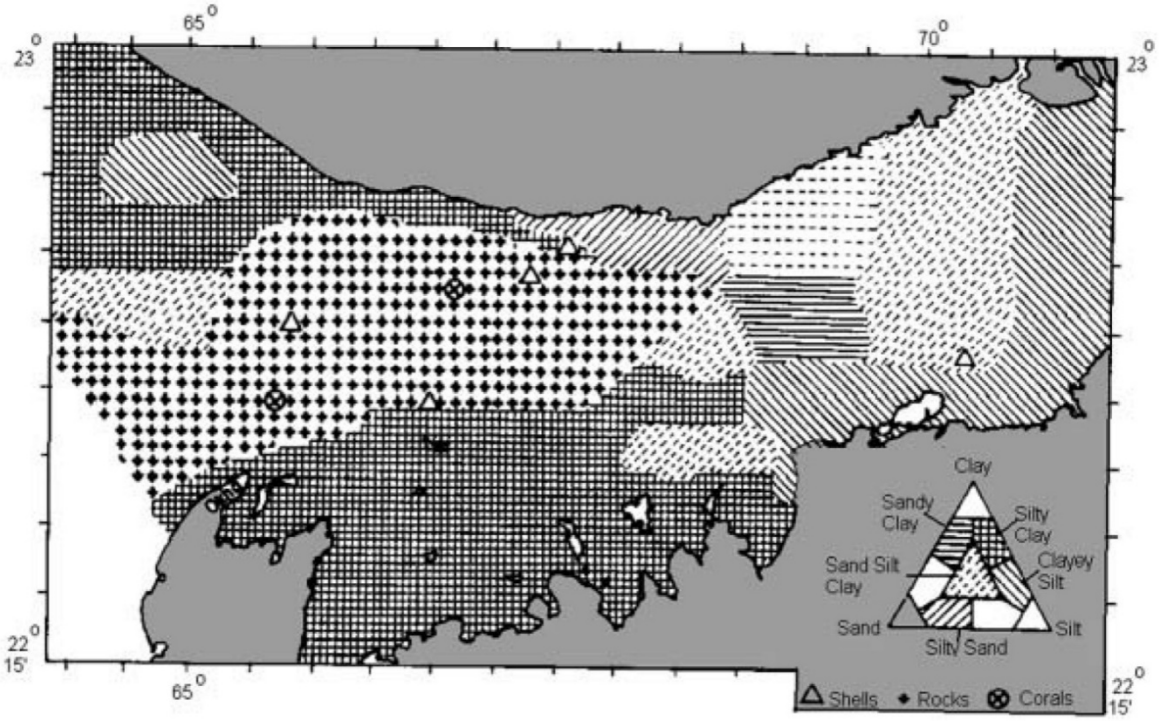


**Fig. 3.11 Generalized surface sediment distribution (Hashami et al., 1979)**

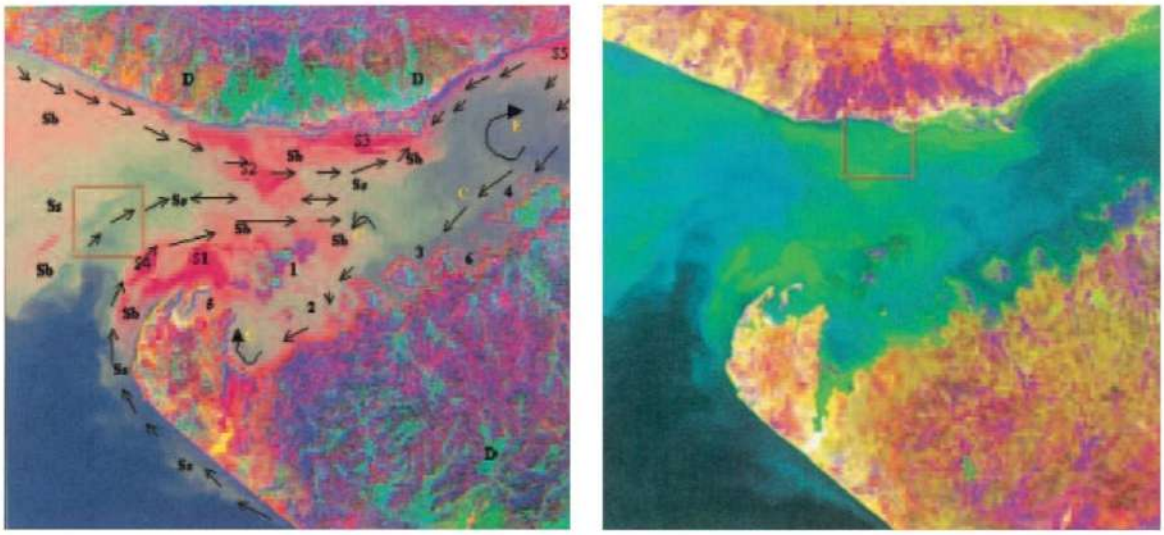

(*a*) (*b*)

**Fig. 3.12 (a) FCC-2 and (b) FCC-3. Principal components of OCM with RGB colours (Pravin et al., 2003)**

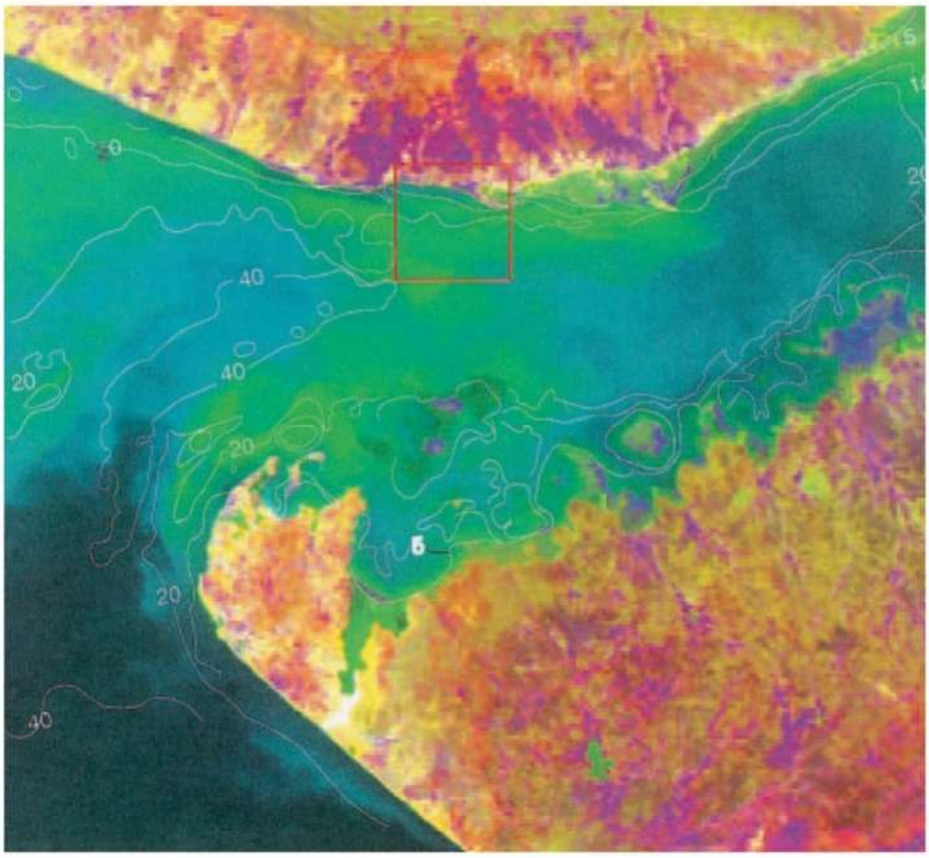


**Fig. 3.13 OCM with RGB colours are superimposed with bathymetry contours (Pravin et al., 2003)**

## 3.4 Suspended sediment concentration

Suspended sediment is generally transported within and at the same velocity as the surrounding fluid (water or wind). The stronger the flow and finer the sediment, the greater the amount of sediment that can be suspended by turbulence.

Only the finer fraction (usually silt and clay fraction) of the suspended sediment can be continuously maintained in suspension by the flow turbulence. This fraction is often referred to as “wash load,” and is typically not found in significant quantities at the bed surface. Its concentration is usually related to the sediment supply and is difficult to determine theoretically.

Most sediment particles are not continuously suspended, but are continuously settling through the surrounding fluid and may eventually return to the bed. This part of the total suspended sediment is referred to as “bed-material load,” and its concentration can be estimated from the hydraulic parameters of the fluid and the composition of the bed material (Veerle., 2014).

Fig. 3.14 shows the OCM derived SSC images of March, April, November, and December vis-à-vis MIKE 21-simulated maps (using HD and MT modules). The analysis of suspended sediment dispersal patterns using OCM and model simulation along with the bathymetry data shows that the entire northern region exhibits higher SSC as compared to southern region during all months of March, April, November, and December. Bathymetry is found to be shallower near to southern and northern part and becomes deep at a distance of 15 km from southern part and shallower at central part at ~18 m depth. In the central part, the suspended sediments come in suspension because of high tidal currents. Tidal currents vary from 1.2-2.3 m/s at the mouth to 3.0-5.0 m/s in the central portion of the GK (Fig. 3.15) (Mukesh., 2015).

The low SSC, as recorded from the time series, on 14 March at Okha is consistent with the OCM image and tide data (Fig. 3.16). For the period of six hours in a day, the SSC pattern at Navlakhi is more uniform than the SSC patterns observed at Okha. This may be because of the reason that Navlakhi lies in the interior of the GK, and the tidal current velocity is comparatively low at that region (Mukesh., 2015). The role of tidal currents in sediment dispersal in the GK is dominant as discernible from the simulated images. Fig. 3.17 shows rose plots of the direction and magnitude of MIKE 21- simulated tidal currents in the GK. The magnitude of tidal currents progressively increases from 0.2-1.2 m/s for March at Okha port.

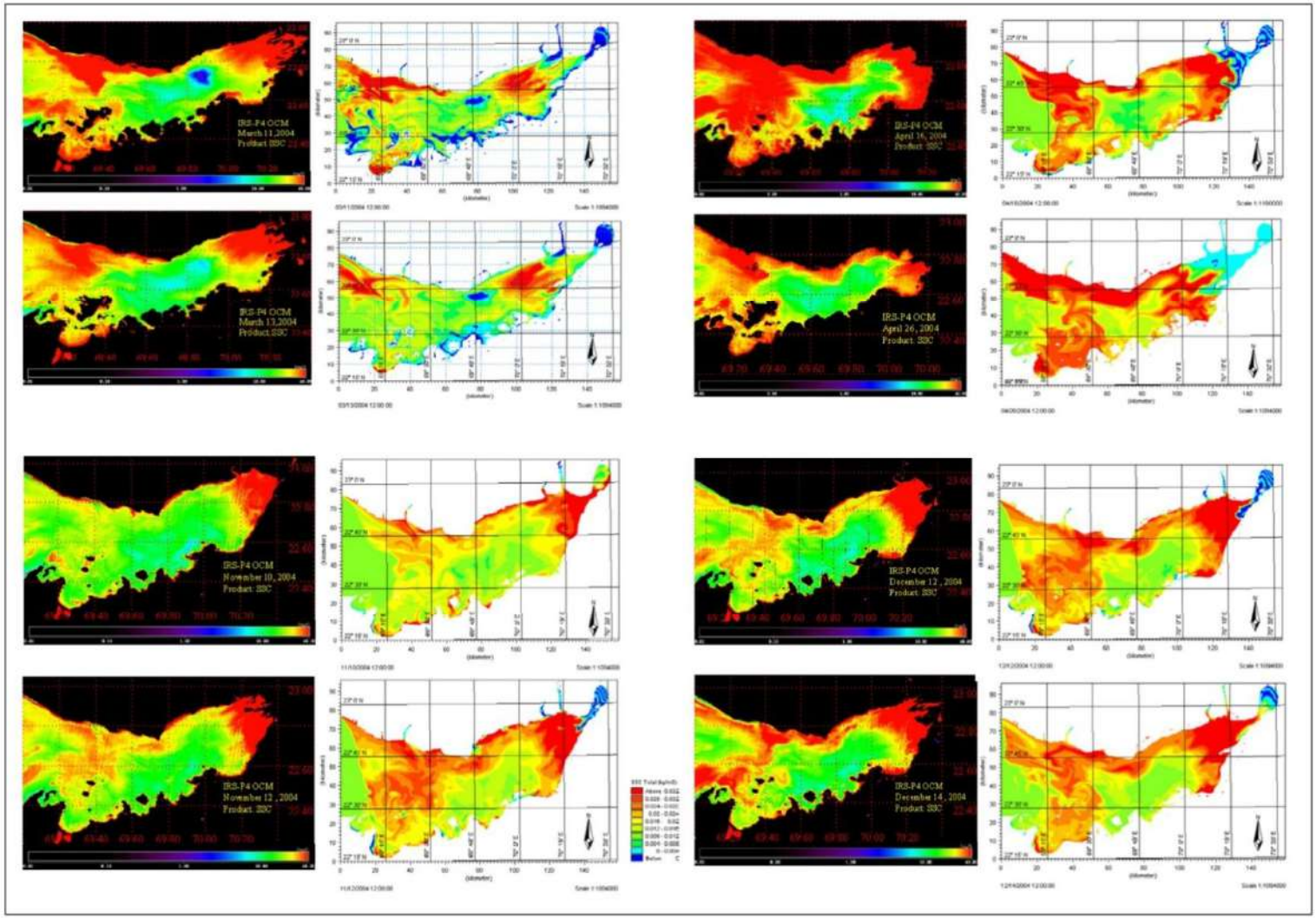


**Fig. 3.14 OCM-derived (left panel) and MIKE 21-simulated (right) (Mukesh., 2015)**

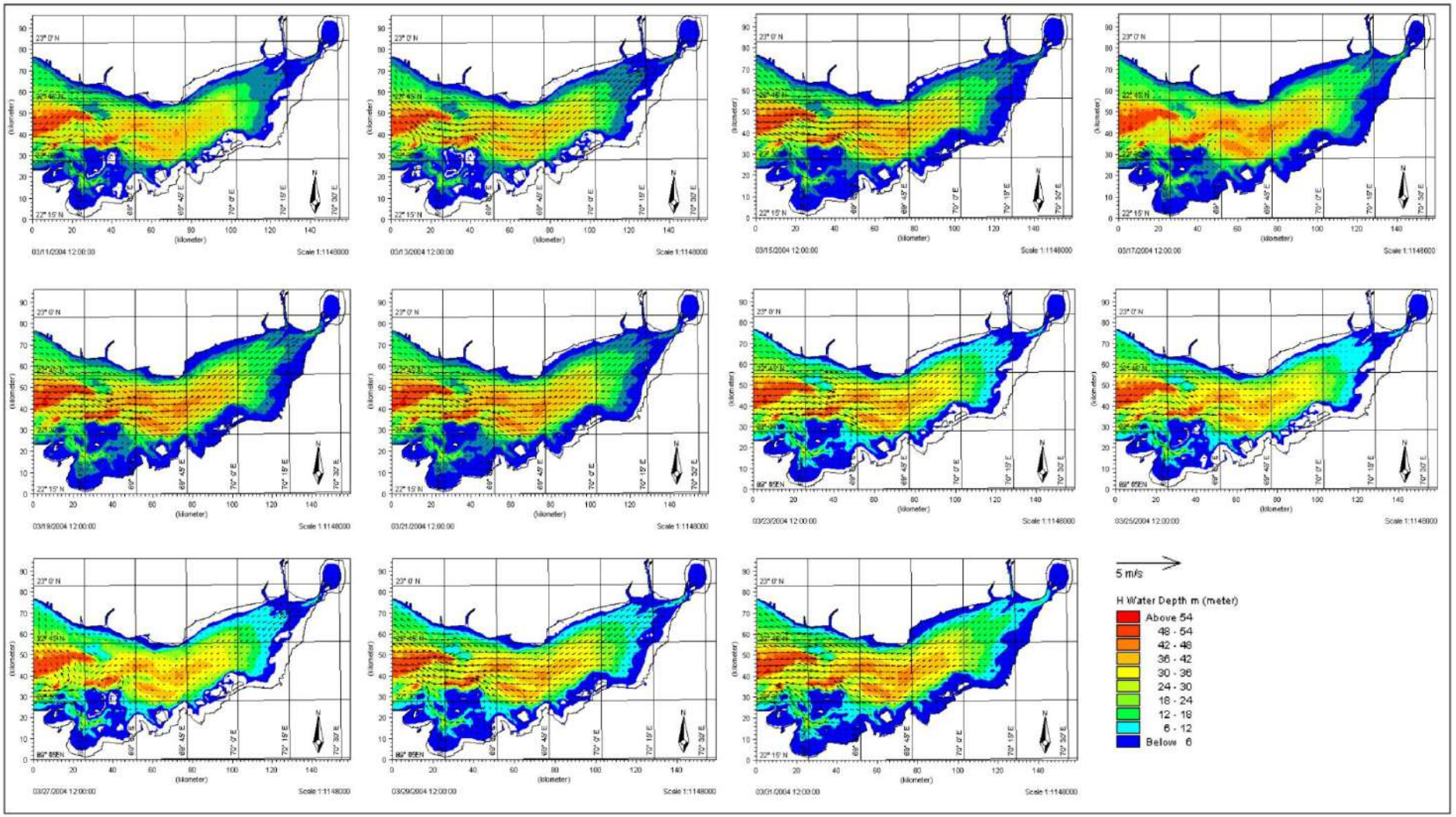


**Fig. 3.15 MIKE 21-simulated current vectors overlaid on the water depth (Mukesh., 2015)**

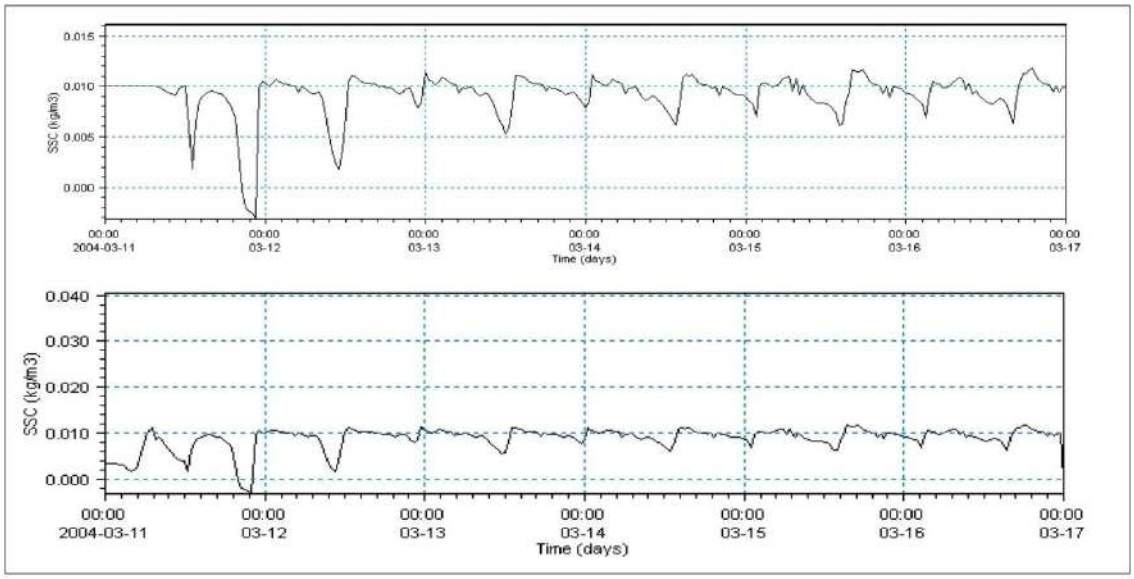


**Fig. 3.16 The SSC time series at Okha (top) and Navlakhi (bottom) (Mukesh., 2015)**

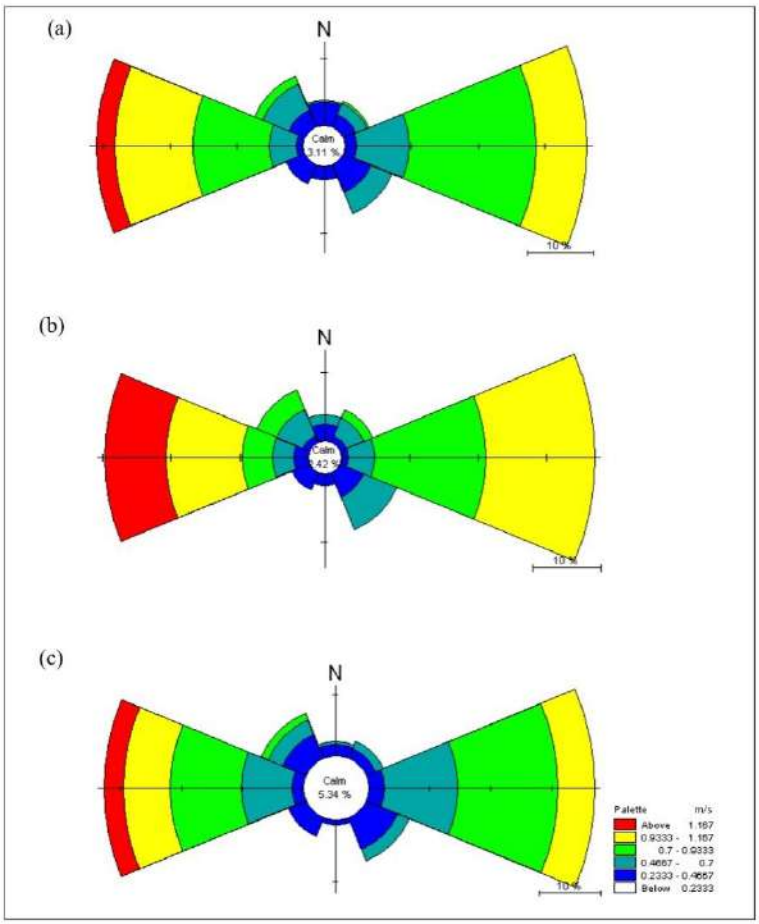


**Fig. 3.17 Typical direction and magnitude of tidal currents (Mukesh., 2015)**

## 3.5 Siltation

Siltation is a common phenomenon in artificially dredged channels due to the reduction in flow velocities and related turbulent motions in these regions, causing the sediments to settle down at the bottom and reducing the depth available for safe navigation of ships. Due to this proper navigation is possible by carrying out maintenance dredging at specific intervals, which involves removal of sediments deposited at the bottom of the channels using dredgers, which incur huge costs annually. This raises the need for an optimum siltation reduction measure, which may help in reducing the amount of money spent for dredging. Before addressing the issues related to siltation, it is essential to have a detailed knowledge about the mechanisms causing siltation. The studies along the Kandla creek reveal that the existing rate of siltation is high along the navigation channel. The typical spatial variation of siltation quantity in Sogal Channel according to the zone wise is shown in Fig. 3.18. Table 3.2 shows the monthly Siltation/Erosion in Sogal Channel for Zone I and Zone II from April 2003 – March 2004 (CWPRS, 2005). From the above information, it can be inferred that the rate of siltation is consistently high in this area. This will lead to the variation in their bathymetry due to siltation which eventually controls the development of the creek. The Creek waters have a salinity ranging from 23 to 25 ppt. The waters of the Creek are heavily silt charged, the range being 1 to 3 ppt.

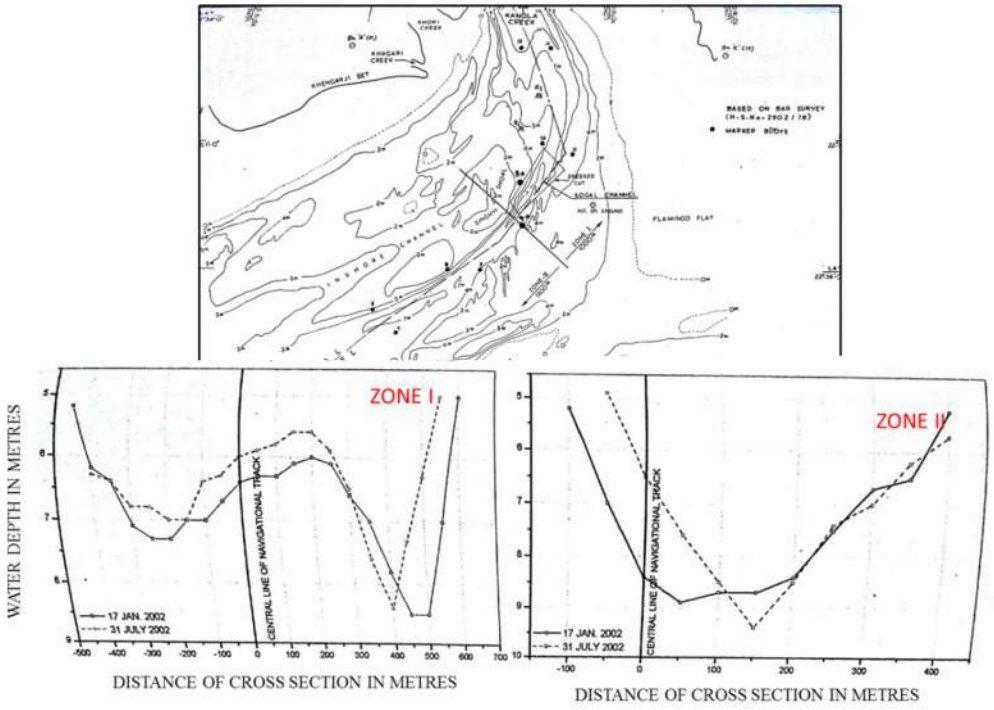


**Fig. 3.18 Typical spatial variation of siltation quantity in Sogal Channel**

**Table 3.2 Monthly siltation/erosion in Sogal Channel from April 2003 – March 2004 (CWPRS, 2005)**

| Period | Zone - I | | Zone - II | |
|---|---|---|---|---|
| | Qty in Cum | | Qty in Cum | |
| | Siltation | Erosion | Siltation | Erosion |
| **Apr 03 –May 03** | **1,93,375** | 1,30,000 | 94,625 | 90,000 |
| **Net Qty** | **+63,375** | | +4625 | |
| **May 03 – Jun 03** | 2,20,000 | 3,05,000 | 2,23,750 | 1,08,750 |
| **Net Qty** | -85,000 | | +1,15,000 | |
| **Jun 03 – Jul 03** | 2,50,000 | 85,625 | 2,30,000 | 28,750 |
| **Net Qty** | +1,64,375 | | +2,01,250 | |
| **Jul 03 – Aug 03** | 2,02,500 | 2,52,500 | 53,250 | 3,91,250 |
| **Net Qty** | -50,000 | | -3,38,000 | |
| **Aug 03 – Sep 03** | 1,15,375 | 3,88,750 | 2,21,250 | 5,35,000 |
| **Net Qty** | -2,73,375 | | -3,13,750 | |
| **Oct 03 – Nov 03** | 1,52,188 | 1,23,750 | 1,29,063 | 1,10,000 |
| **Net Qty** | 28,438 | | 19,063 | |
| **Nov 03 – Dec 03** | 94,500 | 1,62,500 | 91,250 | 94,375 |
| **Net Qty** | -68,000 | | -3125 | |
| **Dec 03 – Jan 04** | 1,88,125 | 1,18,125 | 80,000 | 1,96,875 |
| **Net Qty** | 70,000 | | -1,16,875 | |
| **Jan 04 – Feb 04** | 1,68,125 | 1,82,500 | 1,00,000 | 1,07,500 |
| **Net Qty** | -14,375 | | -7500 | |
| **Feb 04 – Mar 04** | 1,85,000 | 2,37,500 | 2,00,000 | 65,000 |
| **Net Qty** | -52,500 | | 1,35,000 | |

## 3.6 Sea Level Rise

Sea level rise is of great concern, since it will raise the mean sea level. Gujarat has the longest coastline amongst Indian states of about 1,600 km. The coast itself is characterized by creeks and inland waters, classified as submergence type, which is more prone to the effects of sea level rise. Maximum damage is predicted at a rise of 1m. Around 6 % of Gujarat's coastal population likely to be impacted at 1m sea level rise. Trend of sea level rise for Kandla port is 3.37mm per year causing a damage to ground water resources by salt intrusion due to this sea level rise. Sea level changes can be of two types: (i) changes in the mean sea level and (ii) changes in the extreme sea level. Mean sea level changes were estimated by analyzing past tide gauge data at different ports along the Indian coasts (Unnikrishnan et al., 2006).

The LULC assessment was carried out for some of sites of Gulf of Kachchh in the year 1989, 2002 and 2016 from Landsat TM, ETM and OLI satellite image respectively. The

classification maps produced by visual classification techniques are illustrated in Fig. 3.19. Information derived from the analysis of satellite data pertaining to land use and land cover revealed that the major class covered by water body ranged from 76.33 % to 84.38 %. It showed around 8.05 % water level increased from 1989 to 2016. (Disha and Madhusudan., 2017).

The work has demonstrated the capability of remote sensing and GIS techniques for assessing vulnerability of the Gujarat coast due to predicted sea level rise on 1:50,000 scale. Coastal Vulnerability Index (CVI) has been computed for entire Gujarat coast based on integration of five physical variables viz., coastal geomorphology, coastal slope, rate of shoreline change, mean spring tide range and significant wave height in GIS environment. The results show that 785 km (45.67 %) of the Gujarat coast is under high to very high risk category and 934 km (54.33 %) of the Gujarat coast is under moderate to low risk category to the threat of predicted sea level rise. The CVI values obtained ranged from 31 to 74. The entire range of CVI values is divided into four equal parts, each indicating certain risk level of the coastline to sea-level rise (Manik., 2015).

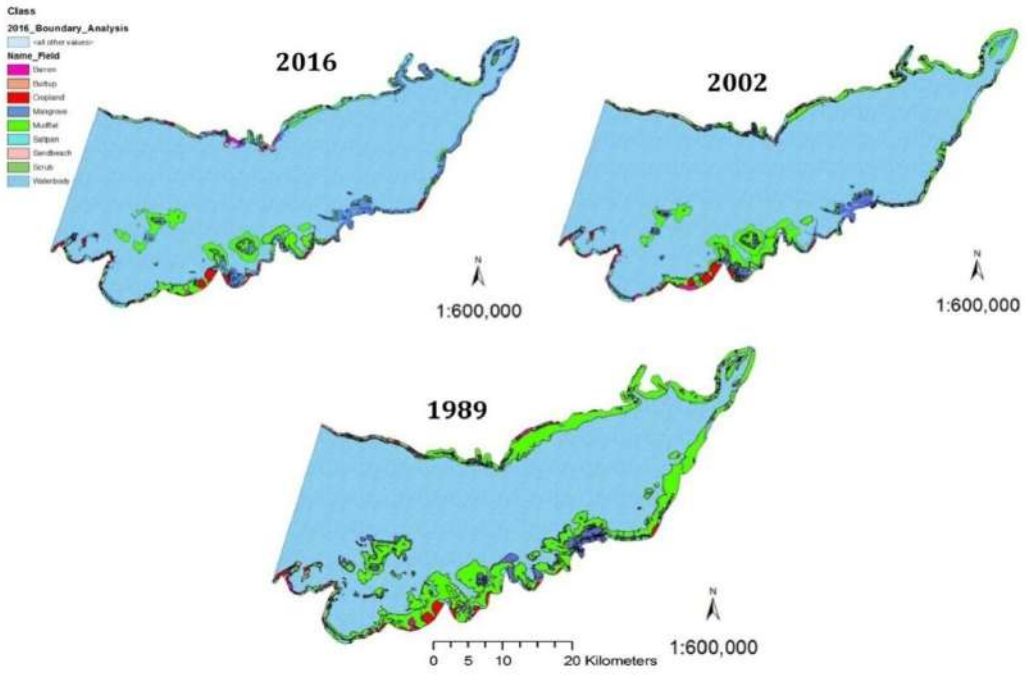


**Fig. 3.19 LULC 1989, 2002, and 2016 (Disha & Madhusudan., 2017)**

## 3.7 Offshore Waves

The wind generated waves that are propagating from offshore to nearshore are of great concerns for sediment transport. The factors influencing the wave characteristics are; wind speed - the wind velocity must sufficient enough for energy transfer to ocean surface; fetch - the uninterrupted distance of open water over which the wind blows without significant change in direction; width of area affected by fetch; wind duration - the time over which the wind has blown over a given area and water depth available in the area of wind blowing. All of these factors work together to determine the size of wind waves and the structures of the flows within. The primary wave parameters that are of interest to engineers are; significant wave heights, peak wave period, mean wave direction. In addition, the percentage of occurrence of the wave characteristics is also important for design of marine infrastructures.

When the wind generated waves propagate from deep ocean towards coastline, they undergo various transformation processes, such as; wave shoaling, refraction, diffraction, reflection and finally breaking near the shore. During these transformation processes, the wave characteristics are also changing, which are important to be understood for coastal developments.

The wind generated waves off Gujarat coast, extracted at location as shown in Fig. 3.23 for the period of one year (2016) from ECMWF (European Centre for Medium-Range Weather Forecast) are statistically analyzed to get the sea-states of normal conditions. For every day with an interval of 6hours, data are collected and analyzed, as shown in Fig. 3.20near to the mouth of Gulf of Kutch. For the proposed location near to Kandla creek, it is evident from the Fig. 3.22 that the significant wave heights are ranging from 0.3 and 3.1, with an average of about more than 1m. Some high waves were also hind casted, in the range of 3.1m, for the year 2016, during July month. The wave periods are in the range of 7sec, with many wave exceeded 8sec during the entire year. The mean wave directions appear to be approaching from west to east, in the directional sector of about 210 to 260deg, which is also confirmed by the wave rose diagrams given in Fig. 3.21.Details of past studies, based on the ship observed data, have shown that joint distribution of higher (4.5m) and the longer waves of 8sec is observed along the Gujarat coastline (Chandramohan et al., 1991), as given in Fig. 3.24.

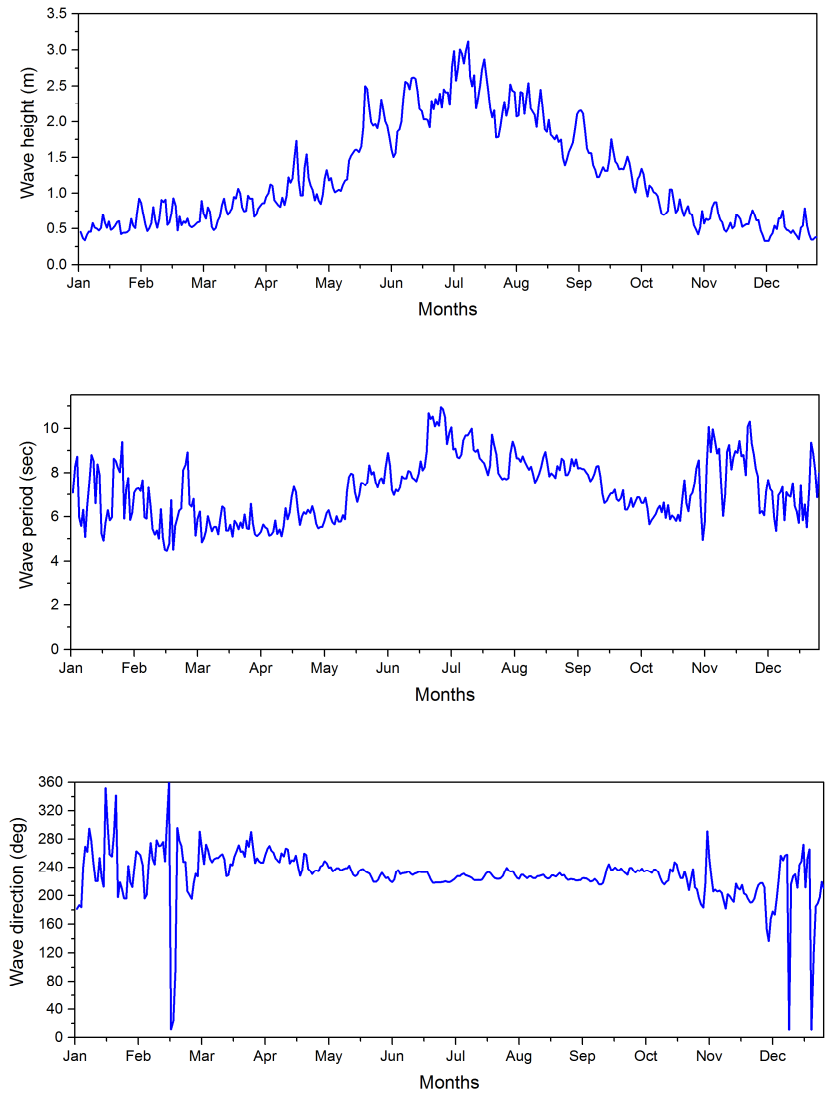


**Fig. 3.20 Typical variations of wave parameters off Gujarat coastline**

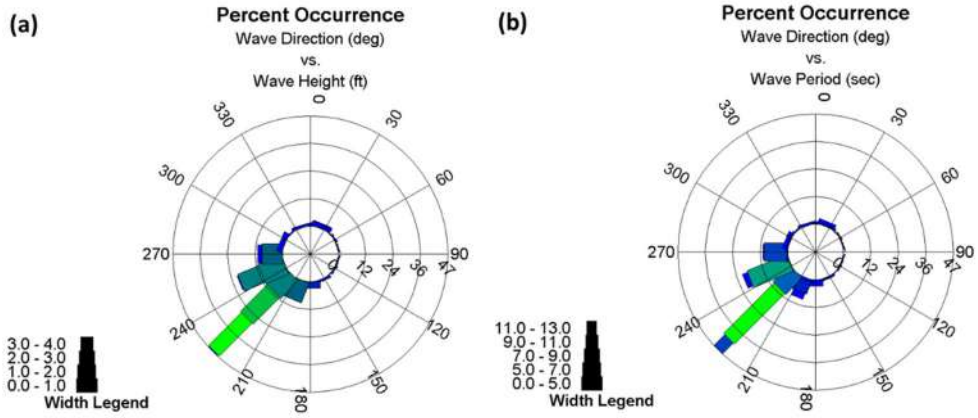


**Fig. 3.21 Typical wave rose diagram at Gujarat for 2016**

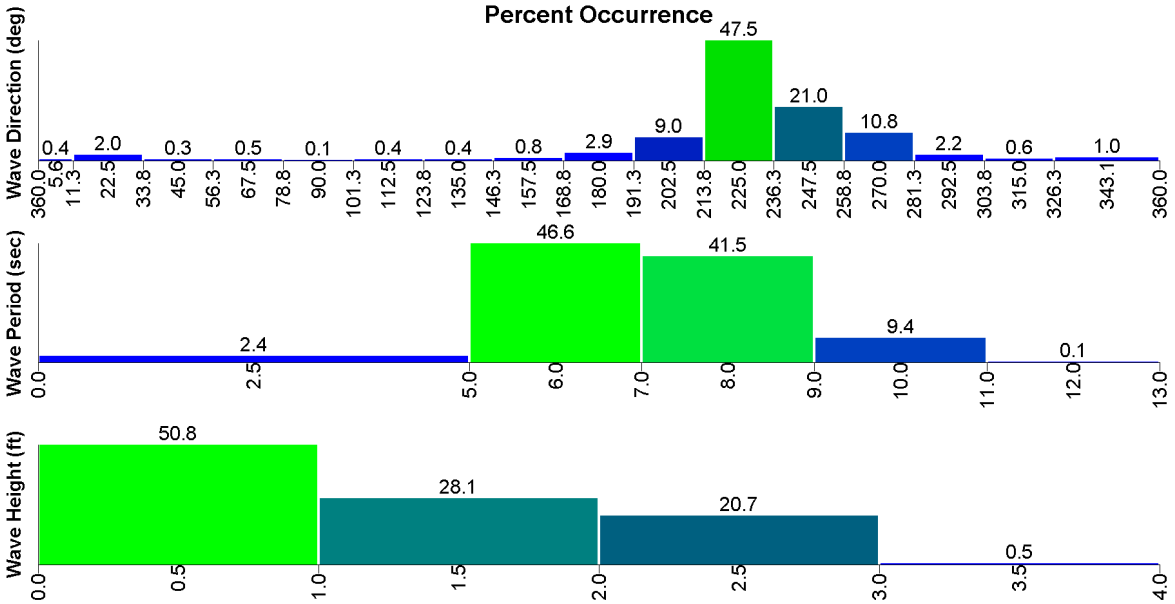


**Fig. 3.22 Typical wave histogram for the year 2016**

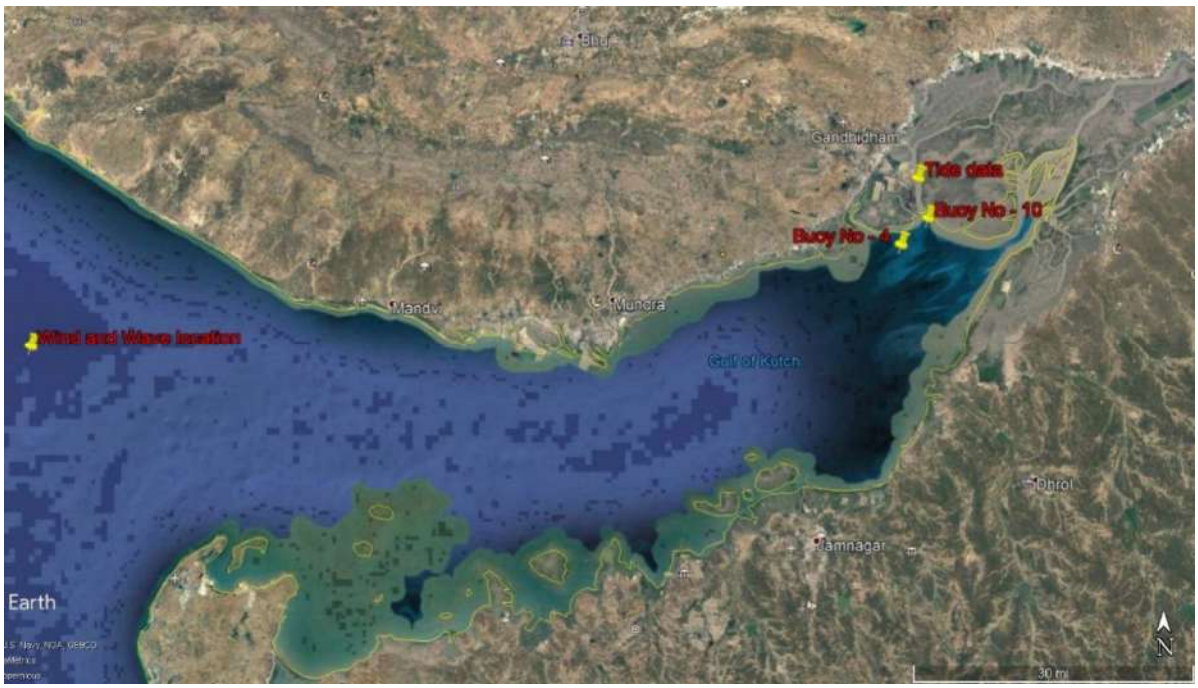


**Fig. 3.23 Geographical view of absorbed wave and wind data location**

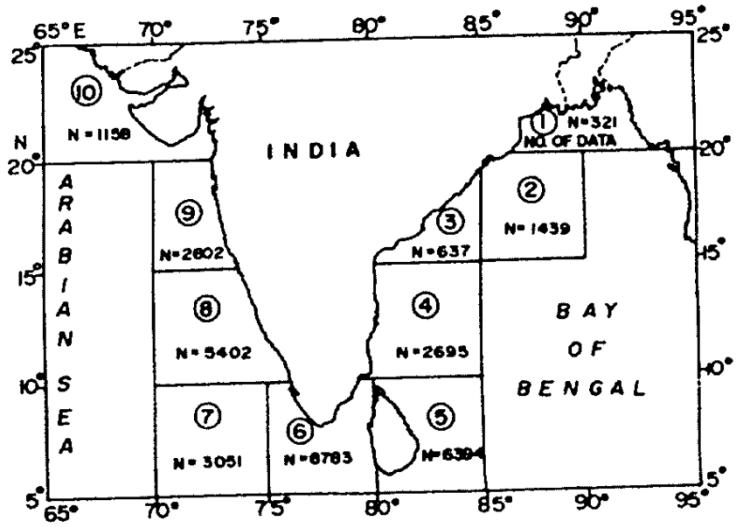


**(a) Grid considered along the Indian coastline**

Table 11 Joint distribution of wave height and period at grid 10 for years 1968-1986

| Wave height (m) | Wave period (sec) 5 | 6 | 7 | 8 | 9 | 10 | 11 | 12 | 13 | 14 |
|---|---|---|---|---|---|---|---|---|---|---|
| Fair-weather (Feb.-May) calm (%) = 9 | | | | | | | | | | |
| 0.5 | 14 | 2 | 1 | 1 | . | 1 | . | 1 | 1 | 2 |
| 1.0 | 15 | 5 | 3 | 1 | . | 1 | . | 1 | 1 | 1 |
| 1.5 | 9 | 4 | 2 | 1 | . | . | . | . | 1 | 1 |
| 2.0 | 5 | 1 | 1 | 1 | 1 | . | . | . | . | 1 |
| 2.5 | 3 | 1 | 1 | 1 | . | . | . | . | . | . |
| 3.0 | 1 | 1 | . | . | . | . | . | . | . | . |
| 3.5 | 1 | . | . | . | . | . | . | . | 1 | . |
| 4.0 | 1 | . | . | . | . | . | . | . | . | . |
| 4.5 | 1 | . | . | . | . | . | . | . | . | . |
| Southwest monsoon (June-Sept.) calm (%) = 1 | | | | | | | | | | |
| 0.5 | 1 | 2 | 1 | . | . | . | . | . | . | . |
| 1.0 | 3 | 3 | 2 | . | . | . | . | 1 | 1 | 1 |
| 1.5 | 6 | 3 | 3 | 2 | . | . | 1 | 1 | . | 2 |
| 2.0 | 2 | 5 | 3 | 3 | 2 | 1 | 1 | . | . | 1 |
| 2.5 | 3 | 5 | 1 | 2 | 2 | 1 | . | . | . | . |
| 3.0 | 3 | 3 | 3 | 4 | 1 | 1 | 1 | . | . | . |
| 3.5 | . | 2 | 1 | 2 | . | 1 | 2 | 1 | . | . |
| 4.0 | 1 | 1 | . | 1 | 2 | . | . | . | . | . |
| 4.5 | . | 1 | 1 | . | . | . | . | . | . | . |
| Northeast monsoon (Oct.-Jan.) calm (%) = 5 | | | | | | | | | | |
| 0.5 | 20 | 3 | 1 | 2 | 1 | 1 | 1 | . | 1 | 2 |
| 1.0 | 16 | 4 | 2 | 2 | 2 | . | . | 2 | 1 | 3 |
| 1.5 | 9 | 2 | 2 | 1 | . | . | . | 1 | 1 | 1 |
| 2.0 | 2 | 1 | 1 | 1 | . | . | . | . | . | . |
| 2.5 | 1 | 1 | 1 | 1 | . | . | 1 | . | . | . |
| 3.5 | 1 | . | 1 | . | . | . | . | . | . | . |
| 4.5 | . | . | . | 1 | . | . | . | . | . | . |

**(b) Joint distribution of wave height and period for Gujarat coastline**

**Fig. 3.24 Ship observed wave data (Chandramohan et al., 1991)**

## 3.8 Offshore Winds

The wind characteristics, speed and direction significantly influence the surface currents and thereby affecting the navigational design parameters. Understanding the offshore as well as nearshore wind characteristics are of important for doing any engineering studies. For the proposed locations, the hind casted offshore wind characteristics were extracted from ECMWF (European Centre for Medium Weather Forecasting).

Typical extracted wind speeds and wind directions for the entire year 2016 for Gujarat coastline are shown in Fig. 3.25 as per the location in Fig. 3.23. It is clear from the figures that the wind speeds are ranging between3 to 7m/sec with the directions changing according to the seasons. For example, during the months Jan to Apr, most of the wind directions are of the order 260-340deg, whereas during the monsoon (Apr-Oct) it is predominantly blowing from 270deg, which is west to east.

The wind rose diagram and histogram, given in Fig. 3.26&Fig. 3.27for Gujarat sites, clearly indicate the various wind directional sectors and the intensity of wind speeds. It is clear from the rose diagrams that the wind speeds are reaching up to 12m/sec at offshore sites.

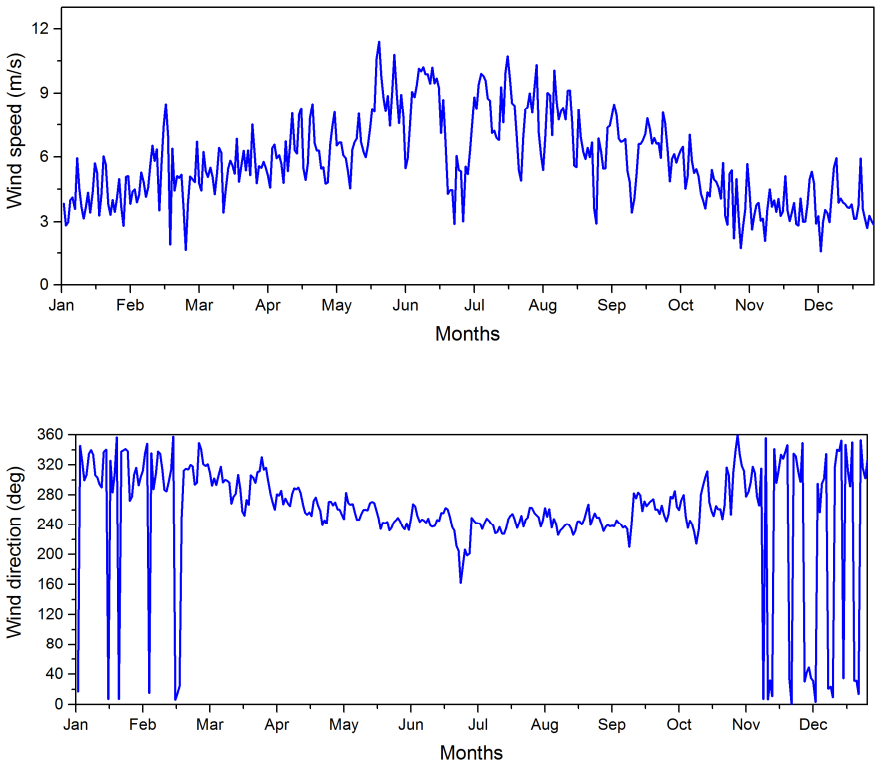


**Fig. 3.25 Typical wind data (intensity and direction) extracted off Gujarat coastline for year 2016**

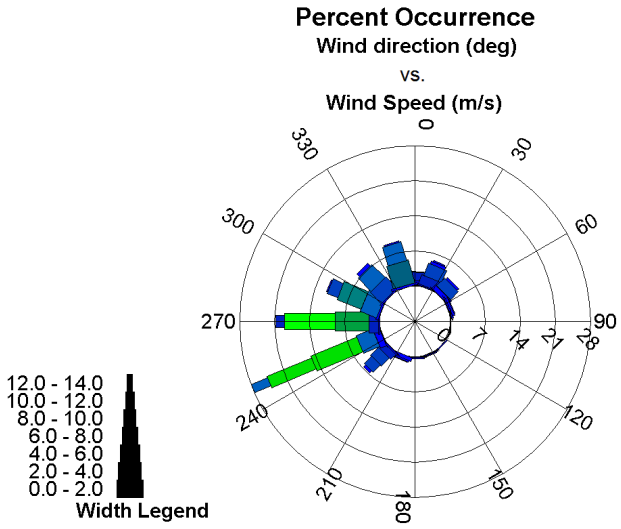


**Fig. 3.26 Typical offshore wind rose diagram for year 2016**

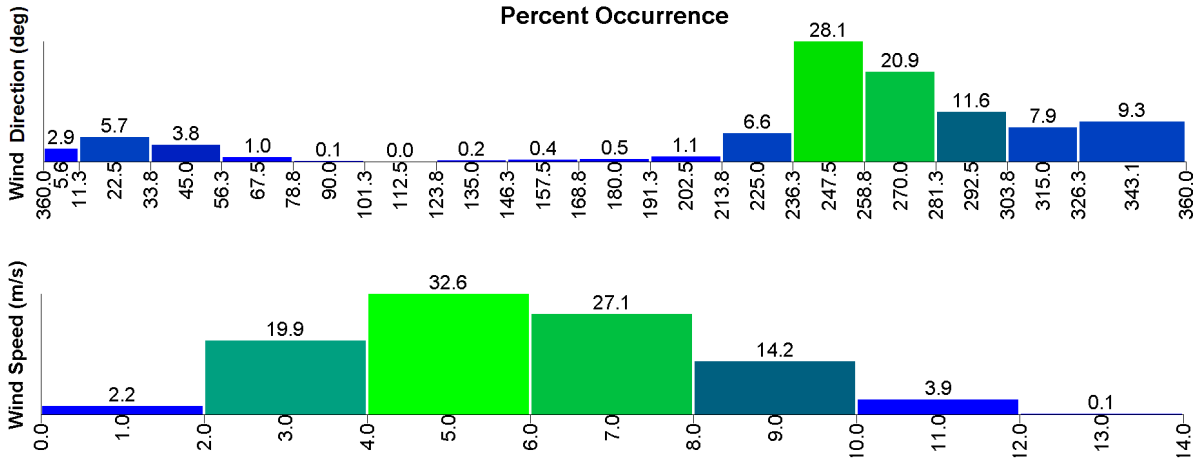


**Fig. 3.27 Typical wind histogram for the year 2016**

## 3.9 Cyclones

A tropical cyclone, which is a rotational low pressure system in tropics when the central pressure falls low with respect to the surrounding, can generate maximum sustained wind speed of about more than 60 kmph. The area of the wind whirl under such tropical cyclones can cover 150 to 800 km, with an eye or center of cyclone and capable of advancing towards land at a rate of 300 to 500 km a day.

The low pressure systems over Indian region are classified as depression, deep-depression and cyclones, depending up on the maximum sustained winds speed associated with the system and the pressure deficit/ number of closed isobars associated with the system. More the pressure drop at the central region of the cyclone pressure field more will be the severity

of the storm. The cyclonic storms are generally categorized according to the maximum wind associated with the storm. If the maximum wind is in the range of about 60-90 kmph then it is called a cyclonic storm. Storms associated with winds speeds of over 90 kmph are called as severe cyclonic storms and if the wind speeds exceed 120kmph, they are called very severe cyclonic storms. When the wind speeds exceed 200kmph, the storms are called super cyclonic storm. The Beaufort scale (Table 3.3), which is an empirical measure, basically relates wind speed to observed conditions at sea or on land. It is observed that size and intensity of storms are insignificantly associated. The intensity of storm shall be either measured by maximum sustained winds or by the lowest central pressure, whereas the size of storm may be represented by radius of gale force winds.

In Fig. 3.28,the central clouds represent the eye of the cyclone relatively a free region of calm winds, the diameter of which shall vary from 10 to 50kms. The surrounding region, called as wall-clouds are characterized by very strong winds and torrential rains, which has a width of about 10 to 150 km. Wind speed fall off gradually away from this core region, which terminate over areas of weaker winds with overcast skies and occasional squall. There may be one or more spiral branch in a cyclone where higher rainfall occurs. In the tropical region, like India, weak pressure waves move from east to west, which are called as easterly waves. For tropical cyclones; the following favorable conditions should be in place, to form as a cyclone; warm ocean waters, of at least 26.5°C, throughout a sufficient depth as warm waters are necessary to fuel the heat engine of the tropical cyclone. In addition, the following conditions are also important for a cyclone to form;

- Relatively moist layers near the mid-troposphere, as dry mid-levels are not conducive for allowing the continuing development of widespread thunderstorm activity.
- A minimum distance from the equator, as for tropical cyclogenesis to occur, there is a requirement for non-negligible amounts of the Coriolis force without which the low pressure of the disturbance cannot be maintained. Because of this reason the narrow corridor of width of about 300 km on either side of the equator is free from cyclones, generally.
- A pre-existing near-surface disturbance is also necessary with sufficient vorticity and convergence. Tropical cyclones need such disturbance to be generated and developed, demanding a weakly organized system with sizable spin and low level inflow.

- Low values, less than about 10 m/s, of vertical wind shear between layers of troposphere is also required. Vertical wind shear is the magnitude of wind distribution with height, large values of which would disrupt the incipient tropical cyclone and can prevent genesis. In case of a tropical cyclone has already formed, large vertical shear is potential to weaken the tropical cyclone.

It is interesting that all the aforementioned conditions fit well over the north Indian Ocean for the development of cyclones.

***Indian Cyclones***

The average annual frequency of tropical cyclones in the north Indian Ocean (Bay of Bengal and Arabian Sea) is about 5 (about 5-6 % of the Global annual average) which contributes to about 80 cyclones around the globe in a year.

The Tropical Cyclone (TC) is developed as an onset vortex at the leading edge of the summer monsoon. A depression formed over the southeast Arabian Sea on the evening of 4 June evolved later on into the Gujarat cyclone of 1998 (Fig. 3.29). Intensities of cyclones are indicated by CS - Cyclonic Storm, SCS - Severe CS, and VSCS - Very Severe CS. In the case of Gujarat, it intensified into a Cyclonic Storm on 5th June over the same area. It further intensified into a Severe Cyclonic Storm by the evening of 6th June. Moving northward, it intensified into a Very Severe Cyclonic Storm on the $7^{th}$, about 700 km southwest of Mumbai. While continuing to move northward, it deepened further with estimated core winds of 140 to 180 km/h on 8th June at about 350 km south-west of Porbandar. The system recurved and crossed the Gujarat coast near Porbandar region on $9^{th}$ of June (Sewa and Manu, 2003). An infrared image of Tropical Cyclone ARB 03A taken from a satellite is shown in Fig. 3.30.

The frequency of cyclones is found to be more in the Bay of Bengal rather than in the Arabian Sea, the ratio being 4:1. The monthly frequency of tropical cyclones in the north Indian Ocean display a bi-modal characteristic with a primary peak in November and secondary peak in May. The months of May-June and October-November are said to produce cyclones of severe intensity. Tropical cyclones developed during the monsoon months (July to September) are generally of less intensity. The frequencies of Cyclonic systems over north Indian Ocean during 1891-2006 are given in Fig. 3.31. Considering the west coast, Gujarat is found to be the most vulnerable state. On the other hand, Maharashtra is less prone to

cyclones. The frequencies of cyclonic storms crossing different coastal states of India during 1891-2006 are shown in Fig. 3.32. However, it is understood that cyclones do not influence the siltation of navigational channels in Kandla.

**Table 3.3 Beaufort scale for wind speeds**

| Force | Wind (Knots) | WMO Classification | Appearance of Wind Effects on the Water |
|---|---|---|---|
| 0 | Less than 1 | Calm | Sea surface smooth and mirror-like |
| 1 | 1-3 | Light Air | Scaly ripples, no foam crests |
| 2 | 4-6 | Light Breeze | Small wavelets, crests glassy, no breaking |
| 3 | 7-10 | Gentle Breeze | Large wavelets, crests begin to break, scattered whitecaps |
| 4 | 11-16 | Moderate Breeze | Small waves 1-4 ft. becoming longer, numerous whitecaps |
| 5 | 17-21 | Fresh Breeze | Moderate waves 4-8 ft taking longer form, many whitecaps, some spray |
| 6 | 22-27 | Strong Breeze | Larger waves 8-13 ft, whitecaps common, more spray |
| 7 | 28-33 | Near Gale | Sea heaps up, waves 13-19 ft, white foam streaks off breakers |
| 8 | 34-40 | Gale | Moderately high (18-25 ft) waves of greater length, edges of crests begin to break into spindrift, foam blown in streaks |
| 9 | 41-47 | Strong Gale | High waves (23-32 ft), sea begins to roll, dense streaks of foam, spray may reduce visibility |
| 10 | 48-55 | Storm | Very high waves (29-41 ft) with overhanging crests, sea white with densely blown foam, heavy rolling, lowered visibility |
| 11 | 56-63 | Violent Storm | Exceptionally high (37-52 ft) waves, foam patches cover sea, visibility more reduced |
| 12 | 63+ | Hurricane | Air filled with foam, waves over 45 ft, sea completely white with driving spray, visibility greatly reduced |

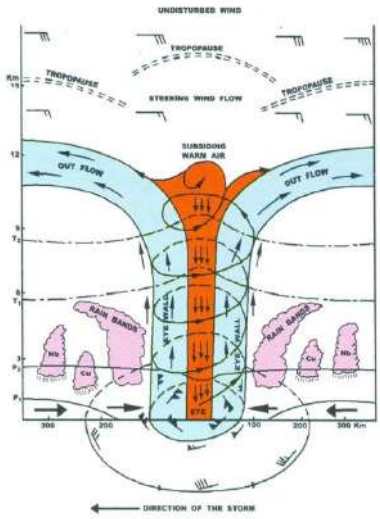


**Fig. 3.28 Ideal wind and cloud distribution in a cyclone**

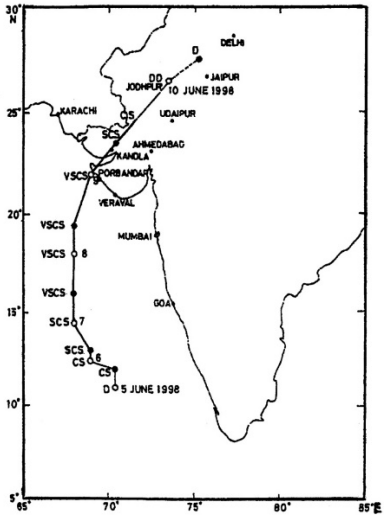


**Fig. 3.29 Gujarat cyclone during 5-10 June 1998 (Sewa and Manu, 2003)**

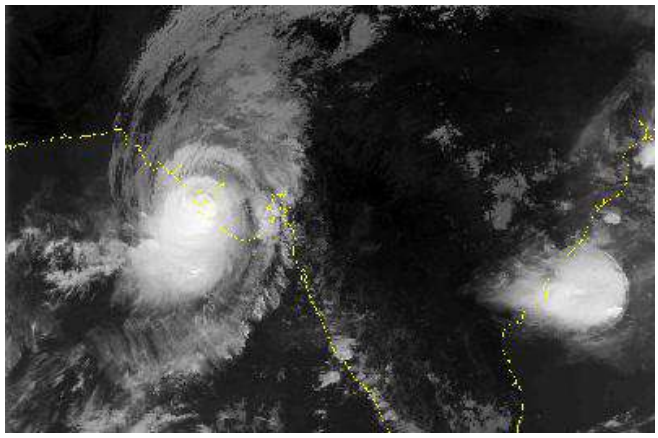

**Fig. 3.30 An infrared image of tropical cyclone ARB 03A taken from a satellite (NOAA)**

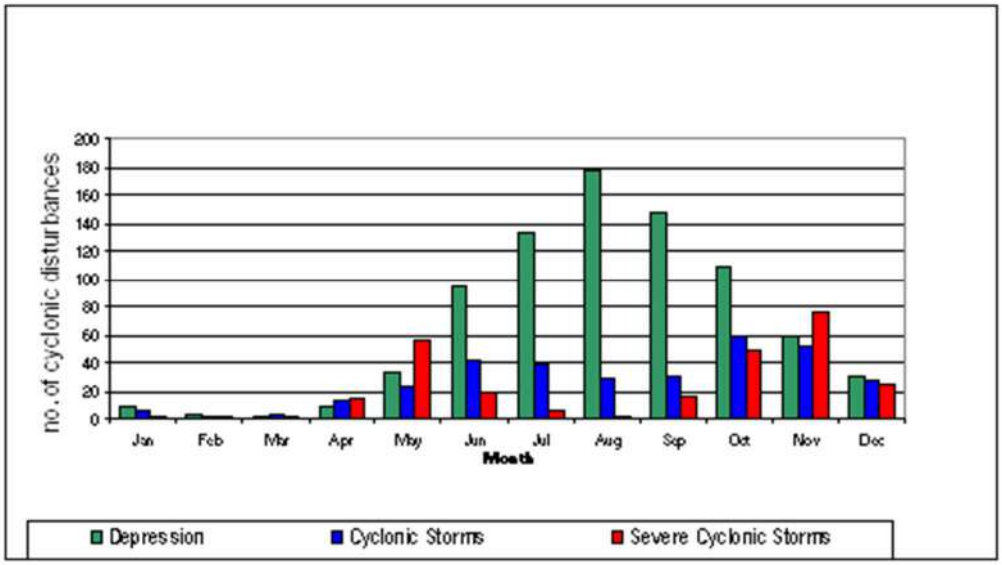


**Fig. 3.31 Frequencies of cyclonic systems over north Indian Ocean during 1891-2006**

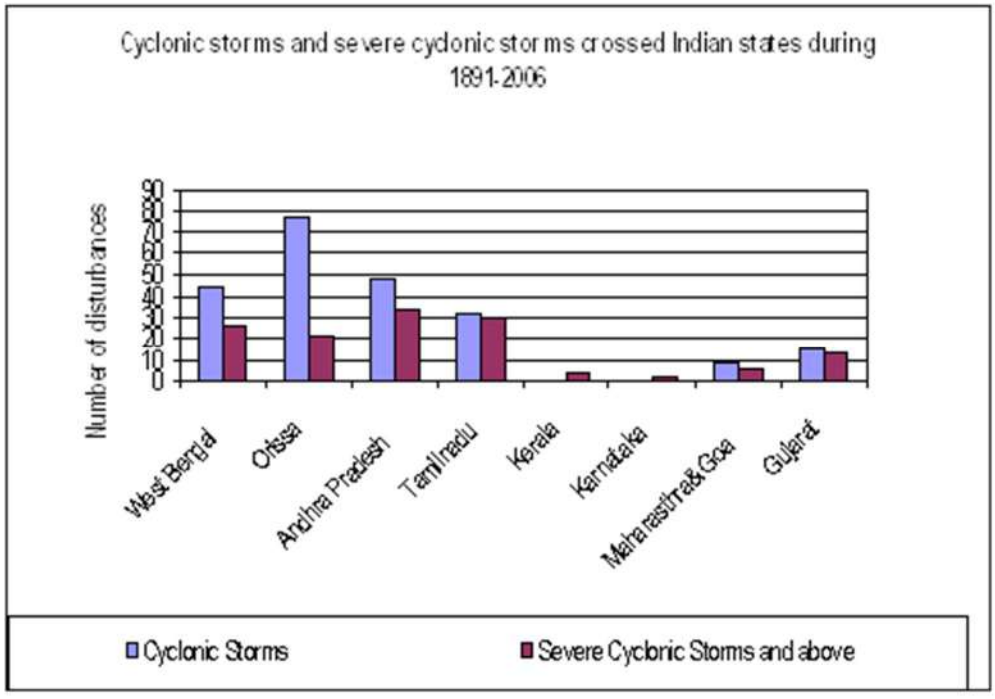


**Fig. 3.32 Frequencies of cyclonic storms during 1891- 2006**

## 3.10 Dredging details

Kandla port trust carries out dredging at three locations; Tuna port, Khori creek and old Kandla while maintenance dredging in front of the general cargo berth is marginal. The area in front of liquid bulk jetties require more dredging. In the 17km long approach channel (see Fig. 3.33) from the outer Tuna buoy to the Kandla creek outfall only a stretch 2.3 km between

buoy 8 and 10 has to be dredged continuously, albeit quite extensively. About 400,000 $m^3$ per month has to be dredged in total in order to ensure ships with a draught of 10.7 m to be able to call on the port of Kandla which costs about 300million rupees. The maintenance dredging was also reportedly increased over these years (Table 3.4) which in turn incurs high costs (approx. 150million rupees per year). According to Jayappa and Narayana (2009), an amount of 500million rupees spent on Kandla port to dredge the quantity of 4.5MCM during the 11th five-year plan period.

Deepening of the harbor requires huge quantities of sediments to be dredged. DPT and Central Water and Power Research Station (CWPRS) calculated that in order to enable ships with a draught of 14m to enter the port, Sogal channel have to be dredged to a depth of 8m (w.r.t. chart datum) with a width of 300m from the existing depth of 5.5m (w.r.t. chart datum) and width 180m. Kandla creek has to be deepened to a depth of 14.2m (w.r.t. chart datum) with a width of 400m. Staggering amount of 3.73 to 5.48MCM per month in Kandla creek and 3.75MCM per month in Sogal channel have been calculated by DPT and CWPRS (1999). This adds up to a total of 90 to 111 MCM per year which costs about 6.3 to 7.8 billion rupees a year. The siltation pattern was changing so drastically within the same season (Fig. 3.34) that the cross section of the navigational channel was displaced several times. This resulted in the modification of the approach channel nearly eight times in the past decades. The siltation pattern was also varying on the spatial scale along the Sogal channel, as shown in Fig. 3.35. It is evident that the maintenance dredging along Sogal channel is a historical challenge (Fig. 3.36) for Deendayal Port Trust.

However, the vital parameters, such as Suspended Sediment Concentration (SSC) and wave characteristics in the vicinity of the approach channel were not available with the port officials. and a typical measured bathymetry is shown in Fig. 3.37. Several measured charts for the year 2015 was digitized to seabed bathymetry as shown in Fig. 3.38, for the project region. The depth varies from -5m landwards to 22m towards the offshore location. Apart from the above data, the DPT also provided some dredging data for the year 2018, which was used on later stages of the analysis.

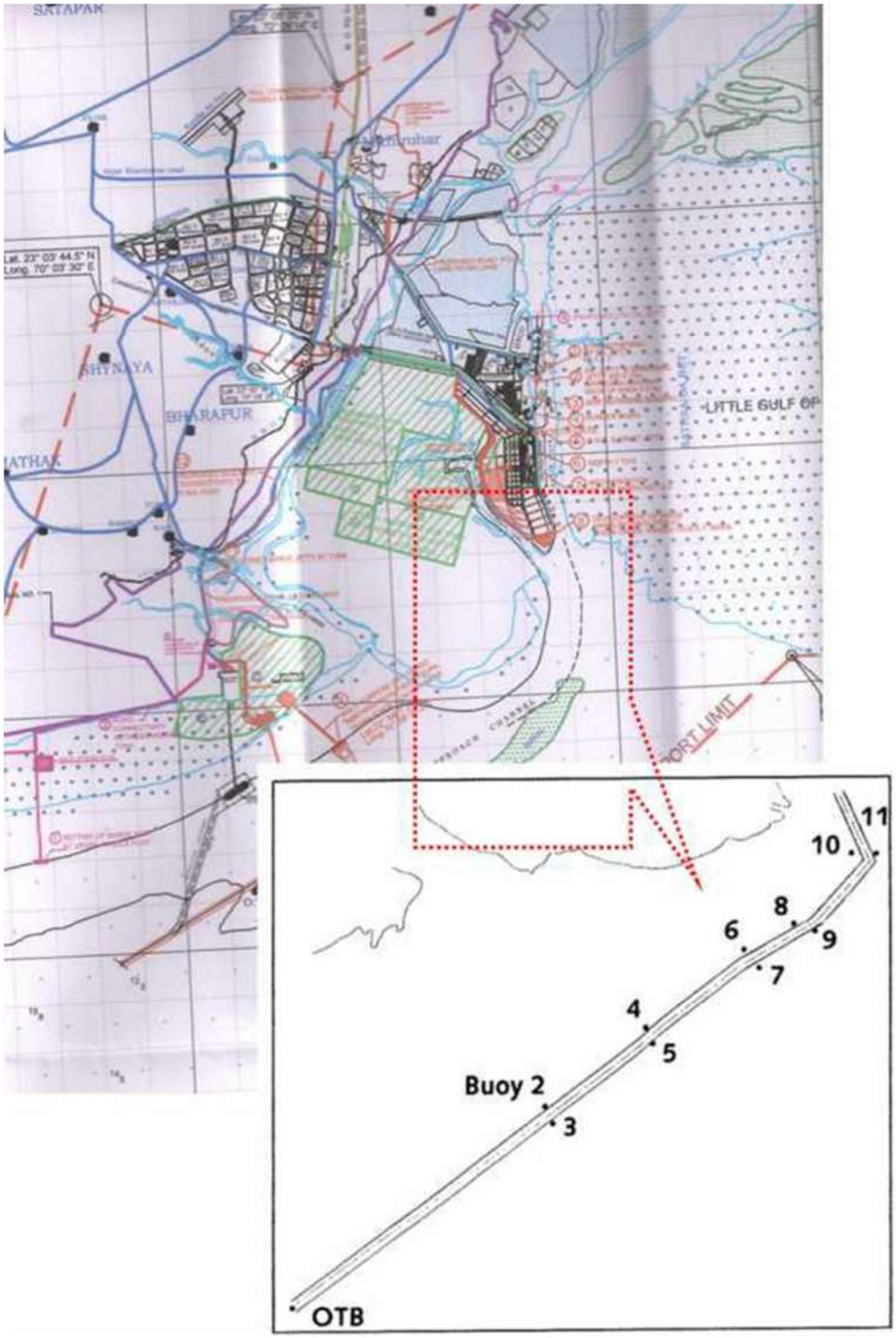


**Fig. 3.33 Approach Channel to Kandla Port**

**Table 3.4 Maintenance dredging quantity (MCM) (Source: Ministry of Shipping, 2011)**

| **11th 5-yr plan** | | **12th 5-yr plan** | | | | | |
|---|---|---|---|---|---|---|---|
| Target | Achieved | 2012-13 | 2013-14 | 2014-15 | 2015-16 | 2016-17 | Total |
| ***41.6*** | 32.36 | 6.5 | 7.5 | 9.0 | 10.5 | 12.0 | ***45.50*** |

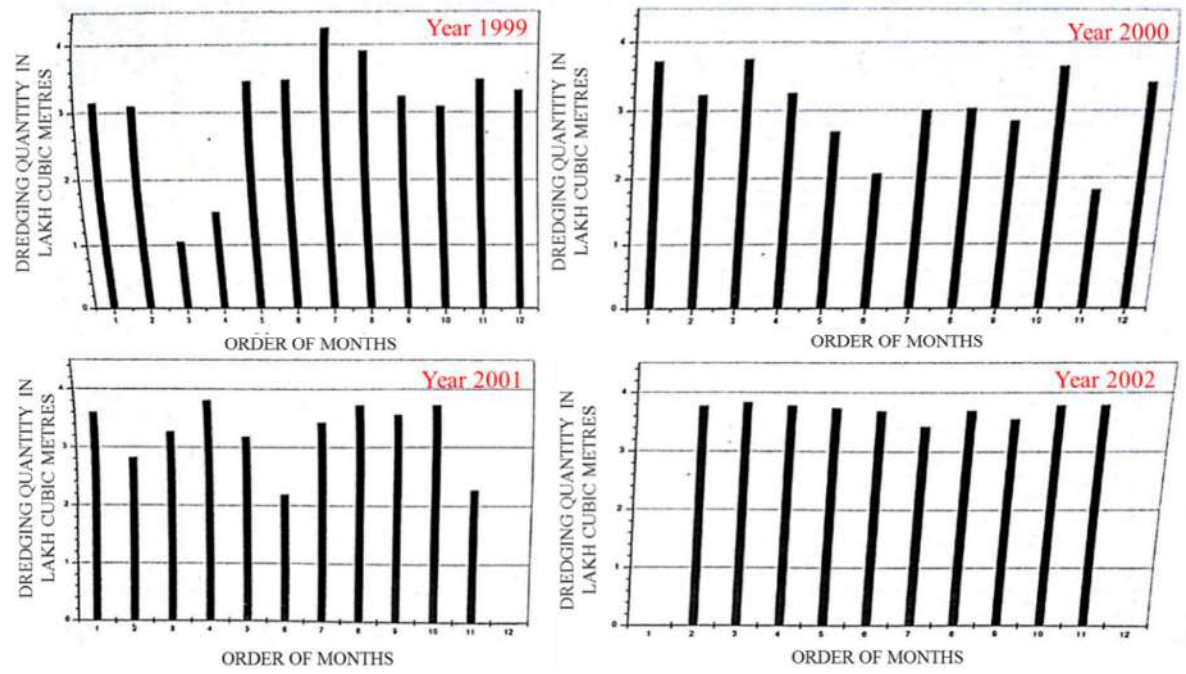


**Fig. 3.34 Monthly dredging quantity in Sogal Channel at Kandla port (1999 – 2002)**

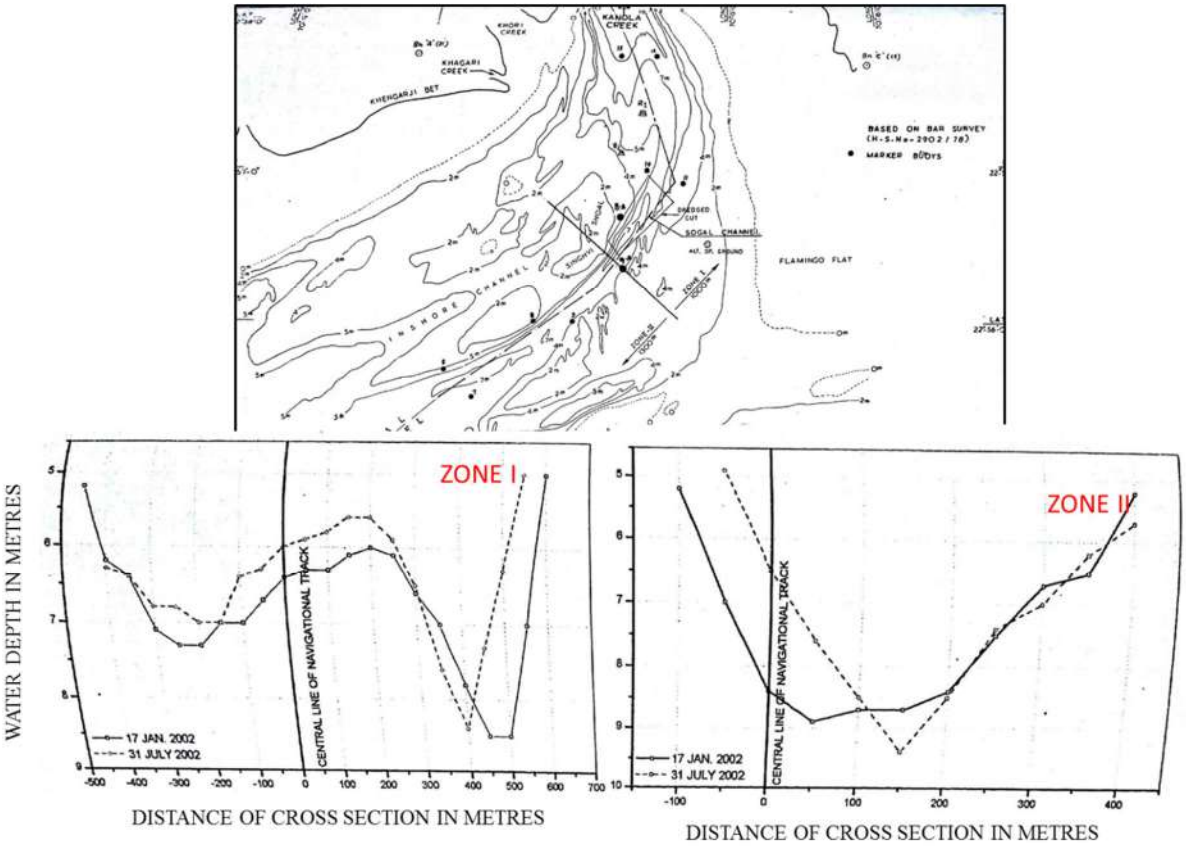


**Fig. 3.35 Typical spatial variation of siltation quantity in Sogal Channel**

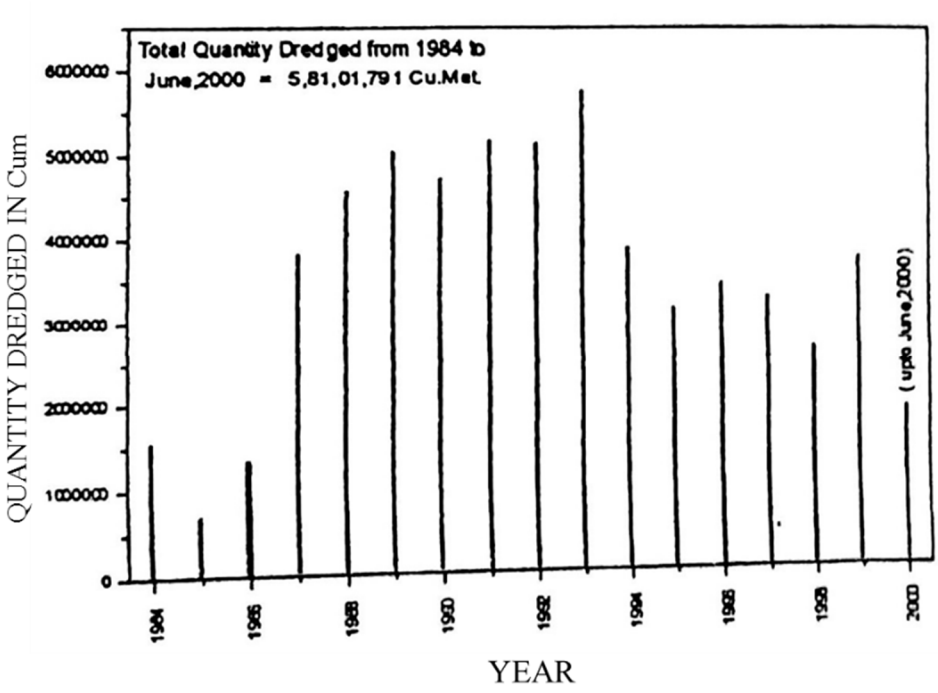


**Fig. 3.36 Historical annual dredging quantity in Sogal Channel**

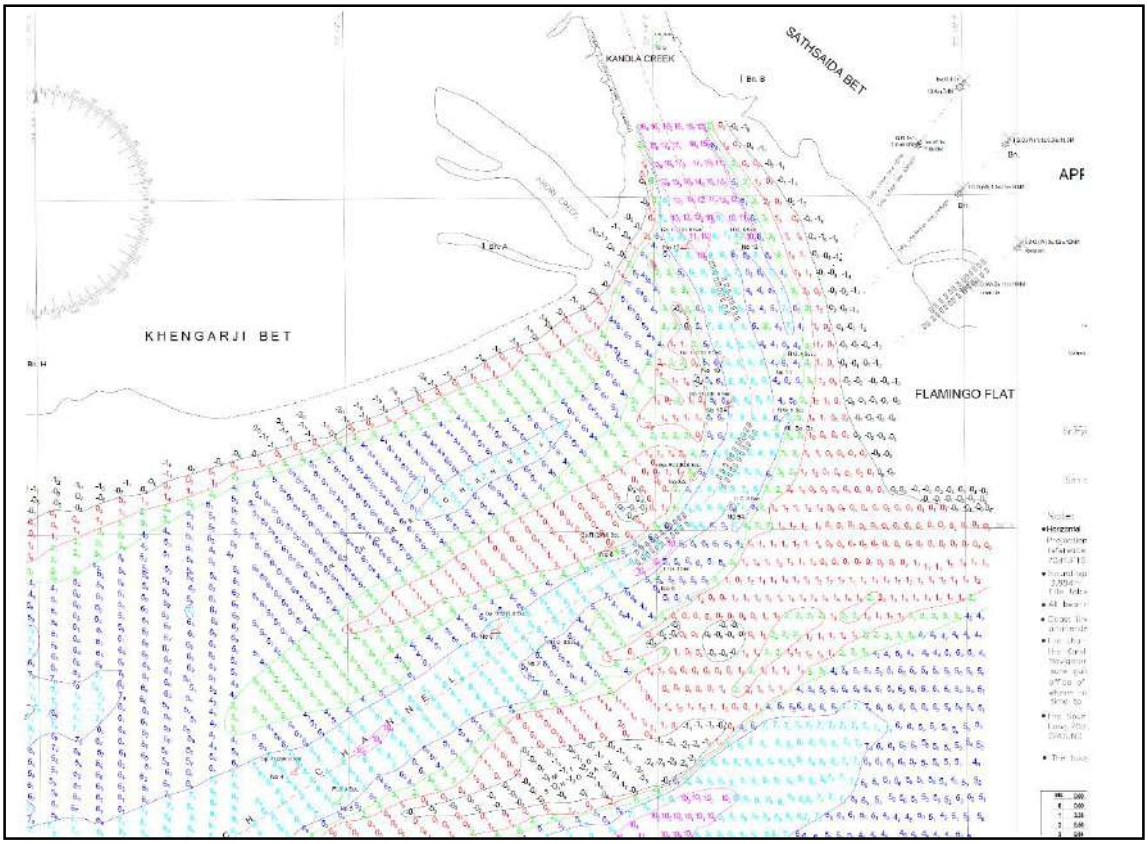


**Fig. 3.37 Typical bathymetry data supplied by Kandla Port**


**Fig. 3.38 Digitized seabed bathymetry(UTM, WGS84, 42**

# 4. Field Measurement Survey

An initial site visit was done by PI, Dr. Balaji Ramakrishnan on 10th August 2017 before proceeding with the field measurement surveys. The meeting was conducted between the Chairman (DPT), the Superintending Engineer (DPT) and PI to discuss the way forward for the successful completion of the project. The PI along with the officers of DPT visited the Kandla creek and the main navigational channel on 11th August 2017 (Fig. 4.1) to know more about the study area. As per the technical discussions done on this meeting, a site visit was again conducted on 11th and 12th of September 2017 (Fig. 4.2) by the associated project staff to officially collect the available data's from the DPT office, like tides, currents, bathymetry, meteorological and dredging details.

**Fig. 4.1 Site visit on 10th and 11th August 2017**

**Fig. 4.2 Site visit on 11th and 12th September 2017**

## 4.1 Pre-Monsoon Survey

### 4.1.1 Survey Plan

The detailed survey plan was drafted (Table 4.1) and discussed with DPT authorities and the same was executed with the help of the port authorities.

**Table 4.1 Detailed survey plan for the field measurement**

| Date | Activity | Measured data |
|---|---|---|
| 19/02/2018 (Monday) | Deploying RCM and ADCP | Tidal current measurements at different depths |
| 20/02/2018 (Tuesday) | Water sample collection along the Kandla creek | For suspended sediment concentration |
| 21/02/2018 (Wednesday) | Drifter (along the Kandla creek) & water sample analysis | Surface current measurements& SSC measurements in lab |
| 22/02/2018 (Thursday) | Water sample collection (along the navigation channel) | For suspended sediment concentration |
| 23/02/2018 (Friday) | Drifter (along the navigation channel) & water sample analysis | Surface current measurements& SSC measurements in lab |
| 24/02/2018 (Saturday) | Retrieval of RCM and ADCP | |

### 4.1.2 In-situ Data Collection

***Deployment of ADCP***

The Acoustic Doppler Current Profiler(ADCP) is one amongst the most widely used instruments in oceanographic research, in a cost effective way to measure profiles of water velocities and directional wave information. The ADCP(Fig. 4.3) uses the basic principle of Doppler Shifting to measure the velocities of waves. The ADCP is normally bottom mounted and upward facing, and the instrument ensonify the entire water column along four beams. The sound pulses are backscattered from small inorganic and organic particles that are

transferred by the wave motion causing a Doppler Shift in the returned sound. The backscatter return is range-gated into a series of bins along the beams to surmise the velocity profile. In addition to the wave orbital velocity measurements, the ADCP also measures the surface height through echo ranging (surface track) and bottom pressure with built in pressure sensor. The ADCP that contains different frequencies namely 300kHz ,600kHz and 1200kHz, has 4sensors on the top which produces the beam at an angle of 20°, whichinturn mesasures velocity and wave by the reflection from the particles present on water bodies.

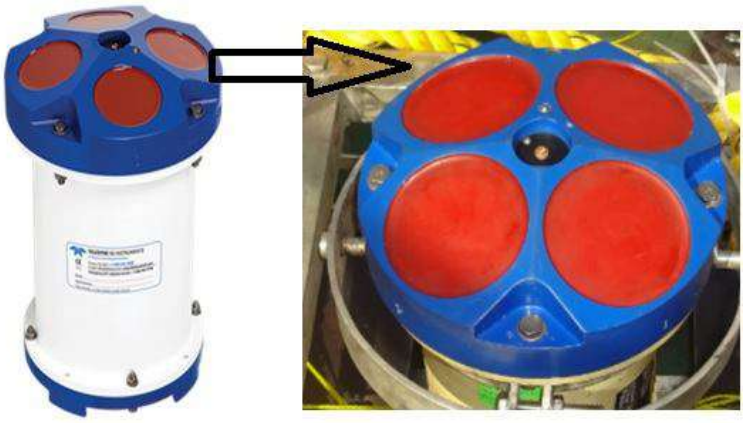

**Fig. 4.3 Typical view of ADCP and a zoomed view of Doppler sensors**

The workhorse sentinel ADCP 600 KHz instrument was set with all the required settings (every 10min data recording) for recording data using the computer and the instrument was sealed and set for deployment. ADCP was fixed on the gimbal with the detachable frame which is of 1m height (Fig. 4.4&Fig. 4.5) and the gimbal portion with the ADCP can rotate on its own to maintain the instrument angel. The deadweight of approximately 250kgs (divided into 8 solid iron bars) was added to the frame at the bottom to make sure the instrument stays intact on the place where it deployed (Fig. 4.6). Fig. 4.7 shows how an ADCP was fixed on the bottom of the desired location and then the ADCP was lowered from the survey launch M.L. Nirishak. The floating buoy (Fig. 4.8) was tied to the instrument for marking with one watch-keeping boat anchored properly to look after the instrument safety. ADCP was deployed at the location 22°56’02” N 70°14’33” E near the marking buoy 9A (Fig. 4.9) at 15:30hrs where the water depth was approximately 10m for taking continuous recording from 19/02/2018 to 24/02/2018. On 24/02/2018, the deployed instrument was recovered with the help of the boat M. T. Ocean Progress at 10:30hrs (Fig. 4.10).

**Fig. 4.4 Assembling the frame for ADCP deployment**

**Fig. 4.5 Assembled frame with gimbal on the top**

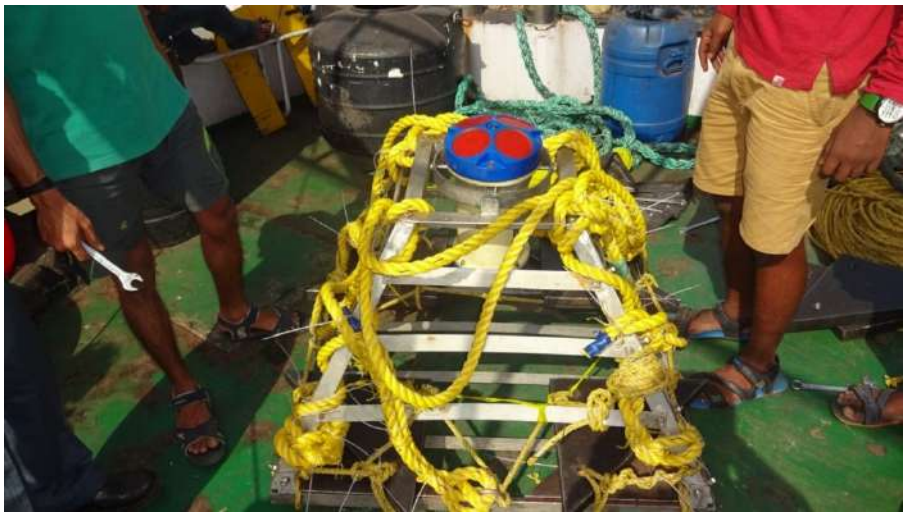

**Fig. 4.6 ADCP set for deployment with all the arrangements**

**Fig. 4.7 Typical graphical picture showing ADCP bottom mounting arrangement**

**Fig. 4.8 View of marking buoy at ADCP installed location with watch-keeping boat**


**Fig. 4.9 Typical view of the ADCP deployed location**


**Fig. 4.10 View of the recovered ADCP using the crane facility**

***Deployment of RCM***

The Recording Current Meter (RCM) is a self-recording current meter with a rotor mounted on the cylindrical body (Fig. 4.11), which is available with PI, also deployed in this field measurement . The rotor has a current sensor ranging between0-300cm/s, with a mean accuracy of ±0.15cm/s. The recording unit is also capable of measuring current direction with a range of 0-360°. It has an on-board turbidity sensor capable of recording turbidity with a

range of 0-125 FTU. It can also record velocity and other parameters like turbidity, salinity, tide level and conductivity.

An RCM, with all the required settings was set to store the data at every 1minute interval on the SD card. RCM was deployed at the location 23°00’38” N 70°13’58” E near the marking buoy 17 (Fig. 4.12)at 17:00hrs where the water depth was approximately 13m. The RCM bottom was tied with approximately 40kgs of deadweight along with a marking buoy tied to the top. The RCM was deployed from the boat and kept at a depth of 2m from the boat (Fig. 4.13). RCM was deployed in the water for making continuous recordings at an interval of 1min starting from 19/02/2018 to 24/02/2018. Fig. 4.14 shows the RCM being recovered from the deployed location on 24/02/2018. Once it was recovered, the data stored in the SD card was retrieved using the Seaguard software for further analysis. The current speed and direction measured by the instrument are illustrated in Fig. 4.15: A maximum current velocity of 1.6m/s was recorded by the instrument with the temperature and turbidity variations at the deployment location as illustrated in Fig. 4.16 and Fig. 4.17, respectively.


**Fig. 4.11 Typical view of RCM with all sensors**


**Fig. 4.12 RCM deployed location**

**Fig. 4.13 Deploying the RCM from the boat**

**Fig. 4.14 Retrieving RCM on 24/02/2018 from the deployed location**

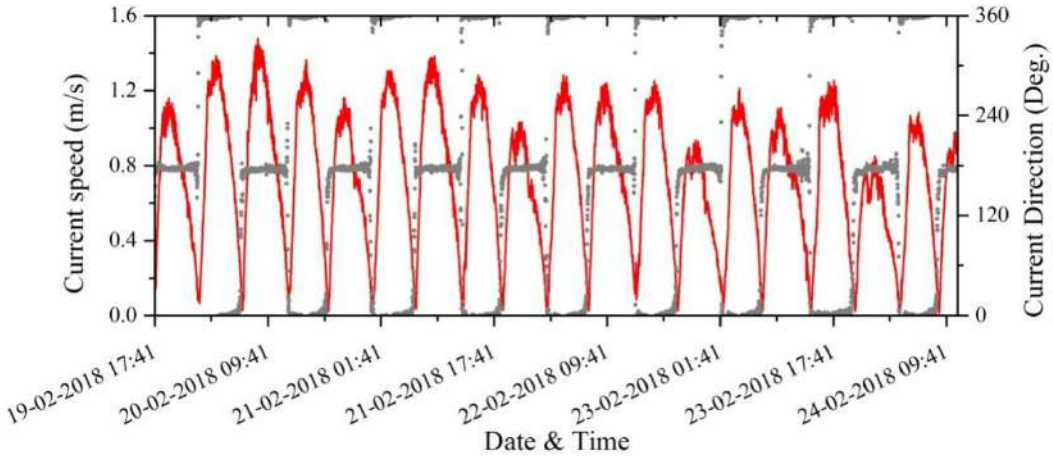


**Fig. 4.15 Typical RCM measured current speed & direction**

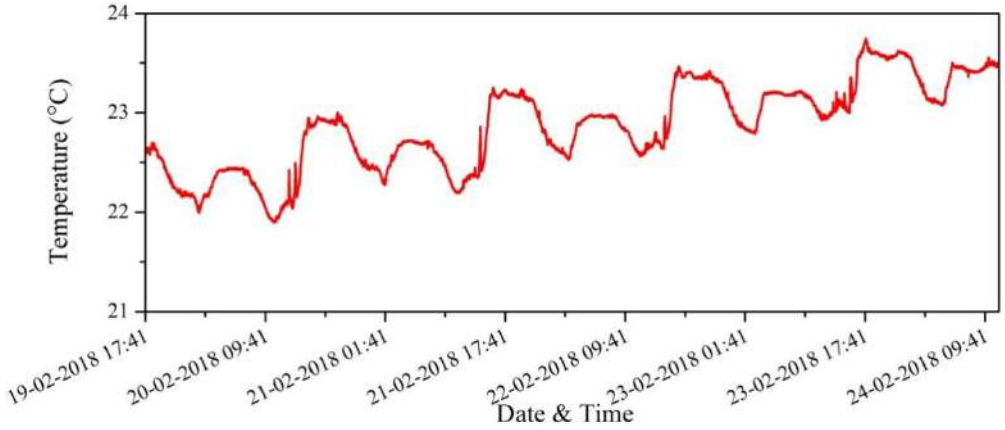


**Fig. 4.16 Typical measures temperature**

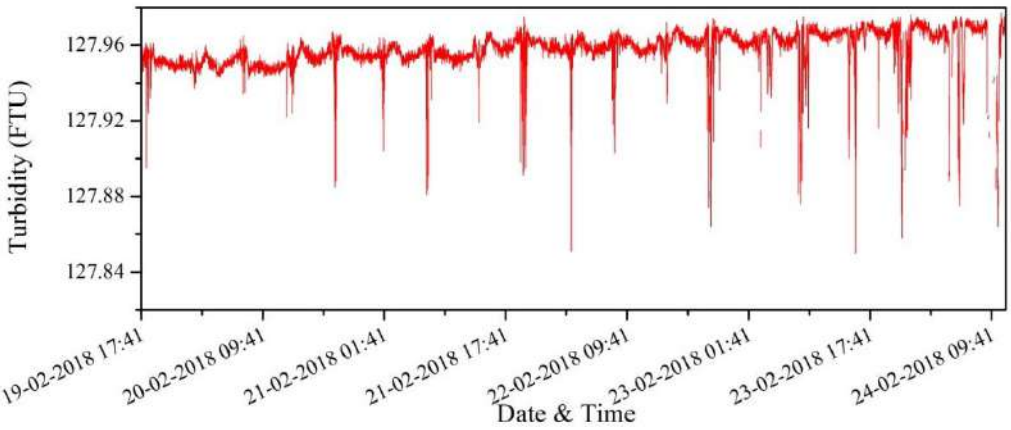


**Fig. 4.17 Illustration of the turbidity difference recorded by the instrument**

### *Suspended Sediment Collection*

Initially, the sample collection points from the creek to end of the navigation channel were marked on the GPS (till Buoy no.3). On 20/02/2018, water samples were collected from the creek side (Fig. 4.18) and on 22/02/2018, from along the navigation channel (Fig. 4.19) using the Niskin samplers. Nearly four samples were collected from different depths over the same proposed location, that are water sample from the surface and at depths 0.2*D, 0.6*D and 0.8*D, where D is total water depth from the surface.

The Niskin sampler (Fig. 4.20) or bottle is a tube, usually made of plastic, opened to the water at both ends. A bronze solid weight known as messenger is used to keep both end caps shut and to seal the tube with the water at the required depth. All the samples were transferred into one-liter water sampler (Fig. 4.21) collection bottles with proper labeling for further analysis in laboratory. The collected samples were transferred to laboratory located in the Seva Sadhan-3 building for the analysis.

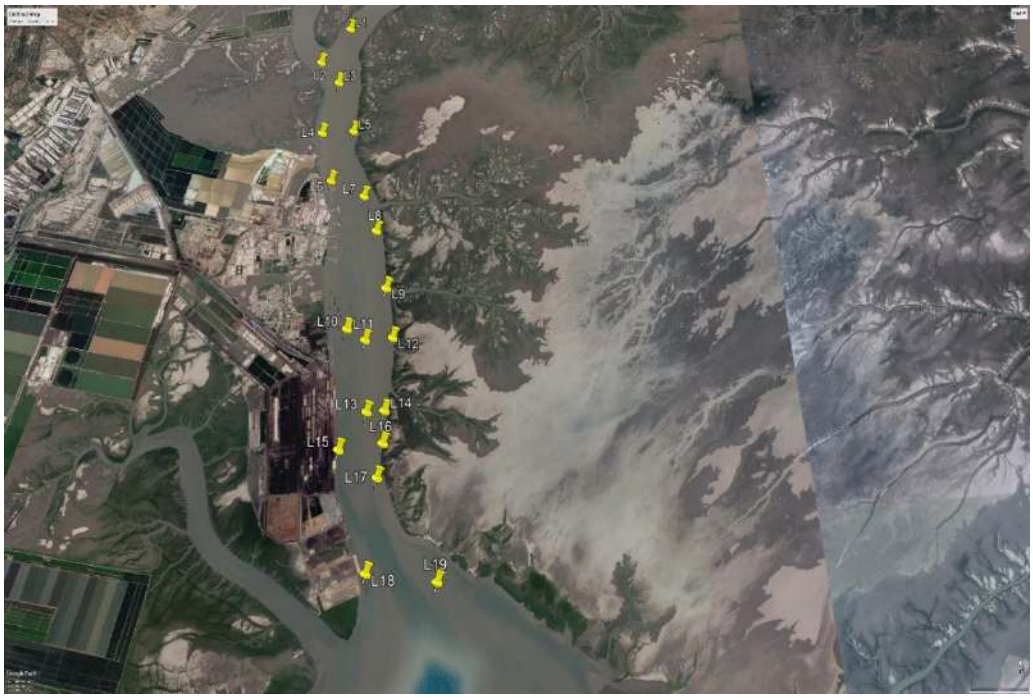


**Fig. 4.18 Locations of water sample collection on 20/02/2018**


**Fig. 4.19 Locations of water sample collection on 22/02/2018**

**Fig. 4.20 Typical view of a Niskin sampler**

**Fig. 4.21 Transferring water sample to collection bottle**

All the sample bottles were kept in the deep freezer (-4°C) to prevent any contamination or microorganism growth over it. Collected samples were filtered through Millipore filter paper, under the vacuum, using a filtration unit. The weight of Millipore filter paper (porous 0.45µm) was measured before the sample was filtered through it (Fig. 4.22). After the filtration process, the papers were kept in the oven for an hour at 105°C, for drying purpose. Then samples were kept in a desiccator for 20min to bring down its temperature and same were again weighed to know the weight of the suspended sediments contained in it. Table 4.2 and Table 4.3illustrated below shows the suspended sediment concentrations at different depths along the Kandla creek and the navigational channel.

**Fig. 4.22 View of the collected samples in the bottles with proper labelling**

**Fig. 4.23 A typical filtration unit and filtered sample on the paper**

**Table 4.2 Data of samples collected on 19/02/2018**

| Location | Longitude (X) | Latitude (Y) | Time | Depth(m) | F.P wt (g) | (F.p + S)wt (g) | SSC (mg/l) |
|---|---|---|---|---|---|---|---|
| L1 | 6252287.93 | 2552209.08 | 5.16pm | surface | 0.08126 | 0.11345 | 321.9 |
| | | | | 2.1 | 0.08125 | 0.11454 | 332.9 |
| 10.5m | | | | 6.3 | 0.08156 | 0.1166 | 350.4 |
| | | | | | | | |
| L2 | 624678.71 | 2511368.04 | 10.23am | surface | 0.07955 | 0.1078 | 282.5 |
| | | | | 3 | 0.0819 | 0.1118 | 299 |
| 5.7m | | | | 4.5 | 0.07945 | 0.11248 | 330.3 |
| | | | | | | | |
| L3 | 625100.63 | 2550852.35 | 10.00am | surface | 0.07945 | 0.10741 | 279.6 |
| | | | | 2.2 | 0.08165 | 0.11023 | 285.8 |
| 11m | | | | 8 | 0.08129 | 0.10784 | 265.5 |
| | | | | | | | |
| L4 | 624806.95 | 2549642.91 | 10.57am | surface | 0.0818 | 0.10505 | 232.5 |
| | | | | 2 | 0.08182 | 0.1056 | 237.8 |
| 9m | | | | 8 | 0.08153 | 0.11121 | 296.8 |
| | | | | | | | |
| L5 | 625473.92 | 2549666.93 | 5.00pm | surface | 0.0868 | 0.11843 | 316.3 |
| | | | | 7.9 | 0.08544 | 0.1178 | 323.6 |
| 13.3m | | | | | | | |

| | | | | | | | |
|---|---|---|---|---|---|---|---|
| L6 | 625065.14 | 2548546.42 | 11.17am | surface | 0.08071 | 0.10502 | 243.1 |
| | | | | 2.4 | 0.08066 | 0.10841 | 277.5 |
| 12m | | | | 7.4 | 0.08061 | 0.114 | 333.9 |
| | | | | 10 | 0.08111 | 0.1095 | 283.9 |
| L7 | 625768.61 | 25486.5 | 4.50pm | surface | 0.08459 | 0.11764 | 330.5 |
| | | | | 3.56 | 0.08549 | 0.12098 | 354.9 |
| 17.8m | | | | 10.68 | 0.086 | 0.1219 | 359 |
| | | | | | | | |
| L8 | 626051.47 | 2547427.42 | 4.30pm | surface | 0.08305 | 0.106 | 229.5 |
| | | | | 3.2 | 0.08438 | 0.1176 | 332.2 |
| 16m | | | | 9.6 | 0.08481 | 0.1187 | 338.9 |
| | | | | | | | |
| L9 | 626284.06 | 2546241.23 | 4.20pm | surface | 0.08304 | 0.1182 | 351.6 |
| | | | | 2.2 | 0.08316 | 0.1192 | 360.4 |
| 11m | | | | 6.6 | 0.08262 | 0.118 | 353.8 |
| | | | | 8.8 | 0.08015 | 0.115 | 348.5 |
| L10 | 625552.03 | 2545460.78 | 11.45am | surface | 0.08237 | 0.1014 | 190.3 |
| | | | | 1.6 | 0.0795 | 0.0992 | 197 |
| 9.7m | | | | 5.8 | 0.08139 | 0.0994 | 180.1 |
| | | | | 7.7 | 0.08207 | 0.10731 | 252.4 |
| L11 | 625913 | 2545234.82 | 11.59am | surface | 0.08206 | 0.1049 | 228.4 |
| | | | | 2.1 | 0.0804 | 0.105 | 246 |

| | | | | | | | |
|---|---|---|---|---|---|---|---|
| 12m | | | | 6.5 | 0.07938 | 0.1088 | 294.2 |
| | | | | 9.6 | 0.07936 | 0.10726 | 279 |
| L12 | 626440.345 | 2545262.93 | 12.10pm | surface | 0.07901 | 0.10167 | 226.6 |
| | | | | 2 | 0.08167 | 0.1079 | 262.3 |
| 12m | | | | 7 | 0.07947 | 0.11546 | 359.9 |
| | | | | 8 | 0.07955 | 0.11603 | 364.8 |
| L13 | 625995.62 | 2543904.35 | 12.10pm | surface | 0.07965 | 0.10817 | 285.2 |
| | | | | 2.3 | 0.08146 | 0.11666 | 352 |
| 11.5m | | | | 6.9 | 0.08128 | 0.11326 | 319.8 |
| | | | | 9.2 | 0.08111 | 0.11632 | 352.1 |
| L14 | 626330.20 | 2543917.37 | 3.47pm | surface | 0.08275 | 0.11314 | 303.9 |
| | | | | 2 | 0.0828 | 0.11815 | 353.5 |
| 7.5m | | | | 4.5 | 0.08185 | 0.11793 | 360.8 |
| | | | | 6 | 0.08181 | 0.11727 | 354.6 |
| L15 | 625513.03 | 2543256.08 | 12.55pm | surface | 0.08031 | 0.09792 | 176.1 |
| | | | | 3 | 0.08026 | 0.11535 | 350.9 |
| 15m | | | | 9 | 0.08117 | 0.11458 | 334.1 |
| | | | | 12 | 0.08063 | 0.11687 | 362.4 |
| L16 | 626315.24 | 2543346.02 | 3.31pm | surface | 0.08132 | 0.11495 | 336.3 |
| | | | | 3.74 | 0.08112 | 0.11731 | 361.9 |
| 18.7m | | | | 11.2 | 0.08107 | 0.11641 | 353.4 |
| | | | | 15 | 0.08193 | 0.11912 | 371.9 |

| | | | | | | | |
|---|---|---|---|---|---|---|---|
| L17 | 626234.78 | 2542760.77 | 2.06pm | surface | 0.0815 | 0.11275 | 312.5 |
| | | | | 3 | 0.081 | 0.10854 | 275.4 |
| 14.5 | | | | 5.8 | 0.0805 | 0.10651 | 260.1 |
| | | | | 8.7 | 0.0805 | 0.1124 | 319 |
| L18 | 626091.94 | 2541219.29 | 2.29pm | surface | 0.08115 | 0.118 | 368.5 |
| | | | | 1.8 | 0.08171 | 0.11727 | 355.6 |
| 9m | | | | 5.4 | 0.08148 | 0.12052 | 390.4 |
| | | | | | | | |
| L19 | 627336.2 | 2541054.29 | 3.10pm | surface | 0.08204 | 0.11402 | 319.8 |
| | | | | 1 | 0.08187 | 0.10854 | 266.7 |
| 5m | | | | 3 | 0.08207 | 0.12528 | 432.1 |
| | | | | 4 | 0.0816 | 0.12222 | 406.2 |

**Table 4.3 Data of samples collected on 21/02/2018**

| **Location** | **Longitude (X)** | **Latitude (Y)** | **Time** | **Depths(m)** | **F.P wt (g)** | **(F.p + S)wt (g)** | **SSC (mg/l)** |
|---|---|---|---|---|---|---|---|
| L20 | 62615.24 | 2539659.91 | 9.50am | surface | 0.08614 | 0.1219 | 357.6 |
| | | | | 1.1 | 0.08555 | 0.12027 | 347.2 |
| 5.5m | | | | 3.3 | 0.08783 | 0.1249 | 370.7 |
| | | | | 4.4 | 0.08766 | 0.12313 | 354.7 |
| L21 | 2539625 | 627064 | 9.30am | surface | 0.08298 | 0.11041 | 274.3 |
| | | | | 2.5 | 0.0824 | 0.11274 | 303.4 |

| | | | | | | | |
|---|---|---|---|---|---|---|---|
| 12.5m | | | | 7.5 | 0.08298 | 0.11997 | 369.9 |
| | | | | 10 | 0.08581 | 0.1278 | 419.9 |
| L22 | 2538822.70 | 626955.29 | 10.01am | surface | 0.08772 | 0.11252 | 248 |
| | | | | 7 | 0.08138 | 0.12622 | 448.4 |
| 8.5m | | | | | | | |
| | | | | | | | |
| L23 | 2538947 | 628713 | 5.46pm | surface | 0.07992 | 0.1058 | 258.8 |
| | | | | 4 | 0.07986 | 0.1062 | 263.4 |
| 5m | | | | | | | |
| | | | | | | | |
| L24 | 2537256.17 | 627268.25 | 10.20am | surface | 0.08307 | 0.1104 | 273.3 |
| | | | | 2.5 | 0.08309 | 0.11967 | 365.8 |
| 12.7m | | | | 7.6 | 0.08342 | 0.12252 | 391 |
| | | | | 10.1 | 0.08165 | 0.1148 | 331.5 |
| L25 | 2537380.65 | 626870.39 | 10.11am | surface | 0.08257 | 0.11715 | 345.8 |
| | | | | 1.3 | 0.08233 | 0.12083 | 385 |
| 6.5m | | | | 3.9 | 0.08039 | 0.11875 | 383.6 |
| | | | | | | | |
| L26 | 2535207.07 | 627588.6 | 5.21pm | surface | 0.08033 | 0.10997 | 296.4 |
| | | | | 1.5 | 0.08021 | 0.1106 | 303.9 |
| 8m | | | | 4.8 | 0.08244 | 0.11268 | 302.4 |
| | | | | 6.4 | 0.08053 | 0.1085 | 279.7 |

| | | | | | | | |
|---|---|---|---|---|---|---|---|
| L27 | 2535934.16 | 625885.25 | 10.39am | surface | 0.08211 | 0.1128 | 306.9 |
| | | | | 1.5 | 0.08475 | 0.1165 | 317.5 |
| 5.3m | | | | 4.6 | 0.08337 | 0.1177 | 343.3 |
| | | | | 6.2 | 0.08505 | 0.1205 | 354.5 |
| L28 | 2536170.07 | 625038.59 | 10.54am | surface | 0.08529 | 0.11293 | 276.4 |
| | | | | 1 | 0.08588 | 0.11583 | 299.5 |
| 5.3m | | | | 3 | 0.08395 | 0.1269 | 429.5 |
| | | | | 4 | 0.08234 | 0.12758 | 452.4 |
| L29 | 2534238.1 | 625355.48 | 5.08pm | surface | 0.08138 | 0.116 | 346.2 |
| | | | | 4 | 0.08164 | 0.1166 | 349.6 |
| 5m | | | | | | | |
| | | | | | | | |
| L30 | 2534332.42 | 624348.81 | 11.41am | surface | 0.08583 | 0.11815 | 323.2 |
| | | | | 1.3 | 0.08589 | 0.11442 | 285.3 |
| 6.5m | | | | 3.9 | 0.08602 | 0.12165 | 356.3 |
| | | | | 5.2 | 0.08729 | 0.12366 | 363.7 |
| L31 | 2535315.9 | 623584.89 | 11.11am | surface | 0.08227 | 0.11994 | 376.7 |
| | | | | 1.6 | 0.08186 | 0.11775 | 358.9 |
| 8.3m | | | | 4.9 | 0.08706 | 0.12918 | 421.2 |
| | | | | 6.6 | 0.08717 | 0.1316 | 444.3 |
| L32 | 253376.46 | 622828.86 | 12.00pm | surface | 0.0811 | 0.10237 | 212.7 |
| | | | | 0.94 | 0.08135 | 0.10315 | 218 |

| | | | | | | | |
|---|---|---|---|---|---|---|---|
| 4.7m | | | | 2.8 | 0.08161 | 0.10495 | 233.4 |
| | | | | 3.7 | 0.08243 | 0.11305 | 306.2 |
| L33 | 2533212.64 | 621399.56 | 4.43pm | surface | 0.08748 | 0.11547 | 279.9 |
| | | | | 3 | 0.08099 | 0.10962 | 286.3 |
| 15m | | | | 9 | 0.08714 | 0.1188 | 316.6 |
| | | | | 12 | 0.08246 | 0.11596 | 335 |
| L34 | 2531643.58 | 622154.88 | 4.24pm | surface | 0.08566 | 0.1185 | 328.4 |
| | | | | 2.7 | 0.08503 | 0.11731 | 322.8 |
| 13.4m | | | | 8 | 0.08549 | 0.12201 | 365.2 |
| | | | | 11 | 0.085 | 0.12001 | 350.1 |
| L35 | 2531779.17 | 623683.22 | 4.01pm | surface | 0.08711 | 0.13211 | 450 |
| | | | | 2.5 | 0.08577 | 0.1315 | 457.3 |
| 10.8m | | | | 6.5 | 0.08209 | 0.12782 | 457.3 |
| | | | | 8.5 | 0.08458 | 0.12962 | 450.4 |
| L36 | 2531712.08 | 621011.8 | 12.35pm | surface | 0.0851 | 0.12576 | 406.6 |
| | | | | 1.96 | 0.08238 | 0.13012 | 477.4 |
| 9.5m | | | | 5.7 | 0.08388 | 0.13195 | 480.7 |
| | | | | 7.6 | 0.08215 | 0.13305 | 509 |
| L37 | 2530485.24 | 621960.98 | 3.48pm | surface | 0.084 | 0.11157 | 275.7 |
| | | | | 1.8 | 0.084 | 0.11591 | 319.1 |
| 9.4m | | | | 5.6 | 0.08433 | 0.1319 | 475.7 |
| | | | | 7.5 | 0.08515 | 0.13784 | 526.9 |

| | | | | | | | |
|---|---|---|---|---|---|---|---|
| L38 | 2530330.05 | 620559.07 | 3.23pm | surface | 0.08225 | 0.1138 | 315.5 |
| | | | | 2 | 0.0834 | 0.116 | 326 |
| 10m | | | | 6 | 0.08386 | 0.1346 | 507.4 |
| | | | | 8 | 0.08366 | 0.13601 | 523.5 |
| L39 | 2529013.17 | 621039.73 | 3.08pm | surface | 0.08206 | 0.0957 | 136.4 |
| | | | | 3 | 0.08471 | 0.1029 | 181.9 |
| 11.2m | | | | 7 | 0.0825 | 0.12103 | 385.3 |
| | | | | 9 | 0.08246 | 0.13728 | 548.2 |
| L40 | 2527995.51 | 619926.23 | 2.41pm | surface | 0.08379 | 0.09863 | 148.4 |
| | | | | 2.4 | 0.08516 | 0.10035 | 151.9 |
| 11.7m | | | | 7.2 | 0.08515 | 0.1327 | 475.5 |
| | | | | 9.6 | 0.0849 | 0.13161 | 467.1 |
| L41 | 2528001.98 | 621068.1 | 2.54pm | surface | 0.08335 | 0.0973 | 139.5 |
| | | | | 2.74 | 0.08373 | 0.10145 | 177.2 |
| 13.7m | | | | 8.2 | 0.08411 | 0.12809 | 439.8 |
| | | | | 11 | 0.08421 | 0.139 | 547.9 |

### *Drifter Experiment*

Drifter is small spherical buoy with an inbuilt GPS system that can be used to calculate the surface velocity of the flow as well as trajectory, based on its own position. The whole system consists of 3 sub-systems, i.e. (i) The drifter, (ii) The coastal relay station sub-system for data transmitting, (iii) Real-time data display and management sub-system that support the in-situ operation. The drifters (Fig. 4.24) with the diameter of 12cm, were found to exhibit good surface flow following capacity. The drifters were capable enough to transmit

the data back to the shore station for every 10sec via digital RF network. The specifications of the drifters are given in Table 4.4.

**Fig. 4.24 Typical floating drifters with the base station kit**

**Table 4.4 Specifications of drifter**

| | |
|---|---|
| Diameter | 12 cm |
| Weight | 600 g |
| Power | Alkaline battery |
| Lifetime | >96 hours |
| Positioning systems | GPS \ GLONASS |
| Positioning accuracy | 2.5 m CEP |
| Positioning precision | 0.167 m |
| Sampling frequency | 1 – 10 Hz |
| Transmitting frequency | 0.1 – 1 Hz |
| Communication systems | RF |

The experiments were conducted on 21/02/2018 and 23/02/2018 with the survey launch M.L. Nirkshak and a roving boat. After completing the initial instrumental setup, one of the drifter (40F82B68) was kept in the launch for tracking the current position of the launch and three of the other drifters (40F82B5F, 40F82B7D, 40F82BDC) were deployed (Fig. 4.25) at 09:14hrs on 21/02/2018 at location 22° 59' 11" N, 70° 13' 54.5" E maintaining enough distance without influencing the drifter's movement. The drifters which were moving towards the shoals were then corrected to follow the path towards the navigational channel. The time taken for the drifters to move up and drop were also noted down. These corrections were taken care during post-processing analysis. The drifters were finally collected (Fig. 4.26) around 16:48hrs and the same procedure was repeated on 23/02/2018 around 08:55hrs at location 22° 57' 56" N,70° 14' 2" E. The whole experiment was conducted based on the ebb and flood tides which are given in Table 4.5.

**Fig. 4.25 Movement of the drifter along with the flow**

**Fig. 4.26 Retrieval of drifters from the water**

**Table 4.5 Predicted tide table provided by DPT**

| Date | Time(HH:MM) | Height (m) |
|---|---|---|
| 21-02-2018 | 05:41 | 6.73 |
| | 12:30 | 0.78 |
| | 18:15 | 6.24 |
| 23-02-2018 | 01:27 | 1.75 |
| | 07:03 | 6.33 |
| | 14:01 | 0.80 |
| | 20:06 | 6.03 |

The data which was recorded by the drifters, were then exported into excel format and then the incorrect values due to various disturbances were removed. The post-processing was done using Matlab software which were then finally plotted as shown in figures below. Fig. 4.27illustrates the surface velocity range varying from 0.3m/s to 1.2m/s (ebb tide) while Fig. 4.28 illustrates the surface velocity range varying from 0.2m/s to 1.6m/s during flood tide. During the flood tide, the surface currents are found to be high (about 1.6m/s) along the sides of the navigational channel.


**Fig. 4.27 Drifters track during ebb tides on 21st and 23rd Feb 2018**


**Fig. 4.28 Drifters track during flood tides on 21st and 23rd Feb 2018**

## 4.2 Post-Monsoon Survey

***Deployment of ADCP***

The ADCP used for the study area was Flow Quest 600 (600kHz frequency). It has 4 sensors at the top which produce the beam at an angle of 20° which measures velocity and wave by means of the reflection from the particles present on water bodies.

The Flow Quest ADCP 600Khz setup was ready for deployment after the battery is connected. The initialization of the input data was given by Flow Quest Studio Windows software through the input cable, and every required data was entered like frequency, salinity of water and time for beginning, the deployment details and other necessary instructions required by the instrument to record the data at every 1min interval. Input cable was then removed after the instructions were passed and the retaining strap was inserted at the bottom to safeguard the input/output plugin. The frame was a detachable type (Fig. 4.29) and it was fitted to fix the instrument on top of the gimbal. The whole setup was tied with a rope for lowering the instrument safely into the water. The instrument was then fixed in gimbal (Fig. 4.29) in such a way to withstand and adjust itself for any alterations of its position occurred due to frame movement or external alterations. The frame was held with dead weight of 4 steel chains, each weighing 12kgs and 4 triangular steel wedges, each weighing 60kgs

altogether amounting to 400 kg approximately (including lifting rope and frame itself) to protect the movement of whole setup from strong currents under the water. The knot of the lifting rope was tied with the hook of hydraulic crane (installed in tug-boat). The instrument was then lifted and the whole setup was slowly lowered into the water (Fig. 4.30) and mounted on the sea bed. Water current profiles are also measured from a depth of 9m, by bottom mounted upward tracking. The free end of the rope was tied with a marker buoy to float on the water surface to indicate the deployment location.

ADCP was then deployed at the location 22°56'4.08"N, 70°14'29.77"E, few meters away from buoy 9A outside navigation channel from 07/12/2018 (10:38 hrs) to 16/12/2018 (15:15 hrs). The instrument was then retrieved from the location as shown in Fig. 4.32 and re-deployed near buoy no. 6 (22°55'20.88"N, 70°12'48.42"E) from 16/12/2018 (16:10 hrs) to 28/12/2018 (15:00 hrs). The depth at the deployment location (near buoy no. 6) was found to be 10m at that point of time. After each retrieval, by inserting the cable to ADCP and connecting it to rugged laptop, data was simultaneously recovered from the instrument via the software. Measured current speed and direction at various depths from 07/12/2018 to 16/12/2018 are illustrated in Fig. 4.33to Fig. 4.36 respectively.

**Fig. 4.29 Clamping of ADCP in detachable frame (with dead weights)**

**Fig. 4.30 Deployment of ADCP with the help of hydraulic crane installed in tugboat**


**Fig. 4.31 Deployment locations of ADCP**

**Fig. 4.32 Retrieval of the instrument with the help of crane from tugboat**

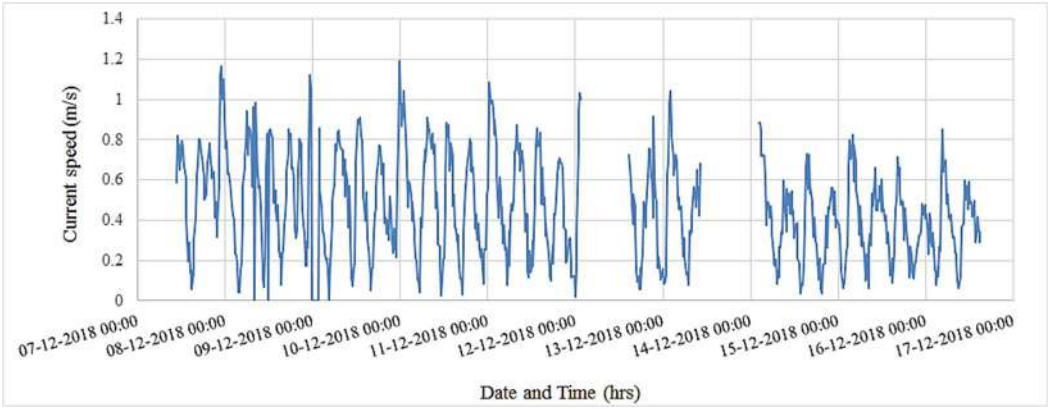


**Fig. 4.33 Typical measured current speed at free surface**

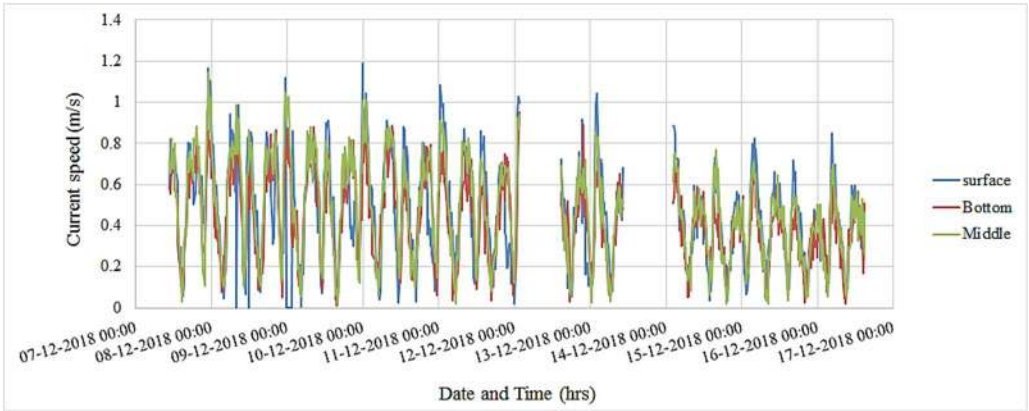


**Fig. 4.34 Typical current speed at free surface, middle and bottom depth**

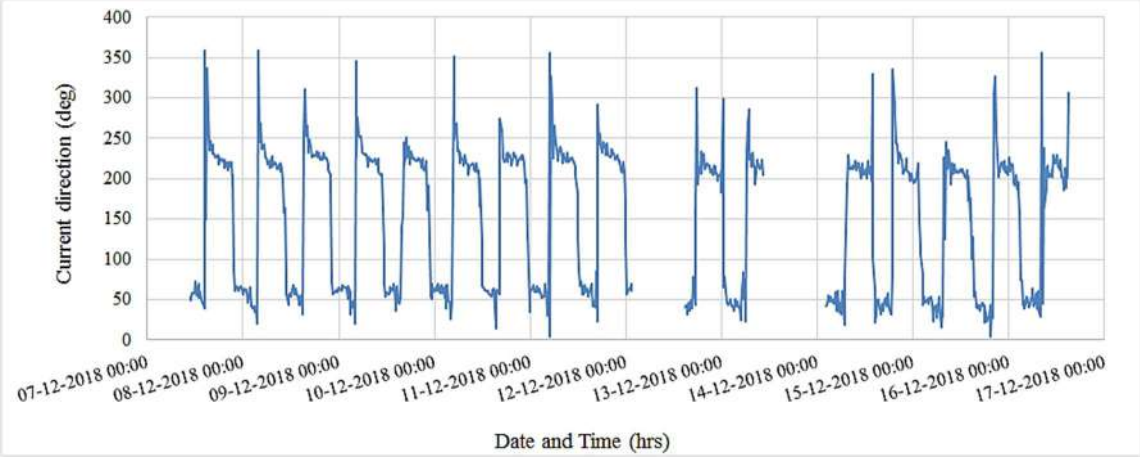


**Fig. 4.35 Typical measured current direction at free surface**

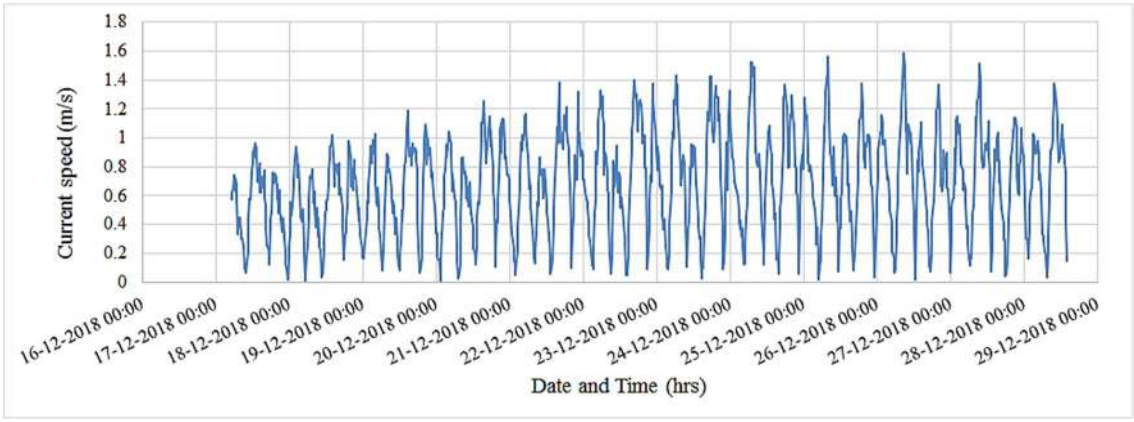


**Fig. 4.36 Typical measured current direction at free surface, middle and bottom depth**

Measured current speed and direction at various depths from 16/12/2018 to 28/12/2018 are illustrated in Fig. 4.37 to Fig. 4.40 respectively.

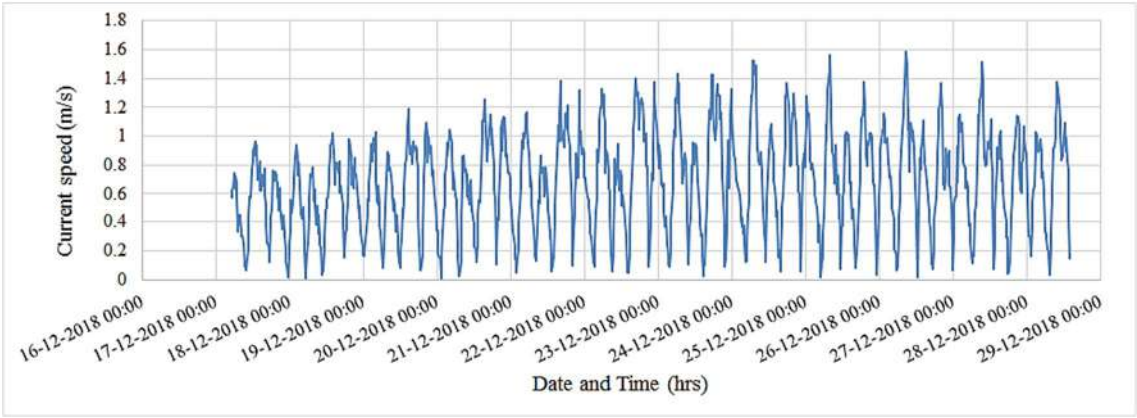


**Fig. 4.37 Typical measured current speed at free surface**

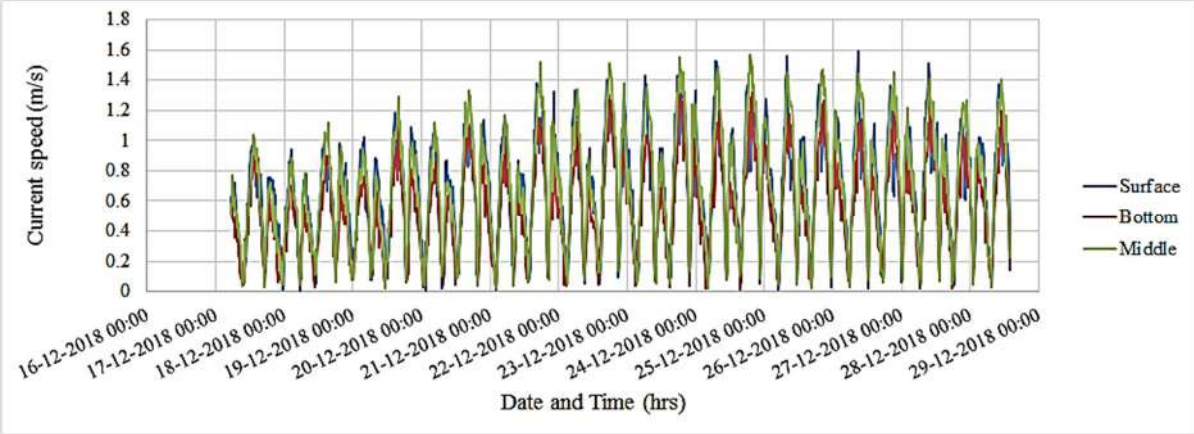


**Fig. 4.38 Typical measured current speed at free surface, middle and bottom depth**

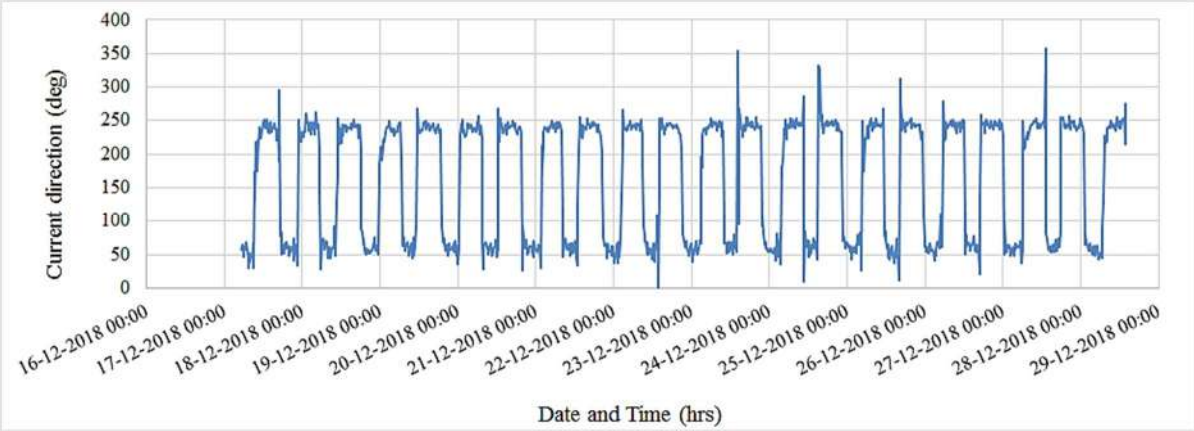


**Fig. 4.39 Typical measured current direction at free surface**

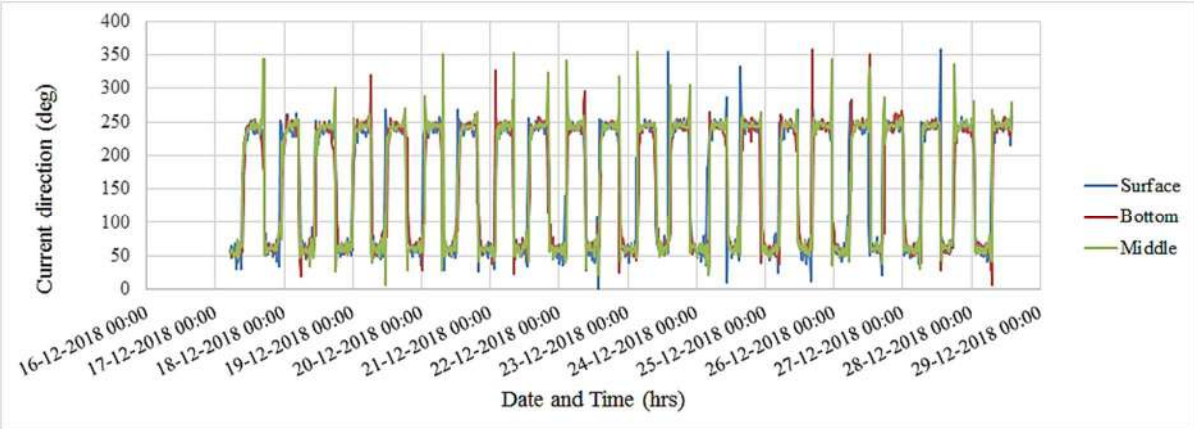


**Fig. 4.40 Typical measured current direction at free surface, middle and bottom depth**

It is observed that the maximum current velocity at first deployment location (near buoy 9A) was observed to be 1.2m/s and 1.6 m/s at second deployment location (near buoy 6).

### *Deployment of RCM*

RCM, with all the required settings to record all current and water level variation was set to store the data at every 10 min. interval on SD card. RCM was deployed at the location 23°00'38"N, 70°13'58"E near Buoy 17 (Fig. 4.41) on 07/12/2018 (13:00hrs) where the water depth was nearly 13m. The free end of rope was tied with the marking buoy to float on water surface such that to indicate the deployment location. The knot of the lifting rope was tied with the hook of hydraulic crane (installed in tug-boat). The instrument was lifted and the whole setup was slowly lowered into the water and mounted on the sea bed. The data collected was retrieved from the SD card using the Sea guard software for further analysis, after the instrument was retrieved on 28/12/2018 (16:30 hrs). Measured water level variations (spring and neap), current speed with direction, temperature and turbidity from 07/12/2018 to 28/12/2018 are illustrated in following figures. The maximum current velocity measured by bottom mounted RCM was 1.132m/s. The measured values of temperature and turbidity are given in Fig. 4.48 and Fig. 4.49 respectively.


**Fig. 4.41 RCM deployed location**

**Fig. 4.42 RCM fitted to frame (with dead-weights)**

**Fig. 4.43 Deployment of RCM**

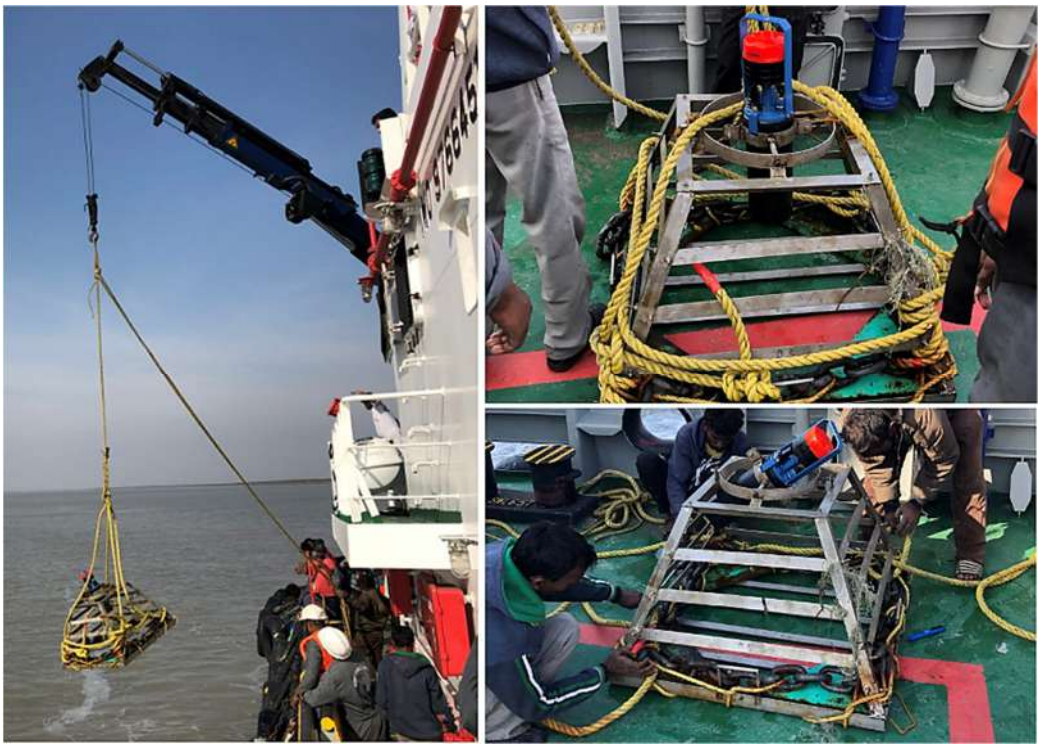

**Fig. 4.44 Retrieval of RCM from the deployed location**

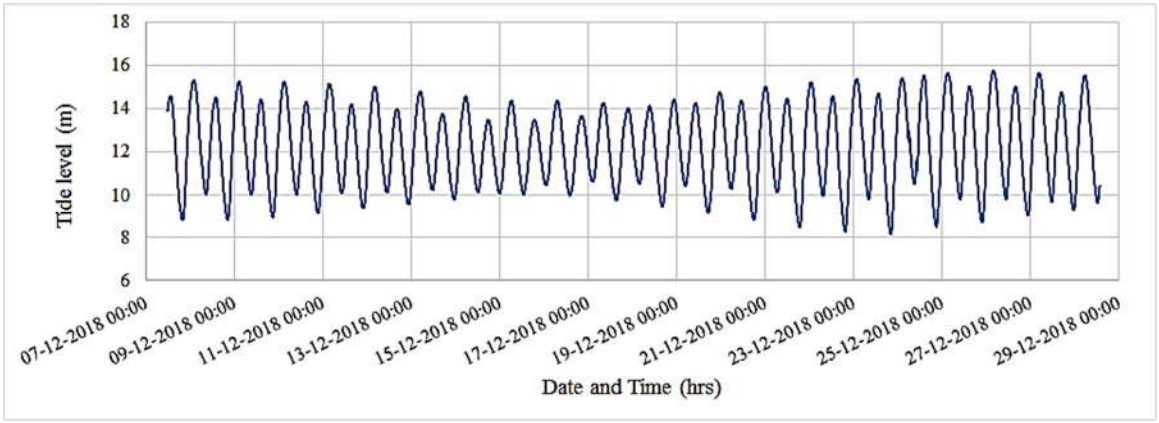


**Fig. 4.45 Typical measured water level variations**

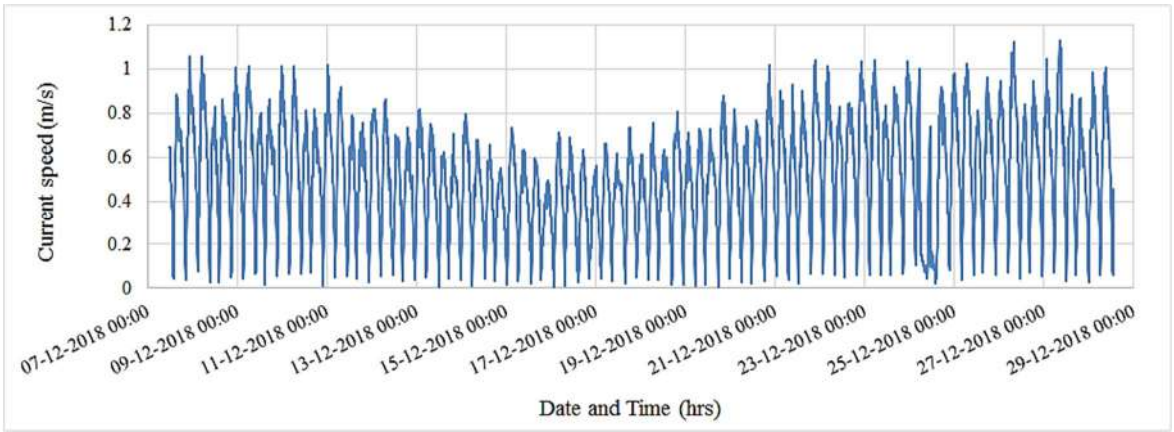


**Fig. 4.46 Typical measured current speed**

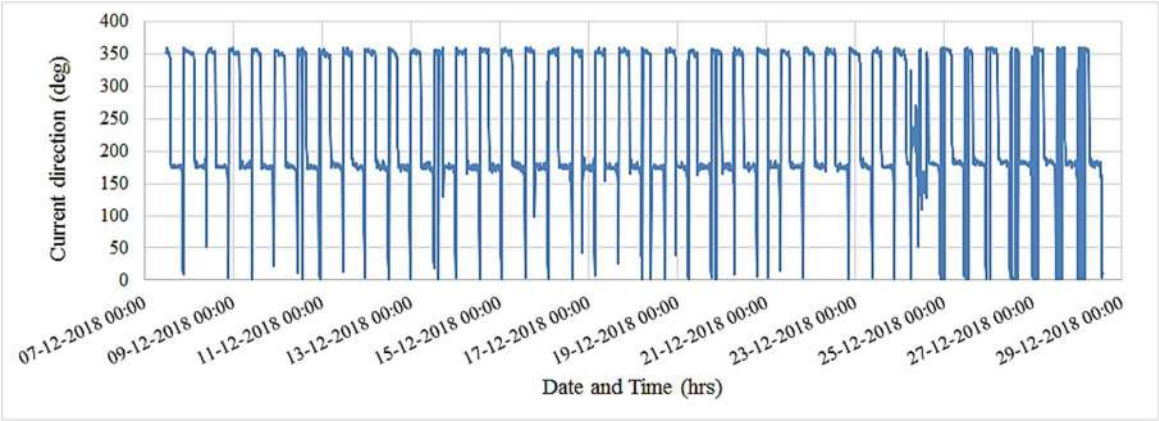


**Fig. 4.47 Typical measured current direction**

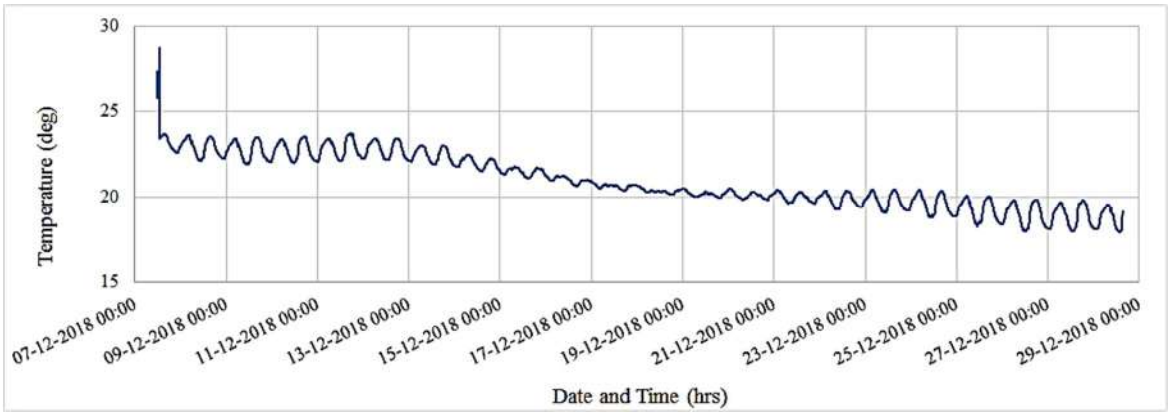


**Fig. 4.48 Typical measured temperature variations**

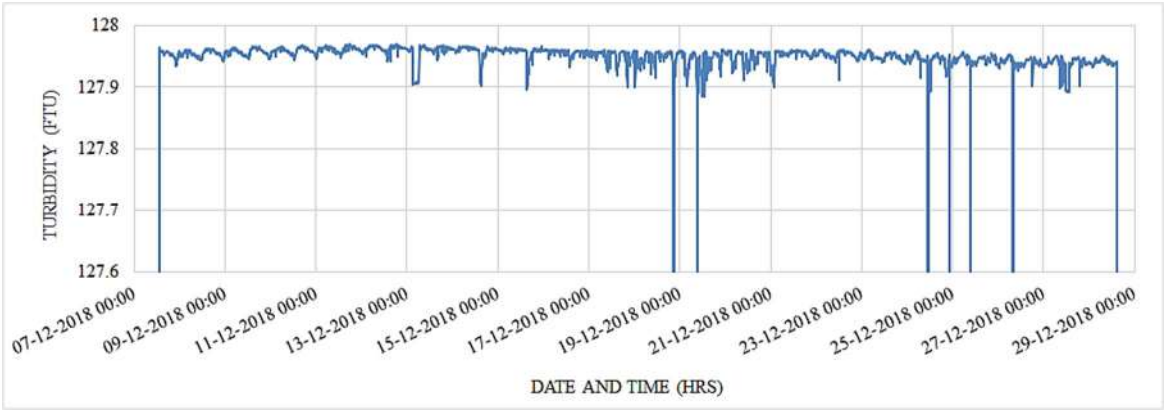


**Fig. 4.49 Typical measured turbidity**

### *Suspended Sediment Concentration*

Initially, sample collection points were marked on the GPS from the creek till the end of the navigation channel (till Buoy no.3). The sample collection points inside and outside Kandla creek are shown in Fig. 4.50andFig. 4.51 respectively. The water sampling survey was conducted in two sessions. The first session included water sampling from 17$^{th}$ Dec ’18 to

20th Dec ’18 (two days after the neap tide) with the help of boats hired from local people in Kandla. The second session of sampling survey was conducted on 24th Dec ’18 and 25th Dec ’18 (two days after the spring tide). Nearly three samples were collected from different depths of the same proposed location i.e., 0.1*D, 0.5*D and 0.8*D, where D is total water depth from the surface.

Niskin sampler was used to collect the water samples at the desired water depth without disturbing the water sample and the samples thus collected were transferred to the bottles with proper labelling (Fig. 4.52&Fig. 4.53). The collected samples were transferred to laboratory located in the Seva sadhan-3 building for the analysis.

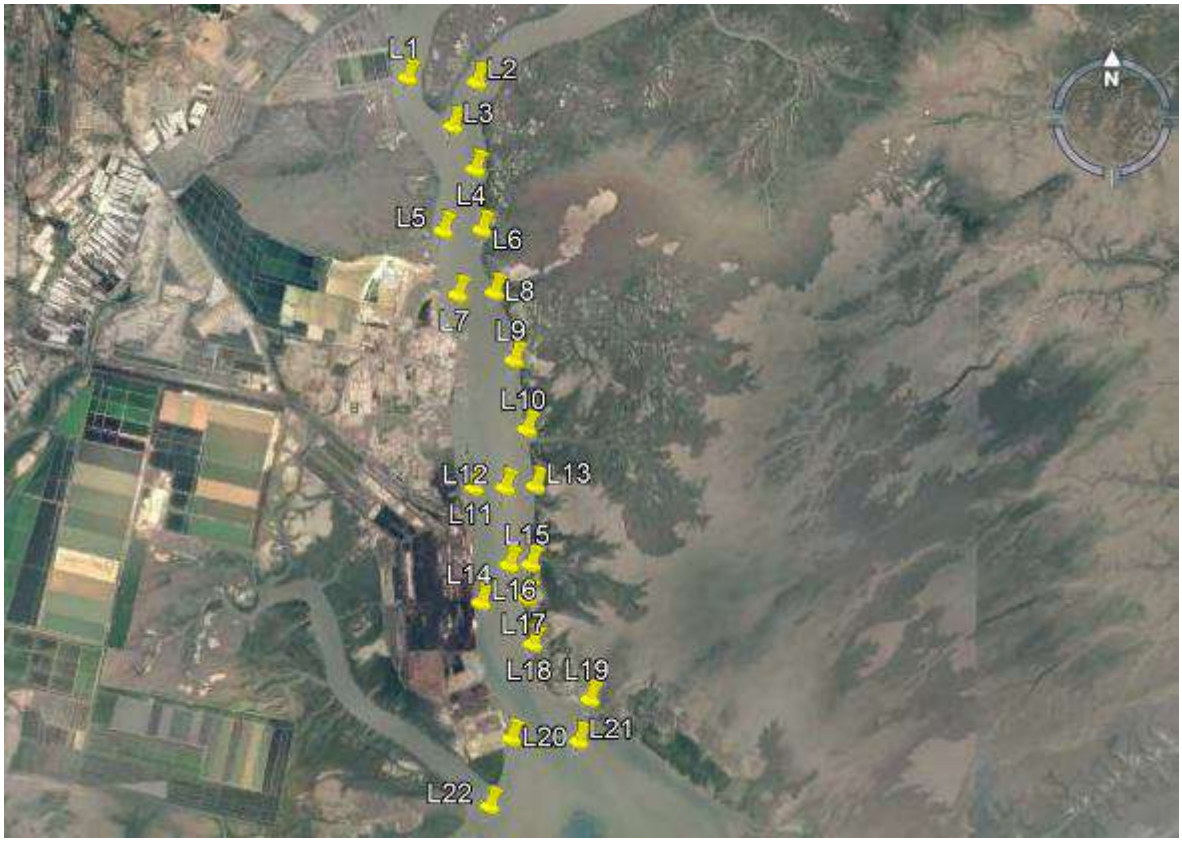


**Fig. 4.50 Locations for water sample collection (inside the creek)**


**Fig. 4.51 Locations for water sample collection (outside the creek)**

All the sample water bottles were kept in the deep freezer (-4°C) to avoid any contamination or microorganism growth. The whole set-up of filtration unit is shown in Fig. 4.54. Collected samples were filtered through Whatman Glass Microfiber filter paper using the vacuum pump of the filtration unit. Whatman Millipore filter paper (porous 0.45µm) weight was measured before the sample was filtered through it (Fig. 4.55). After the filtration, the papers were kept in the oven at 120°C about 15 min for drying. Then samples were then kept in desiccator for 10min to bring down to room temperature and same were weighed again to estimate the weight of the suspended sediments. The spatial variation of estimated suspended sediment concentration inside and outside creek corresponding to both the sessions are represented as contour plots from Fig. 4.56 to Fig. 4.67 respectively.

**Fig. 4.52 Collected water sample transferred to collection bottle**

**Fig. 4.53 View of the collected samples with labelling**


**Fig. 4.54 View of filtration unit set-up**

**Fig. 4.55 View of Whatman Glass Microfiber filter paper with sediments**

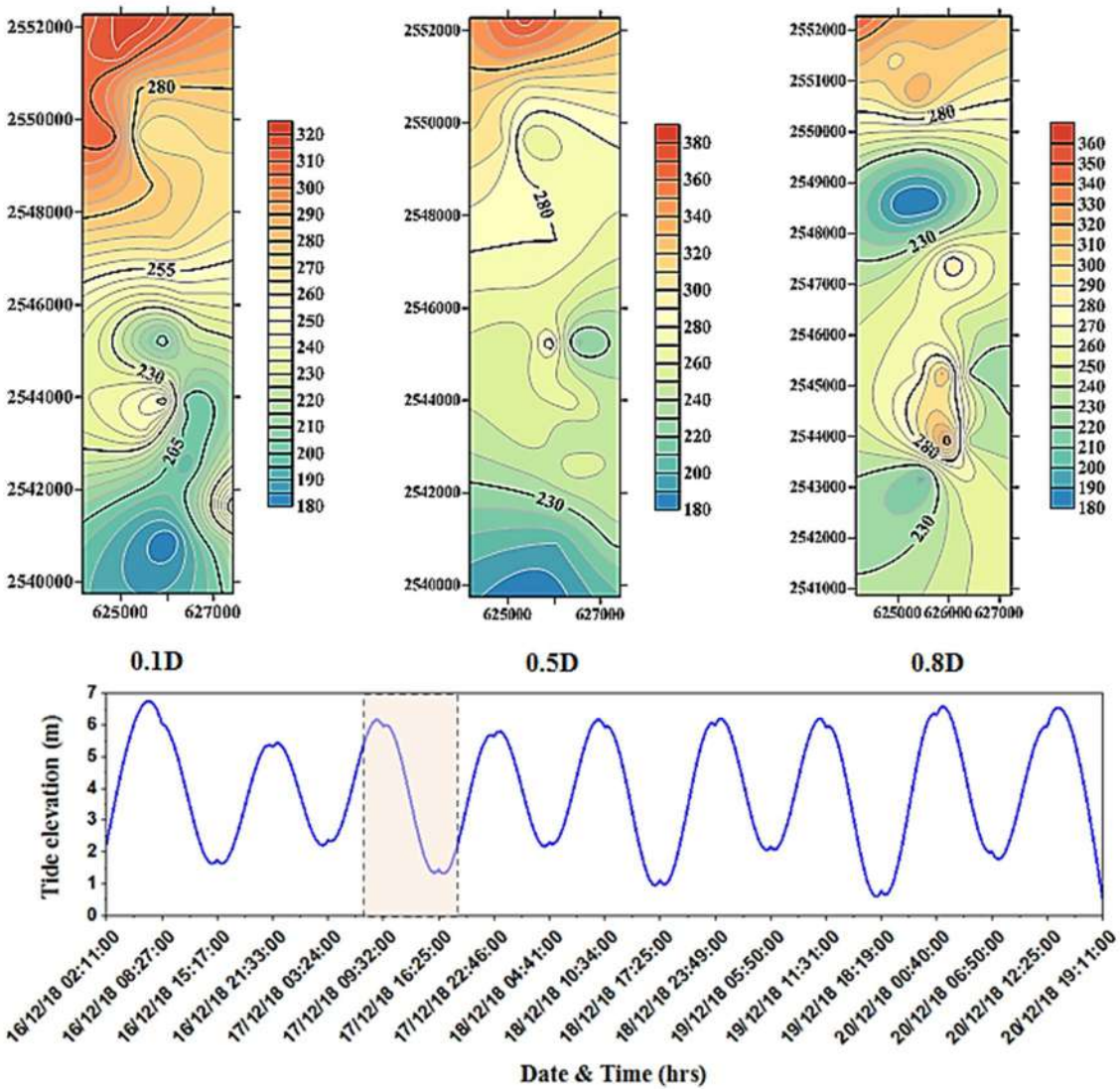


**Fig. 4.56 Contours of SSC at three different depths for 17/12/2018**

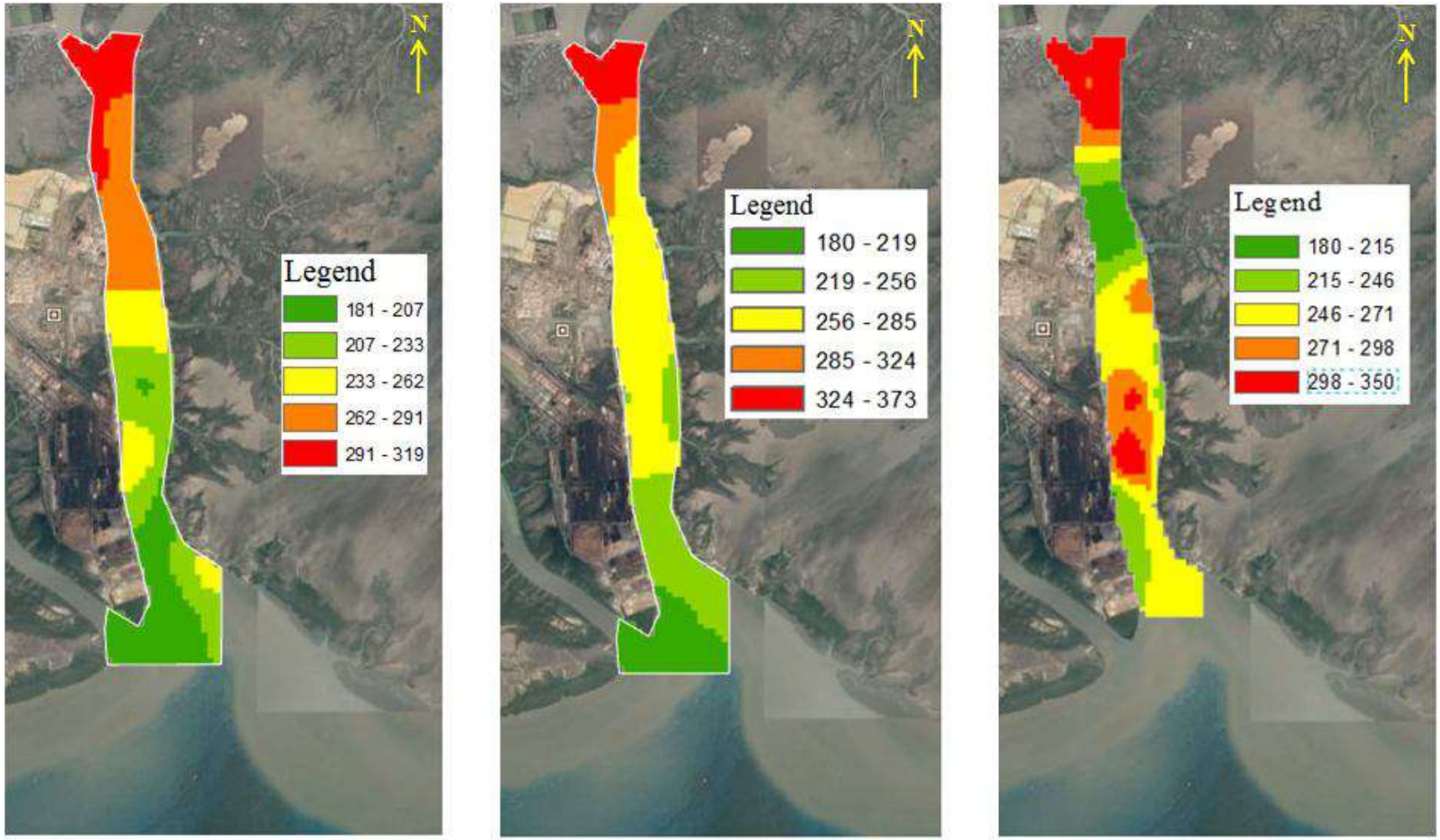


**Fig. 4.57 Spatial spread of measured SSC inside creek (17/12/2018)**

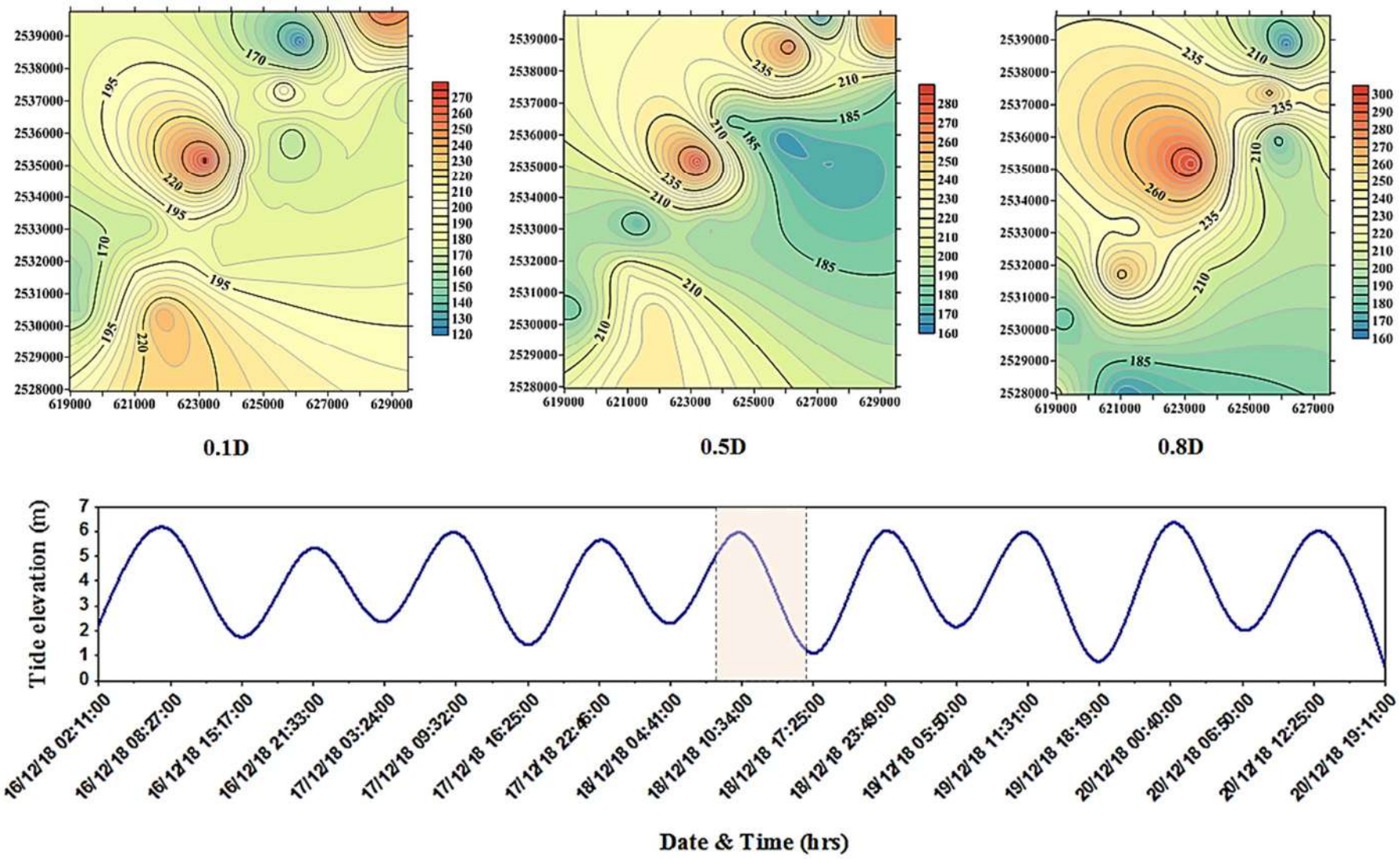


**Fig. 4.58 Contours of SSC at three different depths for 18/12/2018**

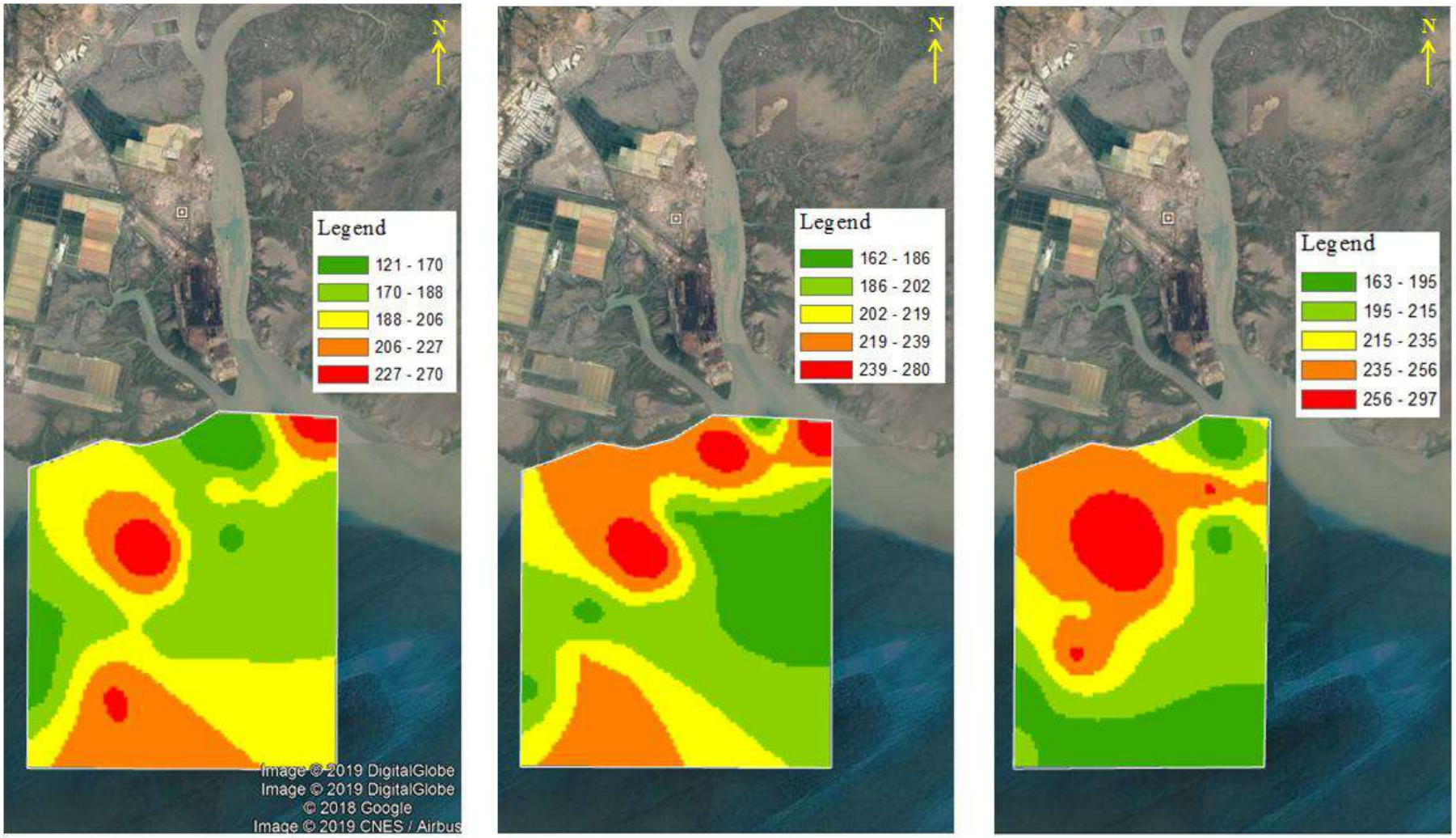


**Fig. 4.59 Spatial spread of measured SSC outside creek (18/12/2018)**

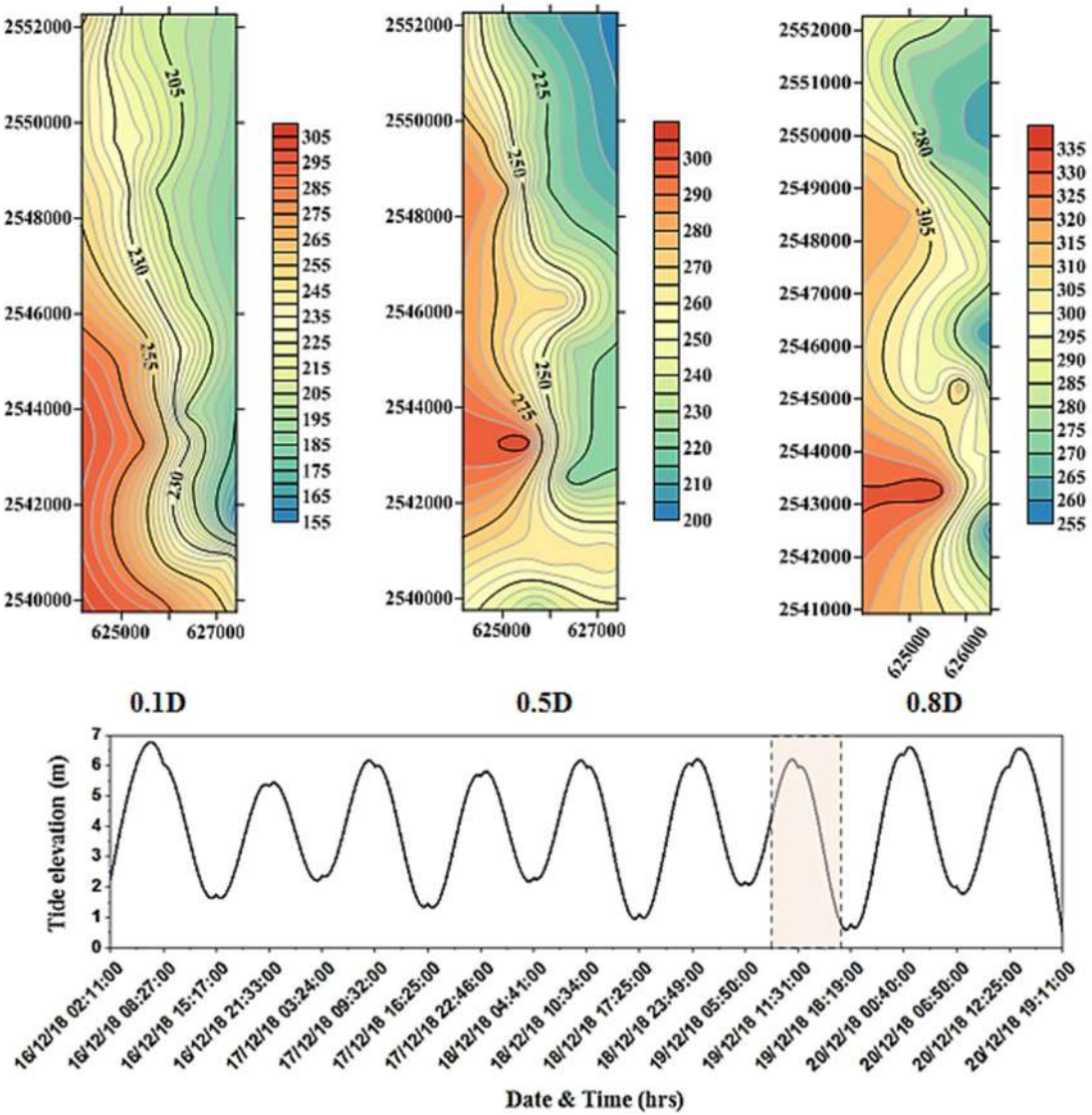


**Fig. 4.60 Contours of SSC at three different depths for 19/12/2018**

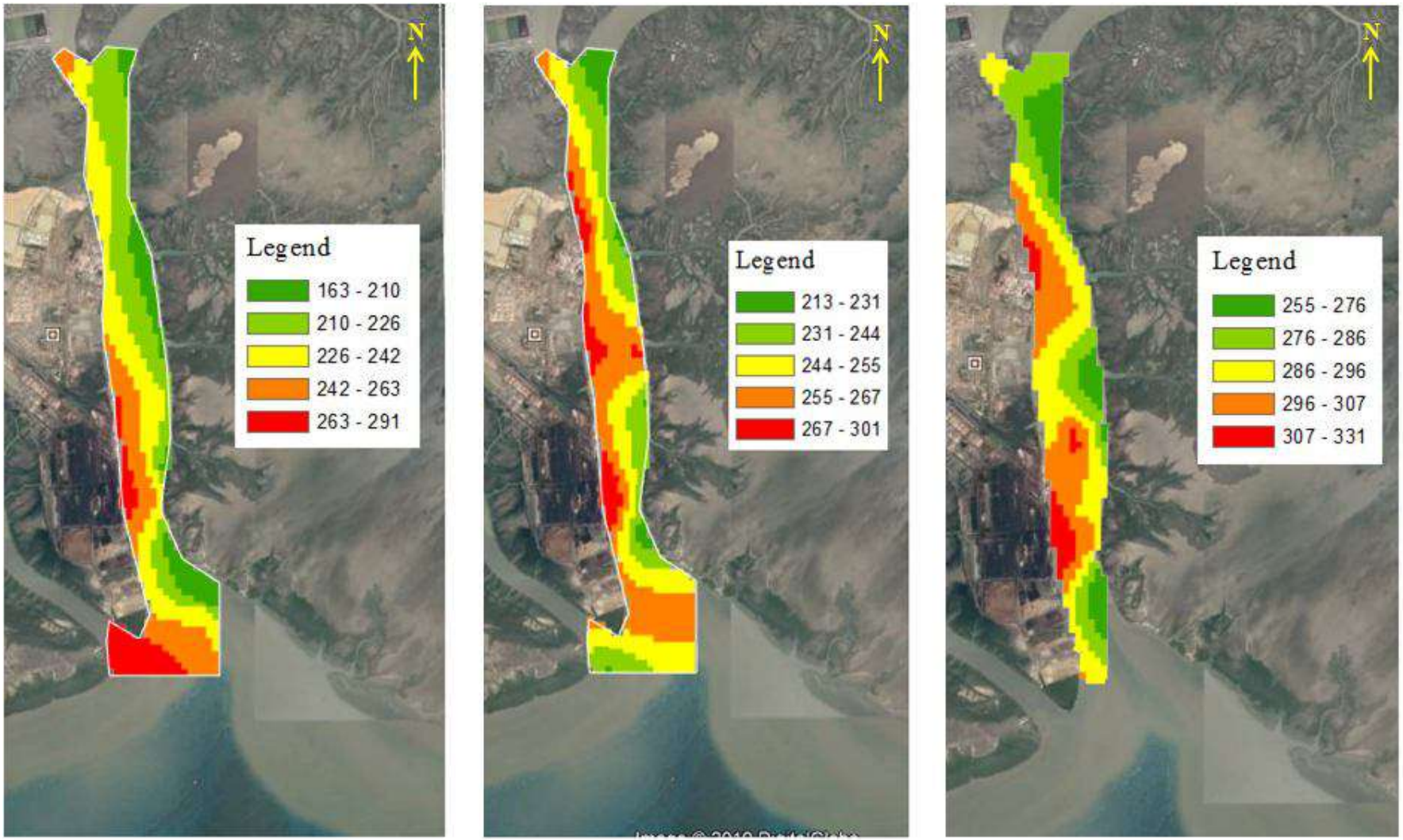


**Fig. 4.61 Spatial spread of measured SSC inside creek (19/12/2018)**

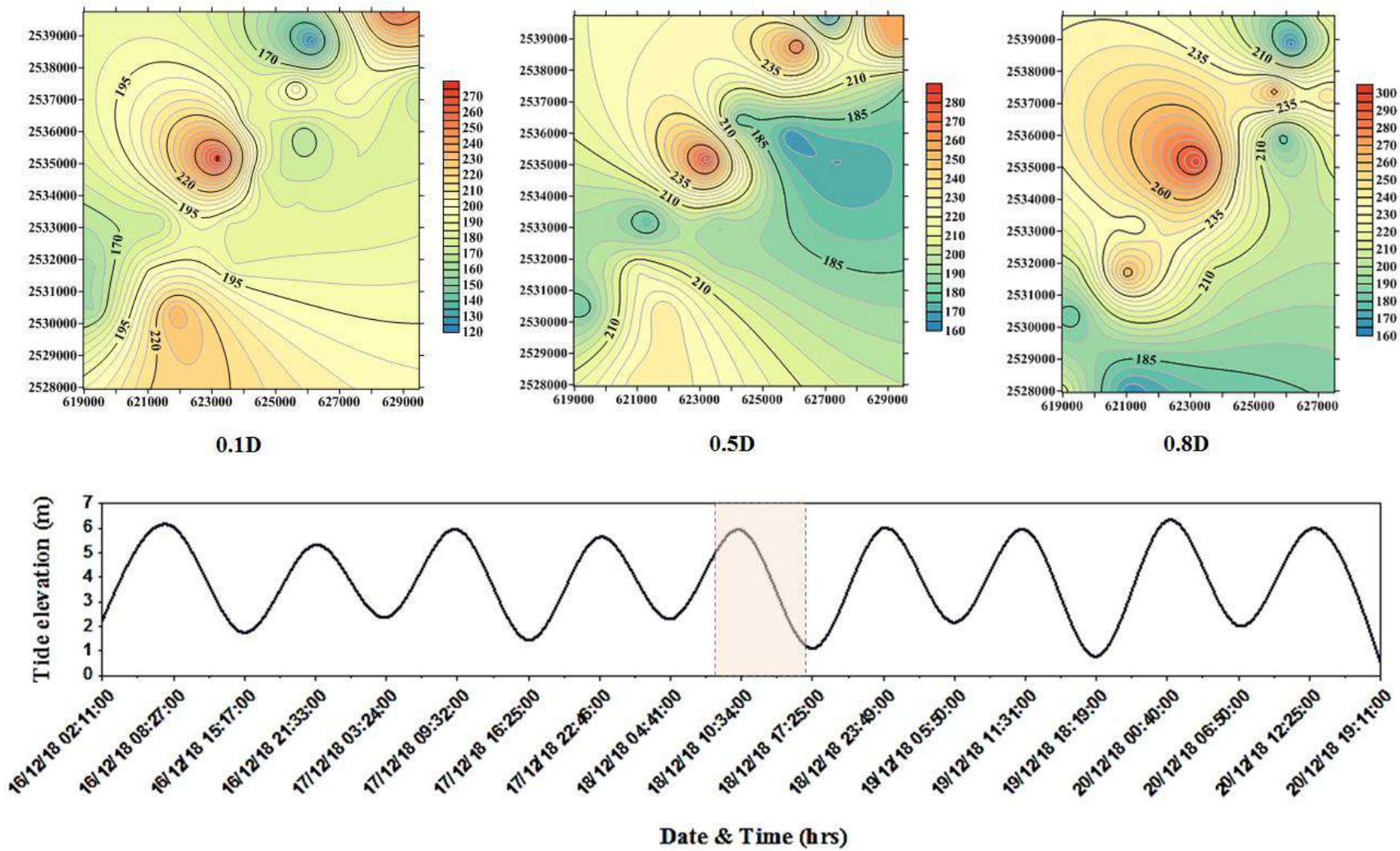


**Fig. 4.62 Contours of SSC at three different depths for 20/12/2018**

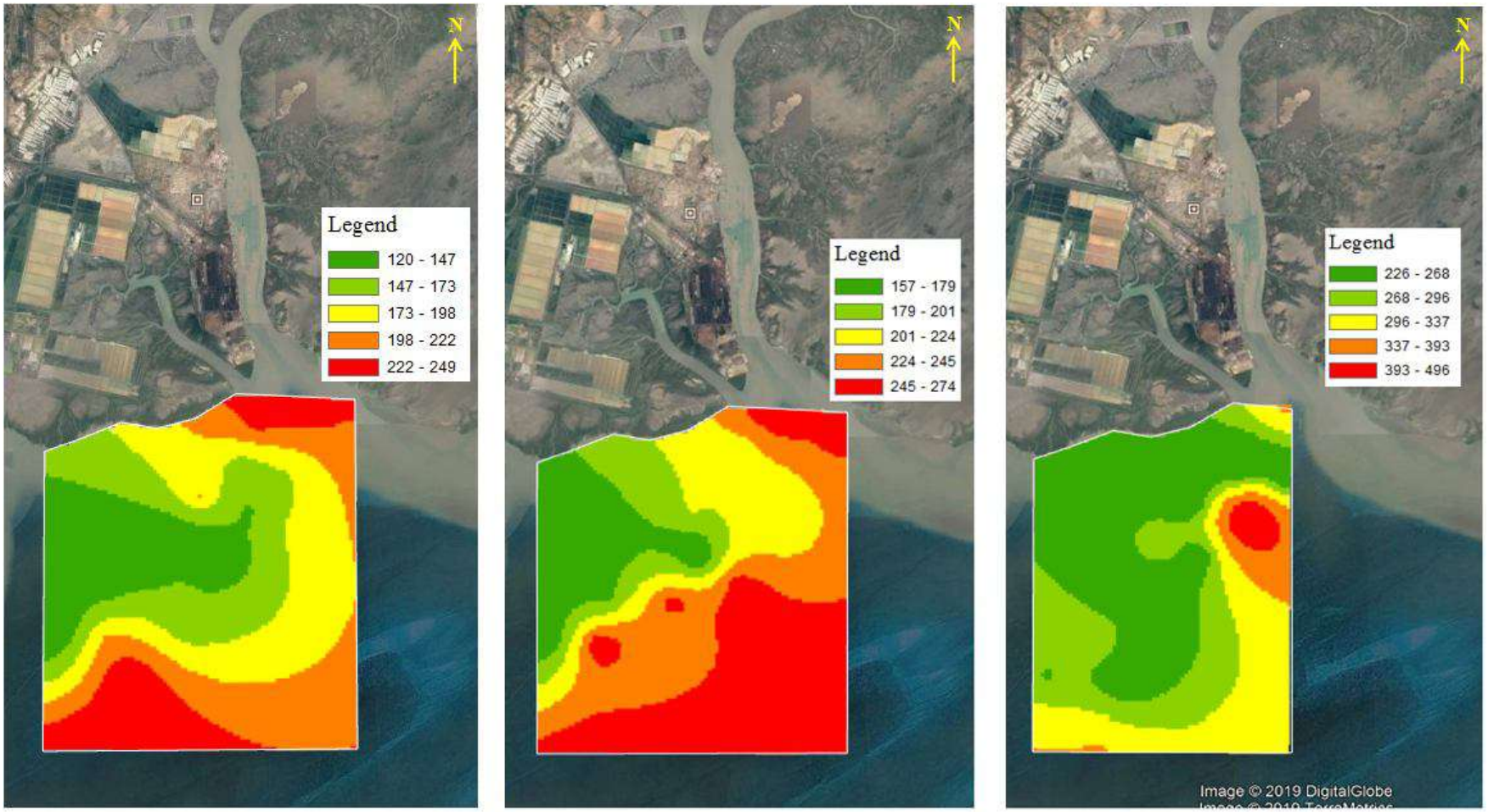


**Fig. 4.63 Spatial spread of measured SSC outside creek (20/12/2018)**

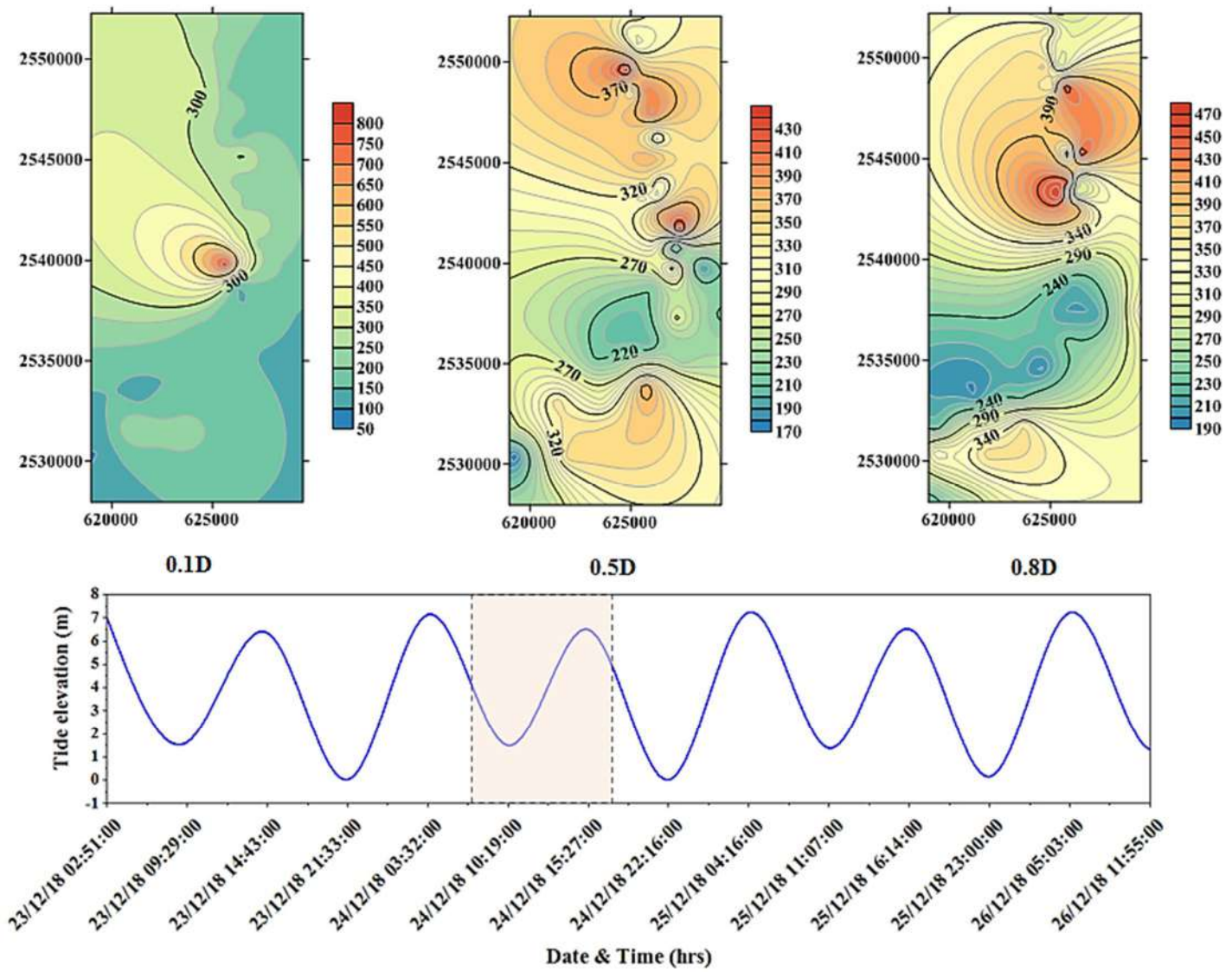


**Fig. 4.64 Contours of SSC at three different depths for 24/12/2018**

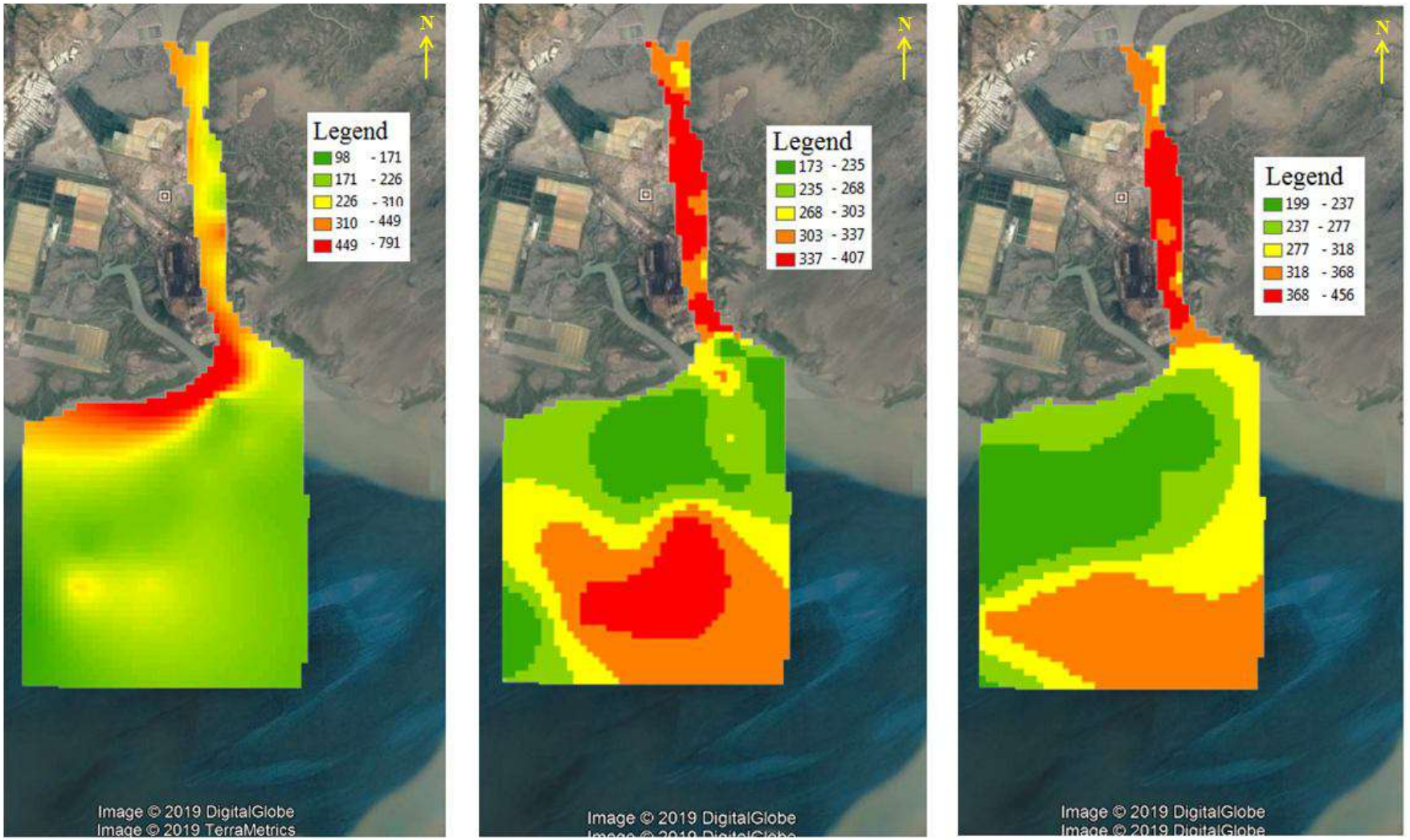


**Fig. 4.65 Spatial spread of SSC (24/12/2018)**

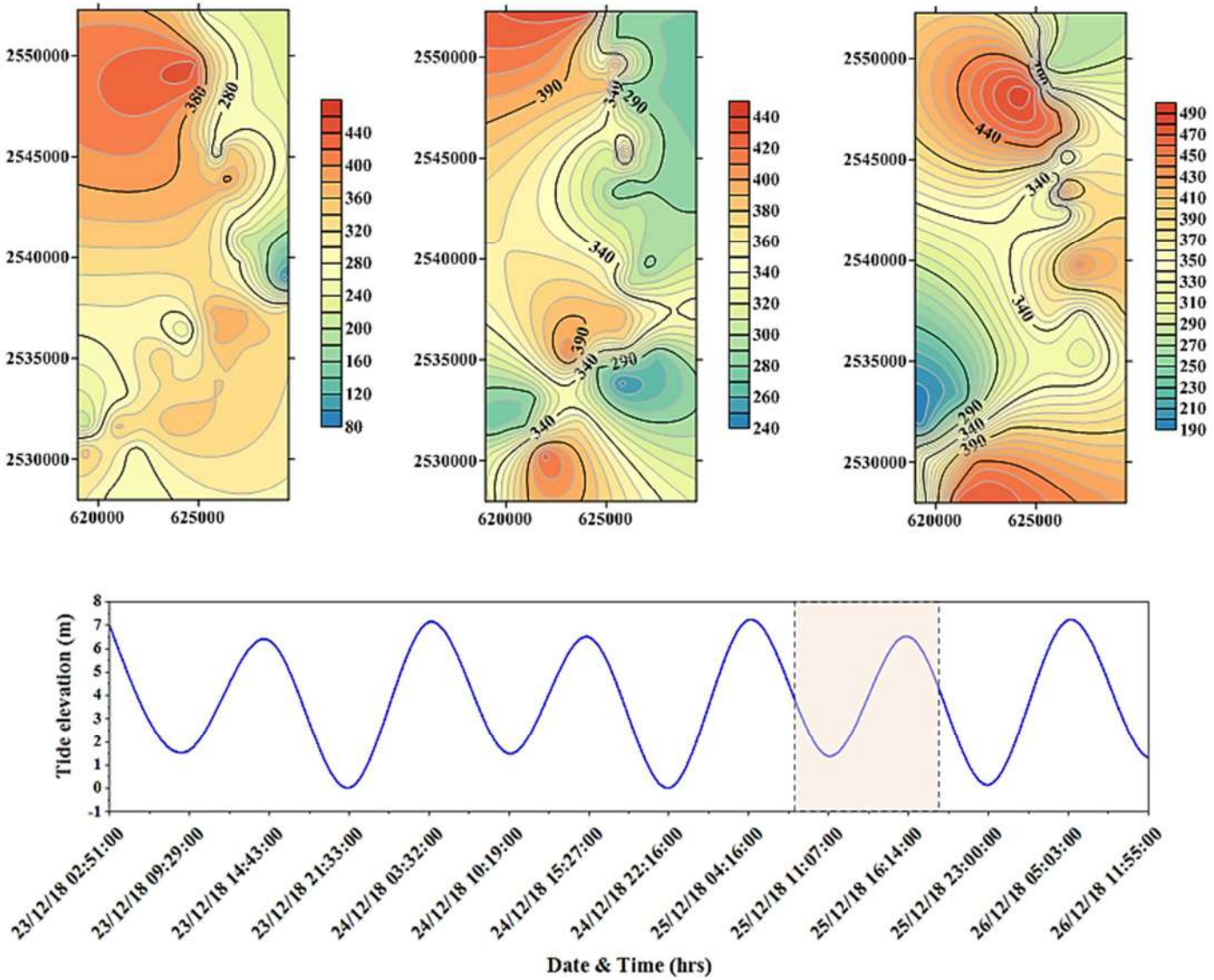


**Fig. 4.66 Contours of SSC at three different depths for 25/12/2018**

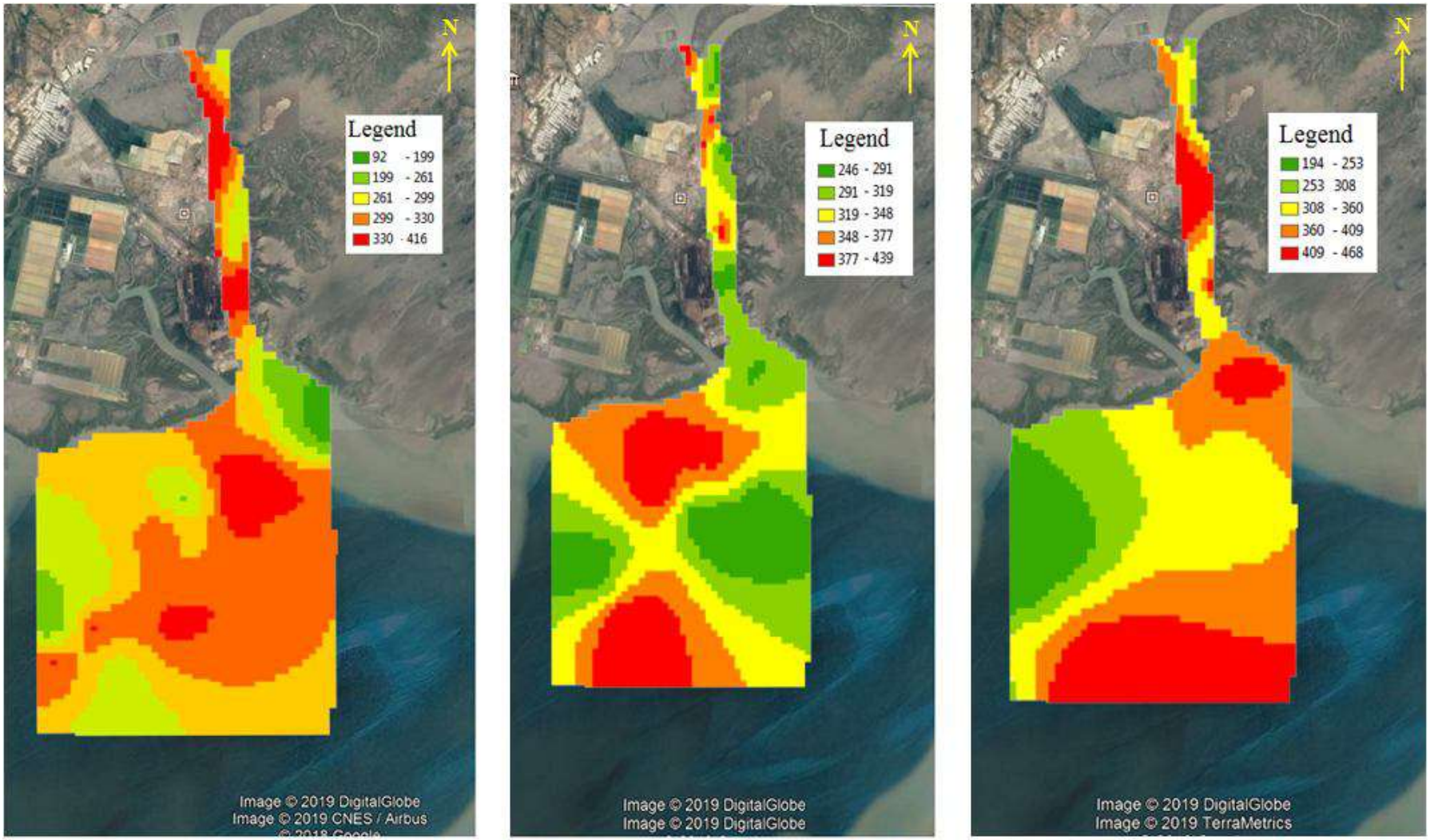


**Fig. 4.67 Spatial spread of measured SSC (25/12/2018)**

In addition to above contour plots, following plots individually depict the variation of SSC at inner point (L1) of the creek (Fig. 4.50), mouth of the creek (L21) and at a point outside the creek (L43 – Fig. 4.51) for each session.

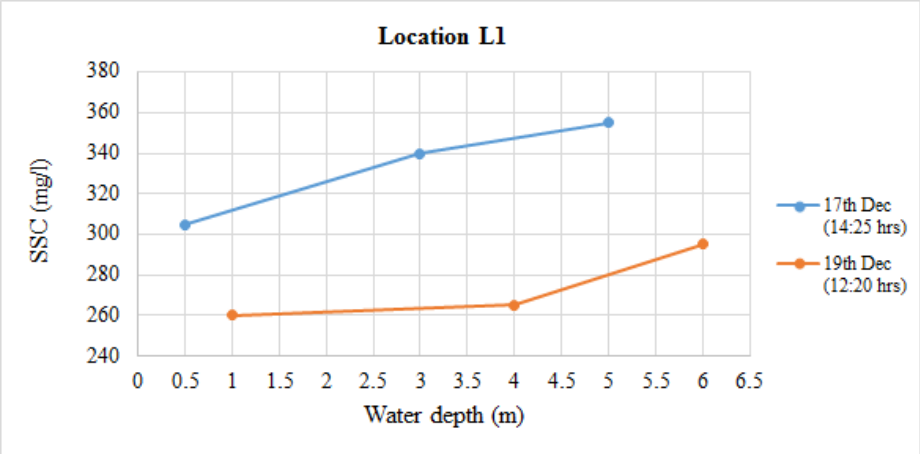


**Fig. 4.68 Variation of SSC on inner point of creek (L1) for session 1 experiment**

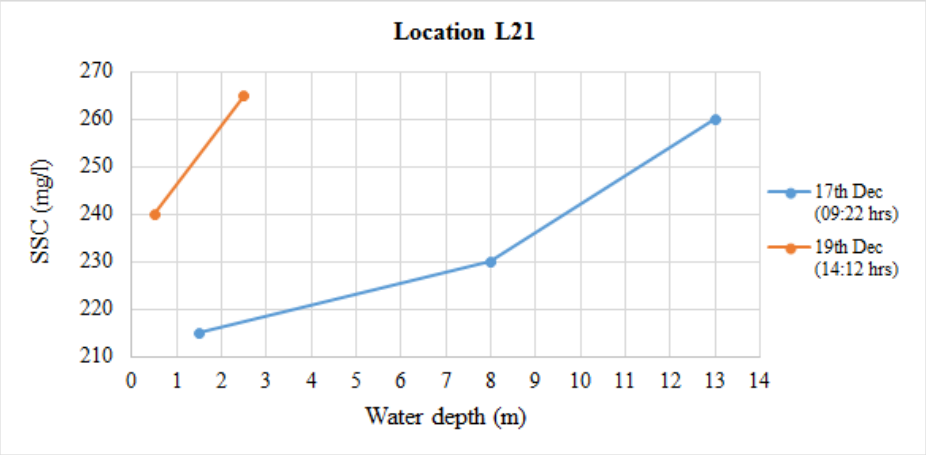


**Fig. 4.69 Variation of SSC on mouth of creek (L21) for session 1 experiment**

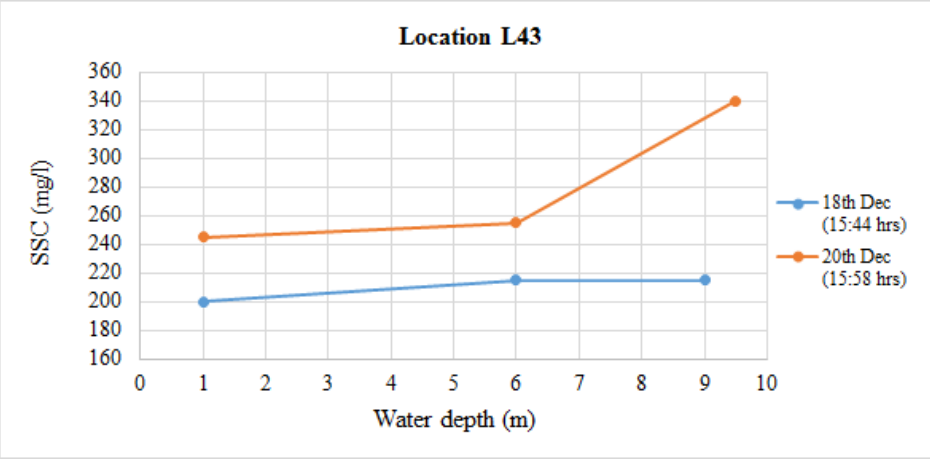


**Fig. 4.70 Variation of SSC outside of creek (L43) on session 1 experiment**

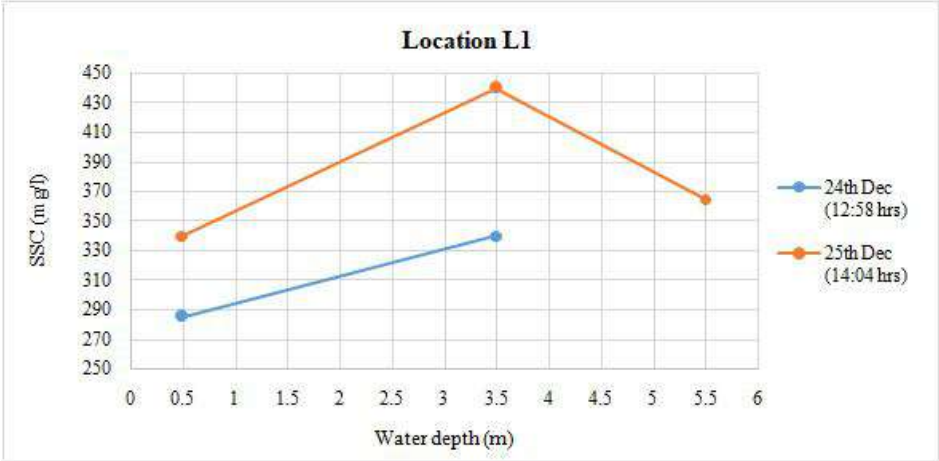


**Fig. 4.71 Variation of SSC on inner point of creek (L1) for session 2 experiment**

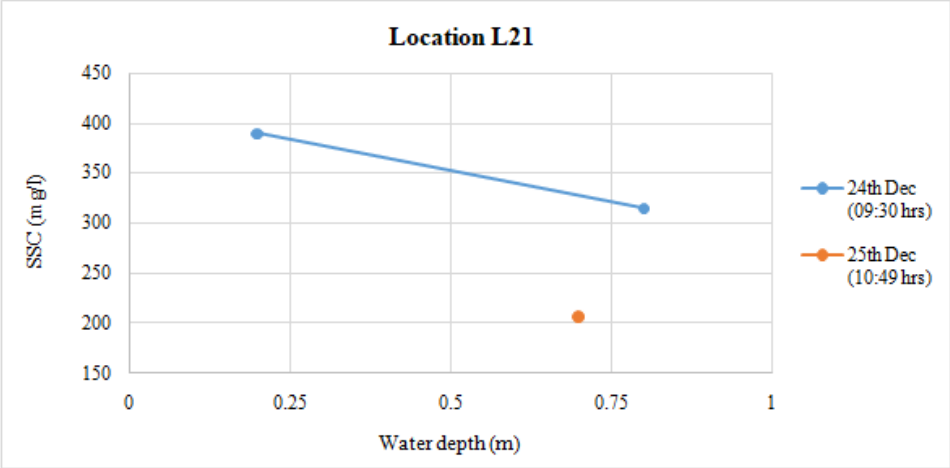


**Fig. 4.72 Variation of SSC on mouth of creek (L21) for session 2 experiment**

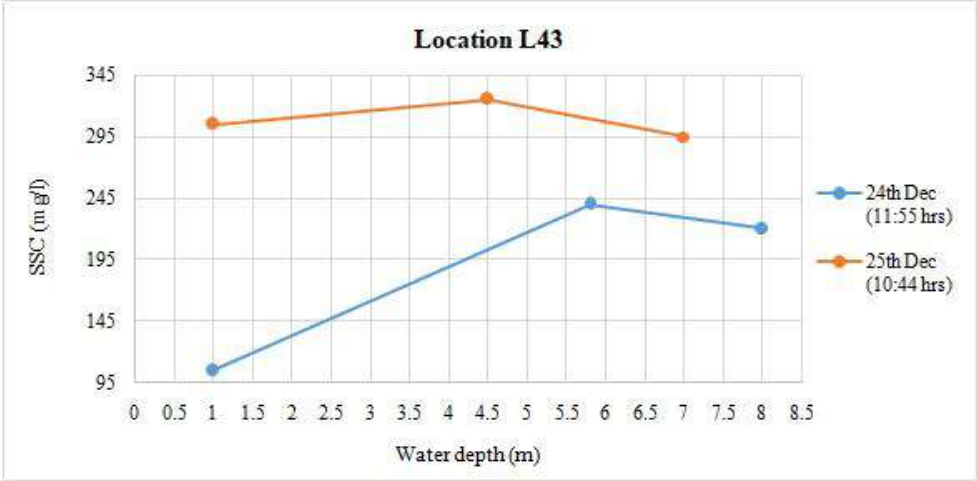


**Fig. 4.73 Variation of SSC outside of creek (L43) for session 2 experiment**

From the above plots, it can be inferred that maximum suspended sediment concentration could be ascertained during low tide than high tide. However, maximum SSC for three locations L1, L21 and L43 are observed to be 440 mg/l (middle), 390 mg/l (surface) and 340 mg/l (bottom) respectively.

***Drifter Experiment***

The setup consists of a GPS transmitter, receiver, drifters and driftrek software. Initially the instrument was setup by entering the co-ordinates and time zone of the current position in the drifttek software. Then the interval at which the drifter was supposed to transmit the data was also specified in the software. Fig. 4.74 shows the typical instrumental setup used for the methodology.

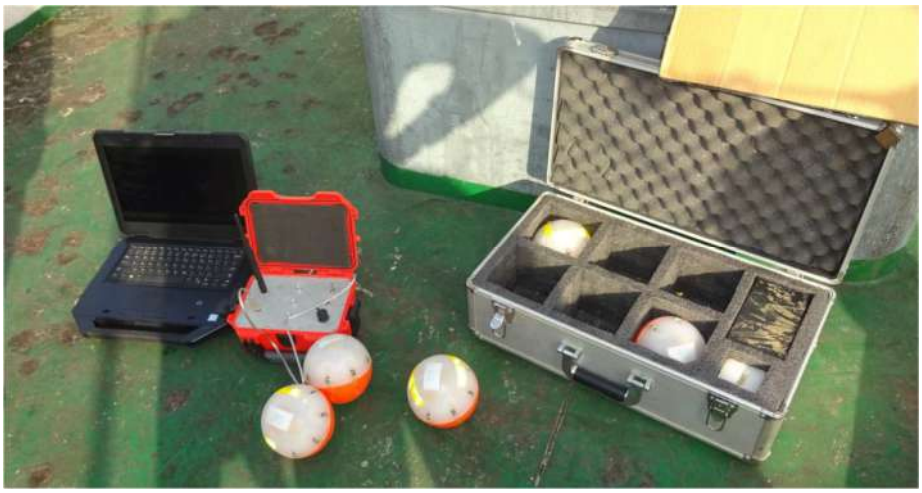

**Fig. 4.74 Typical Drifter instrumental set-up**

After the initial setup, the drifters were deployed into the water noting down the time and position for the corresponding location. The drifter was found to be moving in the direction of flow (Fig. 4.75). The position of the drifters was being continuously updated by the GPS on the driftrek software. These drifters were later on collected using a collecting net.

**Fig. 4.75 Movement of Drifters**

The experiments were conducted on 17th and 18th December as well as on 24th and 25th December using a raw boat. After completing the initial instrumental setup, the drifters were deployed at different locations considering ebb and flood tidal flow. The data's which were recorded in the software were then exported into excel format removing all the incorrect values due to disturbances and then post-processed using Matlab software finally plotted to a figures as shown below.

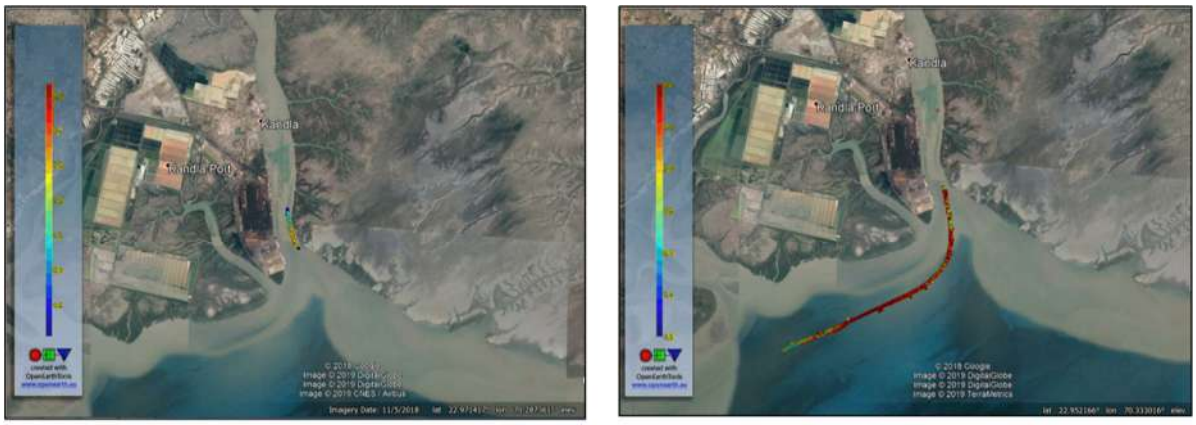

(a) Flood (b) Ebb

**Fig. 4.76 Typical drifter trajectories on 17th Dec 2018**

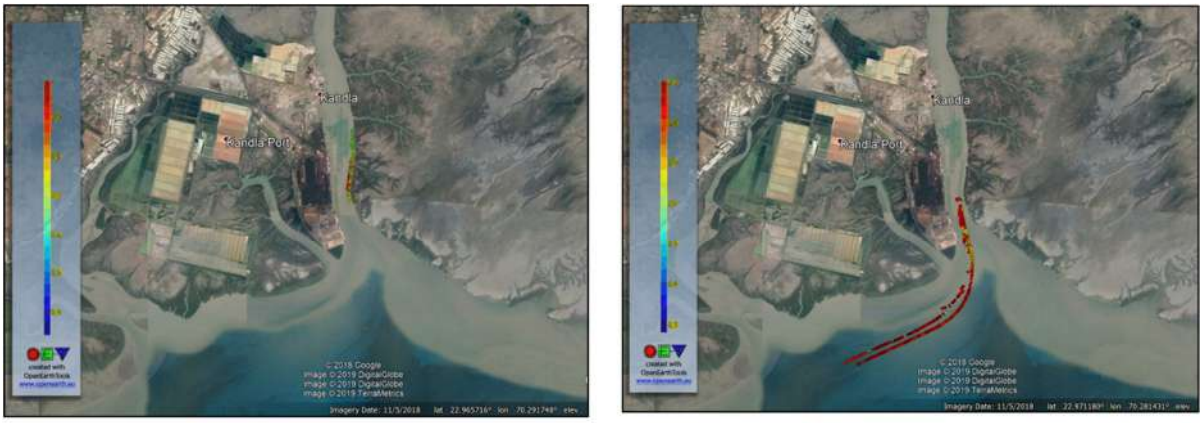


(a) Flood (b) Ebb

**Fig. 4.77 Typical drifter trajectories on 18th Dec 2018 during flooding and ebbing tide**


(a) Flood

**Fig. 4.78 Typical drifter trajectories on 24th Dec 2018 during flooding**

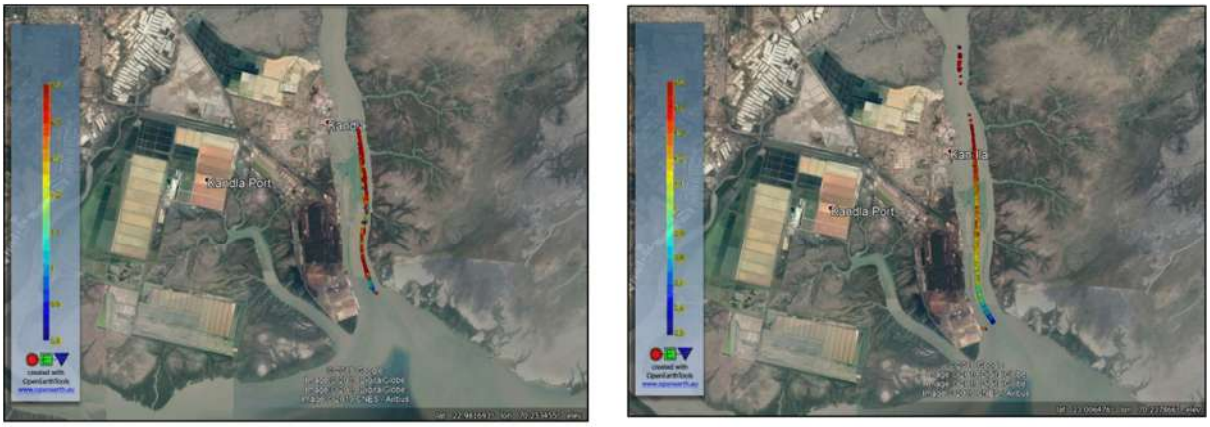


(a) Flood (b) Ebb

**Fig. 4.79 Typical drifter trajectories on 25th Dec 2018 during flooding and ebbing tide**

# 5. REMOTE SENSING BASED TSM ESTIMATION

## 5.1 Introduction

In the coastal environment, the distribution and flux of suspended sediment is highly variable spatially and temporally. This makes the conventional field sampling technique inadequate in studies related to sediment dynamics. Remote sensing can play a valuable role in this regard due to synoptic coverage as well as availability of datasets at variable spatial and temporal scales. A number of studies have been conducted in this regard that demonstrate the potential of satellite remote sensing for sediment transport studies (Tassan and Sturm 1986; Tassan 1994; Kelmas et al. 1974; Warrick et al. 2007; Chauhan et al. 1996). In the current study, TSM is estimated using linear regression between in-situ measurements and satellite reflectance obtained from MODIS Terra 250m band 1 data. The objective is to derive TSM maps that enable to understand the suspended sediment dynamics in this region.

Near-daily MODIS true colour mosaic imagery provide a simple and rapid way to observe the sediment character remotely. MODIS data can be used in a number of ways ranging from observing atmospheric conditions to terrestrial and oceanic processes with pixel resolutions ranging from 1×1 km to 250×250 m pixels at nadir. NASA Ocean color provides MODIS imagery in raw format or as processed mosaic georeferenced true colour enhanced imagery, making it very accessible for product generation or visual interpretation.

## 5.2 Data Processing and Methodology

MODIS data were processed using the SeaWiFS Data Analysis System (SeaDAS) to produce atmospherically corrected band 1 (645 nm) remote sensing reflectance. The MODIS sensors, on board the Terra (EOS AM-1) and Aqua (EOS PM-1) satellites, achieve near-daily global coverage, capturing data across 36 spectral bands is shown in

Table 5.1 (Land Processes Distributed Active Archive Center). The methodology to convert the MODIS raw data to assess sediment character is shown in Fig. 5.3. In this report, the

MODIS raw data was processed to various levels like MODIS Level 1A, MODIS GEO, MODIS Level 1B and Level 2. Further, MODIS Level 2was used to calculate suspended sediment from regionally tuned empirical models to provide quantitative estimates of sediment load.

***MODIS Level 0***

The MODIS Level-0 Production Data Set (PDS) is the raw instrument package consisting of a 5-minute swath of data. It is used to produce calibrated and geo-located MODIS radiances, or Level-1 data.

***MODIS Level 1A***

In MODIS Level 1A, the reconstructed, unprocessed instrument data at full resolution, time-referenced, and annotated with ancillary information, including radiometric and geometric calibration coefficients and geo-referencing parameters are computed and appended. The Level-1A data are used as input for geolocation, calibration, and processing. Quality indicators are added to the data to indicate missing or bad pixels and instrument modes.

***MODIS GEO***

The geolocation fields include geodetic Latitude, Longitude, surface height above geoid, solar zenith and azimuth angles, satellite zenith and azimuth angles, and a land/sea mask for each 1 km sample. Additional information is included in the header to enable the calculation of the approximate location of the center detectors of any of the 36 MODIS bands.

***MODIS Level 1B***

Level 1A data was processed to sensor units. The Level-1B data products contain calibrated radiances for all 36 MODIS bands and reflectance's for the reflective Solar bands (Bands 1 through 19 and 26). The processed Level 1B image is shown in Fig. 5.1.

***MODIS Level 2***

Level 2 data consist of derived geophysical variables at the same resolution and location as Level 1 source data (Fig. 5.2). At level 2, the data was converted into more useful parameters and formats. Additional data were provided, including quality flags, error estimates, and calibration data in the MODIS Level 2.

**Table 5.1 MODIS Spectral Bands (LP DAAC)**

| Band | Range Reflected (nm) | Range Emitted (um) | Key use |
|---|---|---|---|
| 1 | 620–670 | | Absolute Land Cover Transformation, Vegetation Chlorophyll |
| 2 | 841–876 | | Cloud Amount, Vegetation Land Cover Transformation |
| 3 | 459–479 | | Soil/Vegetation Differences |
| 4 | 545–565 | | Green Vegetation |
| 5 | 1230–1250 | | Leaf/Canopy Differences |
| 6 | 1628–1652 | | Snow/Cloud Differences |
| 7 | 2105–2155 | | Cloud Properties, Land Properties |
| 8 | 405–420 | | Chlorophyll |
| 9 | 438–448 | | Chlorophyll |
| 10 | 483–493 | | Chlorophyll |
| 11 | 526–536 | | Chlorophyll |
| 12 | 546–556 | | Sediments |
| 13 | 662–672 | | Atmosphere, Sediments |
| 14 | 673–683 | | Chlorophyll Fluorescence |
| 15 | 743–753 | | Aerosol Properties |
| 16 | 862–877 | | Aerosol Properties, Atmospheric Properties |
| 17 | 890–920 | | Atmospheric Properties, Cloud Properties |
| 18 | 931–941 | | Atmospheric Properties, Cloud Properties |
| 19 | 915–965 | | Atmospheric Properties, Cloud Properties |
| 20 | | 3.660–3.840 | Sea Surface Temperature |
| 21 | | 3.929–3.989 | Forest Fires & Volcanoes |
| 22 | | 3.929–3.989 | Cloud Temperature, Surface Temperature |
| 23 | | 4.020–4.080 | Cloud Temperature, Surface Temperature |
| 24 | | 4.433–4.498 | Cloud Fraction, Troposphere Temperature |
| 25 | | 4.482–4.549 | Cloud Fraction, Troposphere Temperature |
| 26 | 1360–1390 | | Cloud Fraction (Thin Cirrus), Troposphere Temperature |
| 27 | | 6.535–6.895 | Mid Troposphere Humidity |
| 28 | | 7.175–7.475 | Upper Troposphere Humidity |
| 29 | | 8.400–8.700 | Surface Temperature |
| 30 | | 9.580–9.880 | Total Ozone |
| 31 | | 10.780–11.280 | Cloud Temperature, Forest Fires & Volcanoes, Surface Temp. |

| | | | |
|---|---|---|---|
| 32 | | 11.770–12.270 | Cloud Height, Forest Fires & Volcanoes, Surface Temperature |
| 33 | | 13.185–13.485 | Cloud Fraction, Cloud Height |
| 34 | | 13.485–13.785 | Cloud Fraction, Cloud Height |
| 35 | | 13.785–14.085 | Cloud Fraction, Cloud Height |
| 36 | | 14.085–14.385 | Cloud Fraction, Cloud Height |

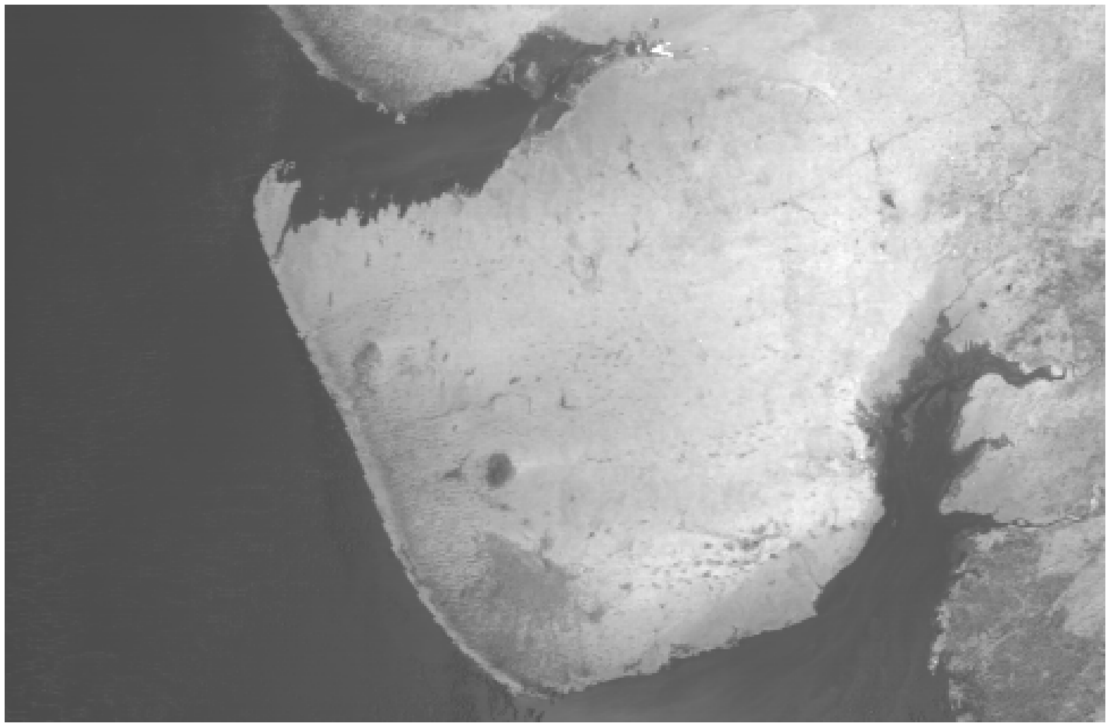

**Fig. 5.1 MODIS Level 1B processed image**

**Fig. 5.2 MODIS Level 2 flag image**

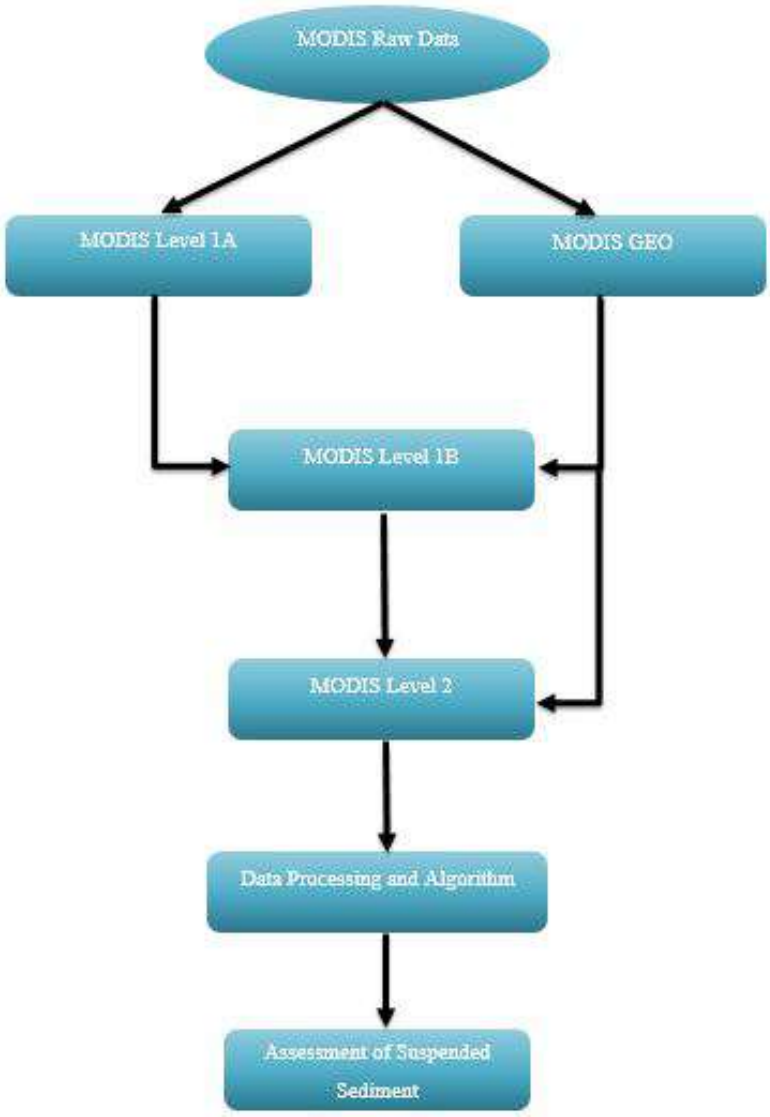


**Fig. 5.3 Flow chart of MODIS data analyzing process**

## 5.3 Data

### *In-situ Measurements*

Surface samples of the water, using Niskin water sampler was collected throughout the in-situ measurement campaign. For analyzing the collected water samples for suspended sediment concentration, Gooch filtration method was adopted which is a standardized methodology. In the filtration technique, a well-mixed sample of seawater was poured into the Gooch crucible and filtered through a weighed standard glass-fiber filter, also called a Gooch filter. In the present study, Whatman 934-AH (47mm-gooch) filter papers were used for this purpose. The residue obtained on the filter was dried to a constant weight at 103 °C for 1 hour, using an oven. After the samples were completely dried, weight of the filter paper was subtracted from

the oven-dried sample weight to obtain the amount of suspended sediment in grams per litter of sample.

***Moderate Resolution Imaging Spectro-Radiometer (MODIS) Data***

The MODIS instrument operates on both Terra and AQUA spacecraft and has a viewing swath of 2,330km which views the entire surface of the earth every 1-2 days. The detectors acquire data in 3 spatial resolutions 250m, 500m, and 1000m and measure 36 spectral bands between 0.405 and 14.385 µm. In this study, available MODIS terra satellite data corresponding to field measurements dates (18,19,20 and 25) were downloaded and used for the analysis. A literature survey conducted prior to this analysis clearly suggests that MODIS data sets can be used extensively for TSM related studies. This is because of the characteristic of MODIS band 1, such as its resolution, red band reflectance and near daily coverage, which makes it very suitable for studying suspended sediments in the coastal region (Misra et al. 2014).

## 5.4 Methodology

The minimum depths attained while field sampling was 0.5m and 1 m while 79 points belong to these depth classes. As reflectance shows relation only when surface samples were chosen, hence, finally only 31 points showed relationship between satellite and in-situ measurement. By applying linear regression with these points, a model was devised to predict satellite derived TSM values as shown in Fig. 5.4.

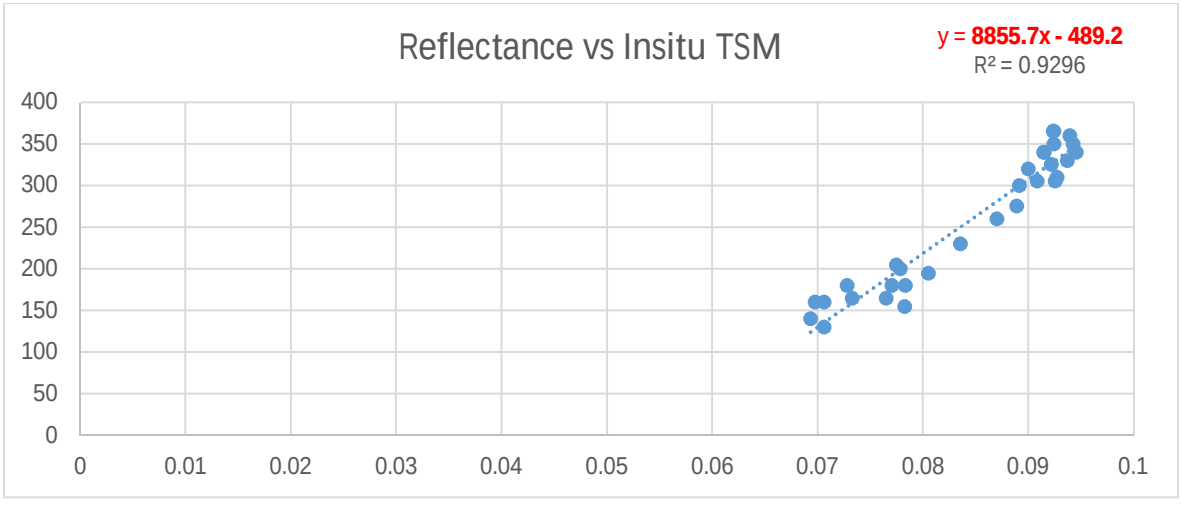


**Fig. 5.4 Linear model developed for study region**

Further, the results obtained from the linear model were compared with the algorithm proposed by Miller and Mckee (2004) given below -

$$TSM = -1.91 + 1140.25 * (MODIS\ band\ 1\ Refelctance) \quad (1)$$

## 5.5 Results

The Table 5.2 typically gives the RMSE obtained for each dataset. The results of the linear algorithm and widely used Mill and McKee (2004) algorithm were compared with each other and it was seen that the former provides better results. Based on this, the final maps for the dates 18th, 19th, 20th and 25th December 2018 were generated as shown in Fig. 5.5.

**Table 5.2 Prediction accuracy of the linear model compared with Miller and Mckee algorithm**

| | No of Valid depth points | Linear Algorithm Based – RMSE(mg/l) | Miller and Mckee 2004 algorithm - RMSE(mg/l) |
|---|---|---|---|
| 18th Dec 2018 | 21 | 57.85 | 117.9 |
| 19th Dec 2018 | 7 | 201.6 | 119 |
| 20th Dec 2018 | 15 | 82.99 | 112.3 |
| 25th Dec 2018 | 36 | 84.03 | 215.5 |

For 18th, 20th and 25th Dec 2018, the TSM values observed lie between 100-500mg/l. In case of 19th Dec 2018, the TSM value were higher (between 400-800mg/l). In all the images it can be clearly seen that there was a gradual decrease in TSM from west to east. It was evident from this analysis that satellite derived TSM maps can be used valuably for understanding the sediment dynamics in a region.

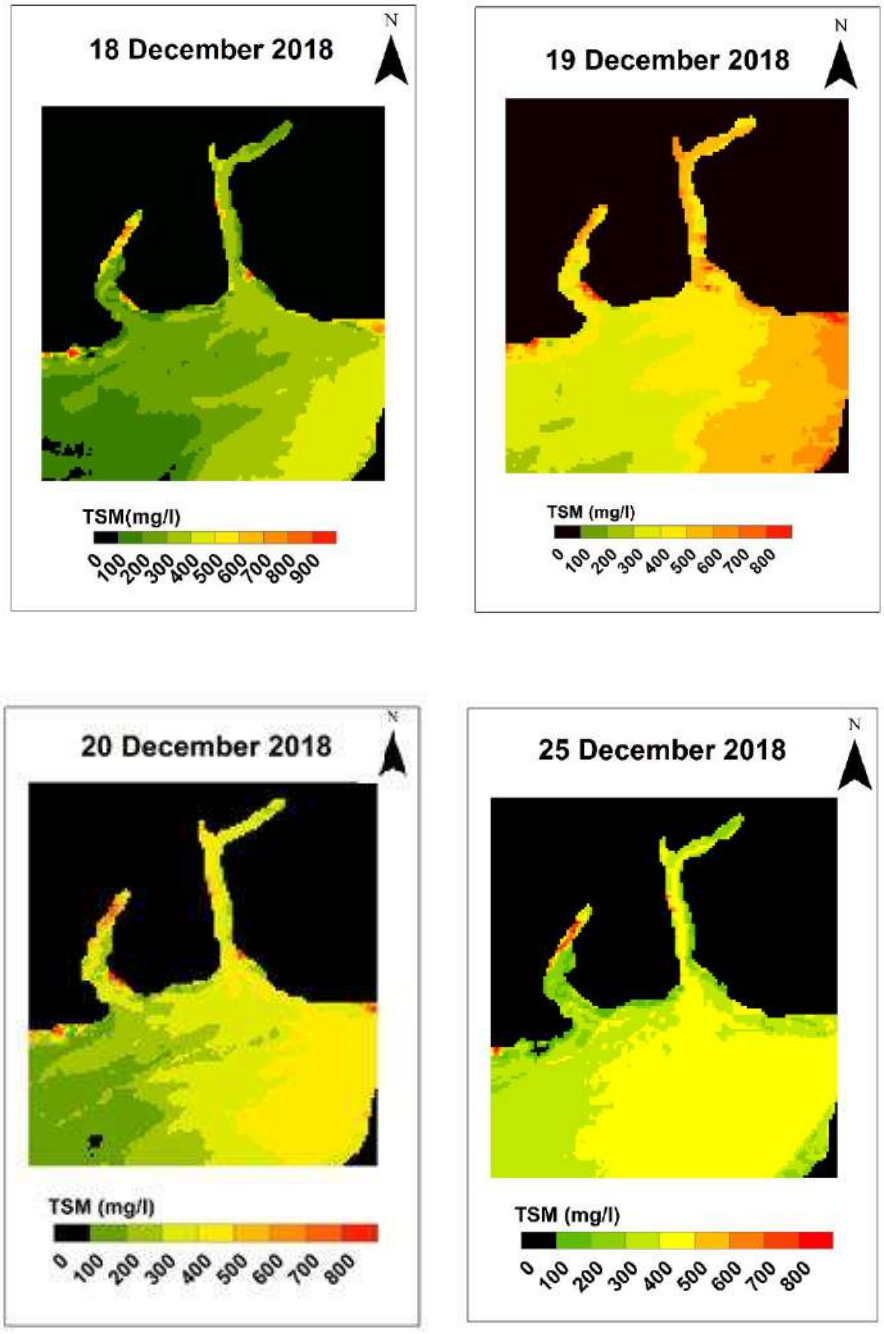


**Fig. 5.5 TSM maps for 18th, 19th, 20th and 25th of December 2018**

# 6. NUMERICAL MODELLING

## 6.1 Tidal Hydrodynamic Modelling

### 6.1.1 Model Description

The numerical modelling was carried out using Delft3D model. For modelling of hydrodynamics the Delft3D-Flow model was utilized. Delft3D-FLOW (Lesser et al, 2004) is a multi-dimensional (2D or 3D) hydrodynamic (and transport) simulation program which calculates non-steady flow and transport phenomena that result from tidal and meteorological forcing on a rectilinear or a curvilinear, boundary fitted grid using finite difference technique, with appropriate initial and boundary conditions. It solves the continuity, eqn. (1) and Navier Stokes eqn. (2 & 3) and advection-diffusion eqn. (7) for an incompressible fluid following the hydrostatic pressure and Boussinesq approximations.

$$\frac{\partial \eta}{\partial t} + \frac{\partial}{\partial x}(d+\eta)u + \frac{\partial}{\partial y}(d+\eta)v = 0 \quad (1)$$

$$\frac{\partial u}{\partial t} + u\frac{\partial u}{\partial x} + v\frac{\partial u}{\partial y} + g\frac{\partial \eta}{\partial x} - fv + \frac{\tau_x}{\rho_w(d+\eta)} - \frac{F_x}{\rho_w(d+\eta)} - \nu\left(\frac{\partial^2 u}{\partial x^2} + \frac{\partial^2 u}{\partial y^2}\right) = 0 \quad (2)$$

$$\frac{\partial v}{\partial t} + u\frac{\partial v}{\partial x} + v\frac{\partial v}{\partial y} + g\frac{\partial \eta}{\partial y} - fv + \frac{\tau_y}{\rho_w(d+\eta)} - \frac{F_y}{\rho_w(d+\eta)} - \nu\left(\frac{\partial^2 v}{\partial x^2} + \frac{\partial^2 v}{\partial y^2}\right) = 0 \quad (3)$$

where *u, v,* are the flow velocities in *x, y,* directions respectively; *f* is the Coriolis parameter; $\rho w$ is the reference density of water; $\tau_x$ and $\tau_y$ are bottom stress parameters; $F_x$ and $F_y$ are the external forces in x and y direction, respectively; $\nu$ is the vertical eddy viscosity.

For two-dimensional depth-averaged flow, the bottom stresses induced by the flow in Eq. (2) and Eq. (3) is governed by a quadratic friction law, given by

$$\tau_x = \frac{\rho g u|u|}{C^2} \quad (4)$$

$$\tau_y = \frac{\rho g v|v|}{C^2} \quad (5)$$

Where$u$and$v$ are the depth-averaged velocity in x and y directions respectively, and C is the Chezy's coefficient.

Under the shallow water assumption, which is valid for large horizontal scales, the vertical momentum equation is reduced to the hydrostatic pressure equation. Vertical accelerations due to buoyancy effects or sudden changes in bottom topography are neglected, and only

gravitational acceleration is taken into account. The hydrostatic pressure equation depicts pressure forces being balanced by weight of the water column, and is given by:

$$\frac{\partial P}{\partial z} \cong -\rho g \tag{6}$$

### 6.1.2 Model Methodology

The bathymetry values for the outer Kandla coast were extracted from GEBCO (General Bathymetric Charts of the Oceans) and inner creek values as well as the values for the approach channel of Kandla port were provided by Deendayal Port Trust. This values were combined with each other and used for the present study. The water depths were varying from 0m to 18m for the model domain as shown in Fig. 6.2. The model boundary line was extracted from shoreline database using Delft Dashboard. The grid used for the model simulation was with a spatial resolution of 115m throughout the domain as shown in Fig. 6.1. Offshore boundary input data is very important for developing numerical model. The boundary was forced with tidal astronomical constituents extracted from a TPXO7.1 global tidal database.

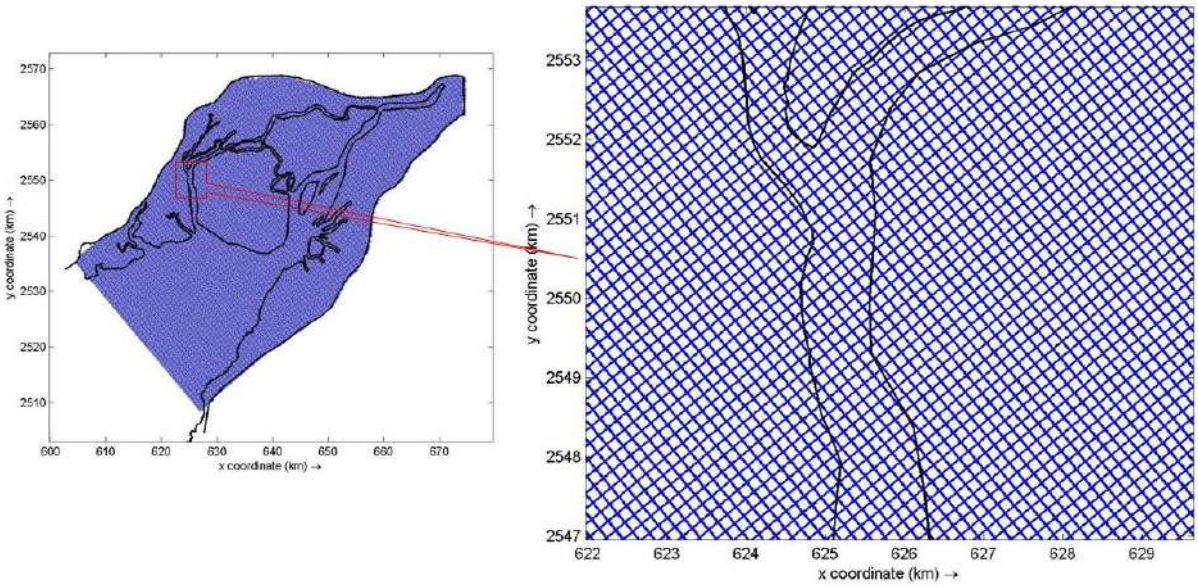


**Fig. 6.1 View of model grid**

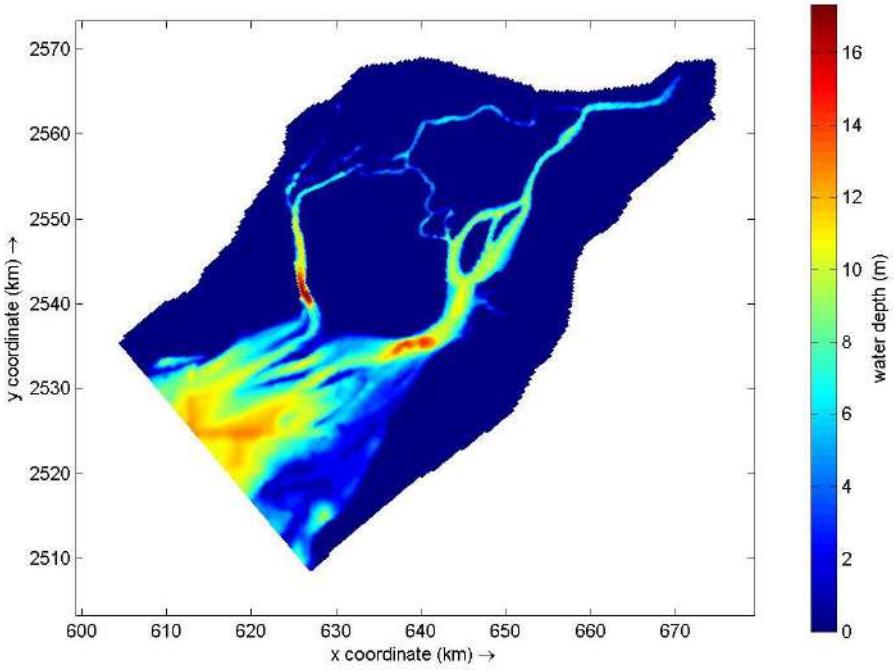


**Fig. 6.2 View of interpolated bathymetry**

### 6.1.3 Model results

The developed model has been simulated for 31 days from 01/12/2018 to 31/12/2018. The in-situ measurement has been conducted from 07/12/2018 to 28/12/2018. The estimated water levels, velocity and directions were extracted at three locations from model output, the contour plots of the water level variation, current velocity and current direction are shown in Fig. 6.7 to Fig. 6.10. Extracted data was compared with field measurement data using graphs as shown in Fig. 6.4 to Fig. 6.6. Observation points are as shown in Fig. 6.3.

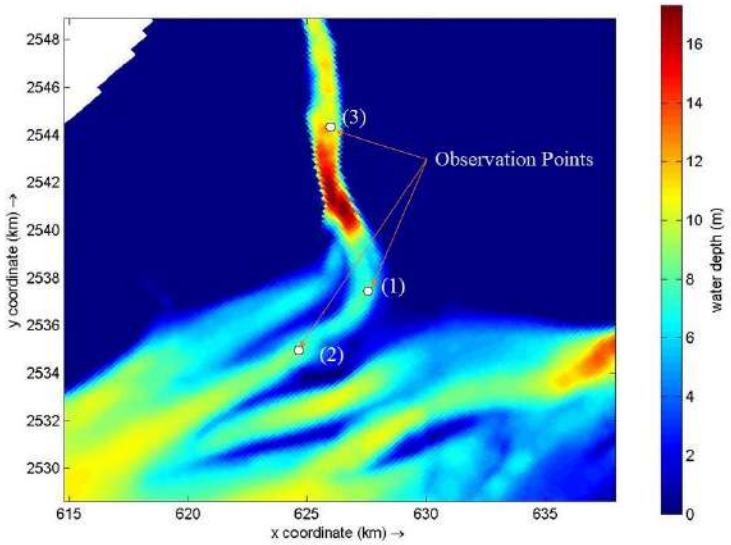


**Fig. 6.3 Observation points**

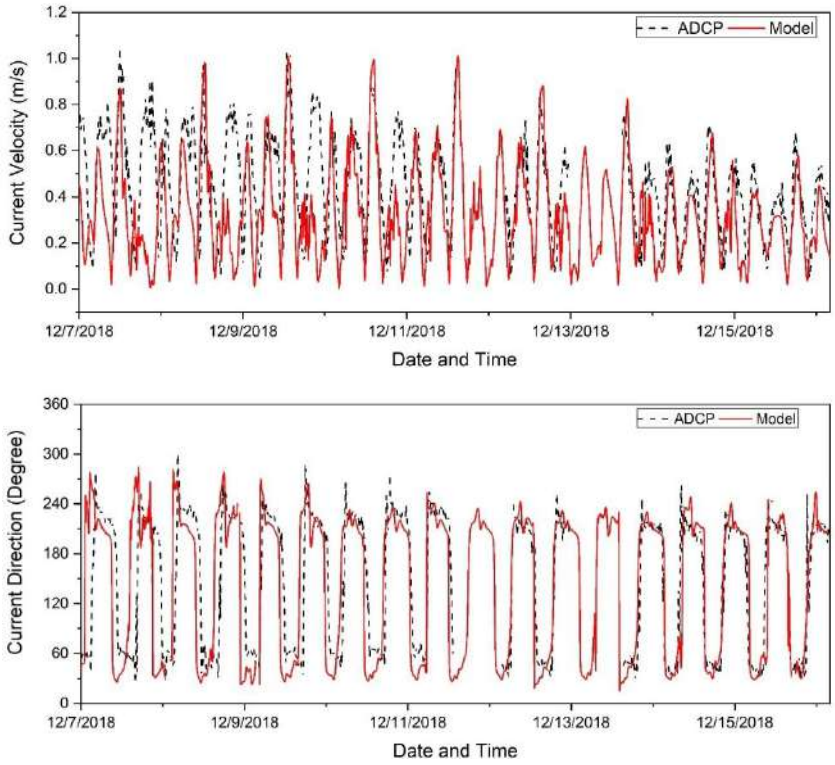


**Fig. 6.4 Comparison of current velocity and directions at 1st observation point**

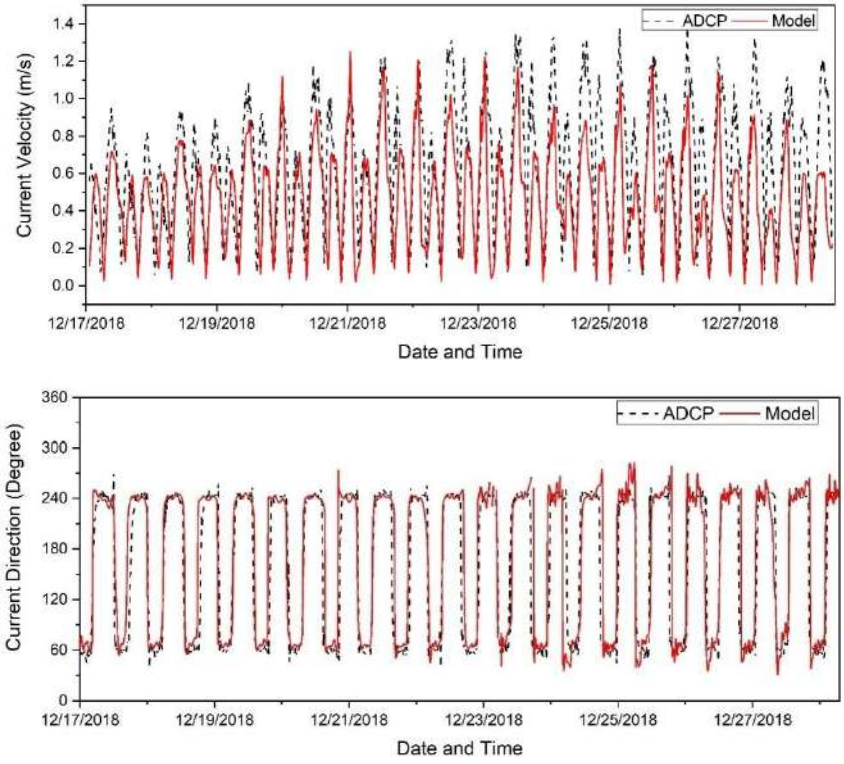


**Fig. 6.5 Comparison of Current velocity and directions at 2nd observation point**

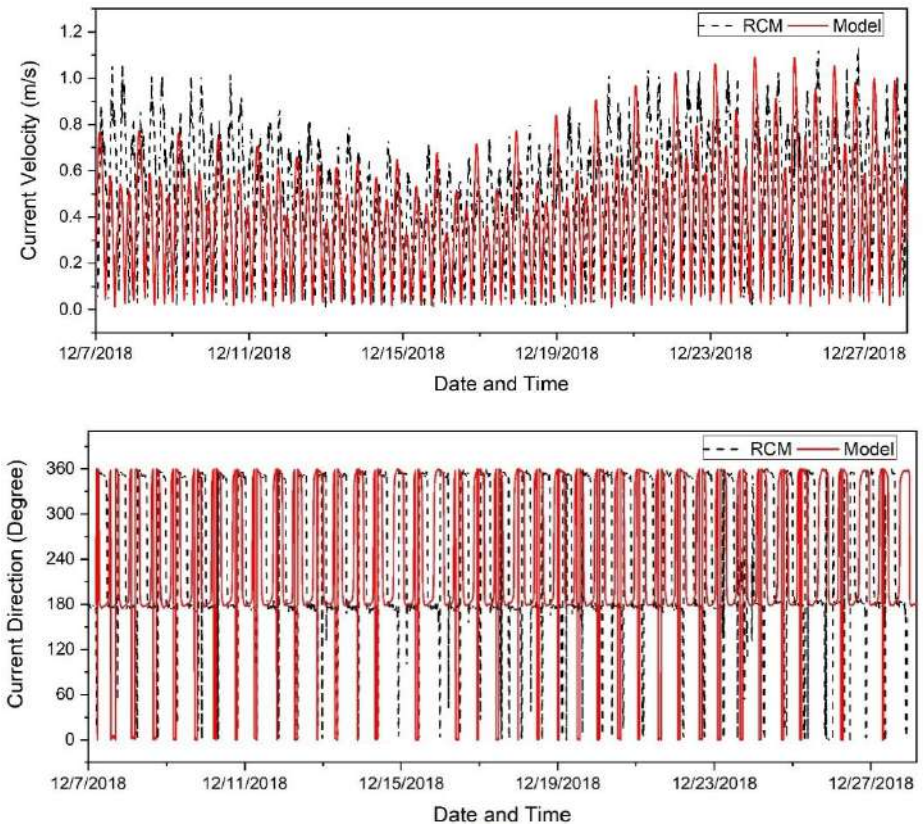


**Fig. 6.6 Comparison of current velocity and directions at 3rd observation point**

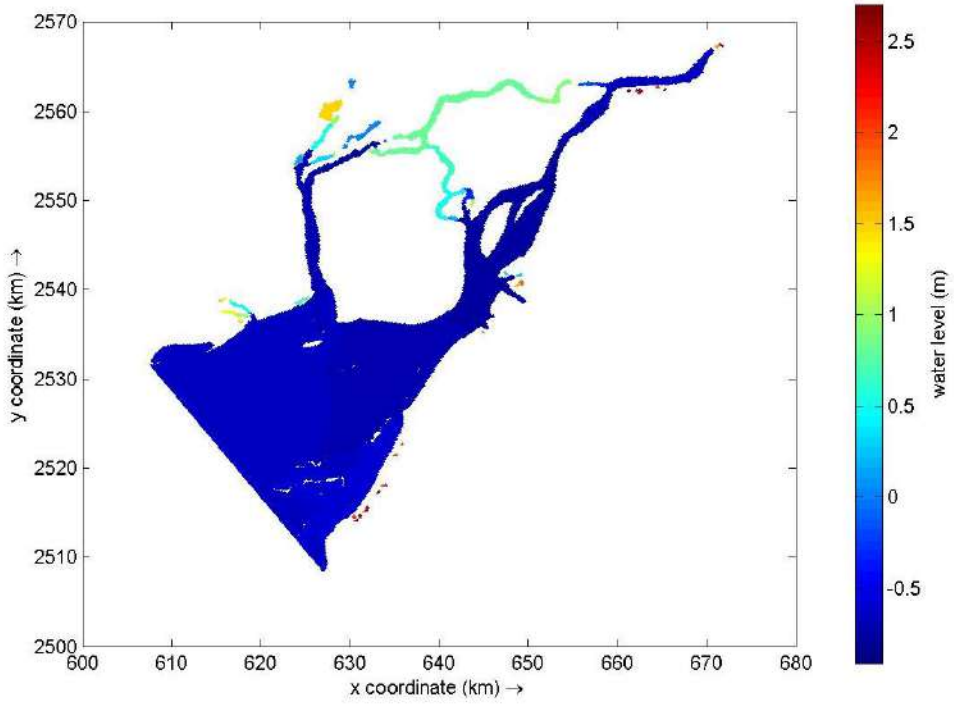


**Fig. 6.7 Water level at ebb**

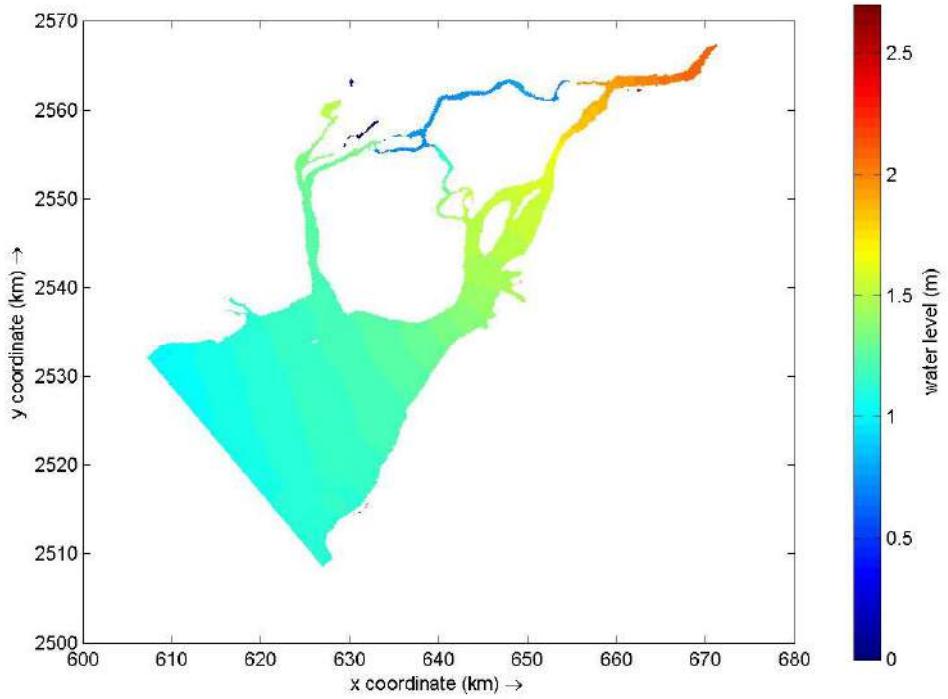


**Fig. 6.8 Water level at flood**

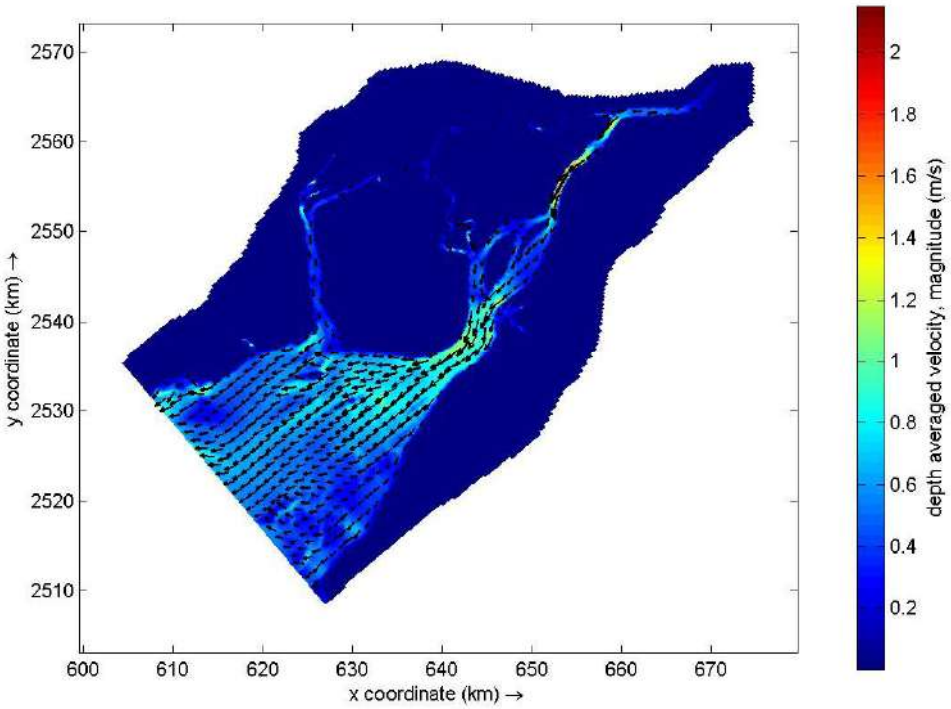


**Fig. 6.9 Current velocity along with current direction at ebb**

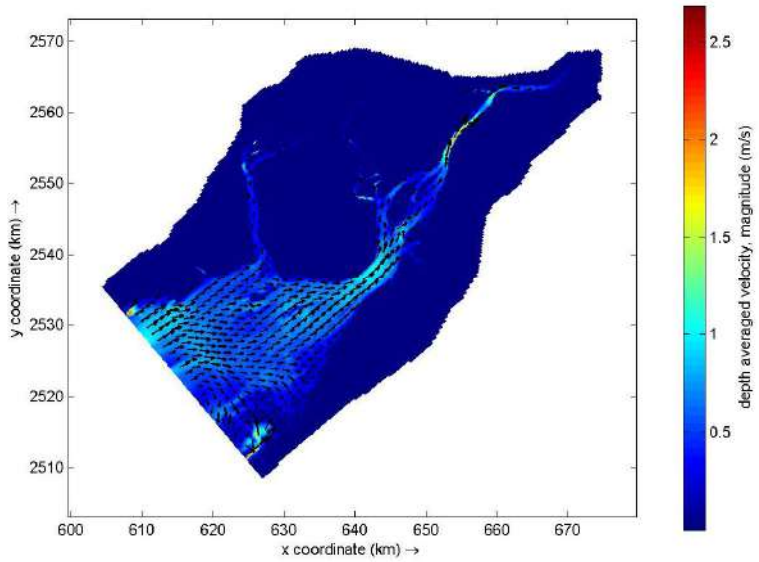


**Fig. 6.10 Current velocity along with current direction at flood**

## 6.2 Morphological Model

### 6.2.1 Model description

The Delft3D morphological module executes processes of flow, wave, sediment transport and morphological updating at every time step according to the 'online' approach shown in Fig. 6.11. In the 'online' approach, the hydrodynamics are solved on a boundary-fitted curvilinear grid, which is provided with initial and boundary conditions. The output flow and wave field is supplied to the sediment transport module, which calculates the magnitude and direction of sand movement, based on the sediment transport formula chosen. In the present study, sediment transport formula given by Van Rijn (1984) is applied, as the formula calculates sediment transport due to tidal currents only. The results from the sediment transport module cause changes in bed level, which are fed back to the hydrodynamic module at every time step.

Sediment transport can be divided into two modes, viz. bed-load and suspended-load transport. Both of them are calculated separately and added together to obtain the total transport. In the present study only suspended-load transport was taken into account. A number of 'tuning' parameters are available which can be adjusted to calibrate the morphological model.

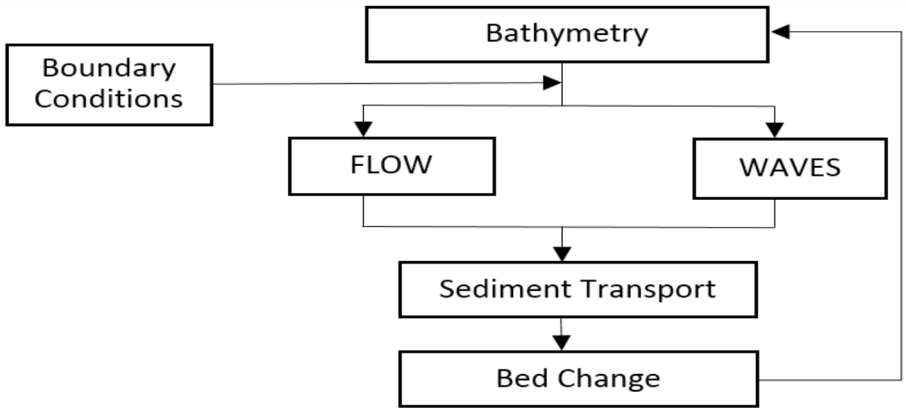


**Fig. 6.11 Delft3D online calculation steps (Roelvink 2006)**

### 6.2.2 Sediment Transport Formulations

Sediment transport in coastal environment is highly influenced by the action of waves and currents, and hence their effects need to be taken into account while computing the rate of siltation. Delft3D offers a number of standard sediment transport formulations for non-cohesive sediment, which consider the effects of waves and currents. These formulations have been derived by Van Rijn (1993), Engelund-Hansen (1967), Meyer-Peter-Muller (1948), Bijker (1971), Van Rijn (1984), and Soulsby (1997). All these formulations are different in a sense that some of them consider the action of waves, while others do not. They also differ in the manner in which they consider the bed load and suspended load. Table 6.1 gives a list of sand formulations which can be solved by Delft3D.

**Table 6.1 List of sand transport formulations**

| Formula | Bed load | Waves |
|---|---|---|
| Van Rijn (1993) | Bed load + Suspended | Yes |
| Engelund-Hansen (1967) | Total transport | No |
| Meyer-Peter-Muller (1948) | Total transport | No |
| Bijker (1971) | Bed load + Suspended | Yes |
| Van Rijn (1984) | Bed load + Suspended | No |
| Soulsby | Bed load + Suspended | Yes |
| Ashida-Michiue (1974) | Total transport | No |

Kandla port is a naturally sheltered port due to which the effect of waves on siltation can be neglected. From the formulations mentioned above, Van Rijn (1984) is the transport formula which is used for fine sediments in situations without waves.

According to Van Rijn (1984), the total volumetric sediment transport rate ($q_t$) is the sum of bed load ($q_b$) and suspended load ($q_s$) transport rates, i.e.,

$$q_t = q_b + q_s$$

Suspended load:

$$q_s = 0.012Uh\left\{\frac{U - U_{cr}}{[(s-1)gd_{50}]^{\frac{1}{2}}}\right\}^{2.4}\left(\frac{d_{50}}{h}\right)D_*^{-0.6}$$

where:

$U$ = depth averaged current velocity,

$U_{cr}$ = threshold current velocity, evaluated according to Van Rijn, 1984 (see below),

$h$ = water depth, and,

$D_*$ = dimensionless grain size

The threshold current velocity is calculated as:

$$U_{cr} = 0.19(d_{50})^{0.1}log_{10}\left(\frac{4h}{d_{90}}\right) \text{ for } 0.1 \leq d_{50} \leq 0.5 \text{ mm (with all SI units)}$$

$$U_{cr} = 8.5(d_{50})^{0.6}log_{10}\left(\frac{4h}{d_{90}}\right) \text{ for } 0.5 \leq d_{50} \leq 2 \text{ mm (with all SI units)}$$

The settling velocity of sand particles is calculated using the method of Van Rijn (1993). A different formulation exists for different range of grain diameter, as seen in above equation.

$$w_s = \begin{cases} \frac{(s-1)gD_s^2}{18\nu} & , 65\ \mu m < D_s < 100\ \mu m \\ \frac{10\nu}{D_s}\left(\sqrt{1+\frac{0.01(s-1)gD_s^3}{\nu^2}}-1\right) & , 100\ \mu m < D_s < 1000\ \mu m \\ 1.1\sqrt{(s-1)gD_s} & , 1000\ \mu m < D_s \end{cases} \quad (14)$$

where:

$s$ = relative density, $\rho_s/\rho_w$ of sediment fraction

$D_s$= representative diameter of sediment fraction

$\nu$= Kinematic viscosity coefficient of water [$m^2/s$]

### 6.2.3 Model Methodology

Optimum values of various model coefficients which was used for simulation of model are shown in Table 6.2.

**Table 6.2 Model coefficients and their values**

| Model Parameter | Value | Description |
|---|---|---|
| U and V | 85 and 85 | Chezy's coefficients in x and y direction |
| D50 | 0.125 mm | Median grain diameter |
| MORFAC | February- 1.6 | Morphological acceleration factor |
| | May- 1 | |
| | September- 2.6 | |
| | December- 1 | |
| Initial Condition | 300 mg/liter and 5m | Sediment Concentration and Sediment layer thickness at bed |
| $\boldsymbol{f_{sus}}$ and $\boldsymbol{f_{bed}}$ | 20 | Current related suspended load and bed-load transport factor |

Morphological model simulation of sediment transport for February, May, September and December month was performed using the above model settings.

### 6.2.4 Model Results

***Validation***

Fig. 6.12 to Fig. 6.15 shows February, May, September and December month sedimentation/erosion pattern predicted by the model using coefficients mentioned in Table 6.2. It can be observed that maximum deposition up to 1.4m in September month and maximum erosion up to 2.8m in same month was predicted by the model in the navigation

channel. The volume of deposition for the four mentioned months are compared with the dredging data provided by the Kandla port for the same time period as shown in Table 6.3.

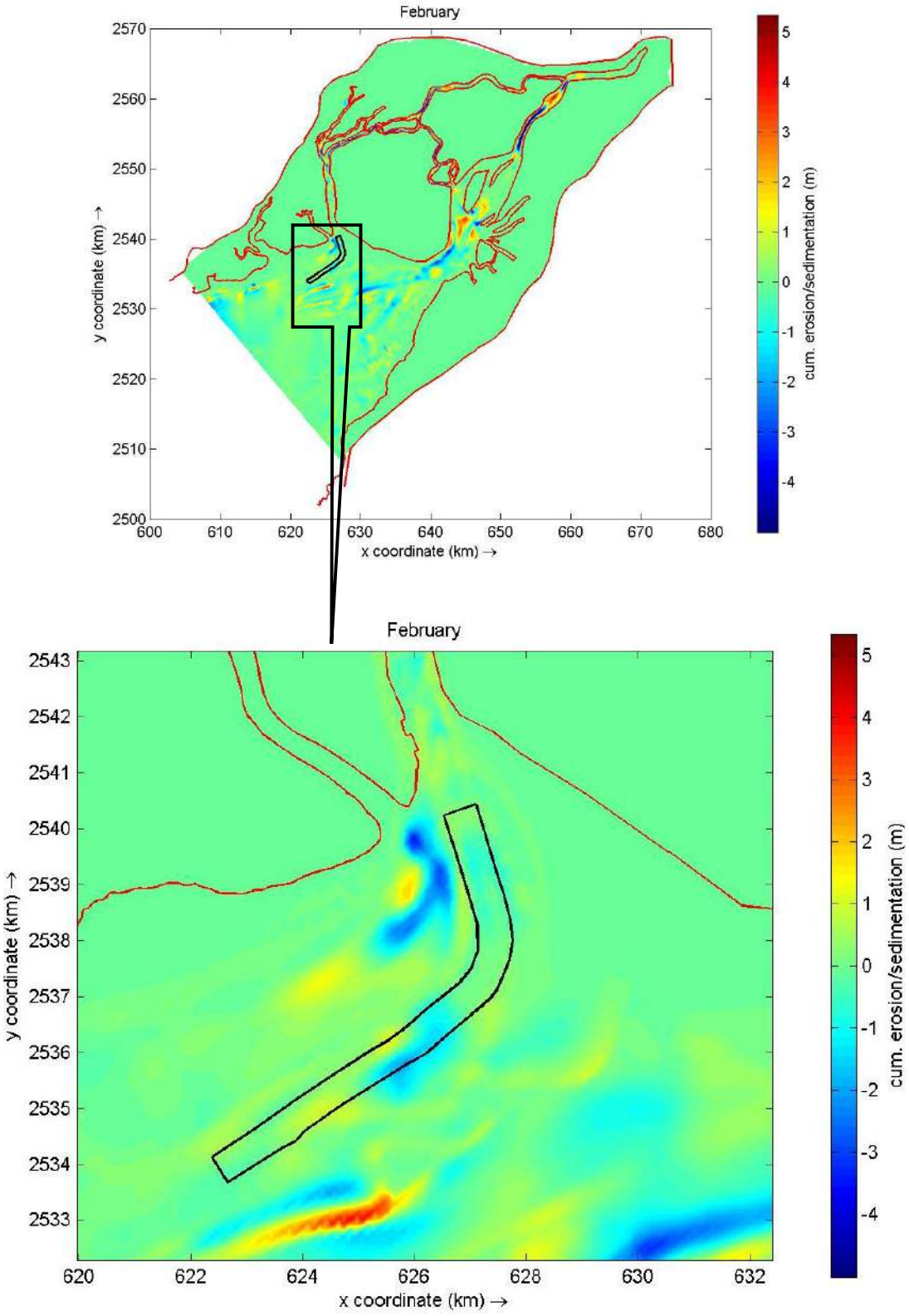


**Fig. 6.12 Cumulative erosion or deposition for February month**

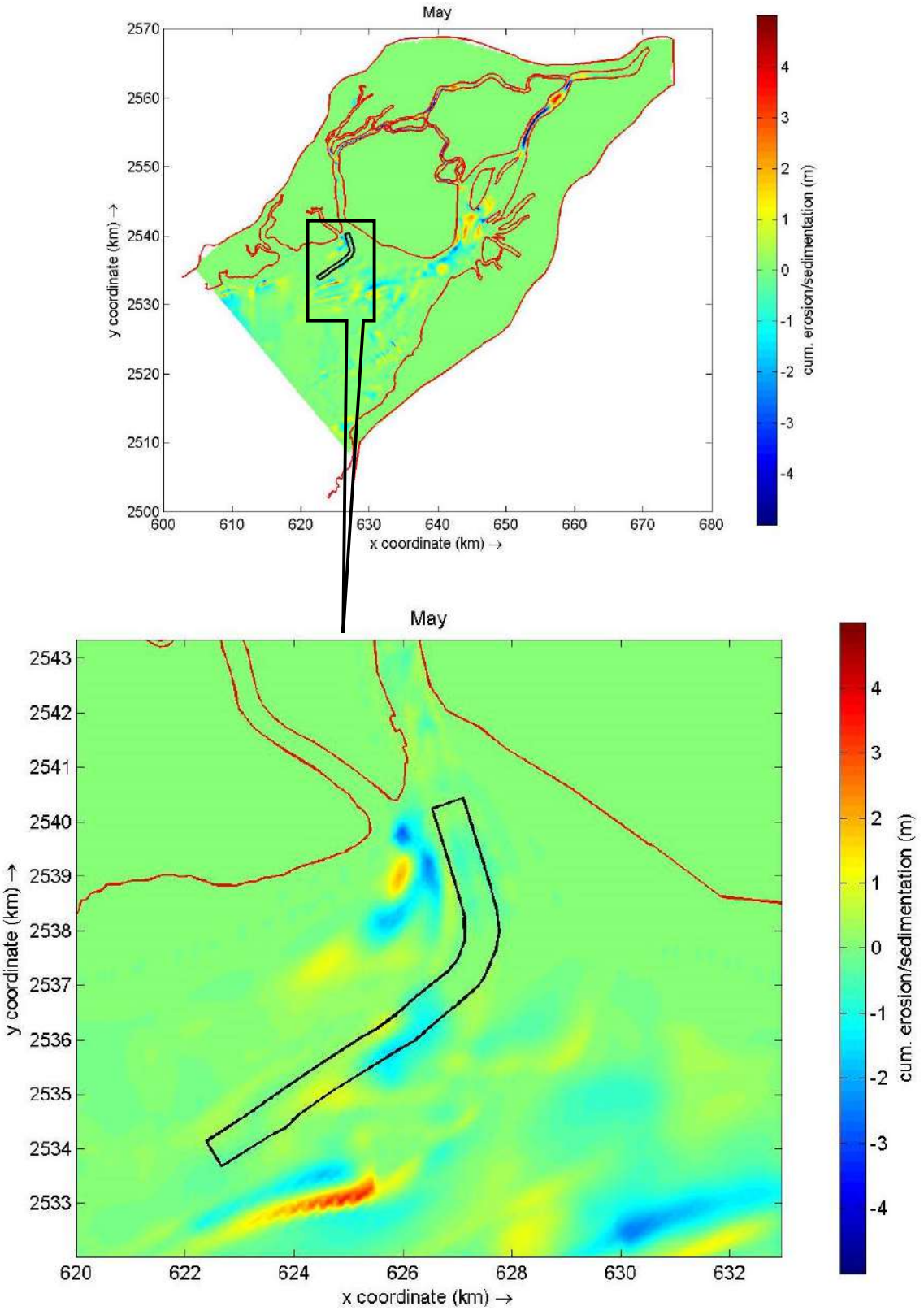


**Fig. 6.13 Cumulative erosion or deposition for May month**

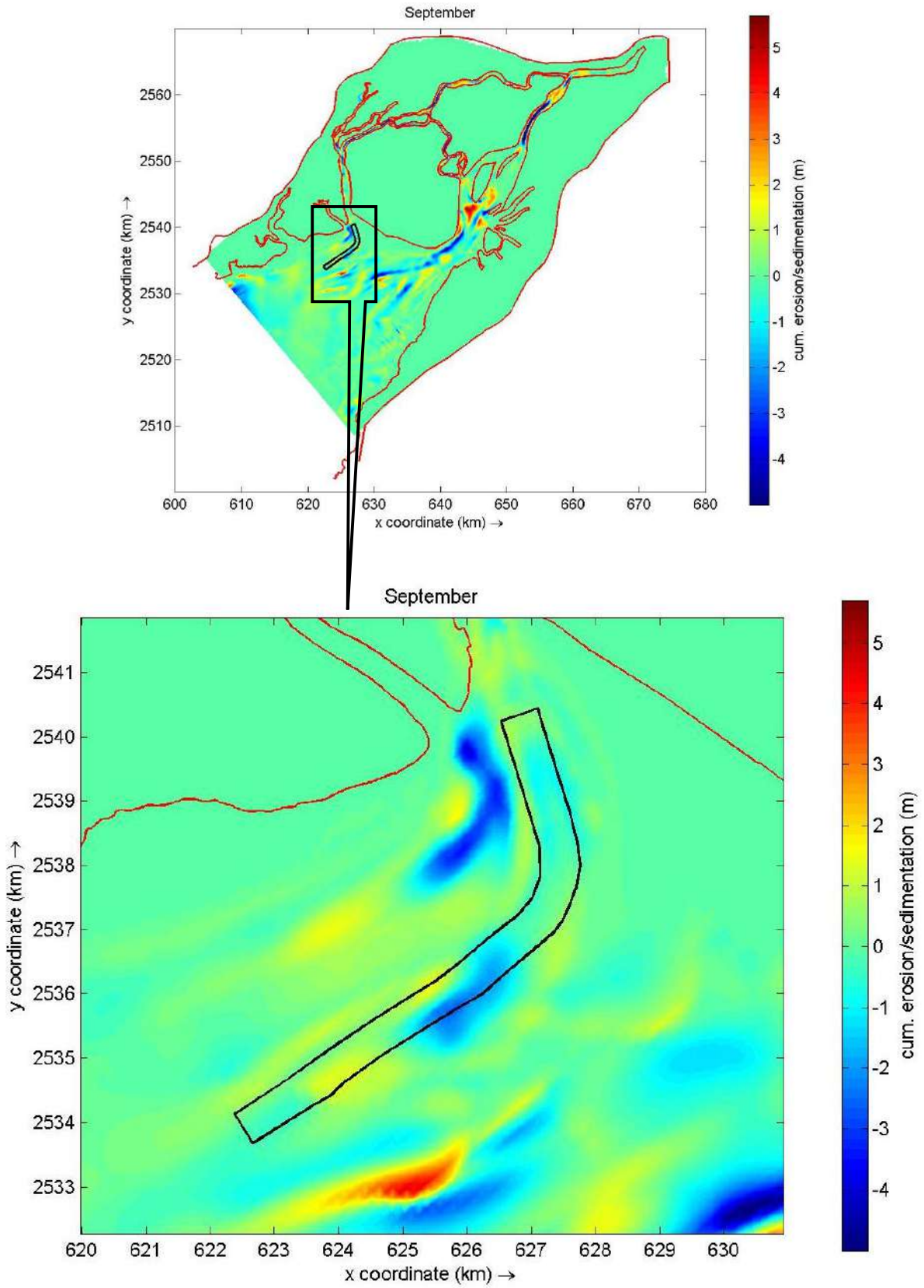


**Fig. 6.14 Cumulative erosion or deposition for September month**

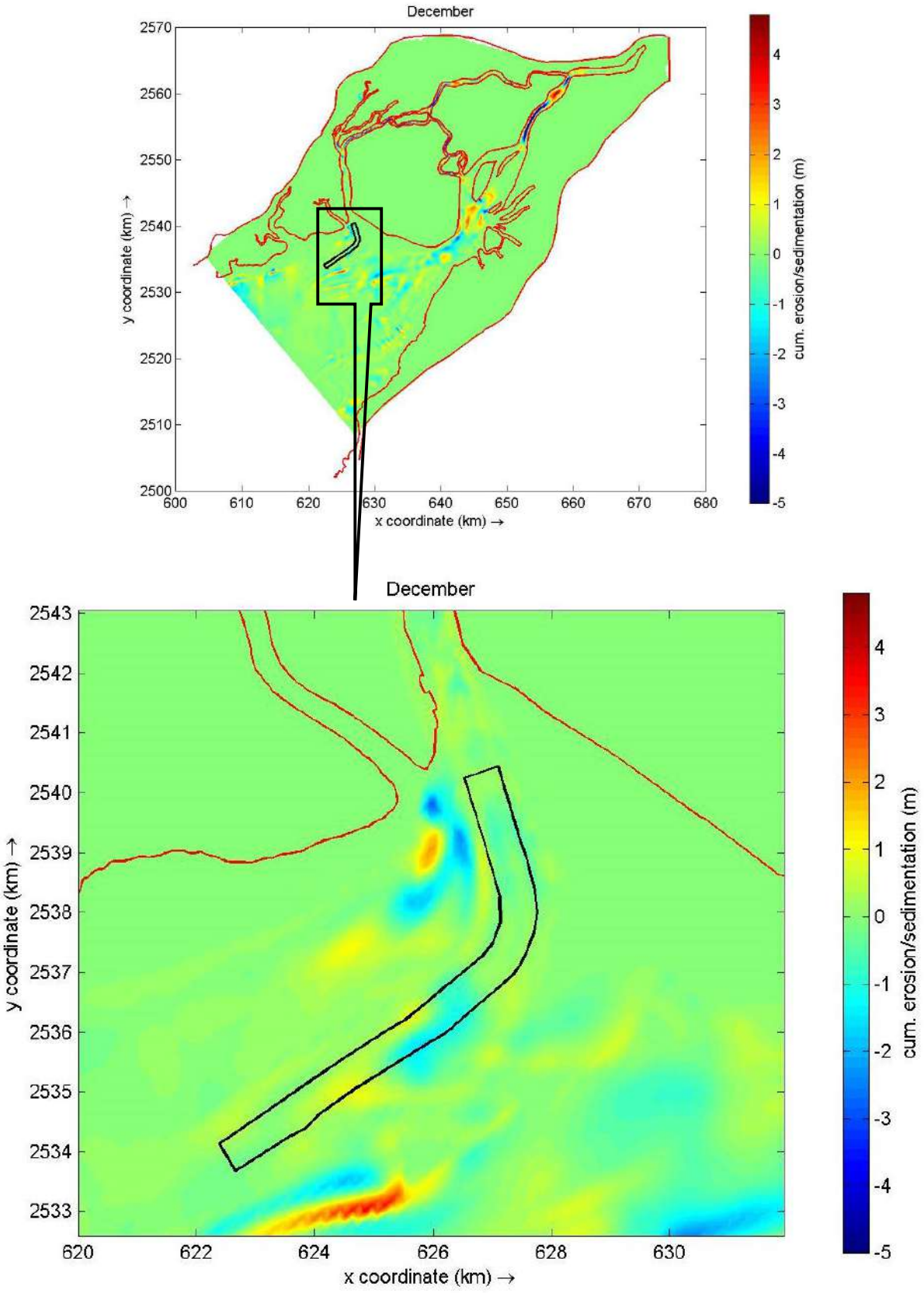


**Fig. 6.15 Cumulative erosion or deposition for December month**

**Table 6.3 Comparison of model results and dredging data provided by DPT**

| Month(season wise) | Siltation Quantity (cubic meter) | |
|---|---|---|
| | Measured | Model |
| February | 5,43,800 | 5,02,400 |
| May | 4,12,000 | 4,12,900 |
| September | 7,37,900 | 6,72,500 |
| December | 4,35,200 | 4,07,000 |

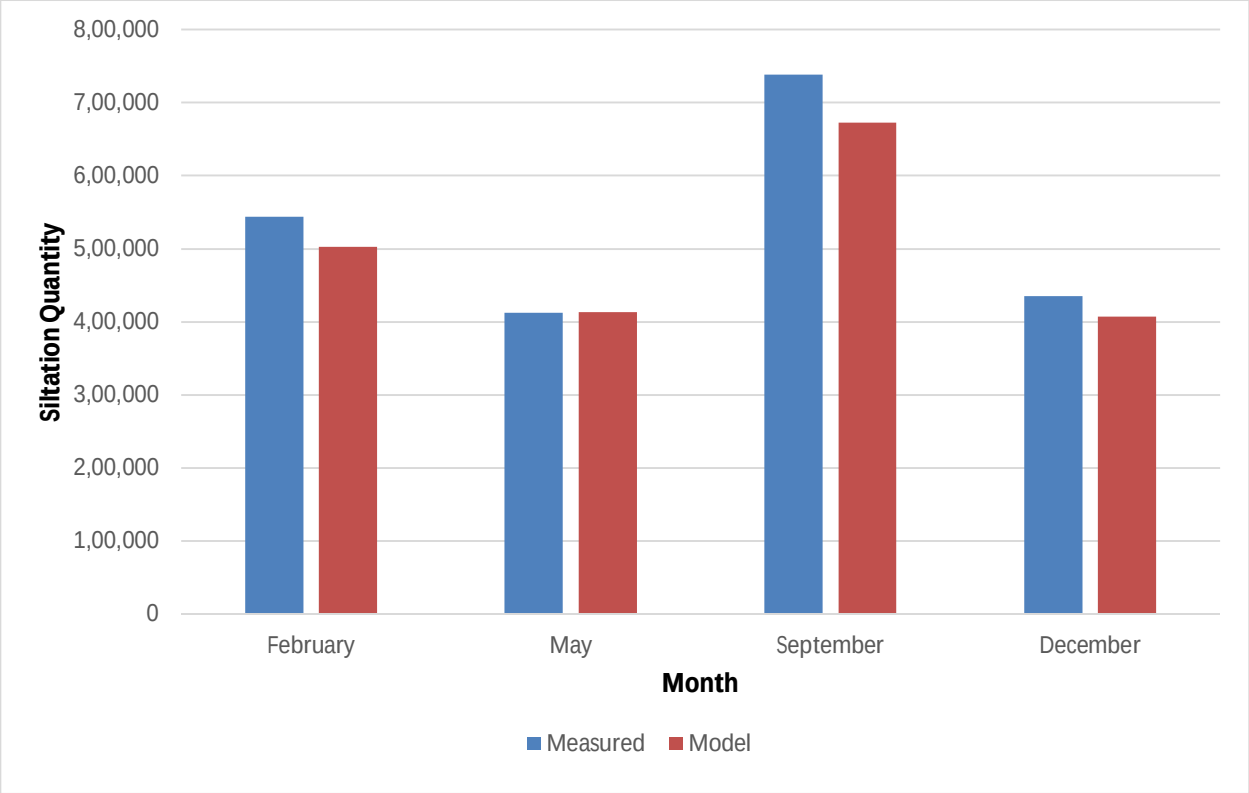


**Fig. 6.16 Comparison showing model results and dredging data provided by DPT**

***Siltation Behaviour with Porous Plate***

Fig. 6.18 to Fig. 6.21 shows the sedimentation/erosion pattern predicted by the model after adding porous plates on adjacent sides of the navigation channel. It can be observed that siltation quantity is significantly reduced after adding the porous plates on adjacent sides of channel as shown in Fig. 6.17. Porous plates specifications are mentioned in Table 6.4.

Comparison of the siltation quantity with and without adding porous plates are given in Table 6.5.

**Table 6.4 Specifications of porous plates**

| Porous Plate | Length (Km) | Spacing |
|---|---|---|
| NP | 3.15 | - |
| SP1 | 1.95 | 1.8 |
| SP2 | 1.95 | |

**Remarks*

*NP- Porous plate on the north side of navigation channel*

*SP1 and SP2- Porous plates on south side of navigation channel*

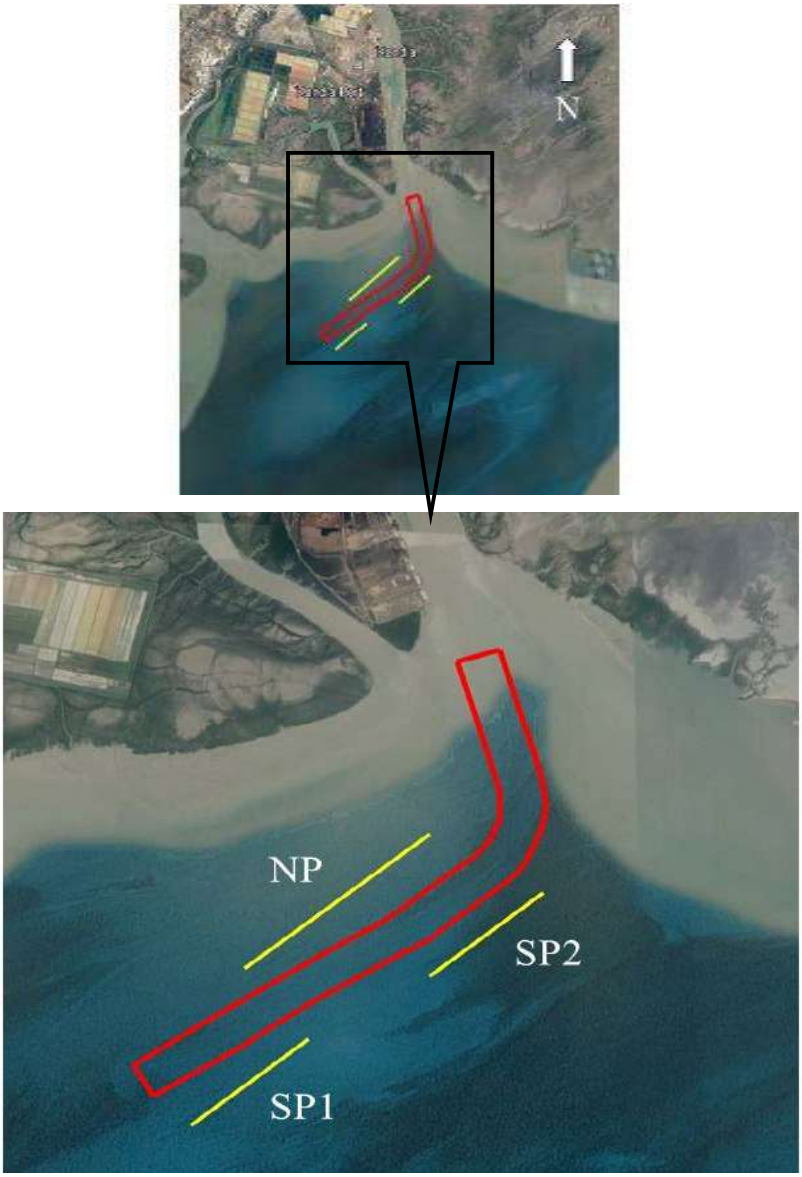


**Fig. 6.17 Google earth image of porous plates with navigation channel**

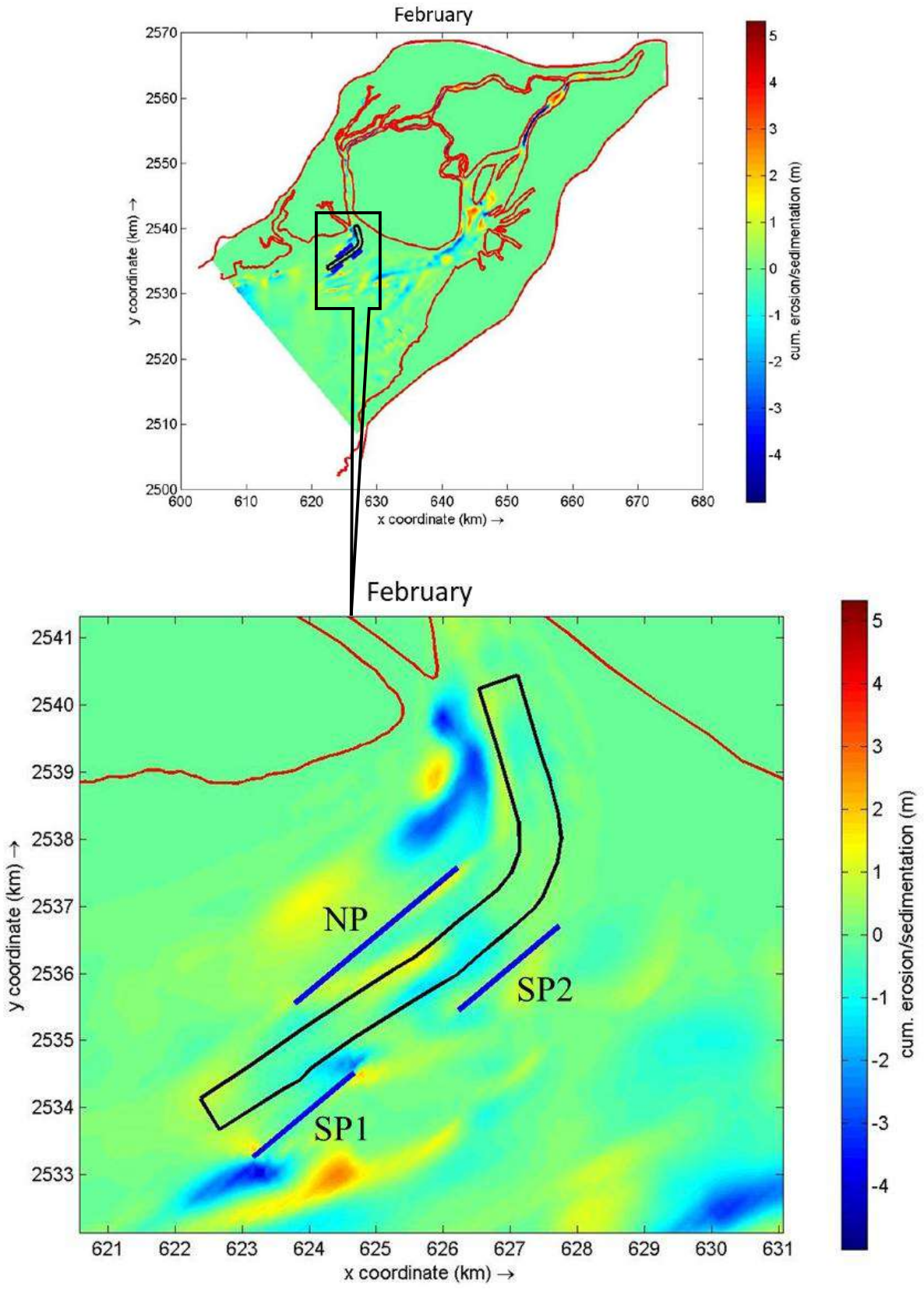


**Fig. 6.18 Cumulative erosion/deposition in February month with porous plate**

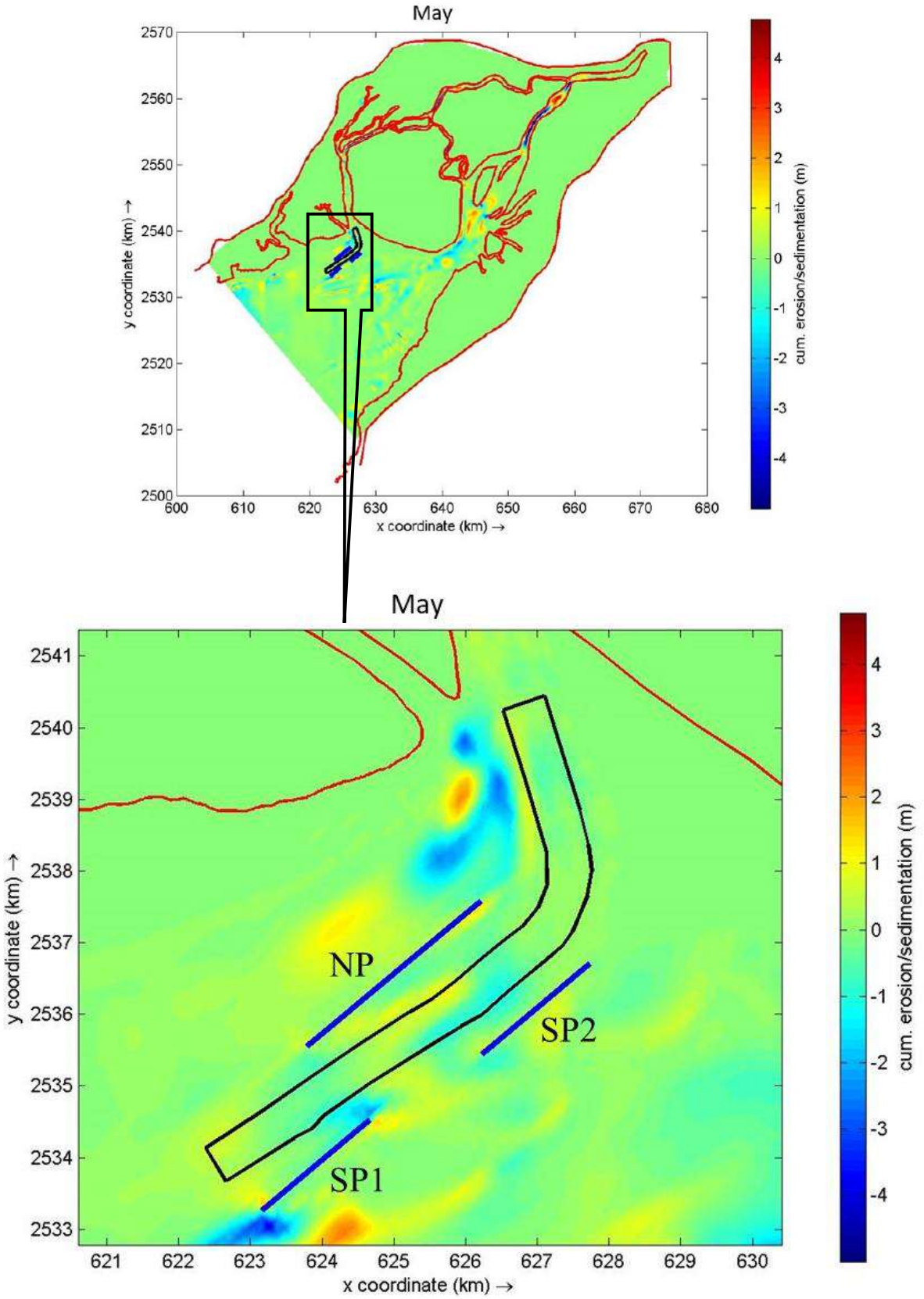


**Fig. 6.19 Cumulative erosion/deposition in May month with porous plate**

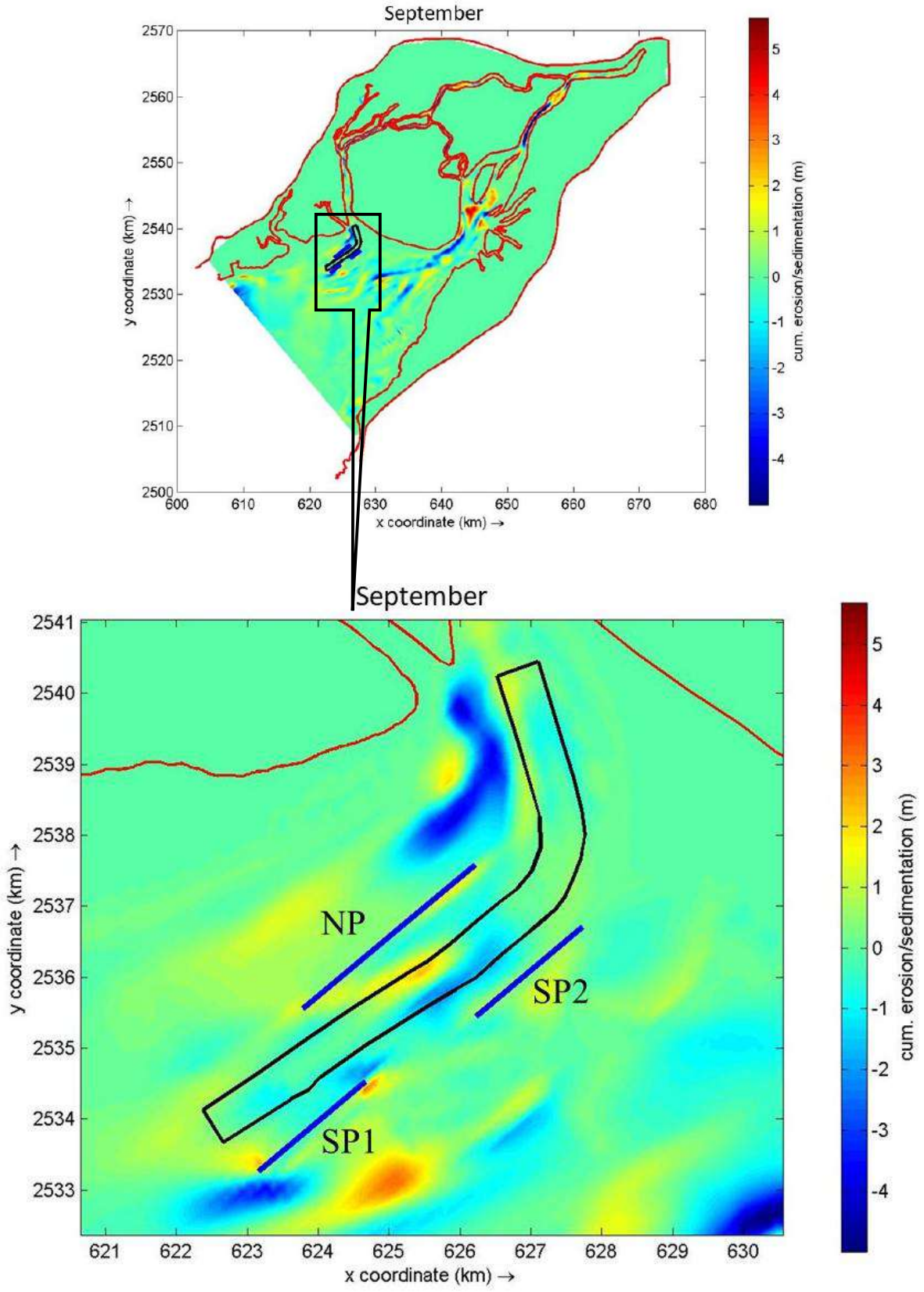


**Fig. 6.20 Cumulative erosion/deposition in September month with porous plate**

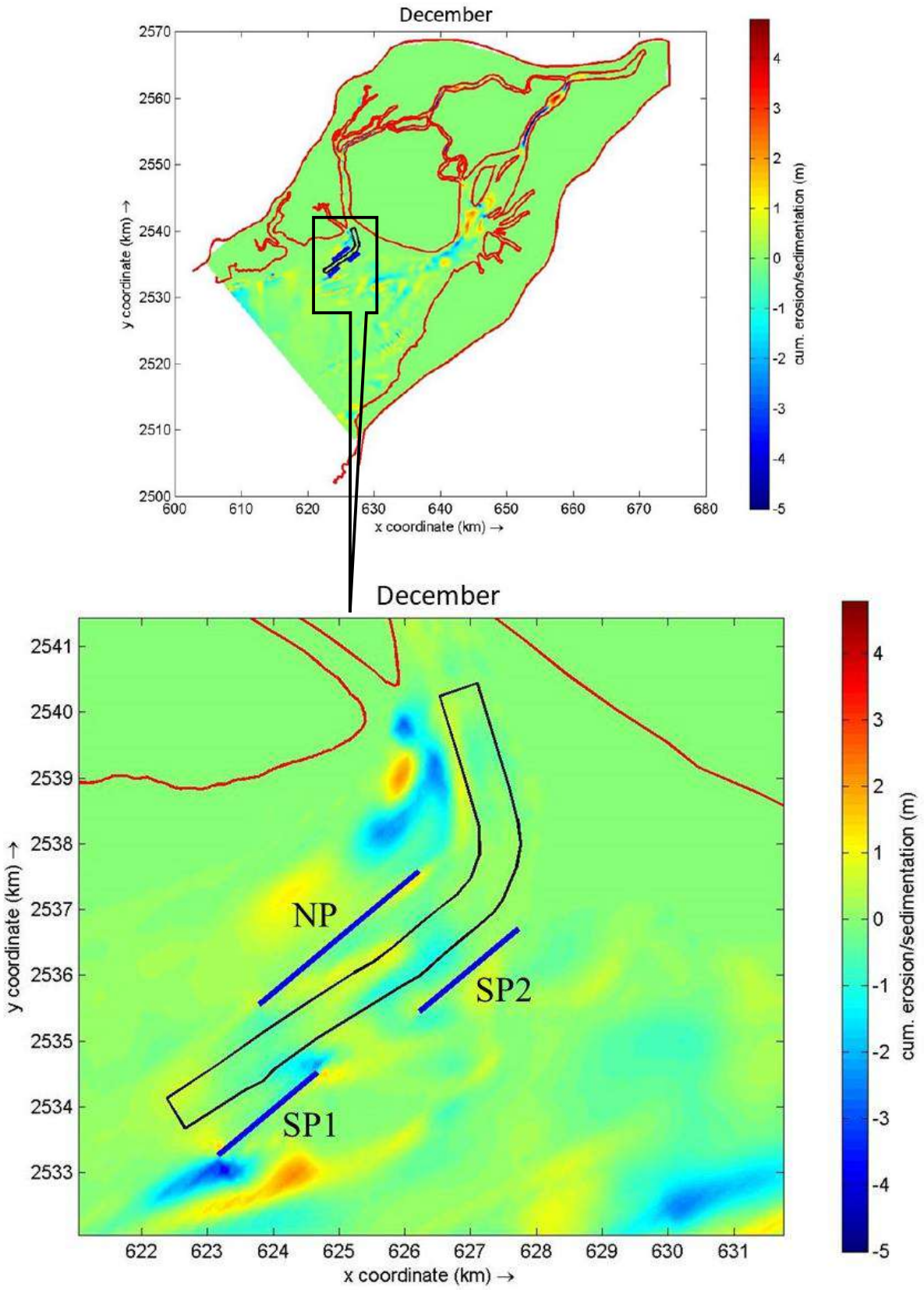


**Fig. 6.21 Cumulative erosion/deposition in December month with porous plate**

**Remarks*

*NP- Porous plate on the north side of navigation channel*

*SP1 and SP2- Porous plates on south side of navigation channel*

**Table 6.5 Comparison of siltation quantity of model results with and without porous plate**

| Month(season wise) | Siltation Quantity (cubic meter) | | Percentage Reduce |
|---|---|---|---|
| | Without Porous Plate | With Porous Plate | |
| February | 5,02,400 | 2,47,300 | 50.77 |
| May | 4,12,900 | 2,22,300 | 46.16 |
| September | 6,72,500 | 3,05,900 | 54.51 |
| December | 4,07,000 | 2,21,300 | 45.62 |

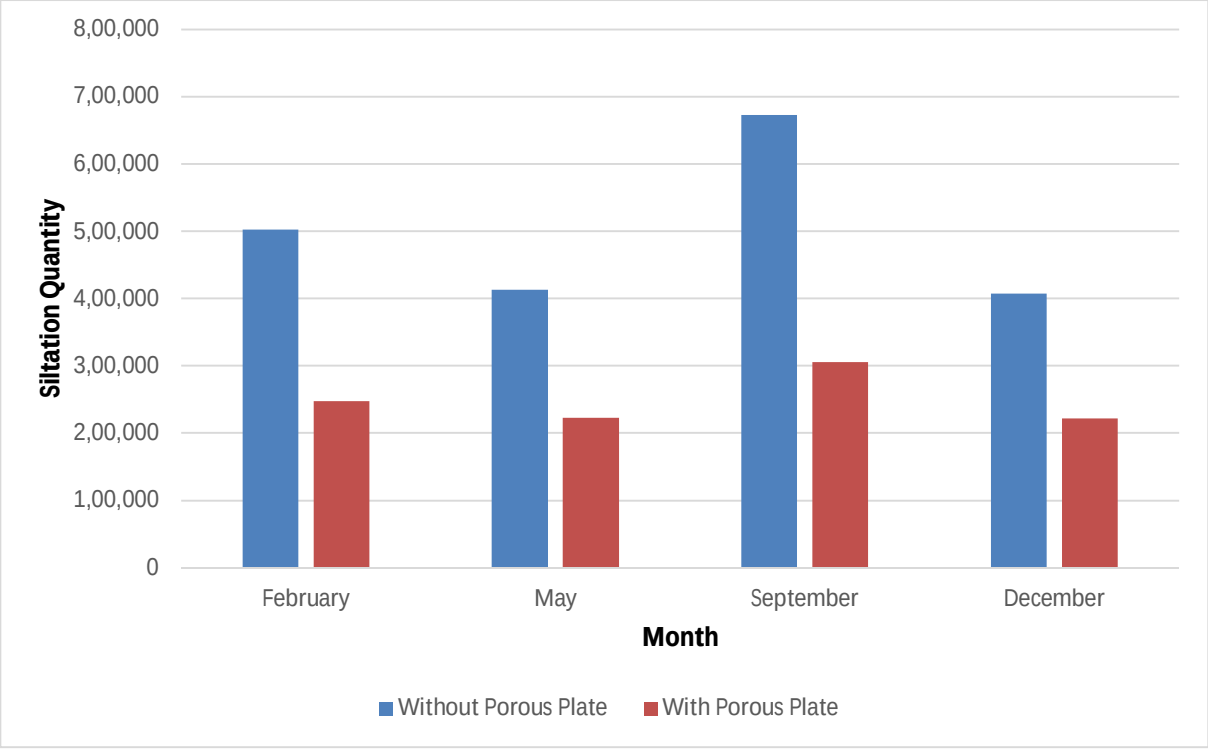


**Fig. 6.22 Comparison showing siltation quantity with and without porous plate**

# 7. RECOMMENDED ENGINEERING SOLUTIONS

After proper analysis of the hydro-morpho-dynamic processes occurring along the Kandla Creek, it was a challenging situation to recommend some engineering solutions which can effectively take down the siltation issue in the region. From the details provided by the DPT, it was clear that significant cost has been spent for the maintenance dredging of the navigational channel. The present study is a comprehensive analysis, including numerical modelling, field measurements and satellite based analyses. Based on the previous experiences, the effective solution that can be provided to mitigate the problem is by using a silt curtain along the navigational channel with the alignment as shown in Fig. 7.1 and specifications as discussed, in the results section. Various numerical simulations had been carried out to depict the presence of silt curtain along the channel. The study included the observations by varying the position and properties of the structure during modelling.


**Fig. 7.1 Silt Curtain along navigation channel of kandla port (Source-Google Earth)**

Silt curtains are impervious or permeable vertical barriers that extend from the water surface to a specified depth, in most of the cases till seabed. In case of Kandla port, magnitude of SSC is fairly uniform throughout the entire depth of water column, as measured from the field measurements. The permeable screen is recommended for movement and circulation of water through the curtain, but to minimize the movement of silts. Silt curtains also called as turbidity curtains, flotation curtains or silt screens. It prevents the process of dispersion of the sediments by allowing them to settle down within the water column. The silt curtain aims to prevent the fine grained suspended material from migrating. In some instances, the use of silt curtains does result in appreciable visual differences between low turbidity 'background' water on one side of a curtain and turbid water on the other side. These very distinct visual differences may truly reflect a significant reduction in turbidity and suspended sediments on other side with the use of the curtain as typical shown in Fig. 7.2.

A silt curtain classification system was outlined in 1997 by the United States Army Corp. Engineers (USACE). Silt curtains were classified into the following three types, according to the prevailing hydrodynamic and met ocean conditions.

- Type I – (Light weight) this is designed for use in lower energy environments where there are no currents and the deployment location is sheltered from any wind and waves
- Type II – (Medium weight) are suited to sites where there is only a small to moderate current of up to about 1 m/s. Wind and wave action can be present but not considered major force.
- Type III – (Heavy duty) is for sites with higher energy environments, with currents in excess of 1.5 m/s. Curtains can be deployed in a tidal region and be subject to wind and wave action.

Components and Manufacturing of silt curtain is typically comprised of following elements; these are described as follows and as shown in Fig. 7.3.

- Screen (or Skirt) – can be woven, non-woven and knitted in construction with compositions varying between polyester, polypropylene fabric and geo-textile. Screen material is predominantly depending upon the implementation of silt curtain. The screen can be single or double layered.

- Floatation system – float diameter ranges between 0.1 m and 0.3 m depending on the type of screen being supported. The floats are held in position by an impermeable PVC sleeve which can vary in quality depending on the class of silt screen and cost associated with construction of the curtains.
- Anchoring – this keeps the curtain in position. This is a very important component of a silt curtain and if done incorrectly can cause major issues relating to effectiveness.
- Ballast – comprises typically of steel or galvanized chain ranging in size depending on the design and class of the silt curtain.
- Connection cable (or Tension member) – is not always present in all the classes or designs and is used to reduce the stress on the connection between each section.
- Connectors – designed to allow the sections of curtain to be joined together whilst preventing any leakage between them. For Type I a polypropylene rope or lace is used, for Types II and III there are a variety of different connectors available.

Anchoring is a very important consideration relating to the use of silt curtains, if done incorrectly it can reduce the effectiveness of the structure. Anchoring and mooring systems are especially critical in situations where tides and / or waves are present causing vertical movement. Different types of anchors can be used to secure the curtain into position. Figure 7.4 shows a simple schematic of a typical anchor system set-up.

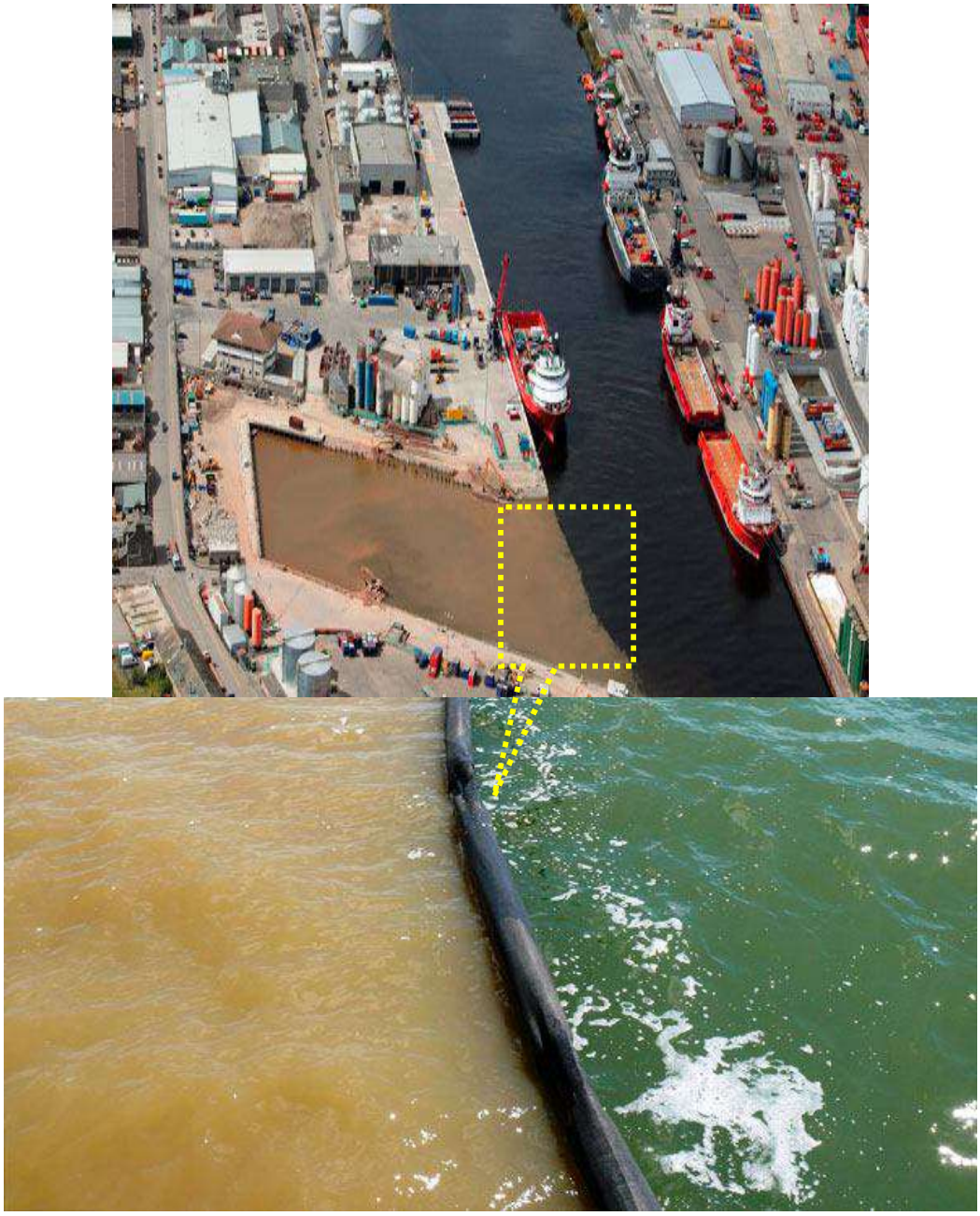

**Fig. 7.2 Visual difference in turbidity due to silt curtain**

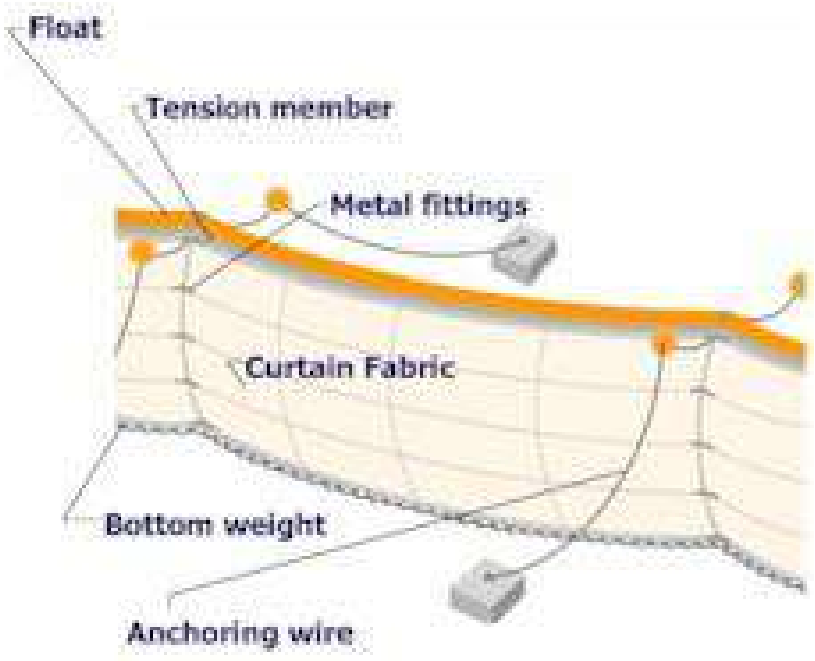


**Fig. 7.3 Typical components of silt curtain (Source-Red Run Drain)**

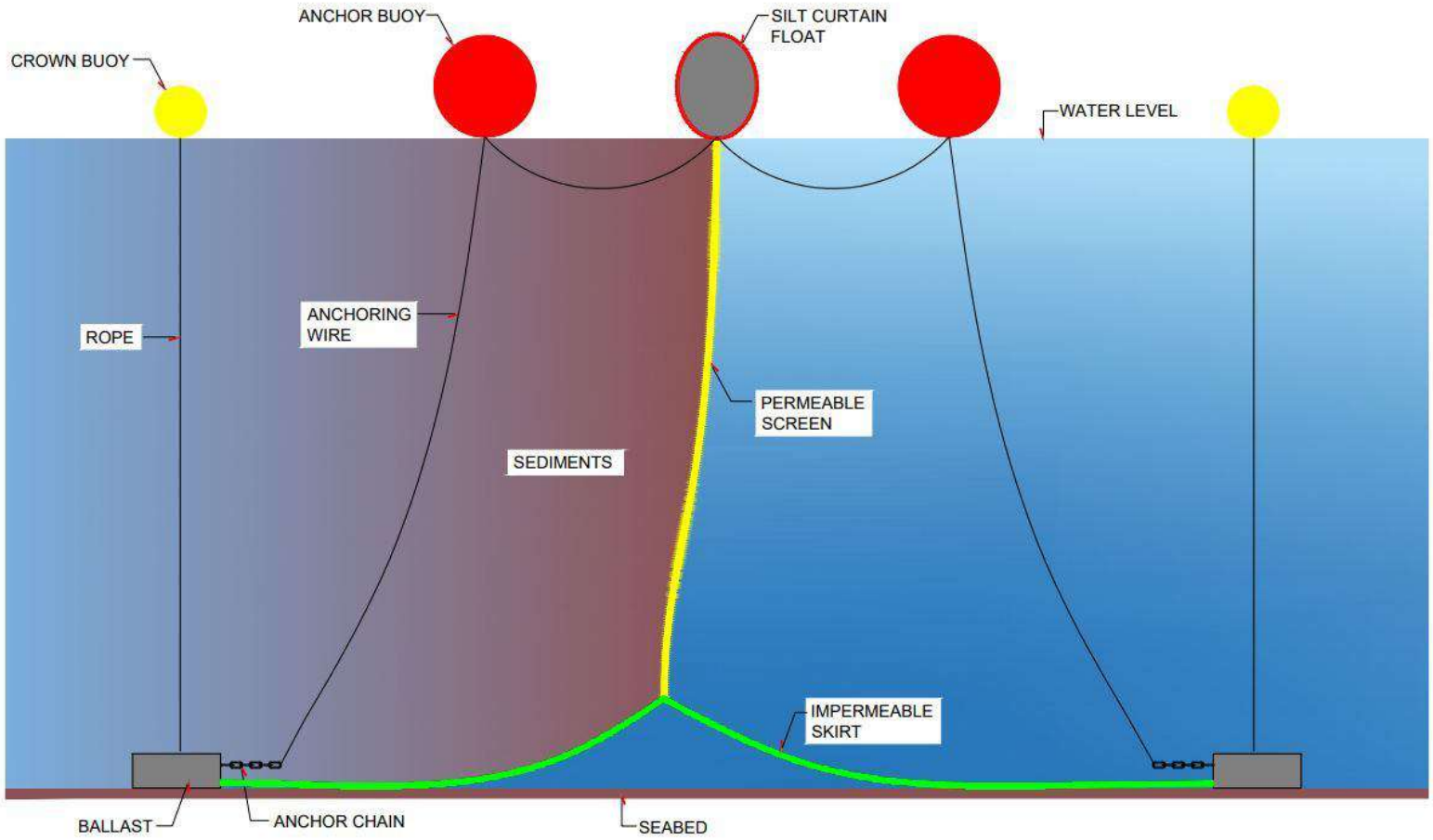


**Fig. 7.4 Schematic drawing of anchoring of silt curtain**

There are many engineering factors to be considered while deploying a silt curtain. The engineering property of the material, its geometry and orientation are already found out and discussed in results by carrying out a number of simulations and then analyzing the optimum solution out of it.

Various studies conducted across the world had found this to be an effective solution against siltation process, provided it would be implemented properly. A flexible silt curtain consisting of hypalon was used in one of the naval basins along the Mare Island Strait (Jenkins et al., 1980) with an entrance width of about 80m and depth of about 10m. The curtain partitioned the basin off from the main channel and extend form the bottom up to the mean low water level. The gap over the curtain (about 1 to 2m) allowed the tidal filling of the basin with low-concentration water. The curtain was constructed in 13 sections, each about 6m in length. The hypalon curtain material on each section was equipped at the lower end with a pipe (0.4m diameter) filled with concrete to function as anchor weight. The 9m high curtain sections were supported vertically in the water by curtain buoys. To raise the curtain, a second set of buoys at the surface was used. The surface buoys are connected to the curtain to raise it at high tide. Due to the presence of the curtain the siltation rate in the Naval basin along Mare Island Strait was reportedly reduced by about 70%. Most of the observed siltation occurred during the period that the curtain was open.

# 8. CONCLUSIONS

In the present study, a comprehensive analysis of the nature and process of sedimentation taking place in the navigational channel of Kandla Port carried out. The study involved a detailed field measurement of tidal currents, which is the prime cause of sediments to be in suspension and also responsible for siltation in navigational channels; along with tidal levels and suspended sediment concentration. A dedicated numerical model for the entire Kandla region is also developed to map the hydrodynamic and morphological characteristics in time and spatial domain, with special emphasis on Kandla creek and Sogal Channel. Numerical hydrodynamic model is calibrated with the data retrieved from the pre-monsoon and post-monsoon field measurements. In morphological model, monthly siltation quantity for each seasonal month was validated with available dredging data. Critical information pertaining to hydrodynamic and morphological behavior around Kandla creek region was obtained and solutions to reduce deposition in navigation channel was discussed in this study. Some of the general findings and conclusions are listed below:

- As Gulf of Kutch has the dominant effect on Kandla Creek, Gulf is well known for the high tidal range and currents, the tidal elevation reaches the maximum of 6.6m at Kandla. From model and field measurement data it was found that maximum current velocity inside and outside creek is 1.2m/s and 1.6m/s respectively.
- From SSC contour maps it was found that sediment characteristics are different from place to place and varies with time. Maximum SSC found at three different locations are as follows, 440 mg/l (middle), 390 mg/l (surface) and 340 mg/l (bottom).
- SSC contour maps indicates that SSC values are high and equivalent throughout the water column hence silt curtains should extend from water surface to the seabed so as to protect the entire water column.
- Turbulent eddies are observed in the vicinity of Kandla creek mouth, due to which significant erosion and deposition are observed at just outside the Kandla creek, from the numerical model simulations. Sediments in suspension tends to settle down after some distance which highly depends on the tidal currents and eventually leads to high siltation rate in navigation channel.
- Current related bed-load ($f_{bed}$) and suspended load ($f_{sus}$) transport factors are found to be the most influential calibration parameters. It was observed that the morphological

changes predicted by the model were very sensitive to changes in the values of $f_{bed}$ and $f_{sus}$.

- Grain size is an important parameter which influences the long term morphological changes in the region. An increase in the value of $D_{50}$ from 100 μm to 200 μm led to significant reduction in the siltation rate, which may be attributed to the reduced capability of sediment to get carried by the flow. Grain size analysis need to be performed in order to obtain accurate $D_{50}$ values for different regions in the domain, before implementing any engineering solution.
- It can be observed that maximum deposition up to 1.4m is predicted by the model in the navigation channel, especially in Zone 1, indicating sensitivity of siltation areas.
- **Attempt to change the alignment of navigation channel did not give any encouraging solution for the siltation issue, as estimated by the developed numerical model.**
- **After extensive modelling for numerous alignments and different structures the use of silt-curtain (porous plate) on the adjacent sides of the navigation channel for the given alignment is found to reduce siltation by approximately 46% - 54%.**
- Practical implementation of porous plates can be silt curtains which could be made of permeable screen to allow water movement and current circulation with minimal sediment passage.

# REFERENCES


1) Central water and power research station, (2005), "Response of Sogal channel to maintenance dredging at Kandla port", Technical Report no. 4200.

2) Chandramohan, P., Sanil Kumar, V and Nayak, U.B. (1991), "Wave statistics around the Indian coast based on ship observed data", Indian Journal of Marine Sciences, Vol. 20, 87-92.

3) Chauhan, O. S., Jayakumar, S., Menezes, A. A. A., Rajawat, A. S., & Nayak, S. R. (2006), "Anomalous inland influx of the river Indus, Gulf of Kachchh, India", Marine Geology, 229(1), 91-100.

4) Disha Nayak. P., and Madhusudan Fulekar. H. (2017), "Coastal Geomorphological and Land Use and Land Cover Study on Some Sites of Gulf of Kachchh, Gujarat, West Coast of India using Multi-Temporal Remote Sensing Data", International Journal of Advanced Remote Sensing and GIS. Volume 6, Issue 1, 2192-2203.

5) Evans Richard, D., Murray Kathy, L., Field Stuart, N., Moore James, A.Y., George Shedrawi, Huntley Barton, G., Peter Fearns, Mark Broomhall, McKinna Lachlan, I.W., Daniel Marrable (2012), "Digitise This! A Quick and Easy Remote Sensing Method to Monitor the Daily Extent of Dredge Plumes", PLOS, Volume 7: Issue 12.

6) Ghosh, L.K., N. Prasad, V.B. Joshi, and S.S. Kunte. (2001), "A study on siltation in access channel to a port", Coastal Engineering 43: 59-74.

7) Gupta, M. (2015), "Modeling and remote sensing of suspended sediments in the Gulf of Kachchh, India", European Journal of Remote Sensing, 48, 201-221.

8) Hashimi, N.H., Nair, R.R., and Kidwai, R.M. (1978), "Sediments of the Gulf of Kutch a high energy tide dominated environment," Indian Journal of Marine Sciences, 7.

9) Jayappa, K. S., and A.C., Narayana. (2009), "Coastal Environments: Problems and Perspectives", New Delhi: I.K. International.

10) Kunte, P. D., Zhao, C., Osawa, T., & Sugimori, Y. (2005), "Sediment distribution study in the Gulf of Kachchh, India, from 3D hydrodynamic model simulation and satellite data", Journal of Marine Systems, 55(3), 139-153.

11) Land Processes Distributed Active Archive Center (LP DAAC). U.S. Geological Survey.

12) Lesser, G. R., J. A. Roelvink, J. A. T. M. van Kester and G. S. Stelling. (2004), "Development and validation of a three-dimensional morphological model", Coastal Engineering Vol 51: 883–915.

13) Manik Mahapatra., Ratheesh Ramakrishnan., and Rajawat. A. S. (2015), "Coastal vulnerability assessment of Gujarat coast to sea level rise using GIS techniques: a preliminary study", J Coast Conserv (2015) 19:241–256, DOI 10.1007/s11852-015-0384-x.

14) Mukesh Gupta. (2015), "Modeling and remote sensing of suspended sediments in the Gulf of Kachchh, India", European Journal of Remote Sensing, 48:1, 201-221, DOI: 10.5721/ EuJRS20154812

15) Nair, R.R., Hashimi, N.H., and Rao, V.P. (1982), "On the possibility of high-velocity tidal streams as dynamic barriers to longshore sediment transport: evidence from the continental shelf off the Gulf of Kutch", India. Marine Geology, 47, 77–86.

16) Pravin, K., Wagle B.G., Yasuhiro Sugimori. (2003), "Sediment transport and depth variation study of the Gulf of Kutch using remote sensing", International Journal of Remote Sensing 24(11) · June 2003 DOI: 10.1080/01431160210164316.

17) Satish Shetye, R., (1999), "Tides in the Gulf of Kutch, India", Continental Shelf Research 19 (1999) 1771 – 1782.

18) Sewa Ram Kalsi. and Manu Gupta. (2003), "Success and Failure of Early Warning Systems: A Case Study of the Gujarat Cyclone of June, 1998", Early Warning Systems for Natural Disaster Reduction.

19) Silt Curtains as a Dredging Project Management Practice, (2005), ERDC TN-DOER-E21.

20) Sinha, P.C., Dube, S.K., Mitra. A.K., Murty. T.S. (2000), "A Tidal Flow Model for the Gulf of Kachchh, India", Marine Geodesy, 23:2, 117-132, DOI: 10.1080/01490410050030689.

21) South Elizabeth Channel Silt Curtain Pilot Study, (2012), U. S. Army Corps of Engineers-New York District.

22) Unnikrishnan, A. S., Rupa, K.K., Fernandes, S.E., Michael, G. S. and Patwardhan, S. K. (2006). "Sea level changes along the Indian coast: Observations and projections", Special section: climate change and India.

23) Van Rijn, L. C. (2014), "Harbour siltation and control measures".

24) Veerle Vanacker. (2014), "Suspended Sediment Concentration", Encyclopedia of Earth Sciences Series, 1125-1126.

25) Wentworth, C.K. (1922), "A scale of grade and class terms for clastic sediments", The Journal of Geology, Vol 30(5):377-392.

26) Winterwerp, J.C.; Eysink, W.D.; Kruiningen, F.E. van; Christiansen, H.; Kirby, R., and Smith, T.J. (1994), "The Current Deflecting Wall: a device to minimise harbour siltation", The Dock and Harbour Authority, 243-246.

27) A.J. McCusker, J. Johnson, M. Hamlin, and C. Guelke, "Full-depth, bottom-sealed filter barriers and their place in comparison with other means of sediment/turbidity control in dredging projects", Dredging Summit & Expo '17 Proceedings.

28) Trey E. Davis and William H. McAnally (2010), "Sediment Management Alternatives for the Port of Gulfport, Mississippi", Mississippi Department of Transportation

29) "Kinnickinnic River Sediment Remediation Milwaukee, Wisconsin", Wisconsin Department of Natural Resources (2010).

30) Jeremy A. Sharp, Hunter N. Johnson, Kimberly C. Pevey, and William H. McAnally (2010), "Sediment Management Alternatives for the Port of Bienville", Civil and Environmental Engineering, Department James Worth Bagley College of Engineering, Mississippi State University.

31) "Silt Curtains as a Dredging Project Management Practice", ERDC TN-DOER-E21 September 2005.

32) "An Analysis of the Functional Capabilities and Performance of Silt Curtains", JBF, Scientific Corporation, Jewel Drive, Wilmington, Mass. 01887, July 1978.

33) JC Ogilvie, D Middlemiss, MW Lee, N Crossouard and N Feates, "Silt curtains - a review of their role in dredging projects", CEDA Dredging Days 2012, Abu Dhabi, United Arab Emirates.

34) United States Army Corp. Engineers (USACE) (1978), "An analysis of the functional capabilities and performance of silt curtains", Technical Report D-78-39, Vicksburg, Miss.

35) United States Army Corp. Engineers (USACE) (1997). Engineering and Design – Handbook for the preparation of Storm Water Pollution prevention plans for construction activities. EP 1110-1-16 Appendix C BMP-27.

# APPENDIX

For better understanding of siltation behaviour, taking May month as reference to simulate the model with structures and to determine the effect of the same on the siltation quantity of navigation channel of Kandla port.

## APPENDIX-I Model Results with Different Alignments of Thin Dam Along the Channel

Keeping various alignments of thin dam, simulations have been done to check sedimentation pattern and the effect of such small obstacle type structures on siltation Fig. A-I. 1 to Fig. A-I. 4 shows the cumulative sedimentation and erosion of Kandla creek with various alignments of thin dams.

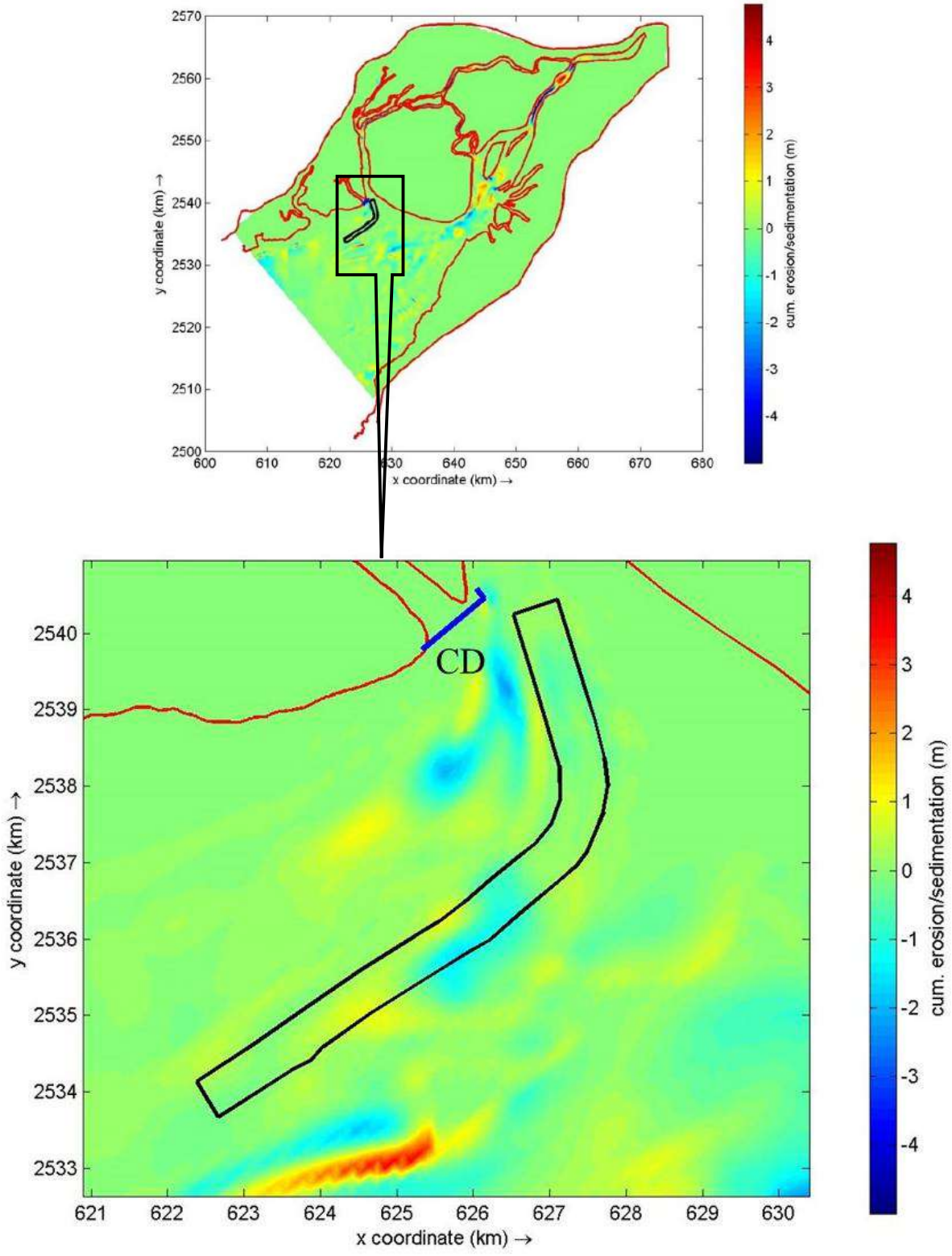


**Fig. A-I. 1 Cumulative erosion/deposition in May month with thin dam- Case 1**

*(Case 1: Keeping the thin dam shown as CD* at the mouth of adjoining creek next to Kandla creek)*

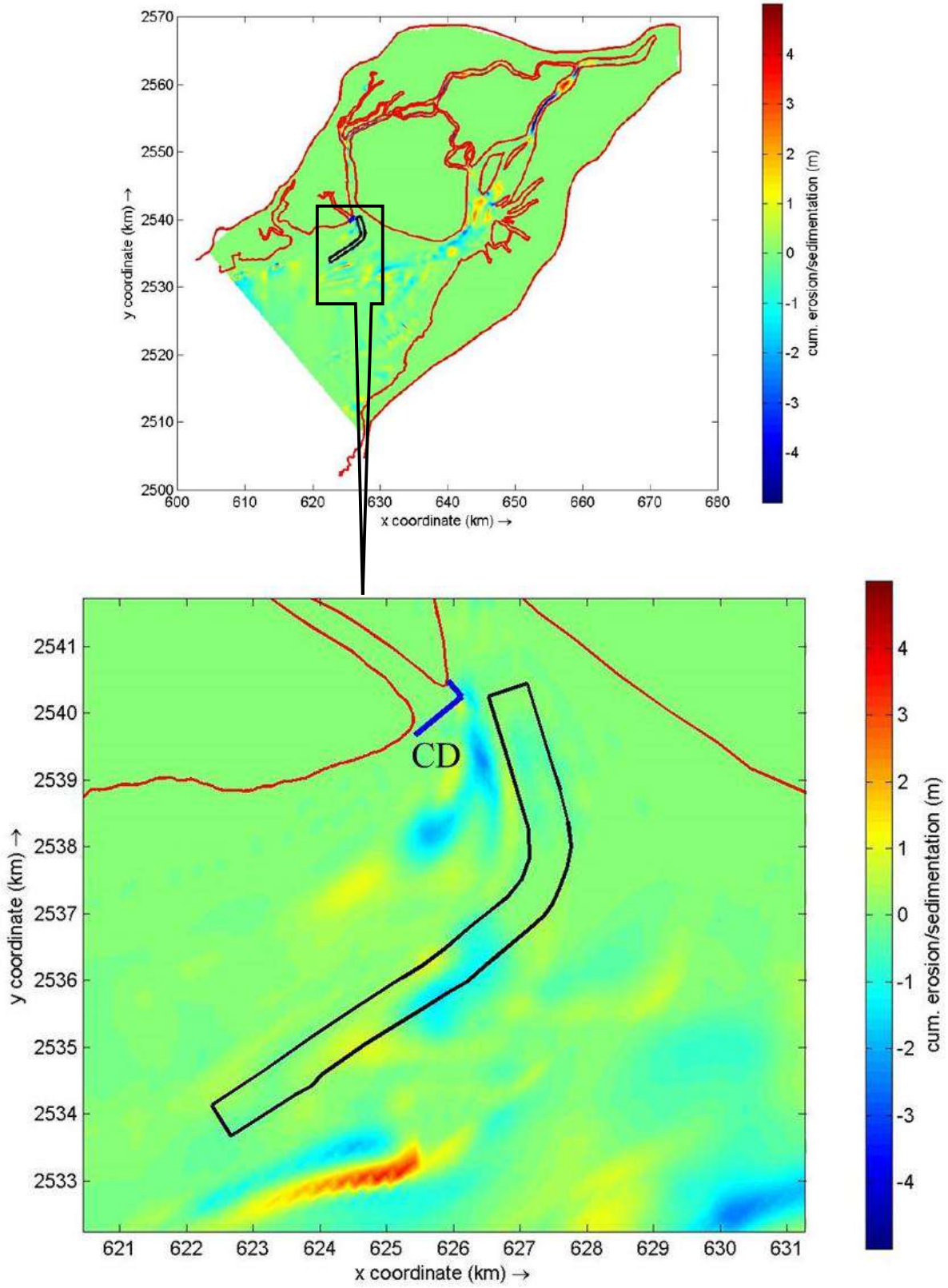


**Fig. A-I. 2 Cumulative erosion/deposition in May month with thin dam- Case 2**

*(Case 2: Keeping the thin dam shown as CD at the mouth of adjoining creek next to Kandla creek but changing the alignment than Case 1)*

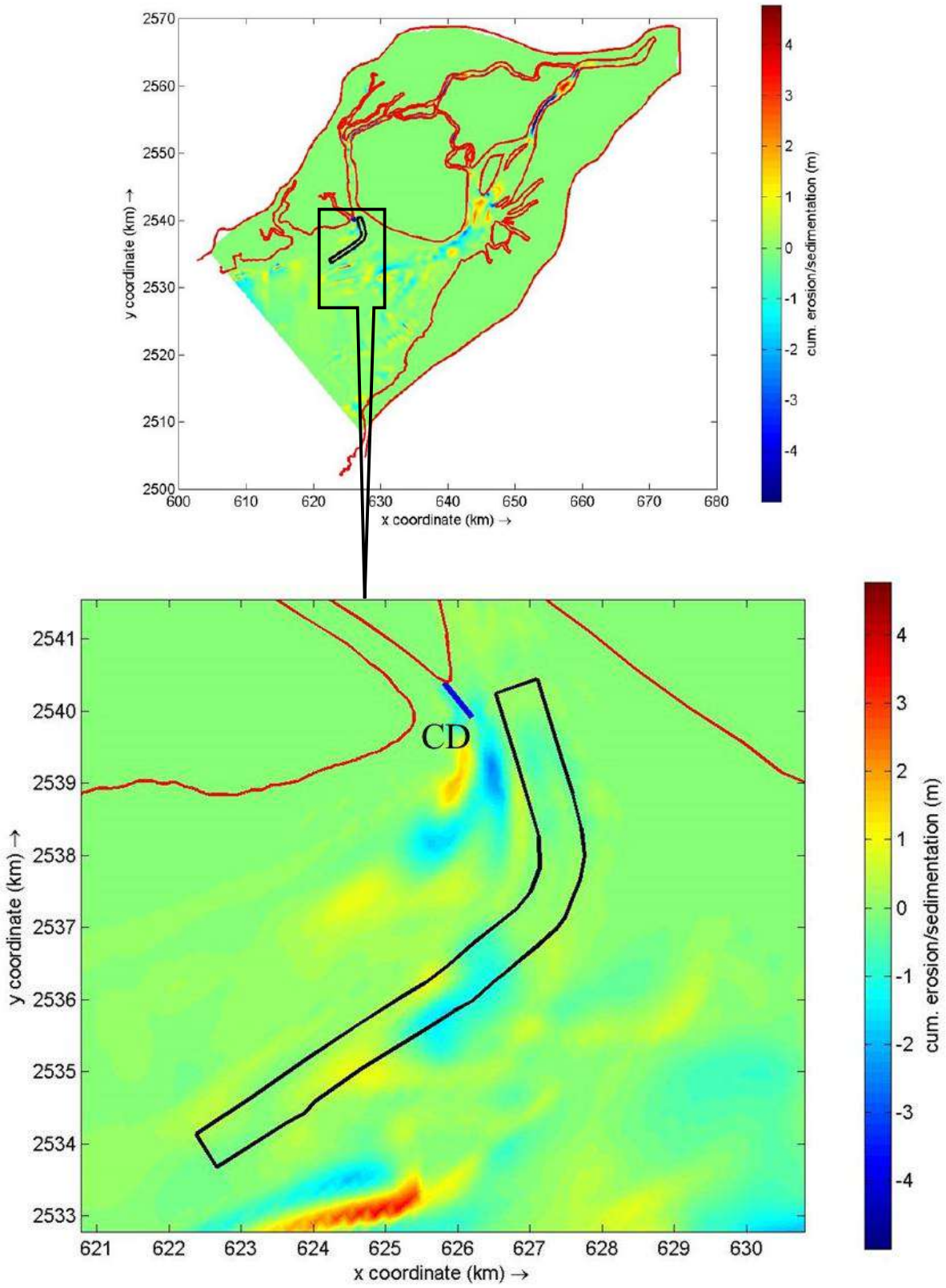


**Fig. A-I. 3 Cumulative erosion/deposition in May month with thin dam- Case 3**

*(Case 3: Keeping the thin dam shown as CD extending along the bank of adjoin creek to Kandla creek)*

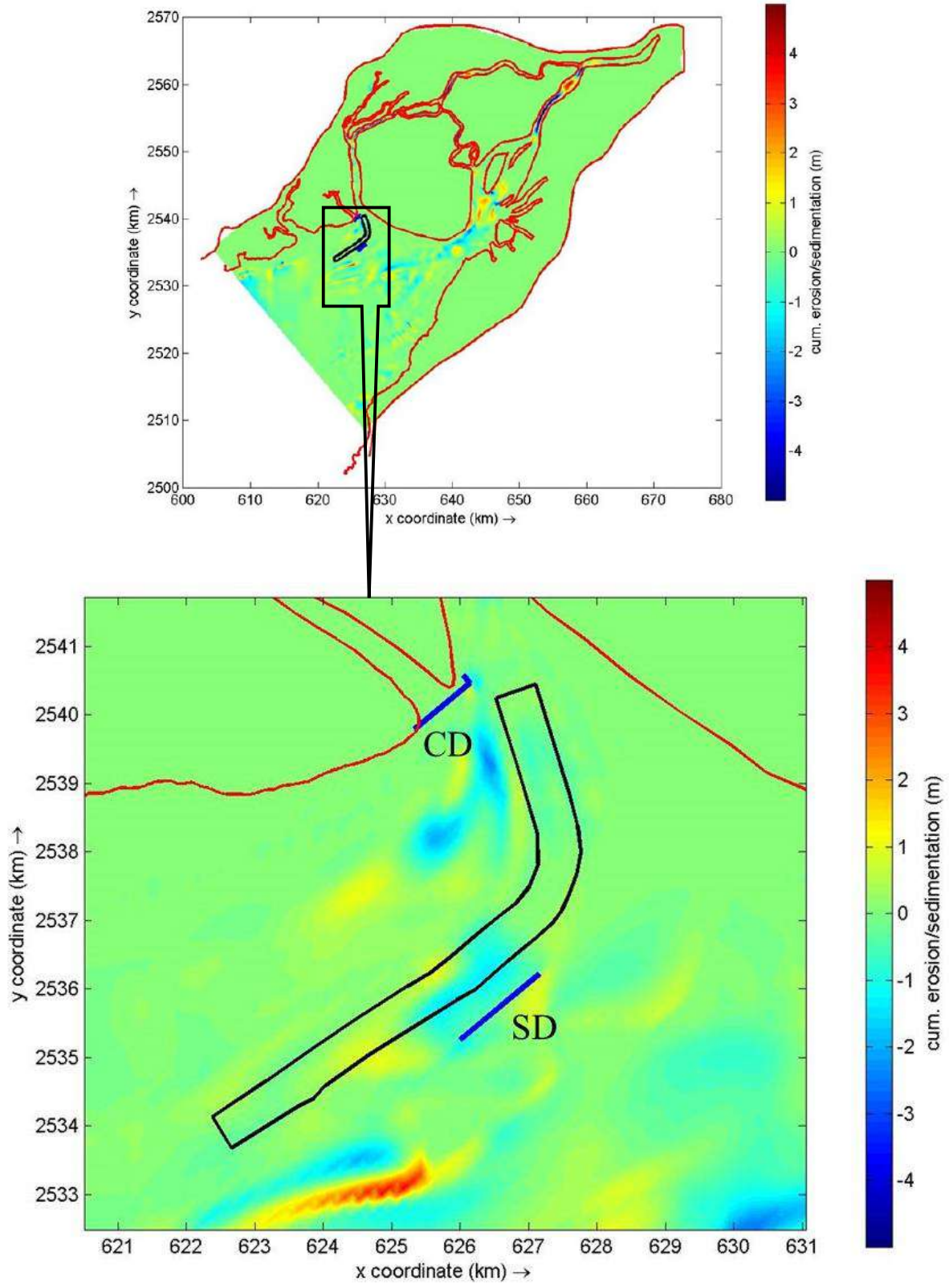


**Fig. A-I. 4 Cumulative erosion/deposition in May month with thin dam- Case 4**

*(Case 4: Keeping the thin dam shown as CD and SD* at the mouth of adjoining creek to Kandla creek and at south of the navigation channel respectively)*

**Remarks*

*CD- Thin Dam near Creek*

*SD- Thin Dam at south of Navigation Channel*

**Table A-I. 1 Thin dam specifications with siltation quantity**

| Case No. | Length of Thin Dam in Km | | Siltation Quantity (meter Cube) |
|---|---|---|---|
| | CD | SD | |
| 1 | 1.2 | - | 3,90,600 |
| 2 | 1.2 | - | 3,93,900 |
| 3 | 0.6 | - | 4,10,800 |
| 4 | 1.2 | 1.5 | 4,18,800 |

## APPENDIX-II Model Results with Different Alignments of Porous Plate Along the Channel

Keeping porous plates close to navigation channel, extensive simulations were done for understanding the effects of barriers like silt curtains, turbidity curtains, filter screens on the siltation behaviour of navigation channel of Kandla port Fig. A- II.1 to Fig. A-II. 20 shows the cumulative sedimentation and erosion of navigation channel with various alignments of porous plates.

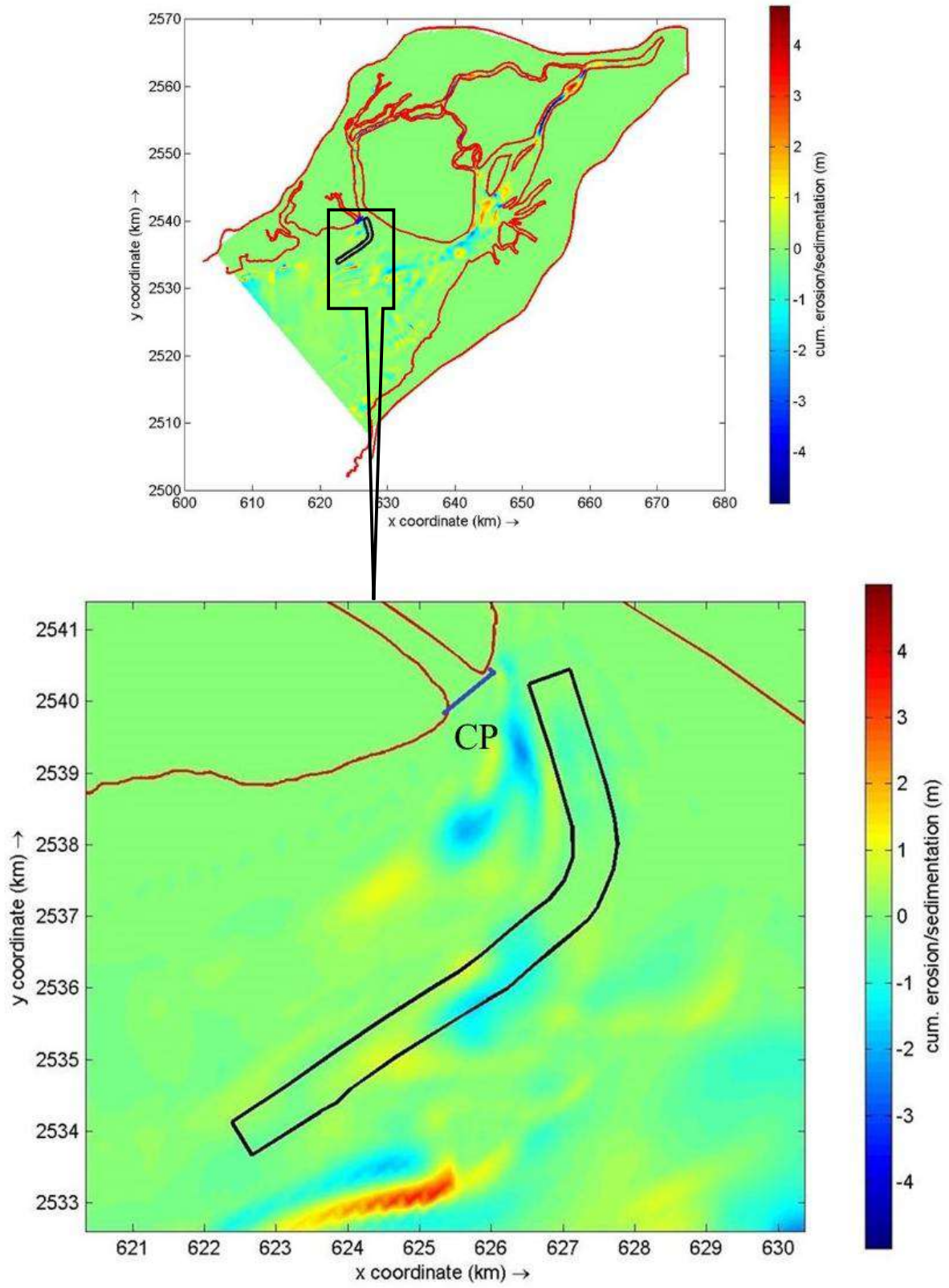


**Fig. A-II. 1 Cumulative erosion/deposition in May month with porous plate- Case 1**

*(Case 1: Keeping porous plate shown as CP* at the mouth of adjoining creek next to Kandla creek)*

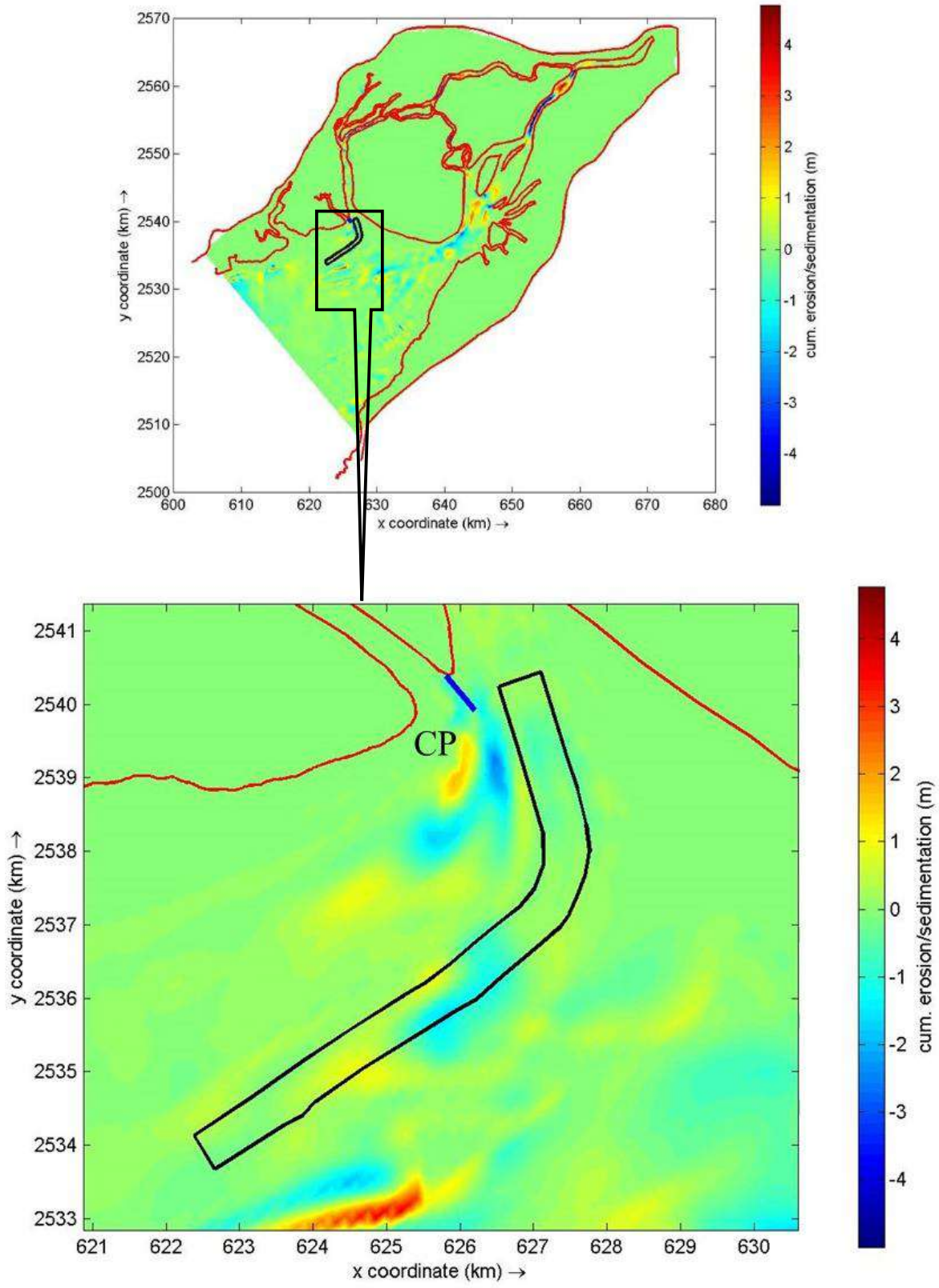


**Fig. A-II. 2 Cumulative erosion/deposition in May month with porous plate- Case 2**

*(Case 2: Keeping the porous plate shown as CP extending along the bank of adjoin creek to Kandla creek)*

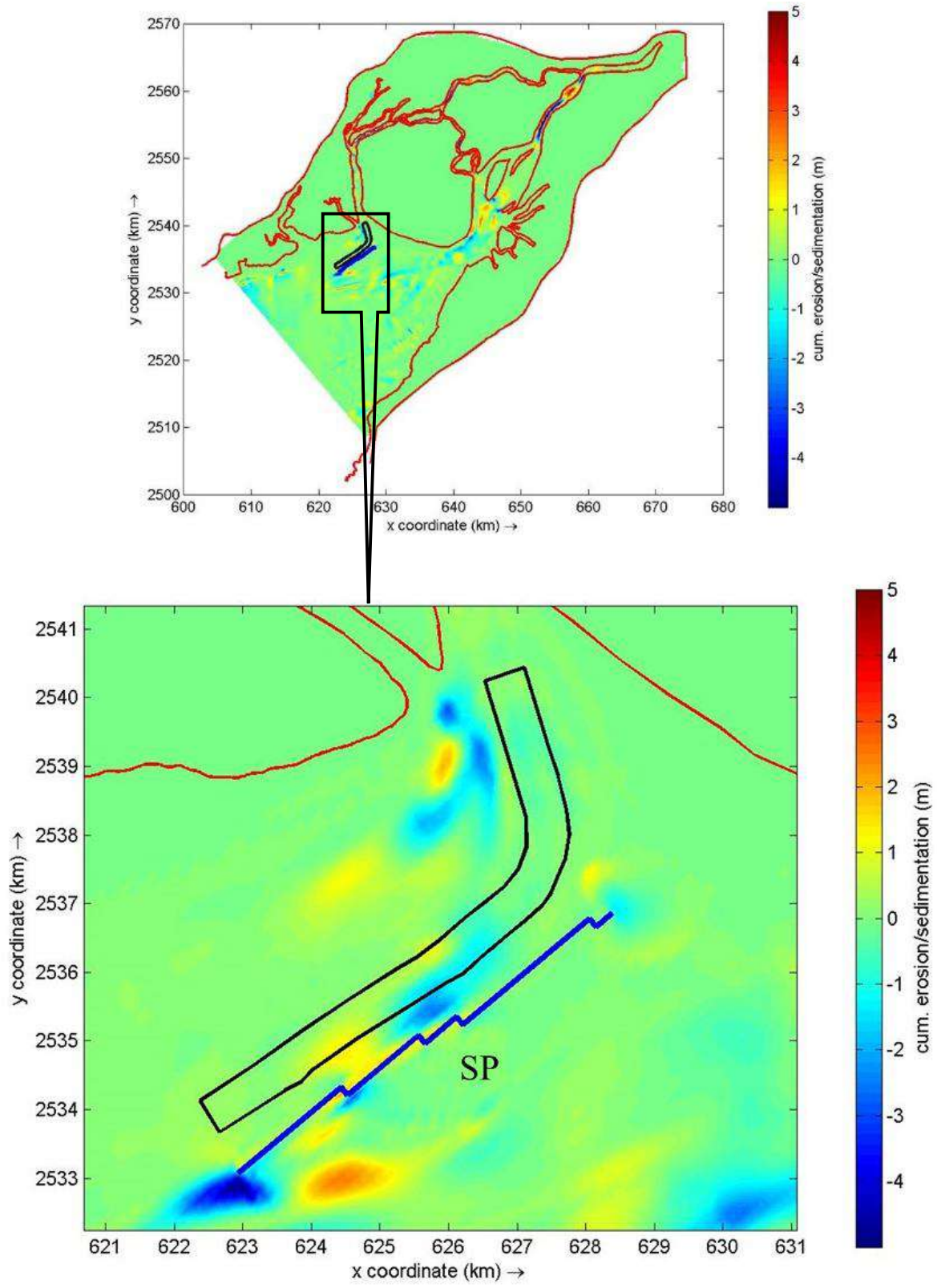


**Fig. A-II. 3 Cumulative erosion/deposition in May month with porous plate- Case 3**

*(Case 3: Keeping porous plate shown as SP* at the south of navigation channel)*

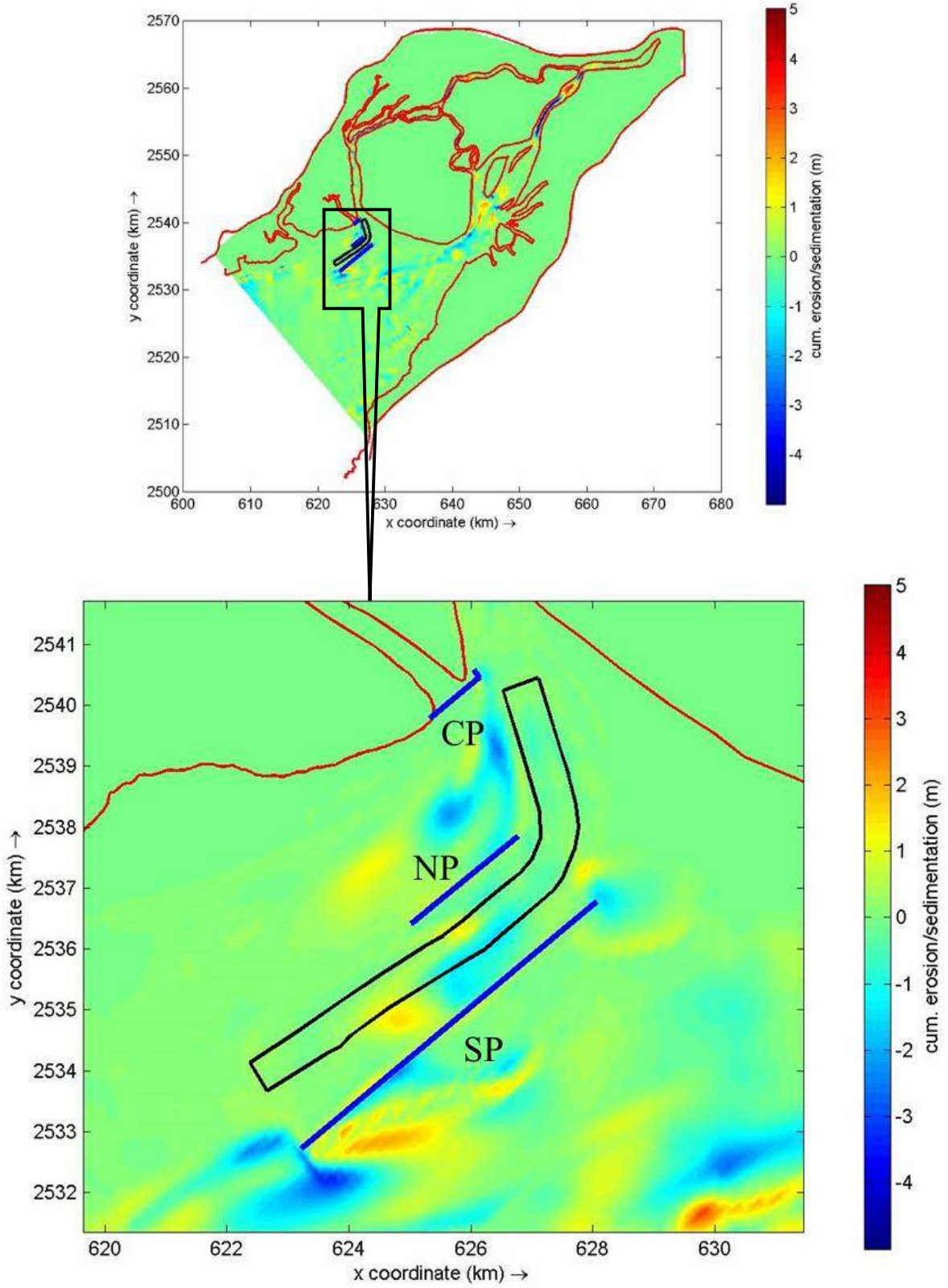


**Fig. A-II. 4 Cumulative erosion/deposition in May month with porous plate- Case 4**

*(Case 4: Keeping the porous plate shown as CP, NP*, SP at the mouth of adjoining creek to Kandla creek, north and south of the navigation channel respectively)*

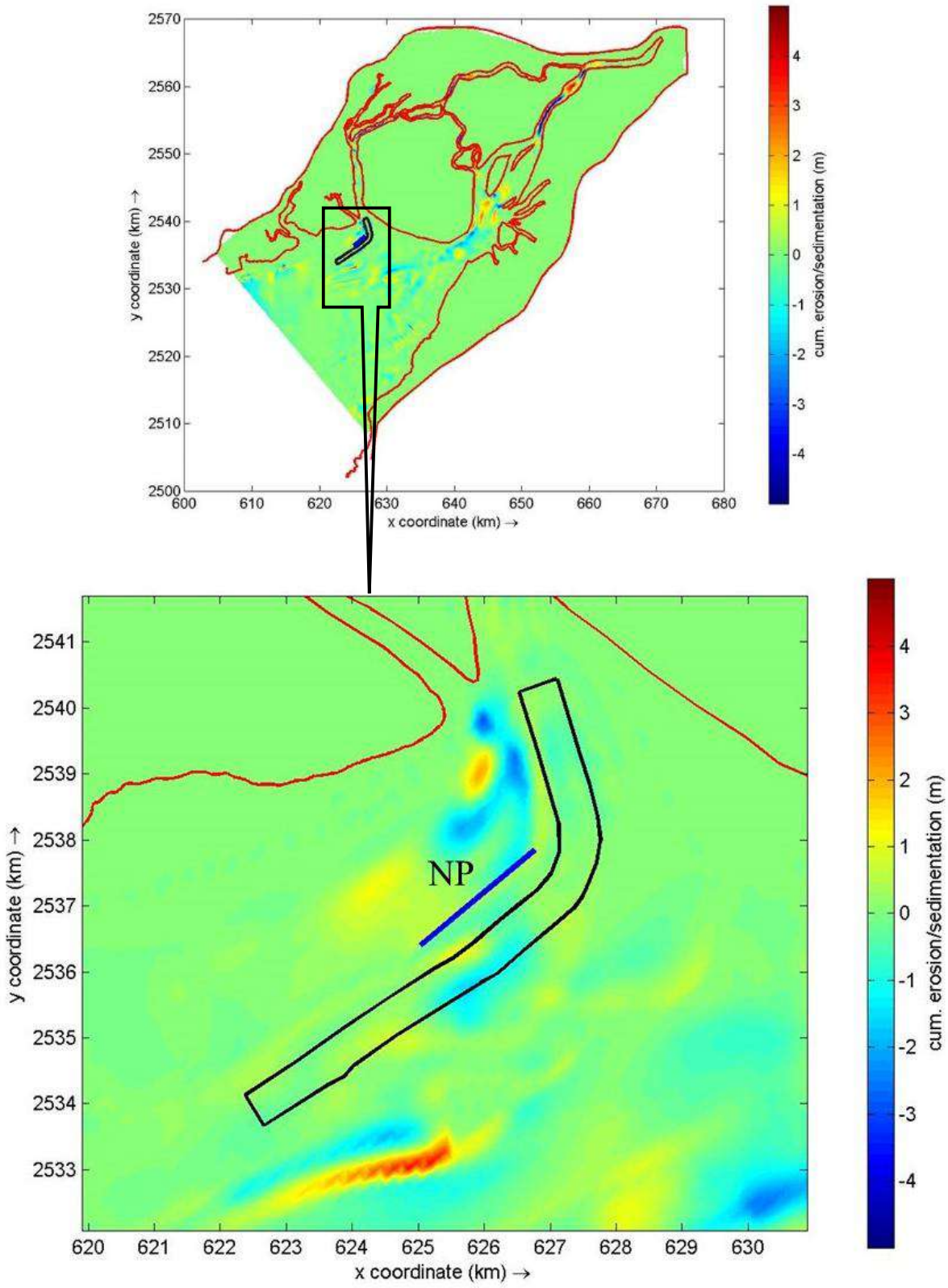


**Fig. A-II. 5 Cumulative erosion/deposition in May month with porous plate- Case 5**

*(Case 5: Keeping porous plate shown as NP at the north of navigation channel)*

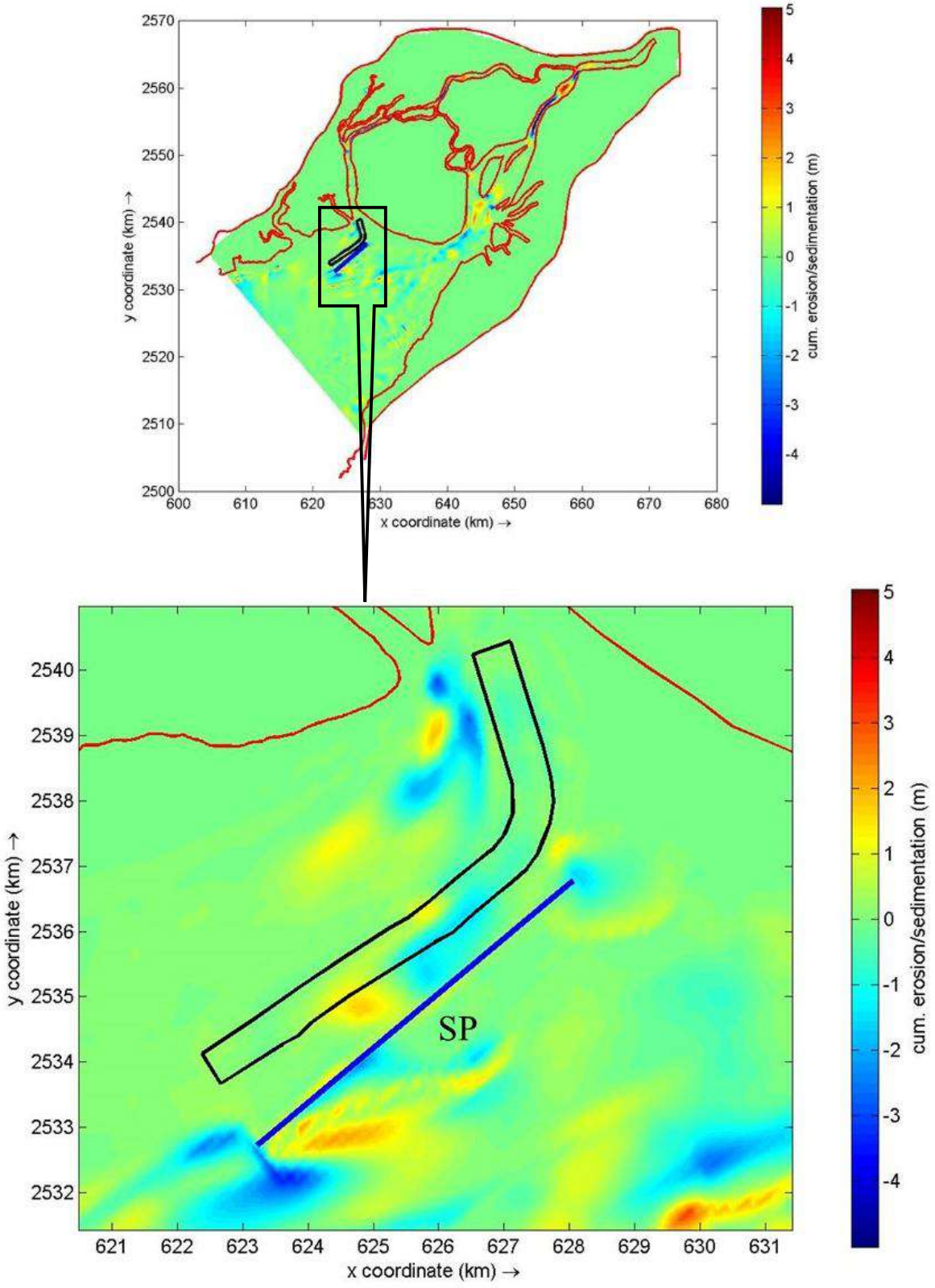


**Fig. A-II. 6 Cumulative erosion/deposition in May month with porous plate- Case 6**

*(Case 6: Keeping porous plate shown as SP at the south and along the navigation channel)*

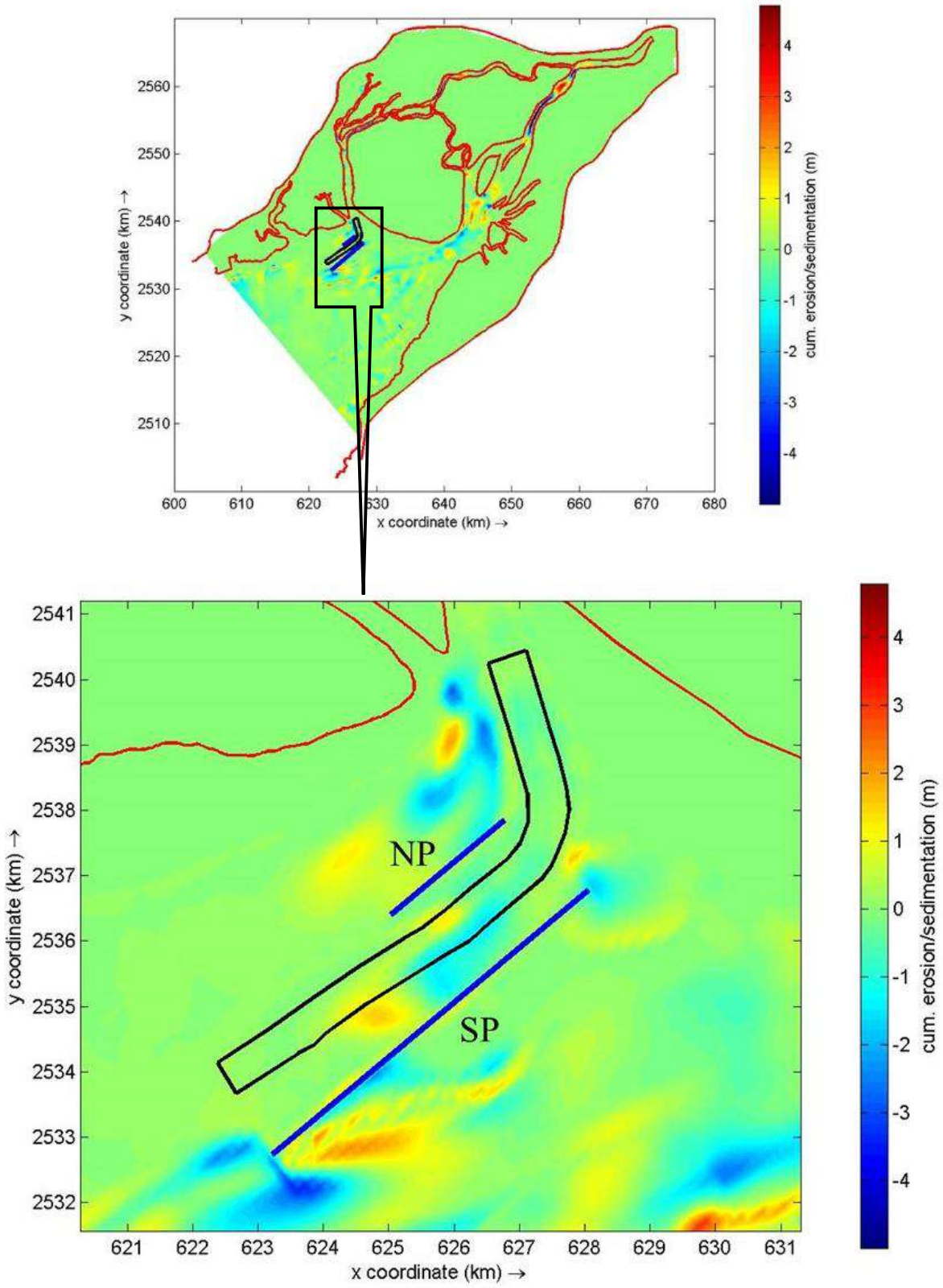


**Fig. A-II. 7 Cumulative erosion/deposition in May month with porous plate- Case 7**

*(Case 7: Keeping the porous plate shown as NP and SP at the north and south of the navigation channel respectively)*

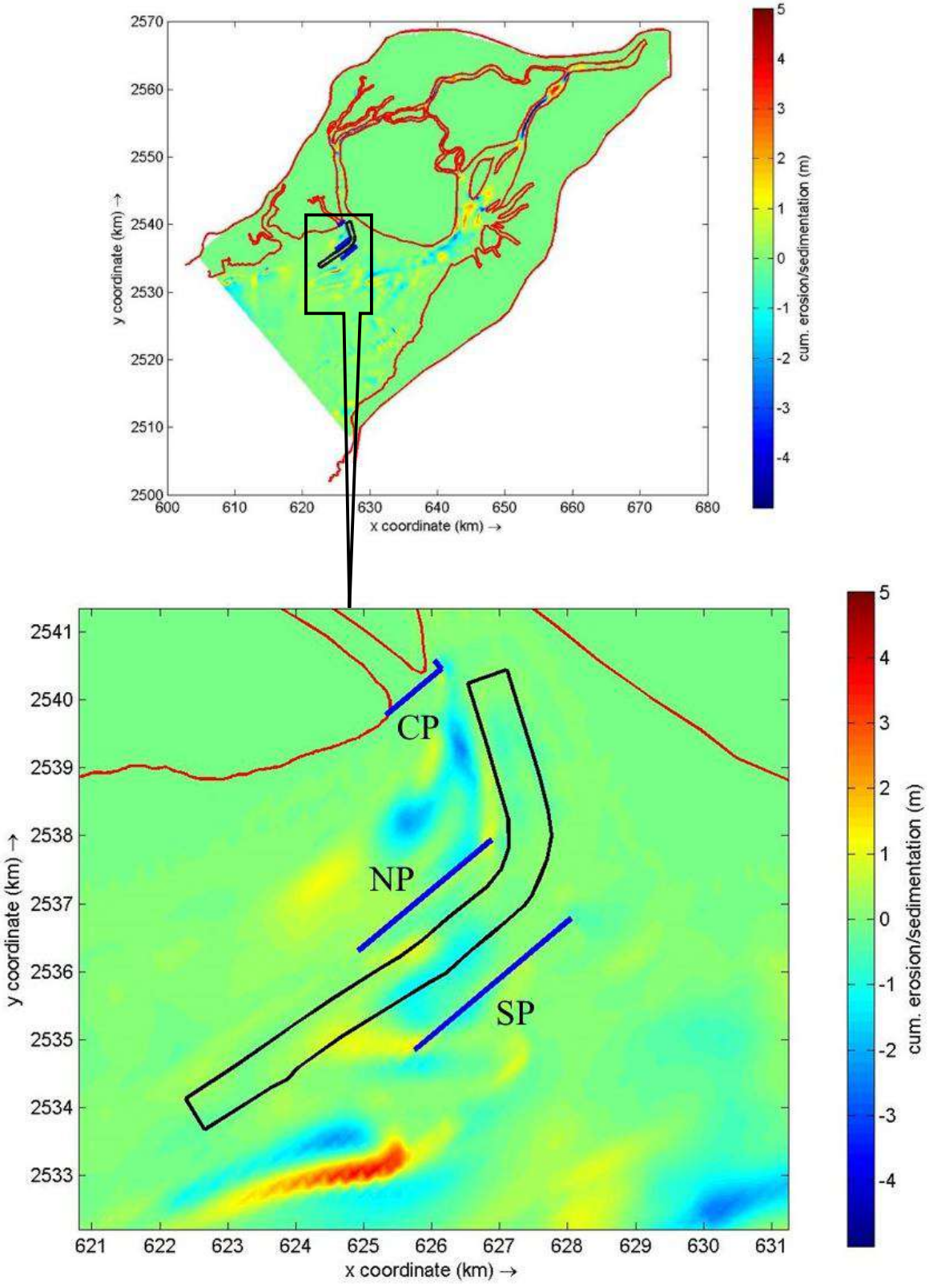


**Fig. A-II. 8 Cumulative erosion/deposition in May month with porous plate- Case 8**

*(Case 8: Keeping the porous plate shown as CP, NP, SP at the mouth of adjoining creek to Kandla creek, north and south of the navigation channel respectively)*

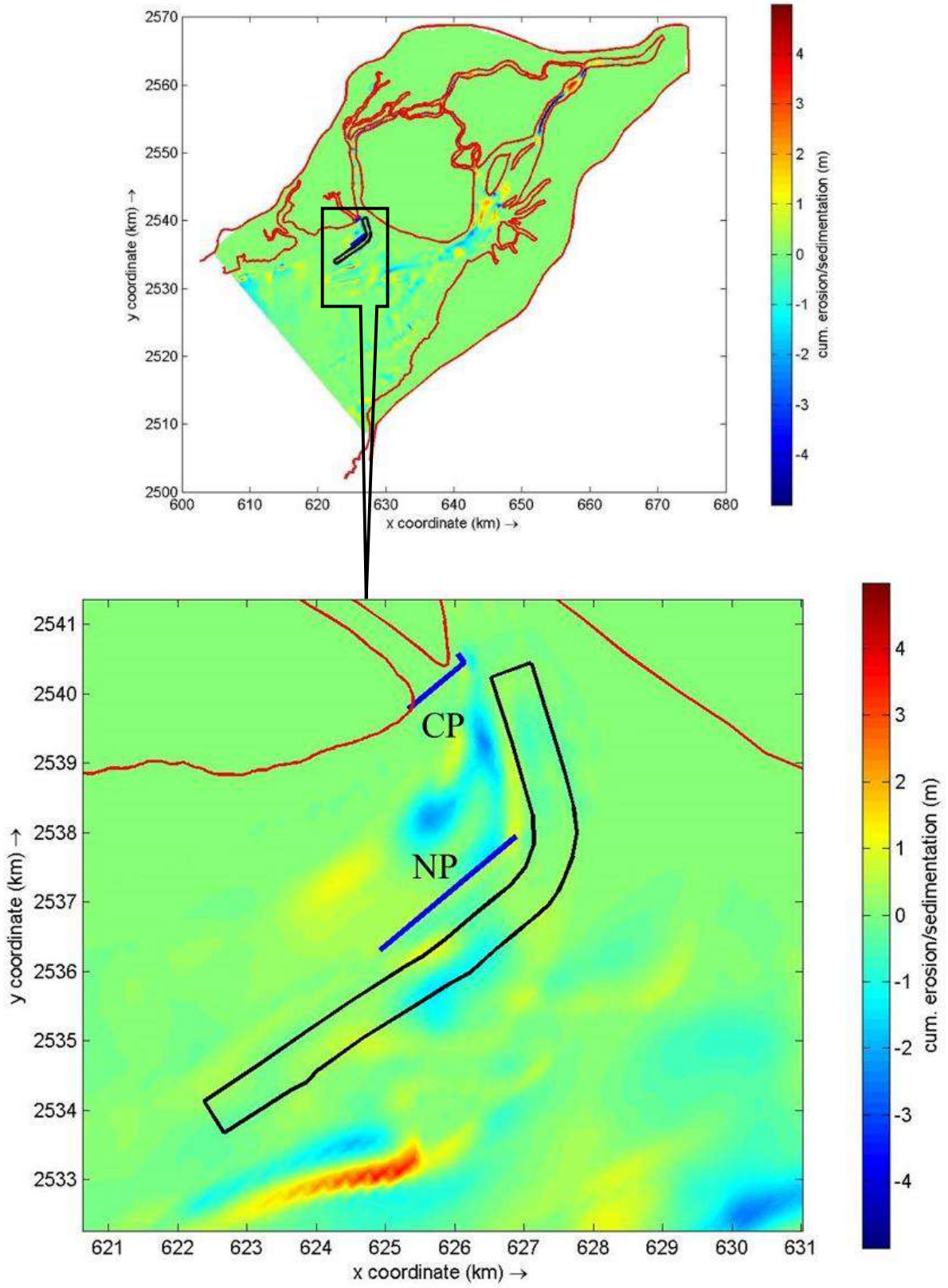


**Fig. A-II. 9 Cumulative erosion/deposition in May month with porous plate- Case 9**

*(Case 9: Keeping the porous plates shown as CP and NP at the mouth of adjoining creek to Kandla creek and at north of the navigation channel respectively)*

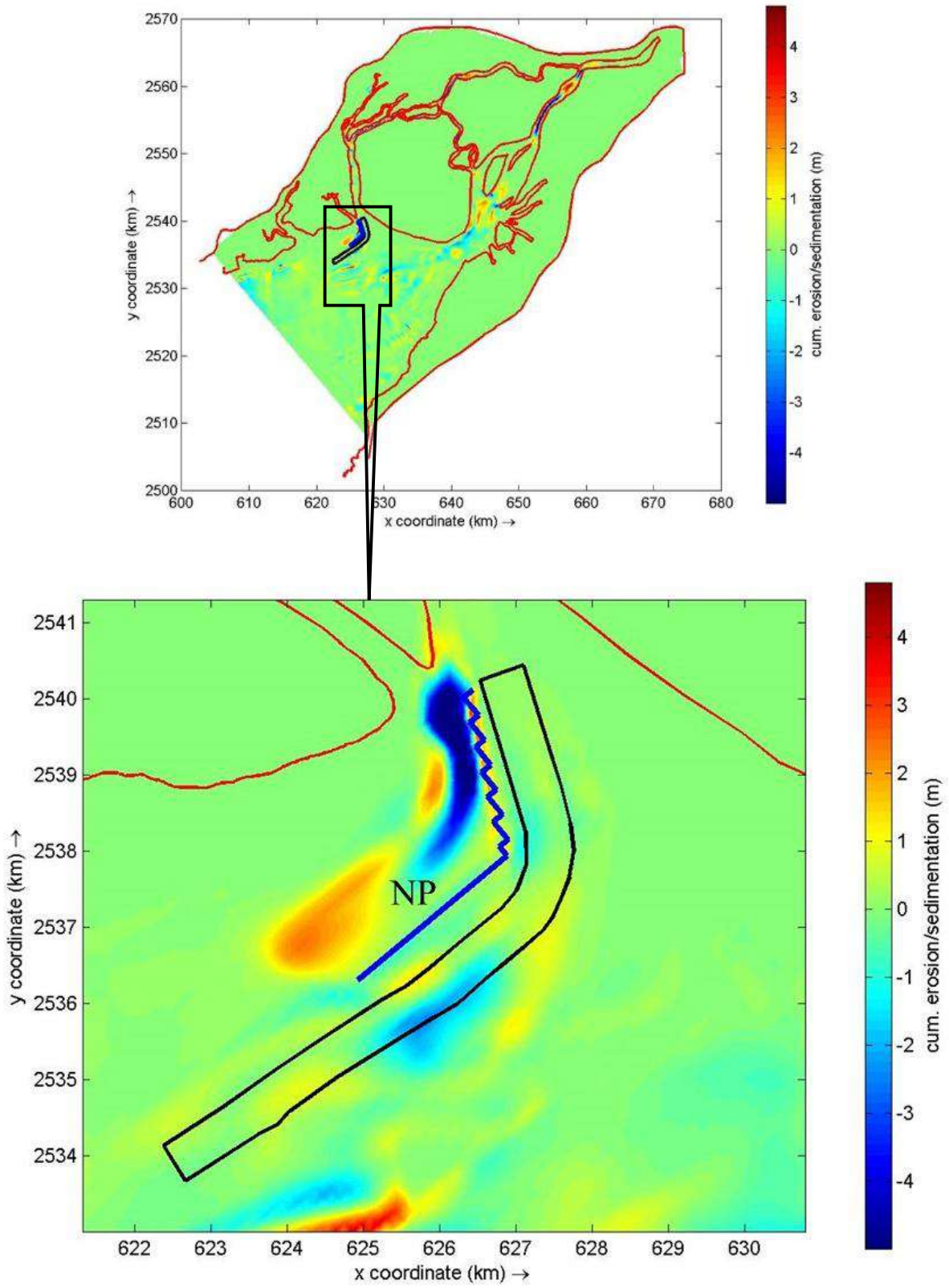


**Fig. A-II. 10 Cumulative erosion/deposition in May month with porous plate- Case 10**

*(Case 10: Keeping porous plate shown as NP at the north and along the navigation channel)*

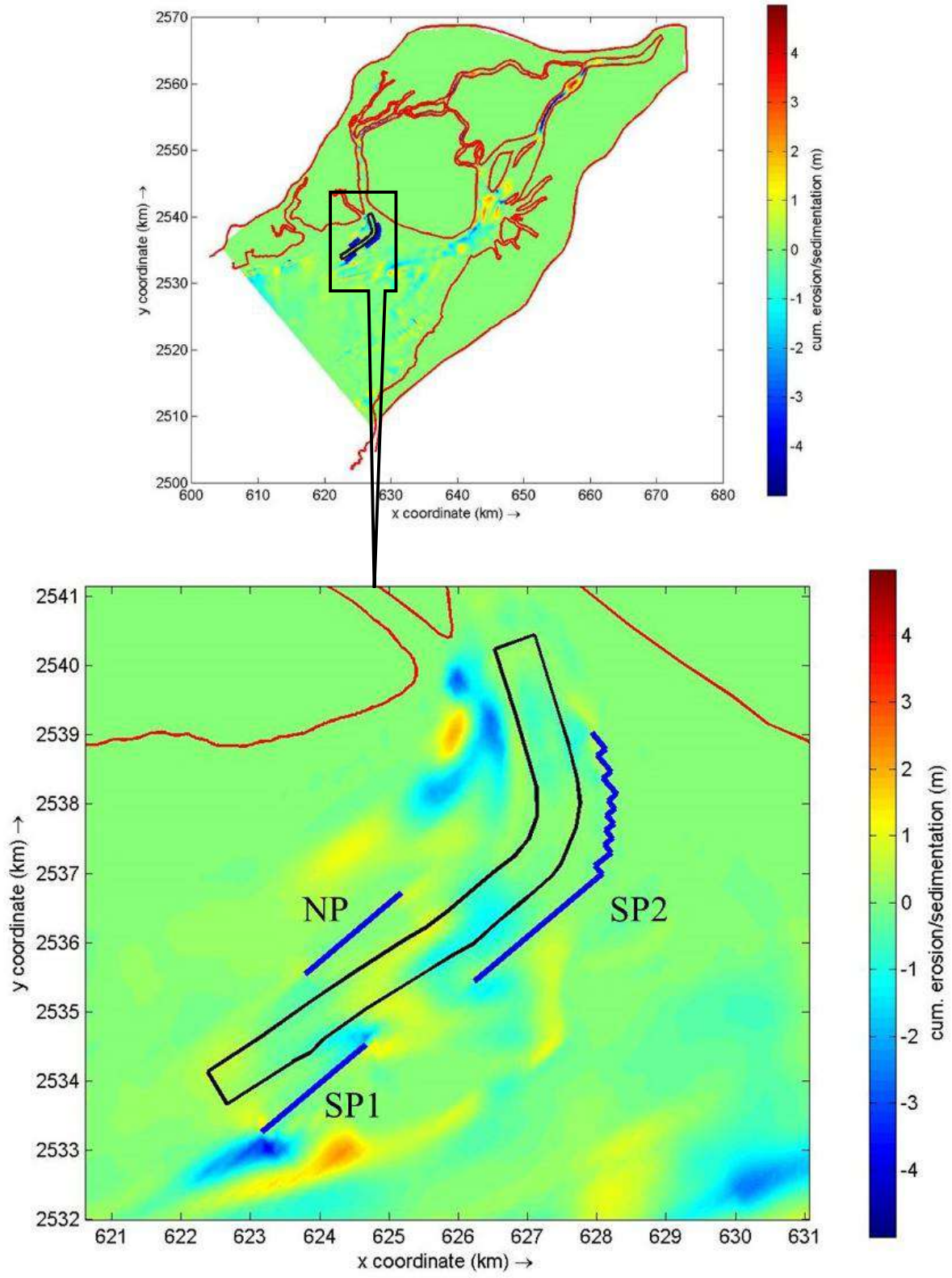


**Fig. A-II. 11 Cumulative erosion/deposition in May month with porous plate- Case 11**

*(Case 11: Keeping the porous plate shown as NP, SP1*, SP2* at the north and south of the navigation channel)*

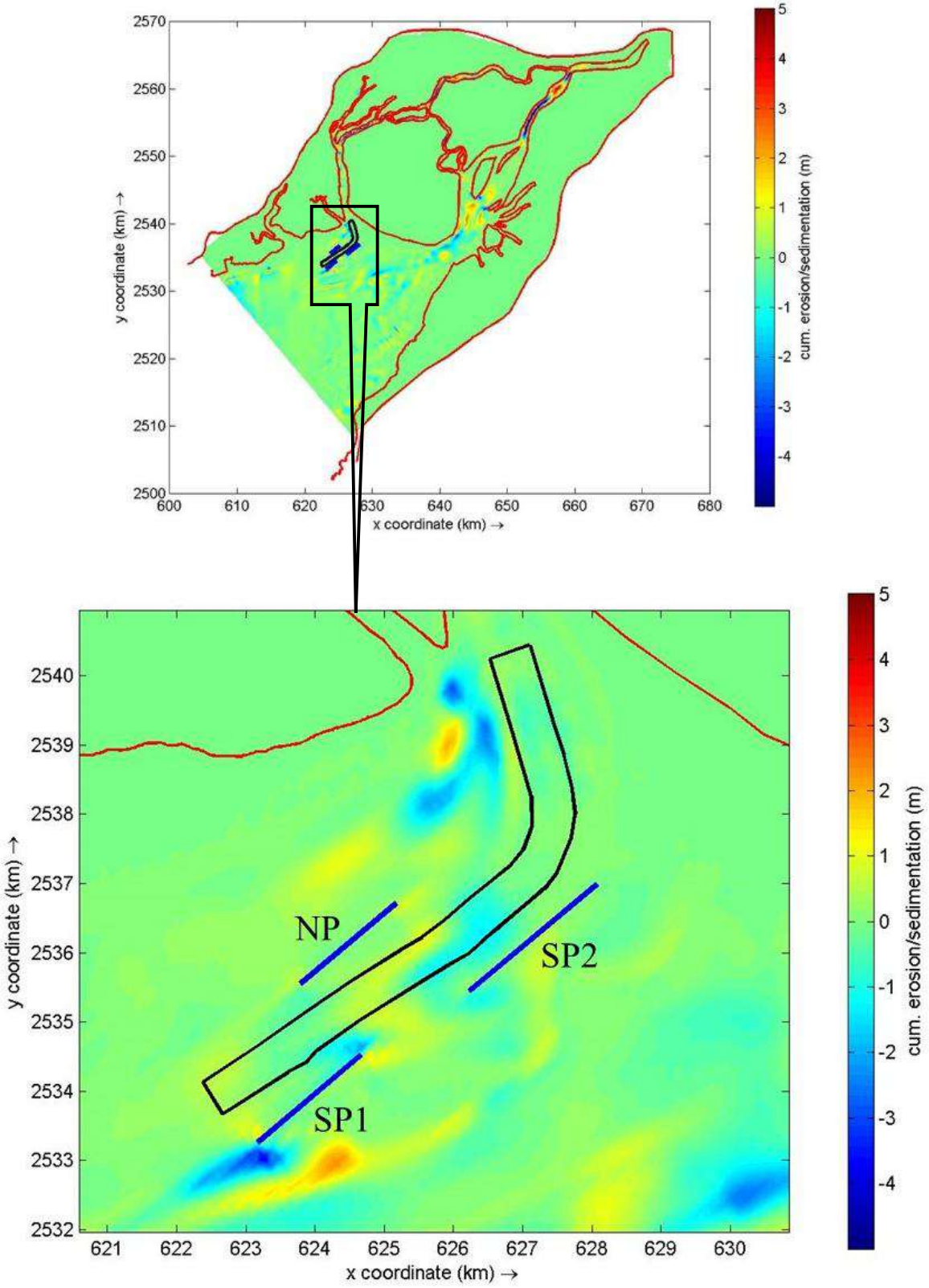


**Fig. A-II. 12 Cumulative erosion/deposition in May month with porous plate- Case 12**

*(Case 12: Keeping the porous plate shown as NP, SP1, SP2 at the north and south of the navigation channel, length of SP2 is reduced in this case than case 11)*

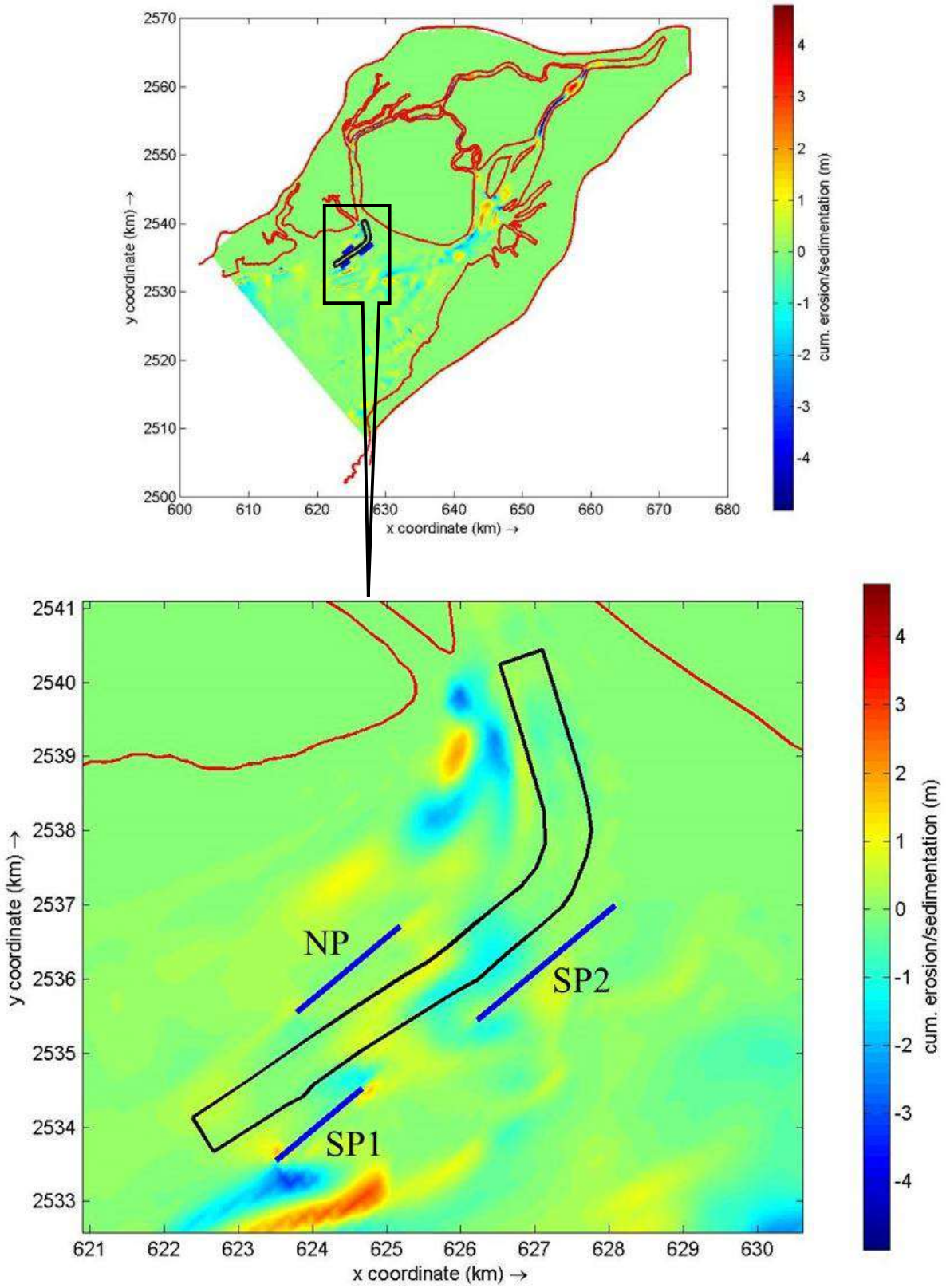


**Fig. A-II. 13 Cumulative erosion/deposition in May month with porous plate- Case 13**

*(Case 13: Keeping the porous plate shown as NP, SP1, SP2 at the north and south of the navigation channel, length of SP1 is reduced from the bottom in this case than case 12)*

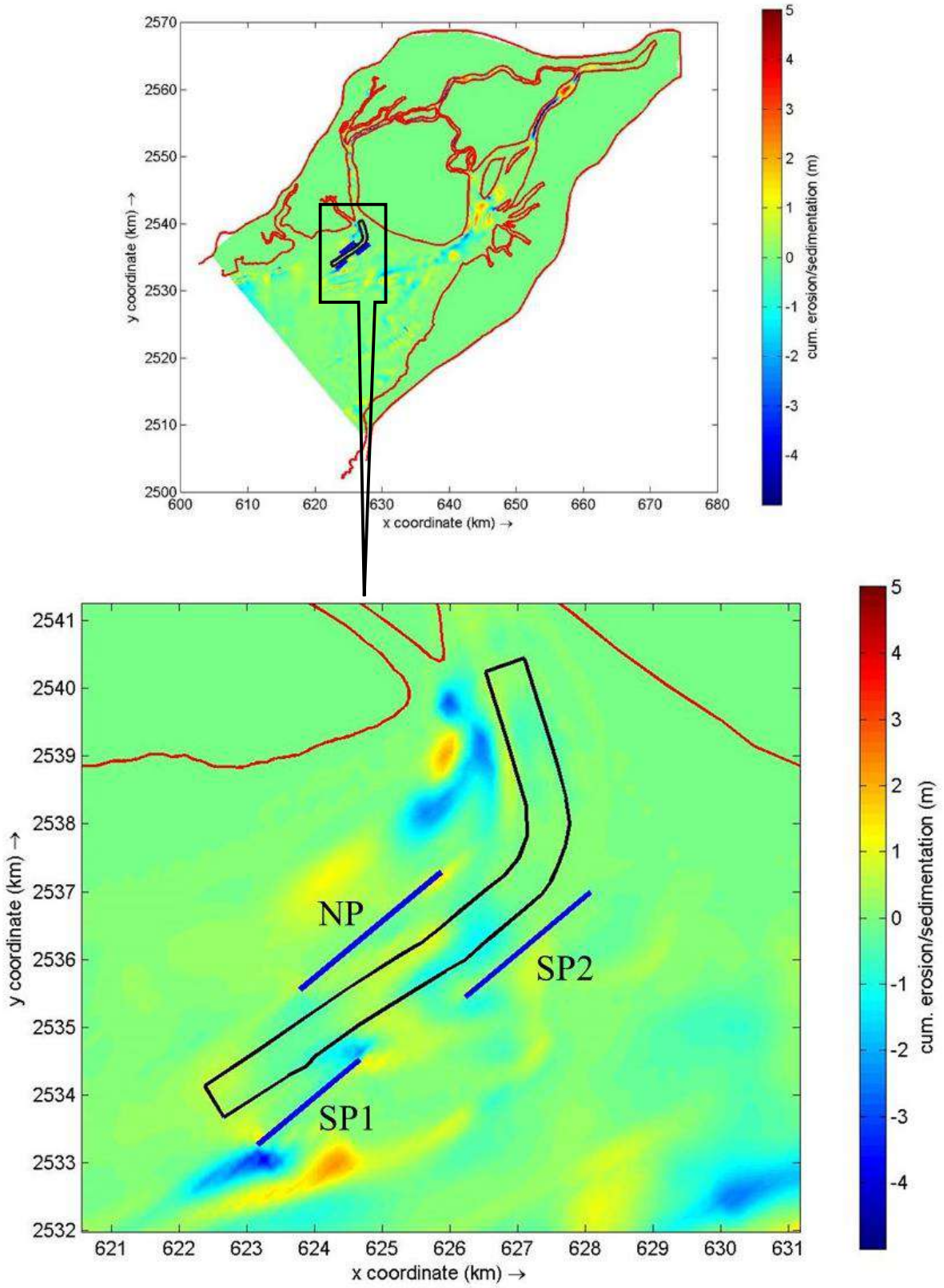


**Fig. A-II. 14 Cumulative erosion/deposition in May month with porous plate- Case 14**

*(Case 14: Keeping the porous plate shown as NP, SP1, SP2 at the north and south of the navigation channel, length of NP is reduced in this case than case 11)*

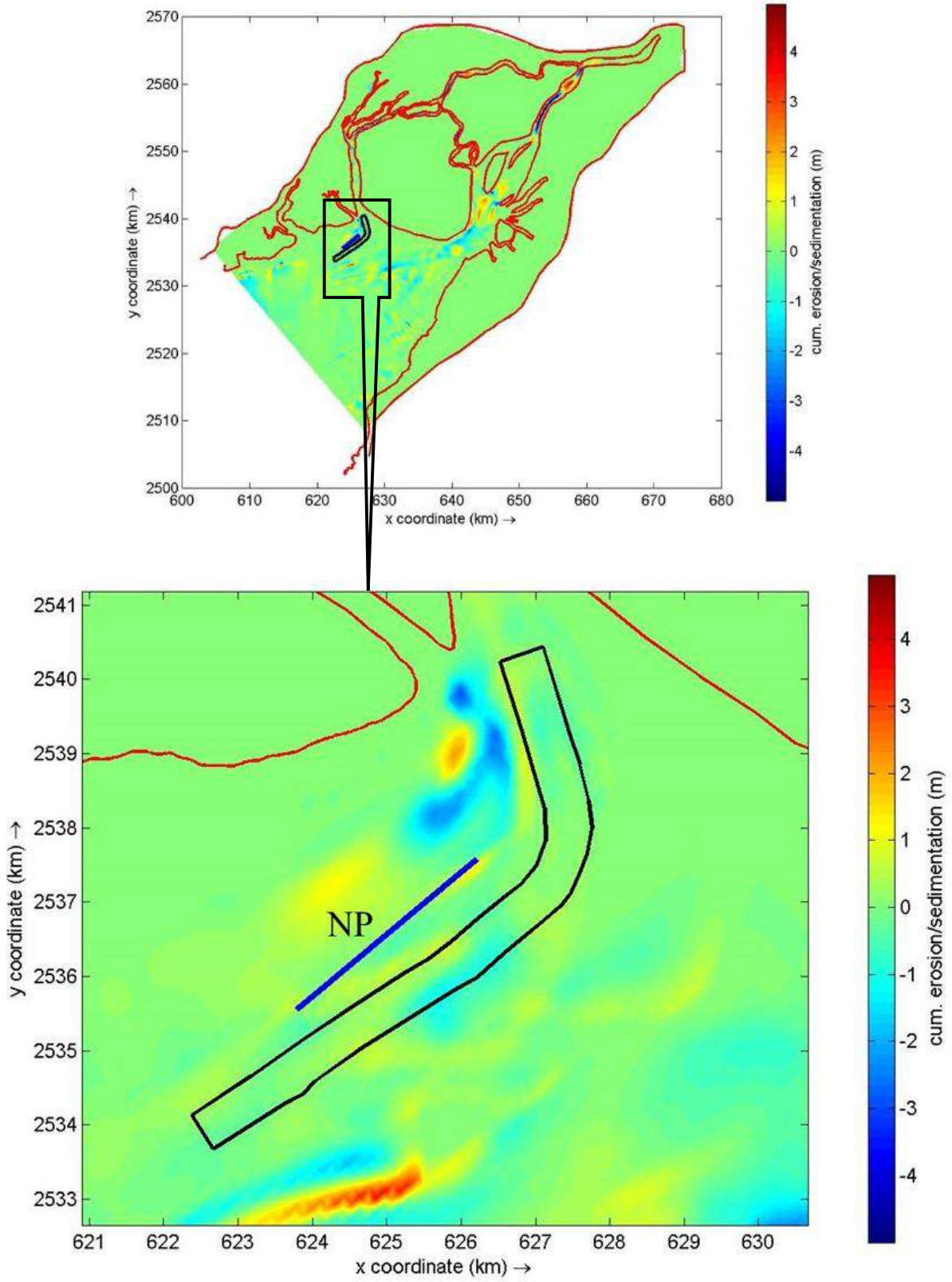


**Fig. A-II. 15 Cumulative erosion/deposition in May month with porous plate- Case 15**

*(Case 15: Keeping porous plate shown as NP at the north of navigation channel)*

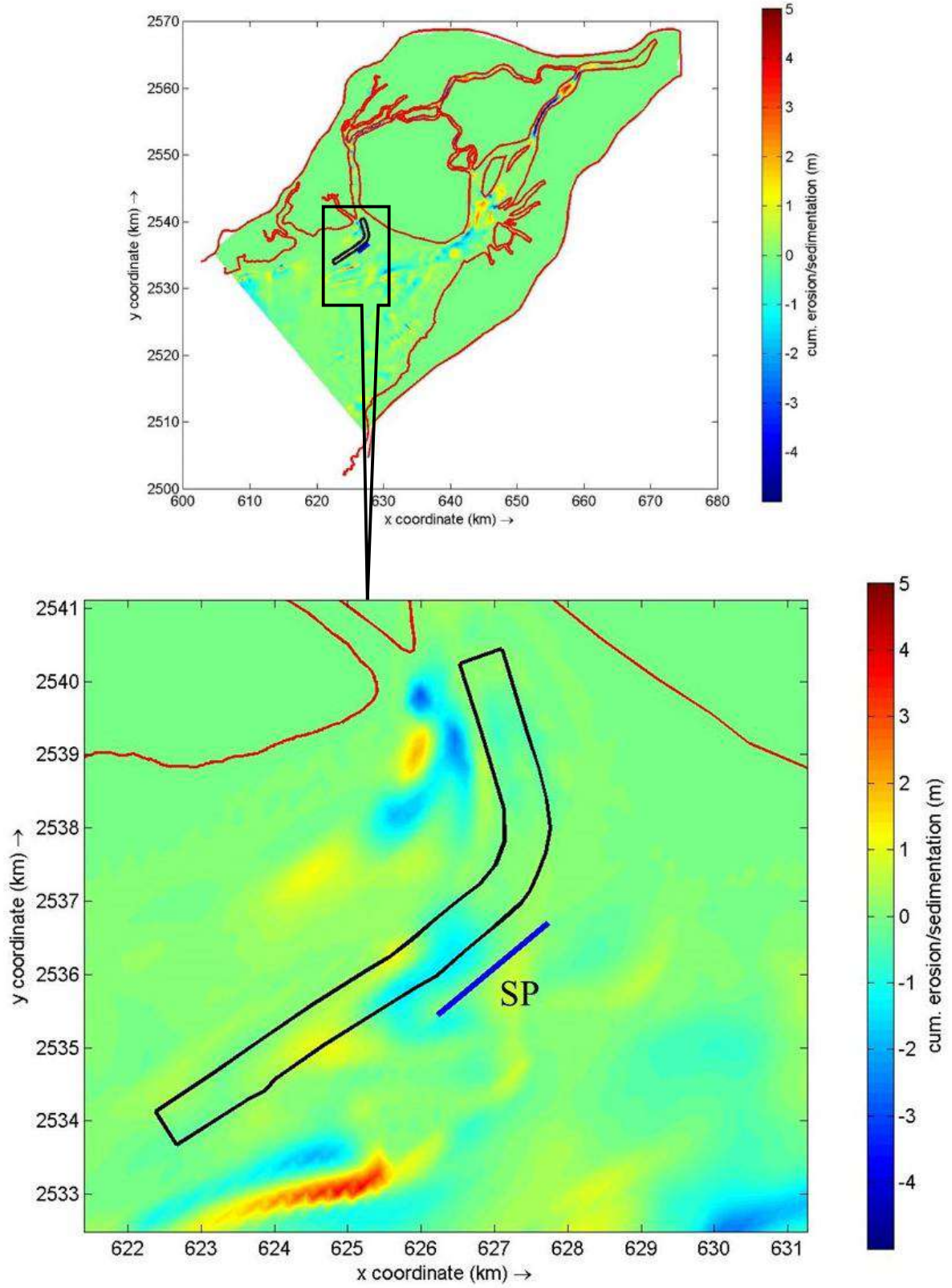


**Fig. A-II. 16 Cumulative erosion/deposition in May month with porous plate- Case 16**

*(Case 16: Keeping porous plate shown as SP at the south of navigation channel)*

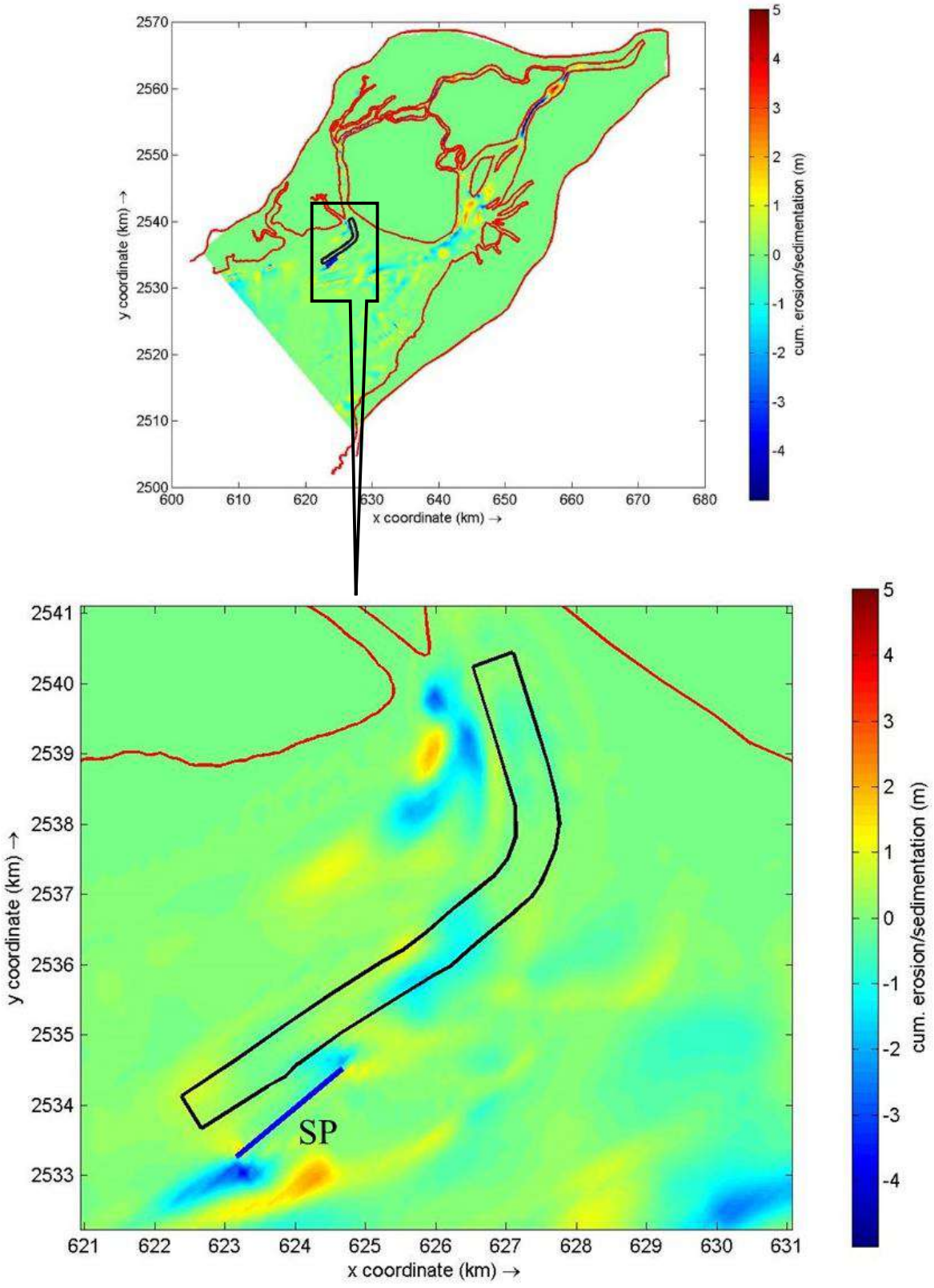


**Fig. A-II. 17 Cumulative erosion/deposition in May month with porous plate- Case 17**

*(Case 17: Keeping porous plate shown as SP at the south of navigation channel)*

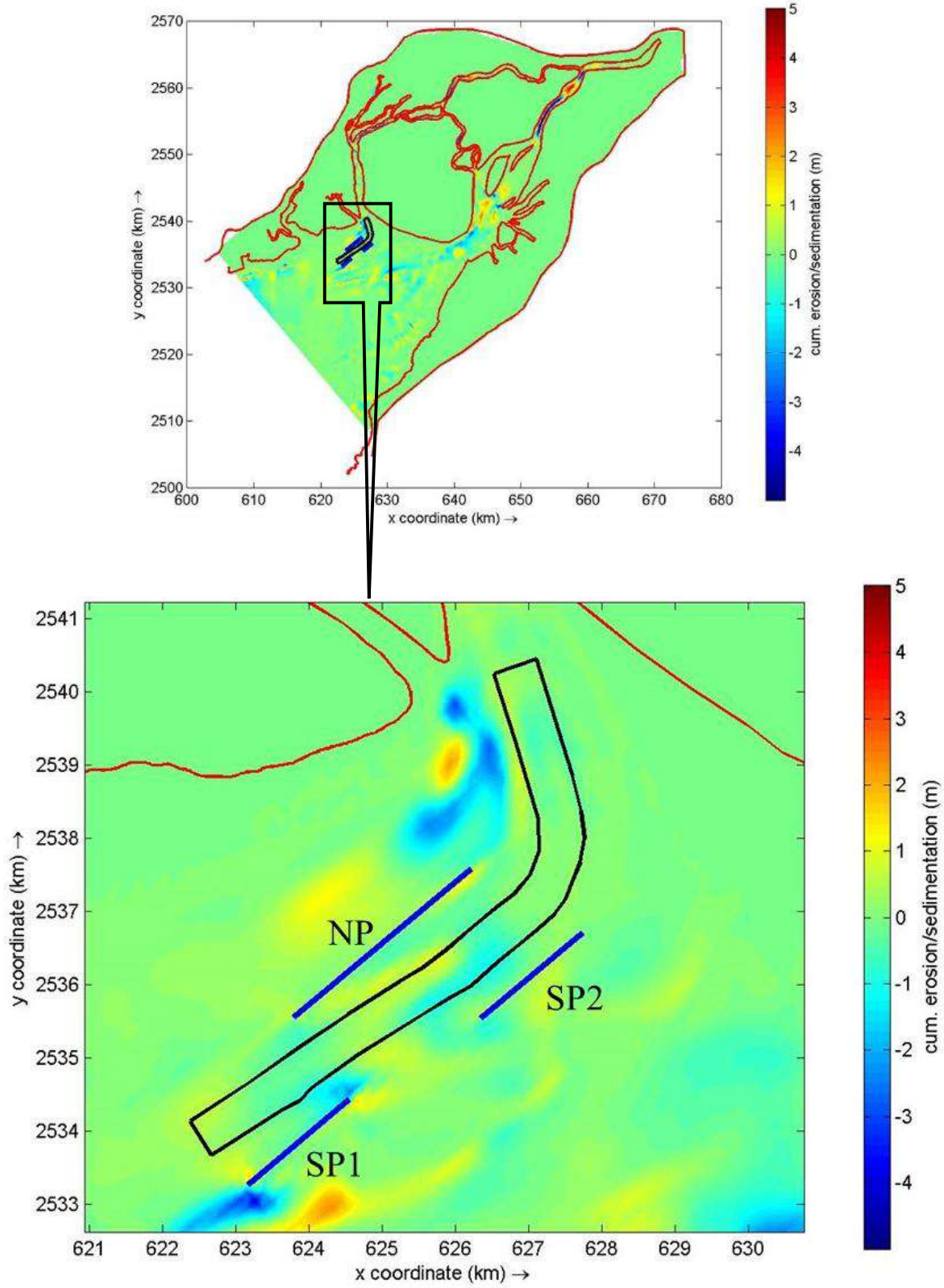


**Fig. A-II. 18 Cumulative erosion/deposition in May month with porous plate- Case 18**

*(Case 18: Keeping the porous plate shown as NP, SP1, SP2 at the north and south of the navigation channel)*

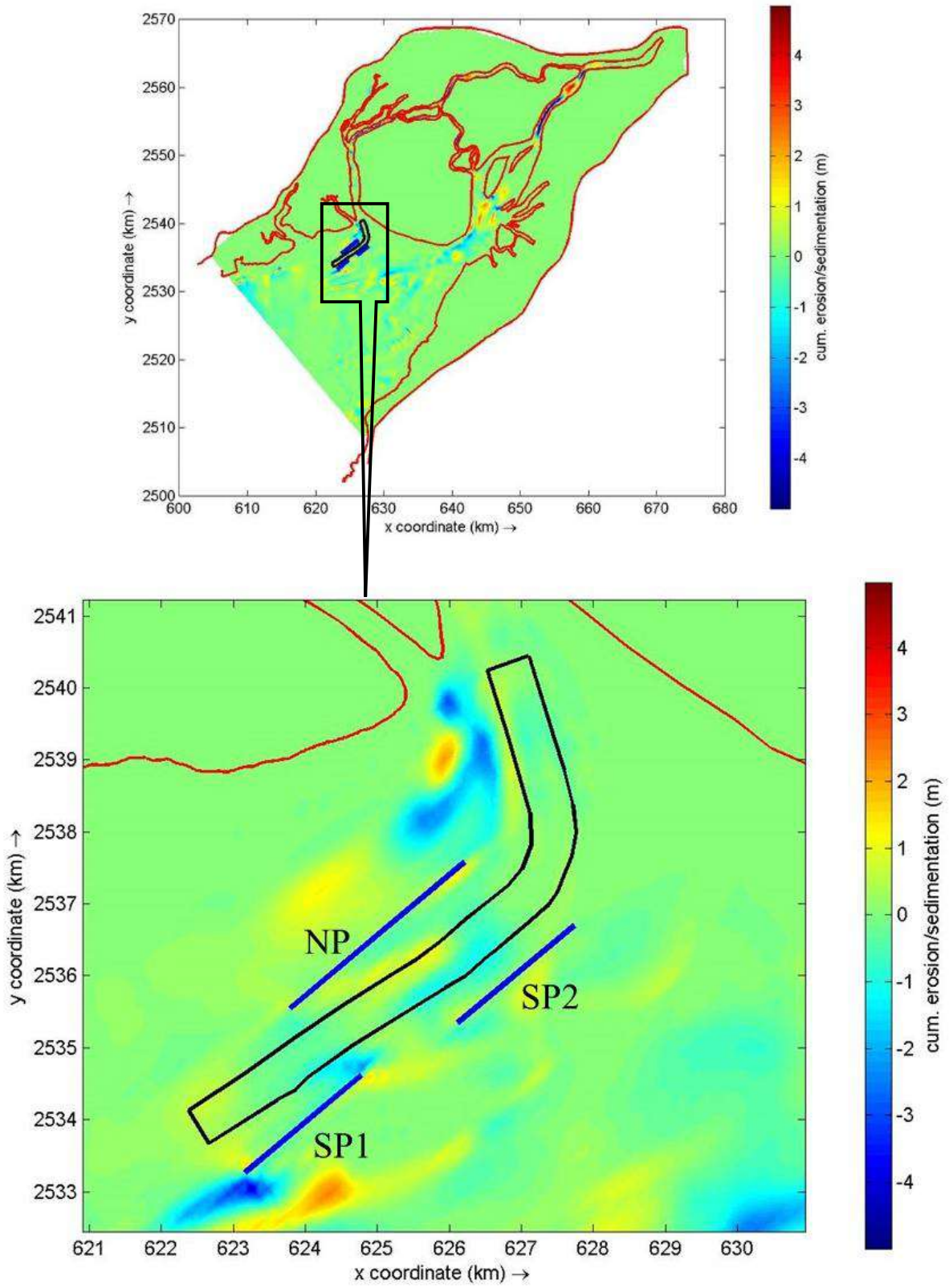


**Fig. A-II. 19 Cumulative erosion/deposition in May month with porous plate- Case 19**

*(Case 19: Keeping the porous plate shown as NP, SP1, SP2 at the north and south of the navigation channel but length of SP1 and SP2 is increased and spacing between them is decreased than case 18)*

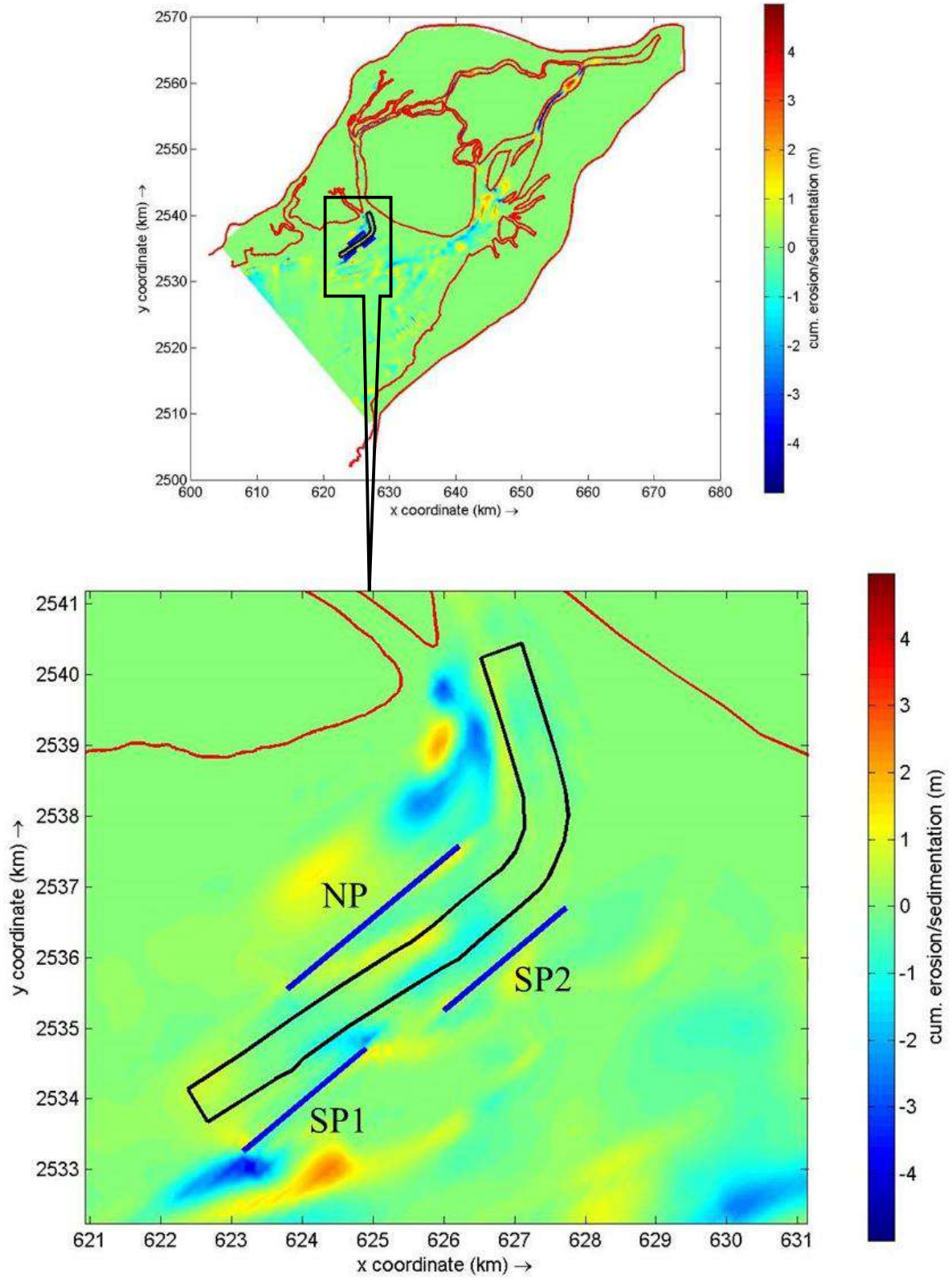


**Fig. A-II. 20 Cumulative erosion/deposition in May month with porous plate- Case 20**

*(Case 20: Keeping the porous plate shown as NP, SP1, SP2 at the north and south of the navigation channel but length of SP1 and SP2 is increased and spacing between them is decreased than case 19)*

**Remarks*

*CP- Porous plate near to mouth of Kandla Creek*

*NP- Porous plate at north of navigation channel*

*SP, SP1, SP2- Porous plate at south of navigation channel*

**Table A-II. 1 Porous plate specification with siltation quantity**

| Case No. | Lengths of Porous Plate in Km | | | | Siltation Quantity (cubic meter) |
|---|---|---|---|---|---|
| | CP | NP | SP/SP1 | SP2 | |
| 1 | 1.2 | - | - | - | 3,91,900 |
| 2 | 0.6 | - | - | - | 4,00,300 |
| 3 | 6.6 | - | - | - | 5,45,900 |
| 4 | 1.2 | 2.25 | 6.3 | - | 4,16,900 |
| 5 | - | 2.25 | - | - | 3,67,700 |
| 6 | - | - | 6.3 | - | 4,93,400 |
| 7 | - | 2.25 | 6.3 | - | 4,38,000 |
| 8 | 1.2 | 2.55 | 3 | - | 3,48,000 |
| 9 | 1.2 | 2.55 | - | - | 3,43,100 |
| 10 | - | 4.8 | - | - | 6,02,800 |
| 11 | - | 1.8 | 1.95 | 4.5 | 3,14,700 |
| 12 | - | 1.8 | 1.95 | 2.4 | 2,97,600 |
| 13 | - | 1.8 | 1.5 | 2.4 | 3,22,200 |
| 14 | - | 2.7 | 1.95 | 2.4 | 2,37,100 |
| 15 | - | 3.15 | - | - | 2,76,500 |
| 16 | - | - | 1.95 | - | 4,47,100 |
| 17 | - | - | - | 1.95 | 2,69,600 |
| 18 | - | 3.15 | 1.8 | 1.8 | 2,29,400 |
| 19 | - | 3.15 | 2.1 | 2.1 | 2,17,700 |
| 20 | - | 3.15 | 2.25 | 2.25 | 2,35,100 |

# APPENDIX-III Porosity of Porous Plate

Porous plate is partially transparent structure and allows mass and momentum to exchange. Porosity in Delft3D morphological model is controlled by the quadratic friction term.

The flow rate Q through a porous plate can often be described by a Q-H relation. They relate the flow rate to the difference between the upstream and downstream water levels:

$$Q = \mu A\sqrt{2g|\zeta_u - \zeta_d} \quad \text{(A.1)}$$

With μ the contraction coefficient ($0 < \mu \leq 1$), the wet flow-through area and the upstream and downstream water level, respectively. The contraction coefficient μ can be used to determine the additional quadratic friction term in the momentum equation.

$$M_\xi = -\frac{c_{loss}-u}{\Delta x} u\sqrt{u^2 + v^2} \quad \text{(A.2)}$$

$$M_\eta = -\frac{c_{loss}-v}{\Delta y} v\sqrt{u^2 + v^2} \quad \text{(A.3)}$$

With $c_{loss}$ is the energy loss coefficient. To determine the porosity, energy loss coefficient has to be discover. After studying various values, energy lost coefficient $(c_{loss})$ is taken as 1000 for model simulations for which approximate 50% porosity is observed. Difference in current velocity with porous plate and without porous plate in ebb and flood time is shown in Fig. A-III.1 and A-III.2 respectively.

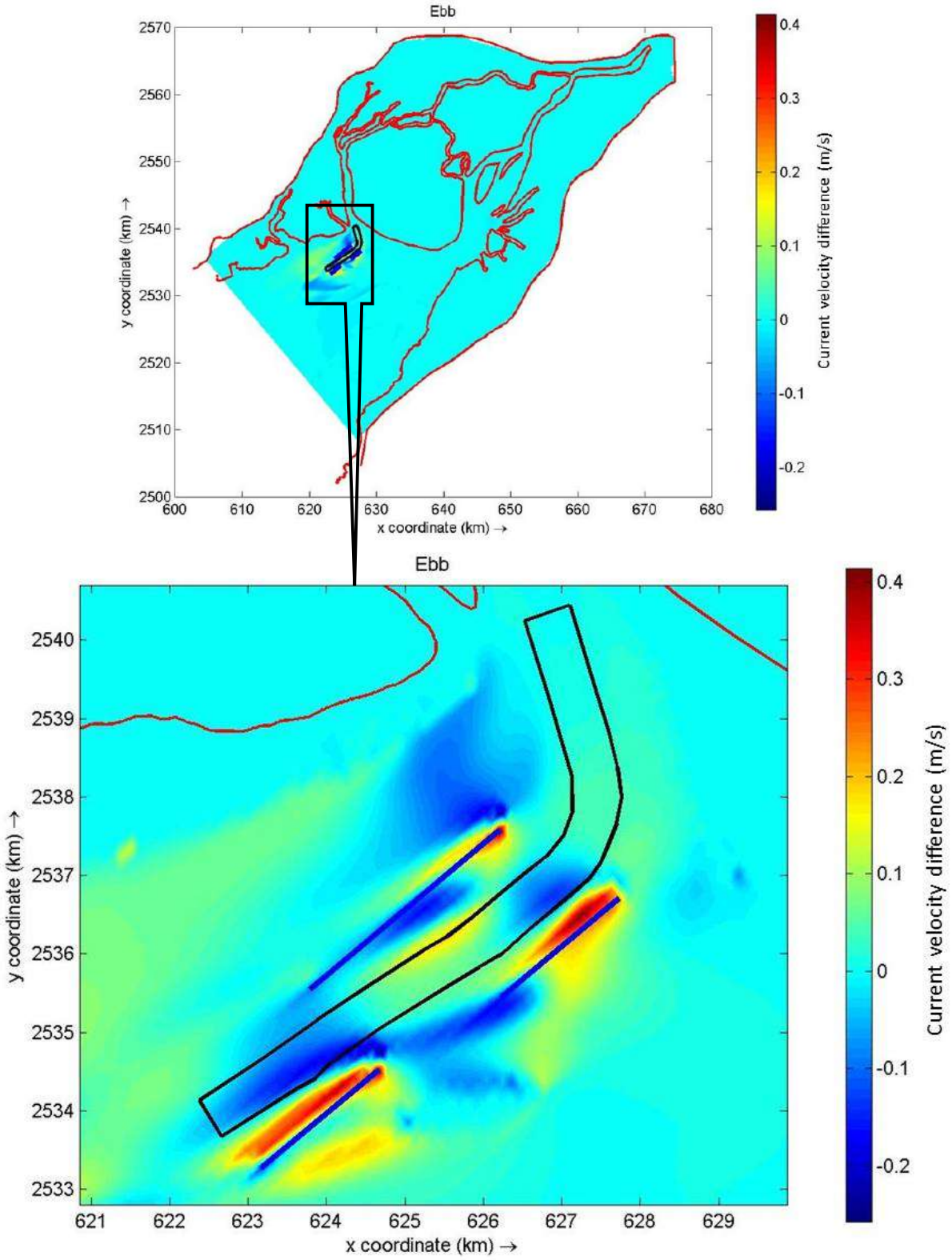


**Fig. A-III. 1 Difference in Current velocity with and without porous plate during Ebb time**

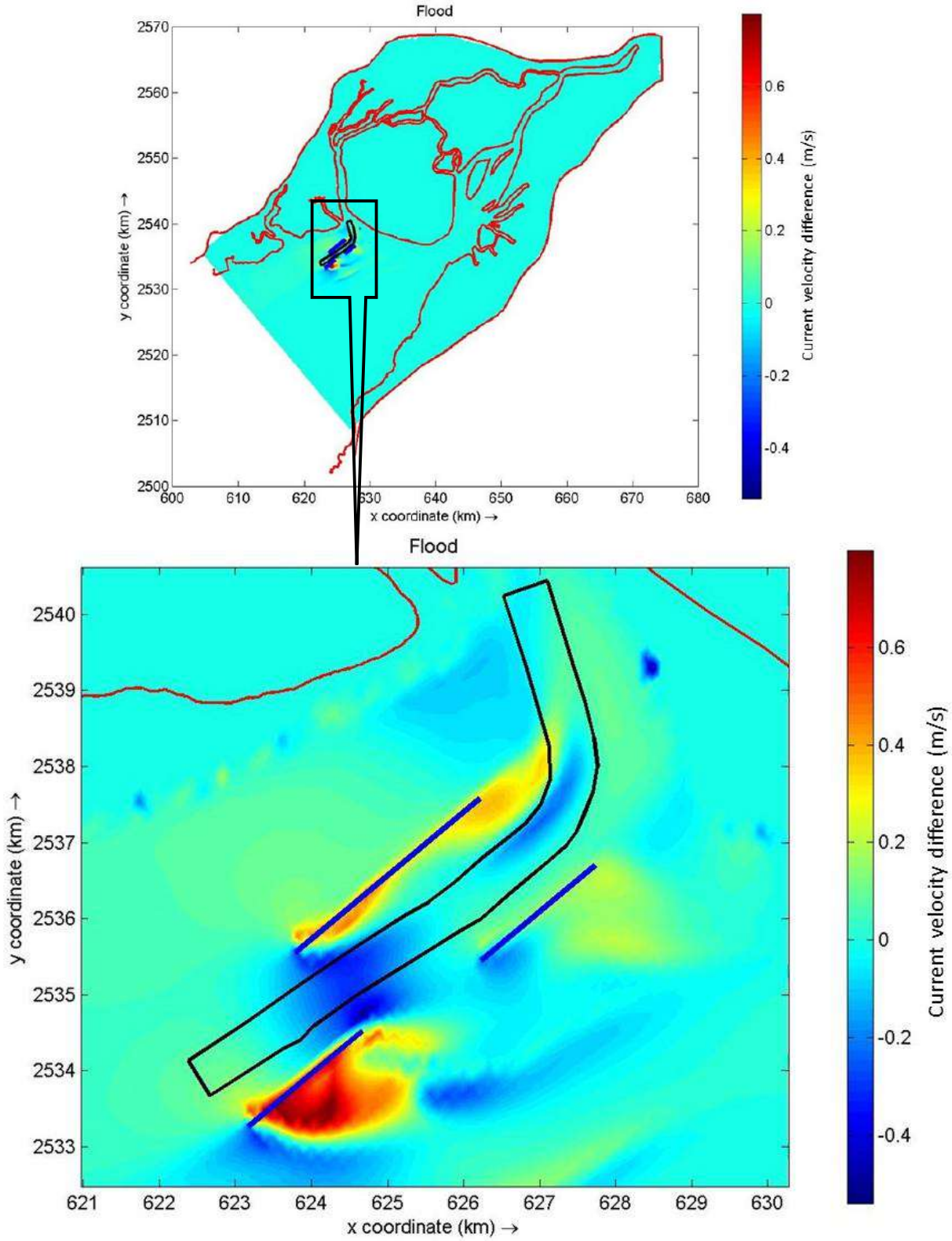


**Fig. A-III. 2 Difference in Current velocity with and without porous plate during Flood time**

## APPENDIX-IV Changing Alignment of Navigational Channel

For understanding the siltation behaviour of Sogal channel in a better way, an attempt was done to change the alignment of existing navigation channel, with the same water depth as of existing channel. The google earth image of attempted alignment is shown in Fig A-IV. 1. However, it was observed that the quantity of siltation had been increased with this orientation of channel. Cumulative erosion/deposition is shown in Fig. A-IV. 2 and quantity is given in Table A-IV. 1

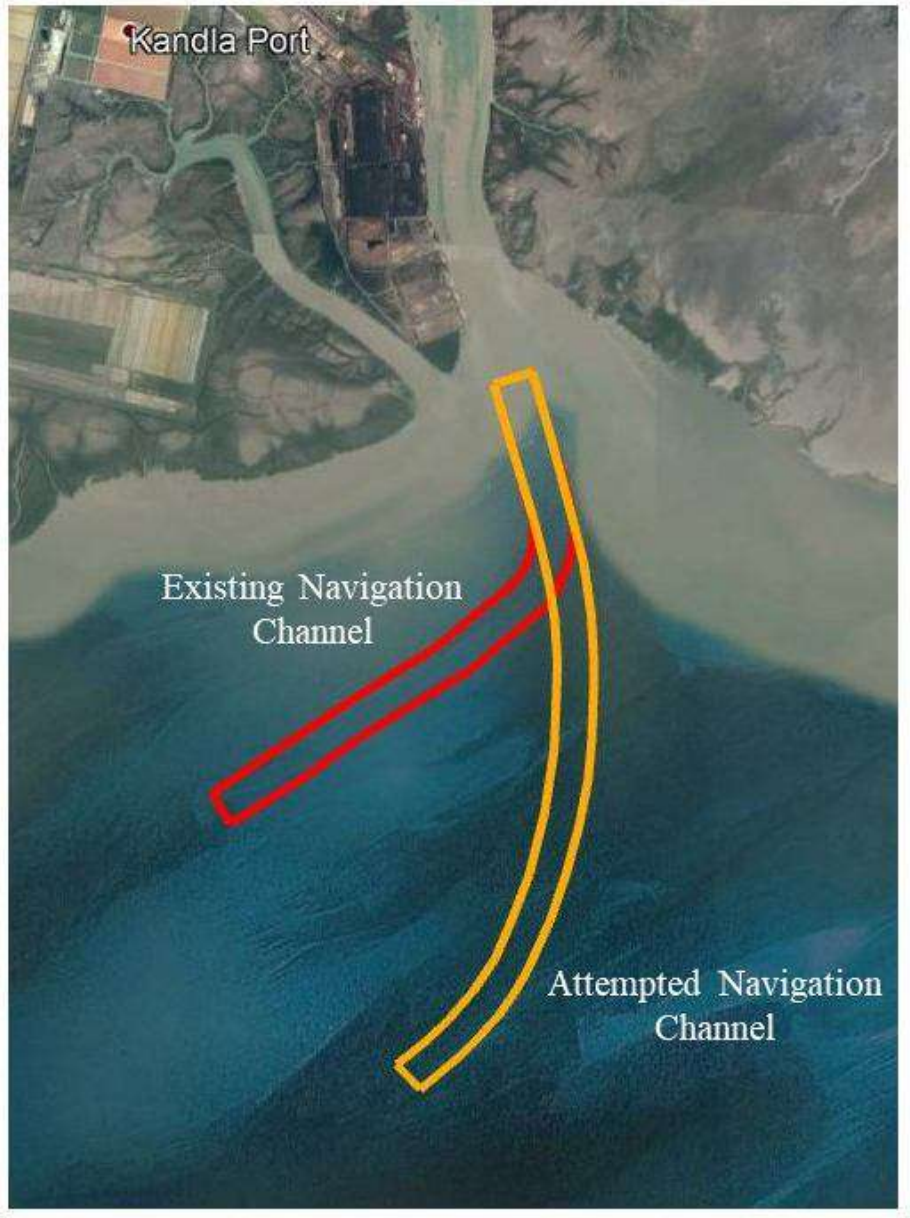


**Fig. A-IV. 1 Google Earth image for new alignment of navigational channel**

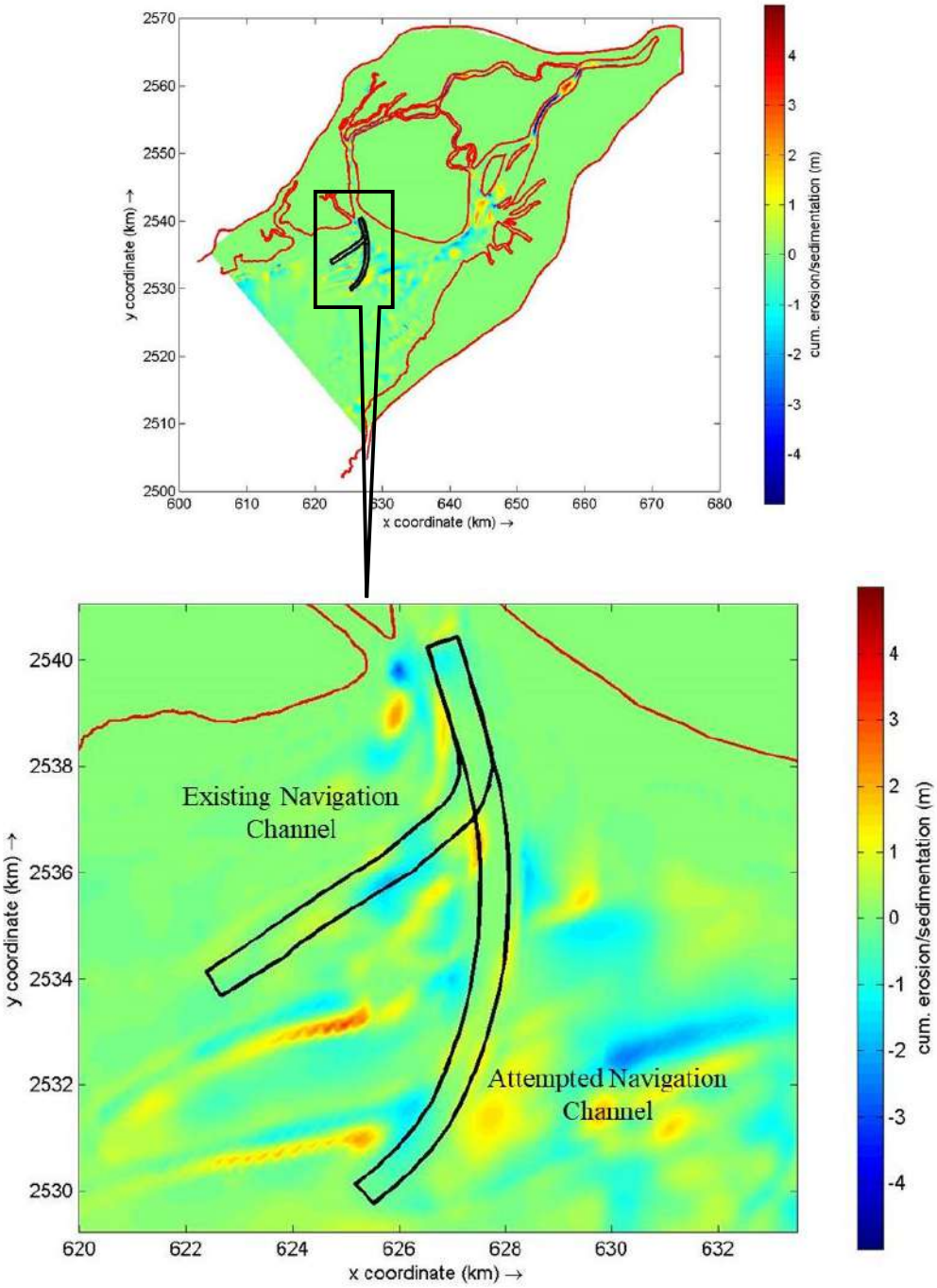


**Fig. A-IV. 2 Cumulative erosion/deposition in May month along attempted navigation channel**

**Table A-IV. 1 Comparison of model results with existing and attempted**

| Month | Siltation Quantity Along Navigation Channels (cubic meter) | | |
|---|---|---|---|
| | Existing Channel | Attempted New Channel | Difference |
| May | 4,12,900 | 5,16,900 | 1,04,000 |

## APPENDIX-V List of Reports and Drawings Provided by DPT

### Table A-V. 1 List of Reports

| SL | Title | Year | Author |
|---|---|---|---|
| 1 | Siltation and Dredging | December 1981 | Kandla Port Trust |
| 2 | Investigations for Approach Channel | March 1983 | Kandla Port Trust |
| 3 | Report for the Approach Channel | February 1984 | CWPRS |
| 4 | Dredging and Siltation in SOGAL Channel | May 1993 | CWPRS |
| 5 | Hydraulic Aspects of Siltation Processes and The Dredging Challenges | 2000 | CWPRS |
| 6 | Behaviour of SOGAL Channel | February 2003 | CWPRS |
| 7 | Morphological Behaviour of Large Range Tidal Creek | 2004 | CWPRS |
| 8 | Behaviour of SOGAL Channel | January 2005 | CWPRS |
| 9 | Impact of Dredging on Stability of SOGAL Channel | December 2006 | CWPRS |
| 10 | Physical and Mathematical model studies for deepening of SOGAL Channel | 2010 | CWPRS |
| 11 | Behaviour of Approach Channel | 1968 | CWPRS |
| 12 | Capital and Maintenance Dredging | 2012 | Kandla Port Trust |

### Table A-V. 2 List of Drawings and field measured data

| Sl. | Title | Year | Author |
|---|---|---|---|
| 1 | Entrance To Nakti Creek – Tuna Bunder | 2005, 2007, 2009 & 2011 | Kandla Port Trust |
| 2 | Marine Boreholes for Capital Dredging in the Approach Channel | 1969 | Kandla Port Trust |
| 3 | Approaches to Kandla Creek | 2005, 2006, 2007, 2009, 2011, 2012, 2013 & 2015 | Kandla Port Trust |
| 4 | Kandla Creek Sheet No. 1 From Mouth of Phang & Sara Creek To South of Oil Jetties | 2005, 2008, 2009, 2011, 2012, 2013, 2014, 2015 | Kandla Port Trust |
| 5 | Kandla Bar Area and Spoil ground | 2005 | Kandla Port Trust |

| | | | |
|---|---|---|---|
| 6 | Approaches to Kandla Creek Tidal Stream Obs Flood Tide | 2010 | CWPRS |
| 7 | Master Plan Of Kandla Port Trust | 2015 | Kandla Port Trust |
| 8 | Kandla Bar Area and Spoil ground | 2007 & 2009 | Kandla Port Trust |
| 9 | Kandla Bar Area and Spoil ground (Pre Monsoon) | 2009, 2011, 2013 & 2014 | Kandla Port Trust |
| 10 | Development of Integrated Facilities Stage II | 2014 | EIA EMP |
| 11 | Port Limit of Vadinar to Kandla | 2015 | Kandla Port Trust |
| 12 | Kandla Creek Sheet No. 2 From South of Oil Jetties to BUOY No 12 & 13 | 2005, 2007, 2009, 2011, 2012, 2013, 2014 & 2015 | Kandla Port Trust |